THE INFLUENCE OF THIOLS ON COPPER BIOAVAILABILITY TO MARINE ALGAE

A Dissertation

Presented to the Faculty of the Graduate School

of Cornell University

In Partial Fulfillment of the Requirements for the Degree of

Doctor of Philosophy

by

Michael Jay Walsh

January 2013

THE INFLUENCE OF THIOLS ON COPPER BIOAVAILABILITY TO MARINE ALGAE

Michael Jay Walsh, Ph. D.

Cornell University 2013

Copper is an essential element for primary productivity in the ocean. However, at concentrations observed surface seawater, copper likely would be toxic to most microbiota if not buffered by a pool of mostly unidentified ligands. These compounds of presumed biological origin can reduce toxicity either by being directly exuded to chelate extracellular bioavailable copper, or by mitigating the toxic effect of copper inside the cell via complexation and subsequent export. This dissertation examines the role of thiols, a presumed component of this pool of ligands, in maintaining copper homeostasis in marine algae.

Stability constants of Cu(I) complexes with cysteine, glutathione, Arg-Cys, and Gln-Cys were measured using a new analytical method that employs fluorescent ion indicators and minimized oxidation of Cu(I). Computational methods were used to support reported constants. Speciation models predict that while thiolate ligands can significantly buffer intracellular copper, at concentrations typically observed in surface seawater, their effect on lowering copper is negligible.

Uptake experiments in the presence of thiols confirmed speciation predictions. Thiols were only partially effective in reducing Cu(I) uptake, while the Cu(II) ligands EDTA and GSSG were able to effectively block uptake. However, cysteine enhances

copper uptake in copper-limited *Emiliania huxleyi* cells and can increase the bioavailability of copper bound to EDTA.

The use of stable isotopes to measure direct uptake of copper in the absence of a ligand, revealed a constitutive copper efflux mechanism in the coccolithophore *E. huxleyi*. This mechanism allows *E. huxleyi* to maintain relatively low cellular levels under exposure to a wide range of high copper concentrations, while the diatom *Thalassiosira pseudonana* only appears to employ export at higher concentrations. Cu-limitation minimizes efflux.

These results suggest that *E. huxleyi* maintains low levels of cellular copper through an intracellular buffering and efflux mechanism. Such a mechanism would give *E. huxleyi* an ecological advantage in water prone to high copper, such as coastal and those experiencing an upwelling event. Results from a survey of marine algae and estuarine field measurements also demonstrate that the thiols Arg-Cys and Gln-Cys may be biologically and geographically widespread.

BIOGRAPHICAL SKETCH

Michael Jay Walsh was born and raised in Concord, New Hampshire, where he graduated from Bishop Brady High School in 2001. He obtained a Bachelor of Arts in Chemistry (A.C.S) from Colby College in 2005. While studying at Cornell, Walsh was a teaching assistant for the courses *Engineering for a Sustainable Society* and *Sustainable Development* and held an appointment as an inaugural Graduate Resident Fellow of Hans Bethe House. He served as Secretary and Vice President of the Graduate and Professional Student Assembly and as a member of the Presidents Climate Commitment Implementation Committee. In 2008 The student body elected him to be a member of Cornell University's Board of Trustees. During his time at Cornell he was awarded the Distinguished Student Volunteer Award from the University's Student Activity Office, The N.G. Kaul Scholarship from the New York Water Environment Association and an Honorable Mention for the Emerging Public Policy Leader Award from the American Institute of Biological Sciences.

Dedicated to my parents,

MARTIN AND SUZANNE WALSH

ACKNOWLEDGMENTS

Foremost appreciation goes to my advisor Beth Ahner for her support, guidance, patience and encouragement throughout this entire process. She has aided my personal and professional development both in the laboratory and the class room. I also am grateful the collaboration and backing of the members of the Ahner Lab: Prayut Bhamawat, Tiffany Gupton Campolongo, Hyun-Su Kim, Colette Kopon, Mark Loria Annie Otwell, Kurt Rhoads, Tim Vadas, and Huijun Yang.

I thank the members of my special committee, Tom Brenna and Lou Derry, for offering guidance and perspective on my work. They also provided instrumentation for this work, support for which was provided by Gavin Saks and Gregg McElwee.

I am very grateful to Rodger Spanswick for use of his radioisotope facility and for his advice and insights whenever I had a question. Michael Rutzke assisted in early ICP-MS method development. An ICP-MS was made available at a critical time by John Helmann with support provided Zhen Ma. Several resources were provided by the Biofuels Research Laboratory led by Larry Walker and supported by Ed Evans. Nancy Fairchild, Debbie Higgins, Brenda Marchewka, Tamara Payne, Allison Pelletier and Peggy Stevens all provided appreciated logistical support in both my research and teaching duties.

I am especially grateful for my partnership with Asha Shama in teaching *Sustainable Development.* I also appreciate the many teaching assistants in that course and in *Engineering for a Sustainable Society*. I am also grateful for all my students especially those who showed a passion for sustainability.

I am indebted to several members of the Cornell Faculty for their mentorship and guidance, including Rosemary Avery, Porus Olpadwala, Norm Scott, Charlie Walcott and Michael Walter. I also had the fortune to work with several admirable role models in the

Cornell administration who led the university though very challenging times, particularly Steve Johnson, Susan Murphy, Mary Opperman, and Kyu-Jung Wang. Additionally I am grateful for the collegial support of the many members of the Cornell University Board of Trustees in particular Carolyn Neumann.

I'd also like to thank several members of Cornell's staff, particularly Corey Earle in Alumni Affairs; Amy O'Donnell, Ari Epstein and Peggy Beach in the Office of Assemblies; Gary Stewart in Community Relations; Phil McPheron, Mary Ann Krisa and Thomas Noel from Campus Life; Kris Corda and Brenda Wicks in the Graduate School; and everyone involved making Cornell's campus more sustainable.

A dream team of fellow students, who were the best of friends and colleagues, made this journey worthwhile. Special thanks goes to Stephanie Whitehouse Barlow, Arnaub Chatterjee, Asa Craig, Kate Duch, Christoffer Heckman, Ben Heavner, Michelle Leinfelder-Miles, Doug Mitarontonda, Amy Richter Blakely, Deondra Rose, Asia Sikora, Ed Strong, and Janet Vertesi and so many others who were also committed to their community.

I was blessed that two of my family members were also fellow students during my studies at Cornell. I owe a great deal of gratitude to my brother Daniel Walsh, particularly for his last minute recommendations to this document and for so much more. My wife, Brianna Walsh, has provided support, patience, love and care from the beginning of this endeavor. She has been my inspiration and my drive.

Finally I thank my parents, Martin and Suzanne Walsh for showing me the mountains and the oceans, for taking me to museums and monuments, for their encouragement and their care, for coaching and teaching me, and for giving me life. They showed me how to turn possibility into reality.

TABLE OF CONTENTS

INTRODUCTION

1. Chemical drivers of productivity

Primary productivity in the oceans is dependent on the presence and chemical form of a variety of nutrients. In most regimes, productivity is limited by the availability of nitrogen and phosphorus (Howarth, 1988). Certain classes of algae can also limited by specific elements. For example diatoms, a globally ubiquitous class of phytoplankton, have a high silica requirement necessary for the production of cell wall frustules (Paasche, 1973). Nutrients can also be present in various chemical forms that have varying degrees of bioavailability. For example, nitrogen may be present as nitrate, ammonia or urea, all of which are processed to varying degrees of efficiency by different cellular pathways. These nutrients are often referred to as *macronutrients* due to their high requirement by marine algae. The total concentration of these essential elements in the ocean is typically low and may vary widely by regime.

In addition to these macronutrients, productivity requires a wide variety of other nutrients for numerous cellular processes and functions which include copper (Cu), cobalt (Co), iron (Fe), manganese (Mn), molybdenum (Mo), nickel (Ni) and zinc (Zn). These elements, predominantly trace metals, are critical cofactors in a variety of enzymes essential to productivity and cellular maintenance. Carbonic anhydrases utilize zinc as a highly electrophilic Lewis acid to dehydrate bicarbonate and maintain a constant supply of CO_2 required for photosynthesis via the RUBISCO pathway (Morel et al., 1994). Nickel is essential for the deamination of urea releasing NH_4^+ (Price and Morel, 1991). Nitrogen fixation in prokaryotic cyanobacteria is facilitated by the molybdenum and iron containing nitrogenase (Cole et al., 1993). Copper is essential for various enzymes including the reactive oxygen species scavenger superoxide dismutase, the

electron transport protein plastocyanin involved in photosynthesis, and cytochrome-c oxidase which facilitates respiration.

Of the suite of micronutrients, iron has an elevated importance due to its higher absolute requirement, role in a number of cellular functions, and low concentrations in surface seawater. Iron is essential to the multi-enzymatic photosynthetic pathway (Geider and Roche, 1994). Photosystem I requires twelve iron cofactors as well as manganese. Photosystem II requires three Fe cofactors. Intracellular nitrogen metabolism employs a number of these micronutrients. Diatoms that use nitrate as a nitrogen source have a higher iron requirement than those grown on ammonia (Maldonado and Price, 1996). Since nitrate concentrations typically far exceed those of ammonia and other nitrogen species, iron sufficiency is essential to nitrogen assimilation.

While the biological requirement of these micronutrients are approximately 1000-fold less than aforementioned macronutrients, they are typically found at far lower concentrations in surface seawater. The lack of certain micronutrients, particularly iron, has also shown to limit primary productivity (Martin et al., 1994). Often this occurs in regions where macronutrient levels are sufficient for growth or high nutrient low chlorophyll (HNLC) zones (Behrenfeld and Kolber, 1999). Low levels of other metals, such as zinc can also result in limitation (Morel et al., 1994) as does the lack of biologically complex forms of some elements. Production in the Southern Ocean can be limited by the lack of the cobalt containing Vitamin B_{12} (Bertrand et al., 2007).

Certain species of marine phytoplankton have evolved numerous strategies to deal with low micronutrient levels. Inside the cell, substitutions are often made for cofactors which are in short supply. The Cu-containing plastocyanin substitutes for iron-containing electron transferring cytochromes in both cyanobacteria (Ferreira and Straus, 1994) and diatoms (Peers and Price,

2006). Flavodoxin, a non-metal enzyme, replaces the iron-sulfur electron transporter, ferrodoxin, in marine diatoms in laboratory studies (Doucette et al., 1996) and in the field (Erdner and Anderson, 1999). Another example of metal replacement is the substitution of cadmium for zinc in a carbonic anhydrase of the marine diatom *Thalassiosira weissflogii* (Lane et al., 2005), which helps to explain the observation that Cd, an element that was long thought to be solely toxic, exhibits a nutrient-like behavior in the ocean.

Another strategy for dealing with low levels of essential trace metals is to increase the availability of the metals to the cell. In addition to upregulating high-affinity transporters, (Blaby-Haas and Merchant, 2012) certain algae and bacteria can change the chemical environment outside the cell to enhance the bioavailabity of certain metals (Morel and Price, 2003). Marine bacteria can produce iron binding siderophores that facilitate iron uptake (Vraspir and Butler, 2009). A similar mechanism appears to facilitate cobalt uptake in the cyanobacteria *Prochlorococcus* (Saito et al., 2002). Redox processes may also enhance uptake. Cell surface reductases reduce Cu(II) to Cu(I) prior to uptake as part of a high affinity copper assimilation pathway. The diatom *Thalassiosira oceanica* utilizes surfaces reductases to assimilate Fe(III) in the presence of a siderophore what would normally limit iron uptake (Maldonado and Price, 2001). Superoxide, which can be biologically produced at the cell surface, can facilitate the reduction of Fe(III) prior to uptake (Kustka et al., 2005).

Frequently, the acquisition of certain nutrients is dependent on the sufficiency of others. Many of the previously mentioned micronutrients are involved in either nitrogen acquisition or photosynthesis. Colimitation occurs when the lack of two nutrients systemically reduces growth (Price and Morel, 1991; Saito et al., 2008). An example of elements intertwined in this fashion includes iron and copper, each of which plays a role in the acquisition of the other. A specific

copper requirement has been demonstrated for a multi-Cu oxidase that facilitates high affinity Fe uptake in the diatom genus *Thalassiosira* (Peers et al., 2005). Genomic searches of these diatoms have found sequences similar to those of multi-Cu oxidases facilitating high-affinity Fe uptake in yeast cultures (Maldonado et al., 2006). Cu limitation of Fe reduction and uptake rates was demonstrated to occur below pCu^{2+} ($-\log[Cu^{2+}]$) = 14, levels that have been observed in the ocean (Moffett and Dupont, 2007). Iron limitation also lowers cellular copper in oceanic phytoplankton species (Guo et al., 2012).

While these micronutrients are essential for growth, some at high concentrations are toxic to algae. Copper and cadmium can induce manganese limitation by blocking its uptake (Sunda and Huntsman, 1998a). The d^{10} electronic configuration of Cd(II) and Cu(I) allows these two enzymes to displace Zn(II) in certain enzymes, disrupting enzymatic functionality. Copper also is highly redox active and can generate free radicals that can have deleterious effects on cellular functions. Tolerance to high levels of both cadmium and copper varies widely among different species of marine phytoplankton (Brand et al., 1986).

Strategies to manage toxic metals mirror some of the approaches used for increasing the bioavailability of essential elements. Copper uptake is regulated in freshwater algae depending upon cellular levels (Hill et al., 1996). At high concentrations eukaryotic cells increase the production of, metallothioneins, which are cystine-rich copper storage proteins (Nevitt et al., 2012).Outside the cell the bioavailability of copper is limited by the presence of a pool of strong copper binding ligands (Coale and Bruland, 1988; Moffett, 1995). Metal-binding ligands are also implicated in the exclusion or efflux of toxic metals. Cadmium stress causes the production of cystine-containing phytochelatins (Ahner et al., 1995) and the diatom *Thalassiosira weissflogii* exudes cadmium with phytochelatin (Lee et al., 1996). Furthermore, transport of Cd-

phytochelatin complexes into vacuoles is facilitated by *Abc2,* an ABC-type transporter in yeast, which also can transport glutathione conjugates (Mendoza-Cózatl et al., 2010). Orthologous transporters are found in plants.

Nutrients, including copper and cadmium are continuously exported out of the surface water by the sinking of fecal matter and dead organisms. This process is referred to as the *biological pump* in which nutrients are assimilated by phytoplankton and bacteria resulting in the depletion of their concentration at the surface. The microbiota can be assimilated into the food chain via consumption or further aggregated. When sinking aggregated microbiota and organic detritus is often referred to as *marine snow*, the descent of which into the aphotic zone removes organic matter, energy, and nutrients from the surface (Alldredge and Silver, 1988). Levels of these nutrients are continuously replenished in surface waters by upwelling of cold, nutrient-rich waters from the deep ocean (Eppley and Peterson, 1979).

Other biological and physical factors drive the availability of certain nutrients. Rivers and other terrestrial sources are common sources of many nutrients and drive increased productivity in neritic zones. Nitrogen fixation by cyanobacteria (Dugdale and Goering, 1967) is the source of a substantial amount of nutrient nitrogen in surface seawater (Karl et al., 2002). Production of the cobalt containing Vitamin B-12 by marine bacteria has been shown to increase diatom growth rates when added with iron, whereas iron alone stimulated the growth of *Phaeocystis antartica* (Bertrand et al., 2007).

Nutrient and chemical factor availability have a significant impact on the composition of phytoplankton communities. Mesocosm experiments have shown diatom dominance when silicate concentrations were higher than 2 μM (Egge and Aksnes, 1992). Diatoms are more likely to be limited by iron, even when surface seawater is enriched with macronutrients nitrogen,

phosphorus and silica (DiTullio et al., 1993). Differences in community structure may arise from evolutionary inheritances as cyanobacteria and eukaryotic algae developed in very different seas. Prior to the buildup of atmospheric oxygen and the proliferation of eukaryotic species, oceanic copper concentrations were much lower than they are now due to the formation of insoluble copper sulfides (Ochiai, 1978). This history may explain why cyanobacteria exhibit greater sensitivities to copper than eukaryotic species (Brand et al., 1986; Mann et al., 2002).

The effects of chemical drivers on phytoplankton community composition have regional and global ecological impacts. At the regional level Haptophytes, a division that includes coccolithophores, are responsible for the production of dimethylsulfide a volatile gas that oxidizes in the atmosphere to form sulfur aerosols which promote cloud formation (Simó, 2001). On a global scale productivity in the oceans facilitates the net removal of carbon dioxide from the atmosphere with removal rates differing by species and community composition (Sweeney et al., 2000). The productivity of calcareous plankton such as coccolithophores can have a significant effect on the carbon cycle, although there remains some disagreement as to the magnitude of this impact (Zondervan, 2007).

Harmful algal blooms (HABs), sometimes referred to as red tides, are of particular concern for their ecological and economic impacts. These events can be caused by blooms of any of a phylogenetically diverse group of algal species which include cyanobacteria, dinoflagellates, and diatoms that produce any one of a number of toxins that are subsequently absorbed into the food chain. HABs are linked to increased mortality in sea lions (Scholin et al., 2000), monk seals (Hernandez et al., 1998), Atlantic dolphins (Hokama et al., 1990), humpback whales (Geraci et al., 1989) and a number of other marine animals. These toxins are also assimilated into human feedstocks such as shellfish (Shumway, 1990). HABs can be naturally occurring, but their

appearances are also have been linked to increased anthropogenic nutrient loading, particularly nitrate from fertilizer (Paerl, 1997; Anderson et al., 2002). Micronutrients may also drive the intensity of HABs. Domoic acid, a neurotoxin, is produced and exuded at high concentrations by the diatom *Pseudo-nitzschia* under copper and iron colimitation. The presence of domoic acid increases growth of colimited *Pseudo-nitzschia*, leading to the hypothesis that this toxin is part of a high affinity metal acquisition system (Wells et al., 2005).

Human activity has long affected the chemistry of surface seawater with increased effects being observed in recent years. Anthropogenic input of various nutrients, such as nitrogen and phosphorous, has caused widespread eutrophication in estuaries and neritic environments (Smith et al., 1999). Despite proliferation of eutrophication and HABs, a recent study has indicated that global phytoplankton concentrations have declined over the past century at a rate of 1% per year (Boyce et al., 2010). This decline is attributed to increasing sea surface temperature resulting from an increase in global atmospheric temperatures driven by elevated emissions of carbon dioxide. Changes in phytoplankton community structure due to these drivers have also been reported (Hare et al., 2007).

Elevation of atmospheric carbon dioxide concentration has driven increased dissolution of carbon dioxide in surface seawater. For organisms such as the coccolithophore *Emiliania huxleyi* this has been a boon, as excess inorganic carbon can increase productivity and calcification rates (Iglesias-Rodriguez et al., 2008). The associated decline in oceanic pH stemming from the dissolution of carbon dioxide threatens other calcifying species (Orr et al., 2005). Furthermore, lower seawater pH causes depressed nitrogen fixation rates (Shi et al., 2012), decreased metal uptake rates (Xu et al., 2012), and decreased iron bioavailability (Shi et al., 2010).

Given the challenges facing the world's oceans and the interconnectedness of this ecosystem, marine research is critical to the understanding of this globally important environmental system. The study of the oceans also provides information on the development of life and its ability to adapt and change over the history of the planet. Ocean life is rich with information that may provide novel tools in the areas of energy, agriculture, biotechnology and medicine (Handelsman et al., 2007). Marine studies also aid in the development of sound global resource management policies as well as in long-term planning for the physical, biological, climatological and economic effects stemming from environmental change. Finally, the seas have challenged and driven the human psyche inspiring exploration, art, literature, and the desire to understand its workings.

2. The role of copper in surface seawater

The research presented in this dissertation examines a small fraction of the complex system described above. It does so by focusing on the role of copper in marine systems and how chemical factors of the extracellular and intracellular environments drive copper bioavailability and homeostasis in marine phytoplankton. Copper occupies a unique niche as a trace-metal nutrient. Its absolute concentration in surface seawater is toxic to most species of marine algae. Its free, bioavailable, ion concentrations however, are buffered to tolerable levels by copper binding ligands. This document investigates the ability of several thiol-containing ligands to bind copper and their ability to influence the bioavailability of copper to marine algae.

In seawater, copper exhibits a depth profile where concentrations are depleted near the surface in the photic zone. Total copper concentrations in the oceanic photic zone ranges from 0.4 – 1.4 nM (Sunda, 1989) and increase to 2.5 nM in the deep ocean (Yeats et al., 1995). Recent

consensus measurements from GEOTRACES North Atlantic 2008 cruise report a surface concentration of 0.83 ± 0.08 nM and a 1000 meter concentration of 1.55± 0.13 nM (Bruland, 2011). Higher concentrations (4.1-260 nM) found in neritic zones are likely due to both natural and anthropogenic inputs (Mills and Quinn, 1984).

In aqueous environments, copper is present as either the cuprous, Cu(I), or cupric Cu(II) ion. Copper is a redox active metal and has a standard reduction potential of 0.159 V ($E°$, $Cu^{2+} + e^- \rightleftharpoons Cu^+$). This low potential allows copper to be exploited for use in numerous proteins that require the transmission of an electron. This ability to easily transfer an electron is also its greatest drawback as high concentrations of Cu(I) can be toxic due to the ability of this ion to generate reactive oxygen species. Because of Cu(I)'s ability to readily react with oxygen, it is kinetically unstable in oxic seawater where it is rapidly oxidized to Cu(II) (Sharma and Millero, 1988). In spite of its high reactivity, Cu(I) concentrations are higher than expected in surface seawater (Moffett and Zika, 1988; Buerge-Weirich and Sulzberger, 2004).

Initially the presence of Cu(I) in seawater was ascribed to the photo-oxidation of dissolved organic matter (DOM) and subsequent generation of the reactive oxygen species superoxide ($O_2^{\cdot -}$) which reduces Cu(II) (Moffett and Zika, 1983; Sharma and Millero, 1988):

$$DOM \xrightarrow{hv} DOM^* + e^- \quad (1)$$

$$e^- + O_2 \rightarrow O_2^{\cdot -} \quad (2)$$

$$O_2^{\cdot -} + Cu^{2+} \rightarrow O_2 + Cu^+ \quad (3)$$

The identification of cysteine (Van Den Berg et al., 1988), glutathione (Le Gall and van den Berg, 1993), and unidentified thiols (Al-Farawati and Van Den Berg, 2001) in seawater opened another possible mechanism for the production of Cu(I) by thiol (RSH) reduction of Cu(II)

which also results in oxidation of the thiol (Pecci et al., 1997):

$$RSH + Cu^{2+} \rightarrow \frac{1}{2} RSSH + Cu^{+} \quad (4)$$

It has also been hypothesized that Cu(I) in surface seawater is a result of the exudation of Cu(I)-thiol complexes produced inside the cell (Dupont et al., 2004). Copper reduction is also biologically facilitated by cell surface reductases (Hill et al., 1996) which is the first step in high affinity copper uptake and common in eukaryotes and prokaryotes (Blaby-Haas and Merchant, 2012), however it is possible that not all copper reduced in this manner is immediately assimilated by the cell.

Cu(II) and Cu(I) behave very differently in aqueous environments. In seawater, Cu(II) tends to form relatively weak inorganic complexes with carbonates, hydroxyl ions, and to a lesser degree chloride and sulfate, leaving 5% of this inorganic copper in the free Cu^{2+} ion form. In contrast Cu(I) forms strong inorganic complexes with chloride and is to a limited degree stabilized from oxidation by the formation of these chloro complexes. The free ion concentration is reduced by four to five orders of magnitude. The two forms also interact differently with organic complexes as carboxylic based ligands form moderately strong complexes with Cu(II), while thiols form very strong bonds with Cu(I). Despite these differences the role of Cu(I) has largely been neglected in studies of copper and its assimilation by phytoplankton in surface seawater. As Cu(I) is readily oxidized, measurement of the reduced form is often difficult. Most techniques used to study copper in surface seawater cannot resolve the redox state. This deficit is problematic for a number of reasons which will be addressed below.

The copper binding capacity of organic ligands in surface seawater and in batch algae cultures is characterized by the conditional stability constant of the ligand with copper:

$$\log K' = \frac{[CuL]}{[Cu_f^{2+}][L_f]} \quad (5)$$

Where [CuL] is the concentration of the copper ligand complex, $[Cu_f^{2+}]$ is the concentration of free Cu(II), and L_f is the uncomplexed ligand. Electroanalytical methods, particularly cathode stripping voltammetry/competitive ligand exchange (CSV-CLE), have been the dominant techniques for measuring the strength of these complexes, and quantifying total ligand concentration and free copper. These techniques typically employ either salicylaldoxime or benzoylacetone as a competing ligand in a copper titration of a copper binding ligand. The formation of the competing ligand-copper complex and its subsequent reactivity with an electrode over the course of the titration is inversely proportional to the strength of the copper binding ligand.

CSV-CLE and other electrochemical techniques have been used to measure nanomolar concentrations of copper binding ligands in a wide variety of culture and field studies (Town and Filella, 2000). Pushed to their limits, these techniques have measured copper concentrations as low as 10^{-15} M in the Northern Pacific (Moffett and Dupont, 2007) and identified a strong copper binding ligand with a conditional stability constant of 10^{13} in exudates of the cyanobacteria *Synechococcus.* The presence of such a ligand may explain that while both *Synechococcus* and *Prochlorococcus*, two closely related cyanobacteria, each exhibit a relatively high copper sensitivity compared to eukaryotes (Mann et al., 2002). Strong copper binding ligands with conditional stability constants ranging from $10^{10.6}$ – $10^{12.3}$ are have also been observed in several eukaryotic algae (Croot et al., 2000; Vasconcelos et al., 2002).

An alternative electrochemical technique, pseudopolarography-anodic stripping voltammetry, provides added resolution to the copper affinity measurements by using

electrochemical standard measurements of known copper ligand complexes (Croot et al., 1999b; Croot et al., 2000). These studies show that despite similar conditional stability constants amongst several eukaryotic algae species, the estimated thermodynamic constants are quite different, indicating that a number of different ligands are being produced. Several estimated thermodynamic constants were far greater than known copper binding ligands and may signify the presence Cu(I) complexes due to an experimental artifact.

These electrochemical techniques often ignore the oxidization states of copper and ligand. Determination of conditional stability constants for CSV-CLE assumes the formation Cu(II) complexes with the competing ligand. The current literature is sparse and vague regarding the behavior of Cu(I) in such systems. Also uncertain is the behavior of Cu(I)-ligands, particularly redox active thiols, with the electrode. Croot (Croot et al., 1999b) observed that electrochemical techniques may cause reduction of the unbound copper binding ligand, clouding electrochemical data. Electrochemical measurements of the interaction of Cu(I)-glutathione and Cu(I)-cysteine in sea water have demonstrated stable Cu(I)-thiol complexes (Leal and Van den Berg, 1998), However, experimental limitations, including those mentioned above, as well as potential thiol oxidation due to the use of Cu(II) as the copper source(Equation 5), suggest that the reported stability complexes of these complexes may be questionable.

Recently the coccolithophore *Emiliania huxleyi* was found to produce the copper binding dipeptides Arg-Cys and Gln-Cys (Dupont et al., 2004) further highlighting the potential importance of thiols in the pool of copper binding ligands. The conditional stability constant of *E. huxleyi* exudates, presumably comprising of both dipeptides, was measured to be $10^{11.6}$ using electrochemical techniques. While this is close to previous measurements of *E. huxleyi* exudates (Croot et al., 2000; Vasconcelos et al., 2002), there was concern regarding the role of Cu(I) in

electrochemical measurements of the exudates.

Despite analytical limitations, it appears that these thiols have a role in copper metabolism and warrant further investigation. Exudation of both thiols increases under copper stress (Dupont and Ahner, 2005). Subsequent to their discovery in laboratory cultures, sub-nanomolar concentrations of dissolved Arg-Cys and Gln-Cys were measured in the Northern Pacific as part of a pool of thiols that included Cys, GSH and γ-glutamate-cysteine (Dupont et al., 2006). A copper-binding ligand with a *m*/*z* of 277, equal to the expected *m*/*z* of Arg-Cys, was found in the Chesapeake Bay (Vachet and Callaway, 2003). Sulfur-containing, copper binding ligands with stability constants similar to those measured above were also observed in the Chesapeake (Dryden et al., 2007).

A biochemical pathway for the production of these dipeptides was demonstrated in *E. coli* by an Arginyl-tRNA synthetase which facilitated deacylation of Arg-tRNA^{Arg} in the presence of cysteine. The synthesis and presence of these ligands may explain why *E. huxleyi* demonstrates an extraordinary tolerance to high copper concentrations (Brand et al., 1986). Such ability may explain why *E. huxleyi* thrives in early spring blooms in the North Atlantic during seasonal upwellings of nutrient and copper-rich waters, while prokaryotic species bloom during later months (Sunda et al., 1981).

Conventional strategies for the management of copper by microbiota could include the reduction of uptake through the downregulation of copper transporters (Hill et al., 1996) and the upregulation of a copper storage mechanisms such as cysteine rich metallothioneins (Cobbett and Goldsbrough, 2002). Both of these strategies are ubiquitous in eukaryotic organisms and may not be sufficient to explain why an organism such as *E. huxleyi* is able tolerate high concentrations of copper. In fact, the second strategy does not appear to be significant in *E. huxleyi* as it

maintains a far lower copper quota than other species of eukaryotic marine phytoplankton in absolute, volume-normalized and phosphorus-normalized terms (Ho et al., 2003), suggesting a lower storage capacity. It is also unlikely that its tolerance and ability to maintain a low quota stems from an ability of *E. huxleyi* to substantially down regulate copper transporters in comparison to others species.

Given the prevalence of copper binding ligands in marine systems and *E. huxleyi's* ability to synthesize two apparently specific copper binding ligands, it is worthwhile to explore the role of copper binding thiols in copper uptake and homeostasis. There are two plausible mechanisms for copper binding ligands to reduce deleterious effects of high copper concentrations: (1) Copper binding ligands limit the bioavailability to and assimilation of copper by marine algae; and, (2) Copper binding ligands help to buffer intracellular levels of copper concentrations prior to export of a copper-ligand complex. This later mechanism is similar to how phytochelatins facilitate the detoxification of cadmium (Lee et al., 1996; Mendoza-Cózatl et al., 2010).

To demonstrate the first mechanism it is necessary to understand the process of copper uptake in marine algae and the effect of certain copper binding ligands on enhancing or limiting uptake. Several studies have explored copper uptake in representative samples of marine algae (Croot et al., 1999a; Vasconcelos and Leal, 2000; Croot et al., 2003; Quigg et al., 2006; Guo et al., 2010), none of which have attempted to control copper redox chemistry . Some of these studies demonstrated copper uptake rates that are surprisingly high given the initial cellular copper concentration. It is possible that such measurements are the result of inefficient cellular washes that may fail to remove Cu(I) from the cell surface.

Further complicating matters could be the simultaneous occurrence of export, due to an efficient detoxification mechanism as described by process (2). Unfortunately in algae, export is

not as well understood. Copper export in the presence of an organic ligand has been observed from thecyanobacterium *Synechococcus.* Specific copper efflux transporters have been identified in yeast and bacteria and have been linked to copper exclusion and homeostasis (Rensing et al., 2000; Burkhead et al., 2009).

The impacts of copper binding ligands on both processes also require further examination. It is well established that Cu(II) ligands such as EDTA and cyclam substantially decrease the bioavailability of copper to marine algae, by reducing the Cu^{2+} concentration (Semeniuk et al., 2009). Little is known about the bioavailability of Cu(I) in the presence of ligands such as thiols. Recent research suggests that they may play a novel role in algal metal uptake. Cysteine can facilitate zinc uptake in the presence of strong ligands such as EDTA (Aristilde et al., 2012) by forming weak complexes that are bioavailable. A similar mechanism could occur by thiol mediated reduction of Cu(II) bound to EDTA, released as Cu(I) and stabilized by a thiol. This possibility suggests a very different role for such ligands than what is proposed by both mechanisms (1) and (2), but could also be biologically relevant in marine systems that are likely to contain both Cu(II) ligands and thiols.

The purpose this dissertation is to clarify the biological importance and biochemical behavior of copper and biogenic thiols in productive surface seawater. To do so requires an understanding of how strongly low molecular weight thiols, such as glutathione, cysteine, Arg-Cys, and Gln-Cys complex with Cu(I). Due to the redox behavior of copper, such measurements are difficult to make. In the first chapter, we describe the development of an alternative method to measure stability constants. A competing fluorometric ligand is used to measure free Cu^{+} ion concentrations in the presence of the thiols mentioned previously. Stability constants are calculated from copper titrations in buffered low oxygen solutions and synthetic ocean waters.

The implications of copper speciation and the relation of these values to those measured in environmental systems are subsequently discussed. In the second chapter, we investigate these complexes further by analyzing the results of density functional theory calculations and optimization of metal-thiol complexes to support the presence of specific complexes observed in chapter one and examine the structure of these complexes for clues to their biochemical behavior.

This document also investigates copper uptake by the globally representative eukaryotic algae *E. huxleyi* and *T. pseudonana*. The third chapter describes the use of stable isotopes as copper-tracers to demonstrate the presence a copper export mechanism in *E. huxleyi* that is concurrently active during copper assimilation. Chapter four subsequently examines uptake in the presence of Cu(I) and Cu(II) ligands and provides evidence of enhanced copper uptake by cysteine, especially when Cu(II) is complexed by EDTA. Chapter five then investigates the biological synthesis of the novel dipeptides Arg-Cys and Gln-Cys and presents evidence for their production by several diverse marine algae as well as in an estuary. This dissertation concludes by discussing the biological and ecological implications of the results presented in these chapters and suggesting new avenues of research related to copper metabolism in marine algae.

3. References

Ahner BA, Kong S and Morel FMM. (1995) Phytochelatin Production in Marine-Algae .1. An Interspecies Comparison. *Limnology and Oceanography* 40: 649-657.

Al-Farawati R and Van Den Berg CMG. (2001) Thiols in coastal waters of the western North Sea and English Channel. *Environmental Science & Technology* 35: 1902-1911.

Alldredge AL and Silver MW. (1988) Characteristics, dynamics and significance of marine snow. *Progress in Oceanography* 20: 41-82.

Anderson D, Glibert P and Burkholder J. (2002) Harmful algal blooms and eutrophication: Nutrient sources, composition, and consequences. *Estuaries and Coasts* 25: 704-726.

Aristilde L, Xu Y and Morel FMM. (2012) Weak Organic Ligands Enhance Zinc Uptake in Marine Phytoplankton. *Environmental Science & Technology* 46: 5438-5445.

Behrenfeld MJ and Kolber ZS. (1999) Widespread iron limitation of phytoplankton in the South Pacific Ocean. *Science* 283: 840-843.

Bertrand EM, Saito MA, Rose JM, et al. (2007) Vitamin B-12 and iron colimitation of phytoplankton growth in the Ross Sea. *Limnology and Oceanography* 52: 1079-1093.

Blaby-Haas CE and Merchant SS. (2012) The ins and outs of algal metal transport. *Biochimica et Biophysica Acta (BBA) - Molecular Cell Research* 1823: 1531-1552.

Boyce DG, Lewis MR and Worm B. (2010) Global phytoplankton decline over the past century. *Nature* 466: 591-596.

Brand LE, Sunda WG and Guillard RRL. (1986) Reduction of marine phytoplankton reproduction rates by copper and cadmium. *Journal of Experimental Marine Biology and Ecology* 96: 225-250.

Bruland KW. (2011) Dissolved Copper: Consensus values (± 1 std. dev.) for North Atlantic GEOTRACES

Reference Samples as of November 2011. *GEOTRACES and SAFe INTERCALIBRATIONS*.

Buerge-Weirich D and Sulzberger B. (2004) Formation of Cu(I) in Estuarine and Marine Waters: Application of a New Solid-Phase Extraction Method To Measure Cu(I). *Environmental Science & Technology* 38: 1843-1848.

Burkhead JL, Gogolin Reynolds KA, Abdel-Ghany SE, et al. (2009) Copper homeostasis. *New Phytologist* 182: 799-816.

Coale KH and Bruland KW. (1988) Copper Complexation in the Northeast Pacific. *Limnology and Oceanography* 33: 1084-1101.

Cobbett C and Goldsbrough P. (2002) PHYTOCHELATINS AND METALLOTHIONEINS: Roles in Heavy Metal Detoxification and Homeostasis. *Annual Review of Plant Biology* 53: 159-182.

Cole JJ, Lane JM, Marino R, et al. (1993) Molybdenum Assimilation by Cyanobacteria and Phytoplankton in Freshwater and Salt Water. *Limnology and Oceanography* 38: 25-35.

Croot PL, Karlson B, van Elteren JT, et al. (1999a) Uptake of 64Cu−Oxine by Marine Phytoplankton. *Environmental Science & Technology* 33: 3615-3621.

Croot PL, Karlson B, van Elteren JT, et al. (2003) Uptake and efflux of Cu-64 by the marine cyanobacterium Synechococcus (WH7803). *Limnology and Oceanography* 48: 179-188.

Croot PL, Moffett JW and Brand LE. (2000) Production of extracellular Cu complexing ligands by eucaryotic phytoplankton in response to Cu stress. *Limnology and Oceanography* 45: 619-627.

Croot PL, Moffett JW and Luther GW. (1999b) Polarographic determination of half-wave potentials for copper-organic complexes in seawater. *Marine Chemistry* 67: 219-232.
DiTullio GR, Hutchins DA and Bruland KW. (1993) Interaction of Iron and Major Nutrients Controls Phytoplankton Growth and Species Composition in the Tropical North Pacific Ocean. *Limnology and Oceanography* 38: 495-508.
Doucette GJ, Erdner DL, Peleato ML, et al. (1996) Quantitative analysis of iron-stress related proteins in Thalassiosira weissflogii: Measurement of flavodoxin and ferredoxin using HPLC. *Marine Ecology-Progress Series* 130: 269-276.
Dryden CL, Gordon AS and Donat JR. (2007) Seasonal survey of copper-complexing ligands and thiol compounds in a heavily utilized, urban estuary: Elizabeth River, Virginia. *Marine Chemistry* 103: 276-288.
Dugdale RC and Goering JJ. (1967) Uptake of New and Regenerated Forms of Nitrogen in Primary Productivity. *Limnology and Oceanography* 12: 196-206.
Dupont CL and Ahner BA. (2005) Effects of copper, cadmium, and zinc on the production and exudation of thiols by Emiliania huxleyi. *Limnology and Oceanography* 50: 508-515.
Dupont CL, Moffett JW, Bidigare RR, et al. (2006) Distributions of dissolved and particulate biogenic thiols in the subartic Pacific Ocean. *Deep-Sea Research Part I-Oceanographic Research Papers* 53: 1961-1974.
Dupont CL, Nelson RK, Bashir S, et al. (2004) Novel copper-binding and nitrogen-rich thiols produced and exuded by Emiliania huxleyi. *Limnology and Oceanography* 49: 1754-1762.
Egge J and Aksnes D. (1992) Silicate as regulating nutrient in phytoplankton competition. *Marine ecology progress series. Oldendorf* 83: 281-289.
Eppley RW and Peterson BJ. (1979) Particulate Organic-Matter Flux and Planktonic New Production in the Deep Ocean. *Nature* 282: 677-680.
Erdner DL and Anderson DM. (1999) Ferredoxin and Flavodoxin as Biochemical Indicators of Iron Limitation during Open-Ocean Iron Enrichment. *Limnology and Oceanography* 44: 1609-1615.
Ferreira F and Straus N. (1994) Iron deprivation in cyanobacteria. *Journal of Applied Phycology* 6: 199-210.
Geider R and Roche J. (1994) The role of iron in phytoplankton photosynthesis, and the potential for iron-limitation of primary productivity in the sea. *Photosynthesis Research* 39: 275-301.
Geraci JR, Anderson DM, Timperi RJ, et al. (1989) Humpback Whales (Megaptera novaeangliae) Fatally Poisoned by Dinoflagellate Toxin. *Canadian Journal of Fisheries and Aquatic Sciences* 46: 1895-1898.
Guo J, Annett AL, Taylor RL, et al. (2010) Copper-Uptake Kinetics of Coastal and Oceanic Diatoms. *Journal of Phycology* 46: 1218-1228.
Guo J, Lapi S, Ruth TJ, et al. (2012) The Effects of Iron and Copper Availability on the Copper Stoichiometery of Marine Phytoplankton. *Journal of Phycology* 48: 312-325.
Handelsman J, Tiedje J, Alverez-Cohen L, et al. (2007) *The new science of metagenomics: revealing the secrets of our microbial planet*: National Academy Press
Hare C, Leblanc K, DiTullio G, et al. (2007) Consequences of increased temperature and CO2 for phytoplankton community structure in the Bering Sea. *Marine Ecology Progress Series* 352: 9-16.

Hernandez M, Robinson I, Aguilar A, et al. (1998) Did algal toxins cause monk seal mortality? *Nature* 393: 28-29.
Hill KL, Hassett R, Kosman D, et al. (1996) Regulated Copper Uptake in Chlamydomonas reinhardtii in Response to Copper Availability. *Plant Physiology* 112: 697-704.
Ho TY, Quigg A, Finkel ZV, et al. (2003) The elemental composition of some marine phytoplankton. *Journal of Phycology* 39: 1145-1159.
Hokama Y, Asahina AY, Hong TWP, et al. (1990) Causitive toxin(s) in the death of two atlantic dolphins. *Journal of Clinical Laboratory Analysis* 4: 474-478.
Howarth RW. (1988) Nutrient Limitation of Net Primary Production in Marine Ecosystems. *Annual Review of Ecology and Systematics* 19: 89-110.
Iglesias-Rodriguez MD, Halloran PR, Rickaby REM, et al. (2008) Phytoplankton Calcification in a High-CO2 World. *Science* 320: 336-340.
Karl D, Michaels A, Bergman B, et al. (2002) Dinitrogen Fixation in the World's Oceans. *Biogeochemistry* 57/58: 47-98.
Kustka AB, Shaked Y, Milligan AJ, et al. (2005) Extracellular Production of Superoxide by Marine Diatoms: Contrasting Effects on Iron Redox Chemistry and Bioavailability. *Limnology and Oceanography* 50: 1172-1180.
Lane TW, Saito MA, George GN, et al. (2005) A cadmium enzyme from a marine diatom. *Nature* 435: 42-42.
Le Gall A-C and van den Berg CMG. (1993) Cathodic stripping voltammetry of glutathione in natural waters. *Analyst* 118: 1411-1415.
Leal MFC and Van den Berg CMG. (1998) Evidence for strong copper(I) complexation by organic ligands in seawater. *Aquatic Geochemistry* 4: 49-75.
Lee JG, Ahner BA and Morel FMM. (1996) Export of cadmium and phytochelatin by the marine diatom Thalassiosira weissflogii. *Environmental Science & Technology* 30: 1814-1821.
Maldonado MT, Allen AE, Chong JS, et al. (2006) Copper-dependent iron transport in coastal and oceanic diatoms. *Limnology and Oceanography* 51: 1729-1743.
Maldonado MT and Price NM. (1996) Influence of N substrate on Fe requirements of marine centric diatoms. *Marine Ecology Progress Series* 141: 161-172.
Maldonado MT and Price NM. (2001) REDUCTION AND TRANSPORT OF ORGANICALLY BOUND IRON BY THALASSIOSIRA OCEANICA (BACILLARIOPHYCEAE). *Journal of Phycology* 37: 298-310.
Mann EL, Ahlgren N, Moffett JW, et al. (2002) Copper Toxicity and Cyanobacteria Ecology in the Sargasso Sea. *Limnology and Oceanography* 47: 976-988.
Martin JH, Coale KH, Johnson KS, et al. (1994) Testing the Iron Hypothesis in Ecosystems of the Equatorial Pacific-Ocean. *Nature* 371: 123-129.
Mendoza-Cózatl DG, Zhai Z, Jobe TO, et al. (2010) Tonoplast-localized Abc2 transporter mediates phytochelatin accumulation in vacuoles and confers cadmium tolerance. *Journal of Biological Chemistry* 285: 40416-40426.
Mills GL and Quinn JG. (1984) Dissolved copper and copper-organic complexes in the Narragansett Bay estuary. *Marine Chemistry* 15: 151-172.
Moffett JW. (1995) Temporal and Spatial Variability of Copper Complexation by Strong Chelators in the Sargasso-Sea. *Deep-Sea Research Part I-Oceanographic Research Papers* 42: 1273-1295.
Moffett JW and Dupont C. (2007) Cu complexation by organic ligands in the sub-arctic NW

Pacific and Bering Sea. *Deep-Sea Research Part I-Oceanographic Research Papers* 54: 586-595.
Moffett JW and Zika RG. (1983) Oxidation-Kinetics of Cu(I) in Seawater - Implications for Its Existence in the Marine-Environment. *Marine Chemistry* 13: 239-251.
Moffett JW and Zika RG. (1988) Measurement of Copper(I) in Surface Waters of the Sub-Tropical Atlantic and Gulf of Mexico. *Geochimica et Cosmochimica Acta* 52: 1849-1857.
Morel FMM and Price NM. (2003) The Biogeochemical Cycles of Trace Metals in the Oceans. *Science* 300: 944-947.
Morel FMM, Reinfelder JR, Roberts SB, et al. (1994) Zinc and carbon co-limitation of marine phytoplankton. *Nature* 369: 740-742.
Nevitt T, Öhrvik H and Thiele DJ. (2012) Charting the travels of copper in eukaryotes from yeast to mammals. *Biochimica et Biophysica Acta (BBA) - Molecular Cell Research* 1823: 1580-1593.
Ochiai E-I. (1978) The evolution of the environment and its influence on the evolution of life. *Origins of Life and Evolution of Biospheres* 9: 81-91.
Orr JC, Fabry VJ, Aumont O, et al. (2005) Anthropogenic ocean acidification over the twenty-first century and its impact on calcifying organisms. *Nature* 437: 681-686.
Paasche E. (1973) Silicon and the ecology of marine plankton diatoms. I. Thalassiosira pseudonana (Cyclotella nana) grown in a chemostat with silicate as limiting nutrient. *Marine Biology* 19: 117-126.
Paerl HW. (1997) Coastal Eutrophication and Harmful Algal Blooms: Importance of Atmospheric Deposition and Groundwater as "New" Nitrogen and Other Nutrient Sources. *Limnology and Oceanography* 42: 1154-1165.
Pecci L, Montefoschi G, Musci G, et al. (1997) Novel findings on the copper catalysed oxidation of cysteine. *Amino Acids* 13: 355-367.
Peers G and Price NM. (2006) Copper-containing plastocyanin used for electron transport by an oceanic diatom. *Nature* 441: 341-344.
Peers G, Quesnel SA and Price NM. (2005) Copper requirements for iron acquisition and growth of coastal and oceanic diatoms. *Limnology and Oceanography* 50: 1149-1158.
Price NM and Morel FMM. (1991) Colimitation of Phytoplankton Growth by Nickel and Nitrogen. *Limnology and Oceanography* 36: 1071-1077.
Quigg A, Reinfelder JR and Fisher NS. (2006) Copper uptake kinetics in diverse marine phytoplankton. *Limnology and Oceanography* 51: 893-899.
Rensing C, Fan B, Sharma R, et al. (2000) CopA: An Escherichia coli Cu(I)-translocating P-type ATPase. *Proceedings of the National Academy of Sciences* 97: 652-656.
Saito MA, Goepfert TJ and Jason TR. (2008) Some Thoughts on the Concept of Colimitation: Three Definitions and the Importance of Bioavailability. *Limnology and Oceanography* 53: 276-290.
Saito MA, Moffett JW, Chisholm SW, et al. (2002) Cobalt Limitation and Uptake in Prochlorococcus. *Limnology and Oceanography* 47: 1629-1636.
Scholin CA, Gulland F, Doucette GJ, et al. (2000) Mortality of sea lions along the central California coast linked to a toxic diatom bloom. *Nature* 403: 80-84.
Semeniuk DM, Cullen JT, Johnson WK, et al. (2009) Plankton copper requirements and uptake in the subarctic Northeast Pacific Ocean. *Deep Sea Research Part I: Oceanographic Research Papers* 56: 1130-1142.

Sharma VK and Millero FJ. (1988) Oxidation of copper(I) in seawater. *Environmental Science & Technology* 22: 768-771.
Shi D, Kranz SA, Kim J-M, et al. (2012) Ocean acidification slows nitrogen fixation and growth in the dominant diazotroph Trichodesmium under low-iron conditions. *Proceedings of the National Academy of Sciences* 109: E3094–E3100.
Shi D, Xu Y, Hopkinson BM, et al. (2010) Effect of Ocean Acidification on Iron Availability to Marine Phytoplankton. *Science* 327: 676-679.
Shumway SE. (1990) A Review of the Effects of Algal Blooms on Shellfish and Aquaculture. *Journal of the World Aquaculture Society* 21: 65-104.
Simó R. (2001) Production of atmospheric sulfur by oceanic plankton: biogeochemical, ecological and evolutionary links. *Trends in Ecology & Evolution* 16: 287-294.
Smith VH, Tilman GD and Nekola JC. (1999) Eutrophication: impacts of excess nutrient inputs on freshwater, marine, and terrestrial ecosystems. *Environmental Pollution* 100: 179-196.
Sunda WG. (1989) Trace metal interactions with marine phytoplankton. *Biological Oceanography* 6: 411-442.
Sunda WG, Barber RT and Huntsman SA. (1981) Phytoplankton Growth in Nutrient Rich Seawater - Importance of Copper-Manganese Cellular Interactions. *Journal of Marine Research* 39: 567-586.
Sunda WG and Huntsman SA. (1998a) Interactive Effects of External Manganese, the Toxic Metals Copper and Zinc, and Light in Controlling Cellular Manganese and Growth in a Coastal Diatom. *Limnology and Oceanography* 43: 1467-1475.
Sweeney C, Smith WO, Hales B, et al. (2000) Nutrient and carbon removal ratios and fluxes in the Ross Sea, Antarctica. *Deep Sea Research Part II: Topical Studies in Oceanography* 47: 3395-3421.
Town RM and Filella M. (2000) Dispelling the Myths: Is the Existence of L1 and L2 Ligands Necessary to Explain Metal Ion Speciation in Natural Waters? *Limnology and Oceanography* 45: 1341-1357.
Vachet RW and Callaway MB. (2003) Characterization of Cu(II)-binding ligands from the Chesapeake Bay using high-performance size-exclusion chromatography and mass spectrometry. *Marine Chemistry* 82: 31-45.
Van Den Berg CMG, Househam BC and Riley JP. (1988) Determination of cystine and cysteine in seawater using cathodic stripping voltammetry in the presence of Cu(II). *Journal of Electroanalytical Chemistry and Interfacial Electrochemistry* 239: 137-148.
Vasconcelos MTSD and Leal MFC. (2000) Adsorption and Uptake of Cu by Emiliania huxleyi in Natural Seawater. *Environmental Science & Technology* 35: 508-515.
Vasconcelos MTSD, Leal MFC and van den Berg CMG. (2002) Influence of the nature of the exudates released by different marine algae on the growth, trace metal uptake, and exudation of Emiliania huxleyi in natural seawater. *Marine Chemistry* 77: 187-210.
Vraspir JM and Butler A. (2009) Chemistry of Marine Ligands and Siderophores. *Annual Review of Marine Science* 1: 43-63.
Wells ML, Trick CG, Cochlan WP, et al. (2005) Domoic Acid: The Synergy of Iron, Copper, and the Toxicity of Diatoms. *Limnology and Oceanography* 50: 1908-1917.
Xu Y, Shi D, Aristilde L, et al. (2012) The effect of pH on the uptake of zinc and cadmium in marine phytoplankton: Possible role of weak complexes. *Limnology and Oceanography* 57: 293.

Yeats PA, Westerlund S and Flegal AR. (1995) Cadmium, copper and nickel distributions at four stations in the eastern central and south Atlantic. *Marine Chemistry* 49: 283-293.

Zondervan I. (2007) The effects of light, macronutrients, trace metals and CO2 on the production of calcium carbonate and organic carbon in coccolithophores—A review. *Deep Sea Research Part II: Topical Studies in Oceanography* 54: 521-537.

CHAPTER 1

Cu(I), Cd(II) & Zn(II) Binding to Cysteine and Cysteine Containing Peptides: 1. Stability Constant Determination Using Fluorescent Probes

1. Abstract

Fluorometric competing-ligand titrations were used to measure stability constants of Zn(II), Cd(II) and Cu(I) complexes of cysteine and glutathione. Cu(I)-stability constants and protonation constants were also determined for the dipeptides Arg-Cys and Gln-Cys which are produced by a marine alga under copper stress. The fluorescent ion indicators FluoZin-1 and BTC were used as competing ligands in titrations involving Zn(II) and Cd(II). PhenGreenSK was likewise used in Cu(I) titrations. Several precautions were taken to prevent unwanted Cu(I) oxidation, including solution deoxygenation and employing EDTA as a masking agent for interfering Cu(II). Stability constants were determined by developing a 5-species chemical equilibrium model and using least squares minimization to fit the model parameters to the titration data. The measured stability constants of Cd(II) and Zn(II) complexes were consistent with previous work, validating our model and assumptions. Our results also include the first general stability constants for Cu(I)-cysteine complexes and an alternative set for Cu(I)-GSH complexes. While these stability constants indicate that Cu(I) forms strong complexes with thiols, they suggest that in the environment where thiol concentrations range from 1 – 100 nM, their presence may not effectively buffer copper when chloride is present.

2. Introduction

Thiol-containing compounds are among the most prevalent biogenic small ligands responsible for metal coordination, regulation and homeostasis. Glutathione (γ-l-glutamyl-l-cysteinylglycine, GSH), often the most abundant intracellular thiol, is involved in antioxidant activity (Millis et al., 1993; Pompella et al., 2003), is also involved in metal coordination (Fuhr and Rabenstein, 1973). Complexes of glutathione with copper facilitate the reconstitution of the copper cofactor of some proteins (Ciriolo et al., 1990), and the metal-thiol complex have been shown to be a source of superoxide (Speisky et al., 2008). Phytochelatins, $((\gamma\text{Glu-Cys})_n\text{-Gly}$, n=2-11), cysteine-rich polypeptides biologically synthesized from GSH, are responsible for heavy metal detoxification and homeostasis in algae and plants (Ahner and Morel, 1995; Cobbett and Goldsbrough, 2002). Thiols also tend to form relatively strong complexes with Zn(II), Cd(II), and Cu(I) (Pearson, 1963; Lenz and Martell, 1964).

In surface seawater, organic ligands lower bioavailable copper from toxic to nutritive levels (Croot et al., 2000). Numerous electrochemical measurements have demonstrated the presence of ligands with a wide range of affinity for copper (Town and Filella, 2000). Some field studies have shown thiols constitute a significant portion of these ligands (Al-Farawati and Van Den Berg, 2001; Dryden et al., 2007). Culture studies of several classes of marine phytoplankton have identified the presence of thiol ligands classified as "cysteine-like" and "glutathione-like" (Leal et al., 1999). The globally abundant coccolithophore *Emiliania huxleyi* has been shown to produce two cysteine-containing dipeptides, Arg-Cys and Gln-Cys (Figure 1), under conditions of metal stress (Dupont and Ahner, 2005) and luxury nitrogen (Kim et al., 2011). In batch cultures, these dipeptides are present at nanomolar levels in the extracellular medium (Dupont and Ahner, 2005), comparable to levels of ligands measured in culture and

A. Cys

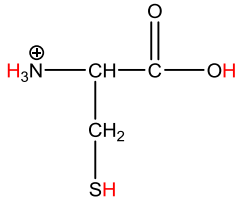

B. GSH

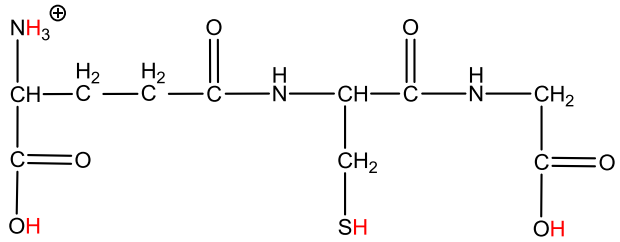

C. Arg-Cys

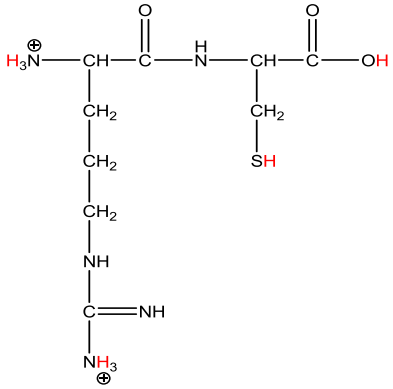

D. Gln-Cys

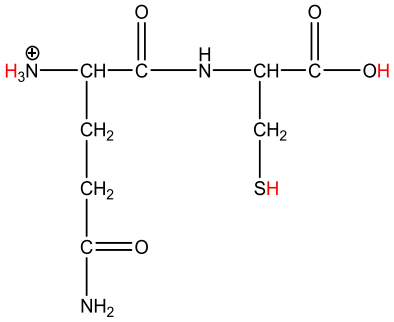

Figure 1. Structures of A. Cysteine (Cys), B. Glutathione (GSH), C. Arginine-Cysteine (Arg-Cys), and D. Glutamine-Cysteine (Gln-Cys) showing dissociable protons in red.

field studies. No metal-binding data currently exists for these dipeptides.

Measurement of the strength of metal-thiol complexes provides critical insight into how these ligands affect metal chemistry and bioavailability. Strong complexation of copper would suggest that these ligands are important players in reducing copper-bioavailability in surface sea water. The general stability constants of glutathione complexes of Cd(II) and Zn(II) have been measured with good agreement using various techniques (Corazza et al., 1996; Jalilehvand et al., 2006). Complexes of cysteine with these metals have also been examined using a range of analytical techniques, but there is less agreement in the literature regarding the relative strength and prevalence of protonated and multi-ligand complexes (Berthon, 1995). In contrast, the general stability complexes for copper with cysteine are not available and only one study reports general stability constants for GSH-Cu(I) complexes (Osterberg et al., 1979).

The limited dataset associated with copper-thiol complexes is due to the fact that ionic copper is highly redox active. While this property enables copper to be an effective enzymatic cofactor, the Cu(I) valence state is highly unstable in aqueous solution as well as seawater, where it is rapidly oxidized to Cu(II) (Sharma and Millero, 1988). Thiol complexation significantly stabilizes Cu(I) (Corazza et al., 1996; Rigo et al., 2004). Additionally thiols (RSH) can facilitate the reduction of Cu(II) to Cu(I) via the following mechanism that results in oxidation of the thiol (RSSR) (Pecci et al., 1997):

$$RSH + Cu(II) \rightarrow \frac{1}{2}RSSR + Cu(I) + H^{+} \quad (1)$$

The reactivity of copper ions renders the traditional methods of determining stability constants of copper complexes problematic (Berthon, 1995). The presence of oxygen, a reactive electrode, and large swings in pH can increase the potential for oxidation. Conditional constants

for cysteine and glutathione have been measured in seawater using voltammetry (Leal and Van den Berg, 1998), but inadvertent thiol oxidation could have resulted from the use of Cu(II) as a titrant. Electromotive force titrations were used to identify a set of Cu(I)-GSH glutathione constants (Osterberg et al., 1979). Avoiding some of the challenges associated with these electrochemical techniques, Rigo et al. (2004) used NMR to measure Cys-Cu(I) stability and coordination under an inert atmosphere. Several Cu(I) complexes of multiple-cysteine containing polypeptides have also been quantitatively evaluated using spectrophotometric measurements of a competing ligand (Rousselot-Pailley et al., 2006; Miras et al., 2008; Pujol et al., 2010; Pujol et al., 2011; Xiao et al., 2011).

Direct measurement of free metal ion concentration using a competing ligand can mitigate problems associated with electrochemical techniques for stability constant determination. Colorimetric ion indicators such as bathocuproine or bathocuproine disulfonate (BCS) have been successfully employed in measurements of high concentrations of strong, multiple-thiol containing compounds (Pujol et al., 2010; Pujol et al., 2011). However, BCS was found to be insufficient to characterize GSH complexation of Cu(I) (Xiao et al., 2011). Fluorescent ion indicators provide a higher degree of sensitivity and analytical ranges lower than those typically achieved using colorimetric indicators. The iminodiacetic-based FluorZin-1 (Molecular Probes) exhibits increased fluorescence upon complexation of $Zn^{2+}$and Cd^{2+} and has been used to characterize GSH-Cd complexes in previous studies (Leverrier et al., 2007; Ogawa and Yoshimura, 2010). The BAPTA-based fluorescent probe BTC (Molecular Probes) was designed for the measurement of Ca^{2+} but also can be used to measure other divalent cations such as Zn^{2+}, Cd^{2+} and Hg^{2+} (Hyrc et al., 2000). The copper-specific high-affinity fluorescent probe Phen Green SK (PGSK, Molecular Probes), a derivative of 1,10-phenanthroline, has been shown

to be a superior indicator for the monovalent copper ion, which quenches the probe's fluorescence upon binding (Kim and Ahner, 2006).

In this paper we report on the use of competing ligand fluorometric titrations for the analysis of thiol-metal complex equilibrium as an alternative to potentiometric or voltammetric methods with the aim of evaluating Cu(I) complexes. We expand upon previous studies that measure conditional stability constants at a single pH, by performing titrations at pH 7.2, 8.1 and 9.0, to determine general cumulative stability constants as well. These probes also allow for the use of 96-well plates as a titration platform, significantly enhancing throughput and reducing reagent usage. Cadmium and zinc complexes of GSH and Cys are first evaluated to demonstrate effectiveness of the method and equilibrium model. PGSK is then used to determine the stability constants for Cu(I) complexes of GSH and Cys and the dipeptides, Arg-Cys and Gln-Cys. The implications of this data on biological and marine chemistry are also discussed.

3. Materials & Methods

3.1. Stock solutions

Numerous steps were taken to minimize trace metal contamination. All laboratory vessels were acid washed overnight in 1M HCl and subsequently rinsed with 18.2MΩ·cm Milli-Q water (Millipore). Milli-Q water was used to prepare stocks and dilutions. Trace metal-free grade pipette tips were used throughout experiments. Buffer solutions of MOPS, TRIS and borate were made at a concentration of 10 mM at pH 7.2, 8.1 and 9.0, respectively and passed through a Chelex-100 (Bio-Rad) ion exchange resin to remove trace metal impurities. The Chelex resin was pretreated using a method described elsewhere to remove contaminating ligands (Price et al., 1989). The synthetic ocean water (SOW) Aquil (Price et al., 1989) was also used in some

titrations. Both SOW and stock solutions of NaCl were also treated with Chelex. No EDTA-trace metal or vitamin amendments, typically a part of this recipe, were made to the SOW. The fluorescent probes, BTC, FluoZin-1 (FZ1), and PhenGreenSK (PGSK, Molecular Probes) were prepared according to manufacturer's instructions, and divided into aliquots that were kept frozen at -80°C until use.

Stock solutions of Zn(II) and Cd(II) were made from the salts $ZnSO_4$, $CdCl_2$ respectively (Sigma). Cu(I) stock solutions were made fresh daily by gaseous reduction (Attari and Jaselskis, 1972). A 10 mM stock solution of Cu(II)O was prepared in 1 mM HCl. Prior to each titration an aliquot of the copper stock was diluted in 0.5 M NaCl and reduced to Cu(I) by bubbling the dilution with $SO_{2(g)}$ for 15 minutes. The solution was sparged with $N_{2(g)}$ for at least 45 minutes to remove excess $SO_{2(g)}$. Chelexed hydroxylamine hydrochloride (Sigma) was added to a concentration of 1.0 mM in the reduced copper stock to maintain a reducing environment. The solution was slowly titrated to a pH of 6.5-7.0 using 0.1 M Ultrapure NaOH (Fluka). Cu(I) concentration and reduction completeness was confirmed via spectrophotometric measurements of a standard dilution of the reduced stock solution in the presence of 1 mM bathocouprine disulfonate (BCS, MP Chemicals, ε=12,700 M^{-1} cm^{-1} at λ_{max} = 483 nm). Cu(I) stock was used within four hours. BCS measurements confirmed that oxidation of the Cu(I) stock was not significant over this time period.

Solutions of cysteine (Baker) and reduced GSH (Sigma-Aldrich) were made fresh daily in nitrogen sparged MOPS, TRIS or borate buffer and titrated with ultra-pure NaOH to maintain desired pH. Arg-Cys and Gln-Cys were synthesized by Anaspec (Fremont CA, USA) at 99% purity. Once dissolved, aliquots were kept frozen at -80°C until use. To reverse potential thiol-oxidation in our long term dipeptide stocks, daily solutions of 1 mM Arg-Cys and Gln-Cys were

prepared with 1mM $NaBH_4$. This was done at least an hour prior to the titrations to allow for hydrolysis of borohydride. Concentrations of reduced thiol stocks were confirmed using Ellman's reagent (Sigma) and subsequent measurement of absorbance at 412 nm (ε = 13,600 M^{-1} cm^{-1}).

3.2. pKa determination of novel thiols

Acid dissociation constants for Arg-Cys and Gln-Cys were determined by titrating a 0.40 mM solution containing each thiol with ultrapure 100 mM sodium hydroxide standardized using potassium hydrogen phthalate. Solution pH measurements were made using a Beckman 511275-AB probe and a Corning 320 meter calibrated using a two point curve of pH 7.0 and 10.0 with standard solutions (VWR). Acid dissociation constants were calculated using the curve fitting software CurTiPot (Gutz, 2007).

3.3. Titrations

Titrations were performed at 25°C in a Class II laminar flow hood. Acid washed flat bottom 96-well plates (Costar Black Opaque) were used for measurements. Plates were stored in a -4°C freezer prior to use. Constant well volumes (200 or 250 µL) were achieved by adding variable amounts of buffer solution prior to the addition of the reagents to balance the changing additions of metal or ligand. In all titrations the ligand was added before the metal to prevent formation of insoluble metal species. Varying concentrations of ligand and metal were added to wells at a predetermined range of concentrations to perform both direct (constant ligand) and indirect (constant metal) titrations. The fluorescent ion probe, diluted in buffer, was added last, except in titrations of Cu(I). Final probe concentrations for the various titrations are listed in Table 1. All

Table 1. Analytical conditions and probe calibration constants (K'_P) used in this study.

Probe	Ion	$[Probe]_T$	$\log K'_P$ pH 7.2 (10 mM MOPS)	$\log K'_P$ pH 8.1 (10mM TRIS)	$\log K'_P$ pH 8.1 (SOW)	$\log K'_P$ pH 9.0 (10mM Borate)	Excitation (nm)	Emission (nm)
BTC	Cd^{2+}	400 nM	10.1 ± 0.2	10.2 ± 0.1	N/A	10.3 ± 0.0	424	524
	Zn^{2+}	400 nM	7.3 ± 0.1	7.5 ± 0.3	N/A	8.3 ± 0.1	424	524
FZ1	Cd^{2+}	400 nM	5.6 ± 0.1	5.5 ± 0.1	N/A	5.2 ± 0.1	495	525
	Zn^{2+}	400 nM	5.4 ± 0.1	5.6 ± 0.2	N/A	6.2 ± 0.1	495	525
PGSK	Cu^{+}	200 nM	11.8 ± 0.1	12.2 ± 0.1	12.0 ± 0.1	12.4± 0.1	490	520

titration points were made in triplicate. Titrations involving Cu(I) were performed in the presence of 1 µM EDTA to prevent any cupric ion interference with the probe.

Fluorescence measurements were made immediately after mixing (<15 min) using a Synergy4 Microplate Reader (BioTek) Spectrophotometer and a Xenon flash lamp light source. Excitation and emission wavelengths for each metal-ligand system are listed in Table 1. The same instrument was used for absorbance measurements of Cu(I)-BCS and thiols. For Cu(I) titrations the plate reader's liquid dispenser was used to minimize time between metal addition and fluorescence measurement to minimize oxidation and loss of Cu(I). Dispenser lines were flushed with 1M HCl and Milli-Q water prior to use. Following titrations, pH measurements of a sampling of wells were measured to ensure that buffer pH was retained.

4. Equilibrium Modeling

4.1. General stability constants

Calculation of general stability constants was based upon the following general metal ligand complex equilibria:

$$mM + lL^{-} + hH^{+} \rightleftarrows M_m L_l H_h \qquad 2$$

$$\beta_{mhl} = \frac{[M_m L_l H_h]}{[M^{+}]^m [L^{-}]^l [H^{+}]^h} \qquad 3$$

Where *m*, *l* and *h* are stoichiometric coefficients for the free metal concentration [M^{+}], the unprotonated-free ligand concentration [L^{-}], and the proton concentration [H^{+}], respectively. β_{mhl} is the general cumulative stability constant for a given (*mhl*) species.

Preliminary speciation calculations using some previously measured stability constants predicted that polynuclear species ($m > 1$), hydroxyl species ($h < 0$), and complexes with more

than two coordinating ligands ($l > 2$) would be negligible at the concentrations and pH levels used this study. Also, in the pH range of this study, only the terminal amine group would be likely to undergo a significant degree of protonation. These constraints allowed for the determination of stability constants of at most five species (ML, MLH, ML_2, ML_2H, ML_2H_2).

Proton concentration used in calculations was determined from measured pH. Free metal concentrations were measured using the fluorometric probe method described below. The concentration of all metal-ligand species was found by a mass balance of the metal:

$$M_T = [M^+] + [M]_{inorg} + \sum \beta_{mhl}[M^+][L^-]^l[H^+]^h \quad 4$$

$[M]_{inorg}$ was calculated using the free metal concentration and the inorganic species formation constants listed in Table 2. Using the total complex concentration, the free unbound ligand concentration $[L_f]$ is calculated using the mass balance of the ligand:

$$L_T = [L_f] + \sum l_i\beta_{mhl}[M^+][L^-]^l[H^+]^h \quad 5$$

The stoichiometric coefficient, l, was assumed to be 1 unless the titration showed a completely saturated fluorescence at an endpoint of M:L = 1:2 in which case it was assumed to be 2. $[L^-]$ could then be calculated from $[L_f]$ using the pKa values of the individual ligands (Table 3).

4.2. Conditional stability constants

Constants conditional to the ligand concentration (K_l') for mono (l=1) and bis (l=2) complexes can be derived for a particular pH from the general stability constants using the following relationship:

Table 2. Inorganic species and formation constants used in study. All values were obtained from the NIST Database (Smith et al., 2003)

M	L_i (Cl^-)	H (H^+)	Zn(II)	Cd(II)	Cu(I)	Cu(II)
1	0	-1	-9.0	-10.1		-7.5
1	0	-2	-16.9	-20.3		-16.2
1	0	-3	-28.4	-33.3		-26.6
1	0	-4	-41.9	-47.3		-39.7
1	1	0	0.46	1.98	3.1	0.3
1	2	0	0.45	2.6	5.42	-0.3
1	3	0	0.5	2.9	4.75	-2.3
1	4	0	0.2			-4.6

$$[M_m L_i H_h] = \beta_{mlh}[M]^m[L_i]^i[H^+]^h$$

Table 3. Protonation constants for organic ligands used in this study. *protonation of guanidine group was not considered.

Reference	Cys Measured	Cys (Smith et al., 2003)	GSH Measured	GSH (Smith et al., 2003)	Arg-Cys* Measured	Gln-Cys Measured	NTA (Smith et al., 2003)
p*K*a1	No fit	1.71	1.9	2.08	2.0	2.0	10.3
p*K*a2	8.4	8.36	3.5	3.49	7.2	7.5	3.0
p*K*a3	10.4	10.74	8.9	8.64	9.4	9.6	1.7
p*K*a4			9.8	9.51	11.7		1.0
HL	10.4	10.74	9.8	9.51	9.4	9.6	10.3
H_2L	18.8	19.10	18.7	18.15	16.7	17.1	13.3
H_3L	No fit	20.81	22.2	21.64	18.7	19.1	15.0
H_4L			24.1	23.72			16.0

Table 4. NTA formation constants (Smith et al., 2003).

Species	Zn	Cd
ML	10.45	9.76
ML_2	14.88	14.47
MLOH	1.43	-.64

$$K_l' = \frac{[ML_l]_T}{[M^+][L_f]^l} = \frac{\sum_h^1 \beta_{1lh}[M^+][L^-]^l[H^+]^h}{[M^+]\left([L^-]^l + \sum_h \beta_{01h}[L^-]^l[H^+]^h\right)^l} = \frac{\sum_h^1 \beta_{1lh}[H^+]^h}{(1 + \sum_h \beta_{01h}[H^+]^h)^l} \quad 6$$

Where $[ML_l]_T$ is the sum of the concentrations of all protonation states of the mono or bis complex. The conditional stability constant is thus a function of pH, the general complex stability constants, and the ligand's protonation constants (β_{01h}). The protonation constants used in this study can be found in Table 3.

An overall concentration and pH-specific conditional stability constant (K'') for total complexed metal, can be determined using the equation:

$$K'' = \frac{[ML]_T + [ML_2]_T}{[M^+]\left[L_f\right]} = K_1' + K_2' \left[L_f\right] \quad 7$$

As $\left[L_f\right]$ becomes small, K''approaches K_1'. Such constants have been determined in previous studies using log-log linearization, however non-linear fitting has been shown to give more optimal fits (Gerringa et al., 1995), and therefore preferable when fitting multiple species.

4.3. Fluorescent indicator calibration

Determination of $[M^+]$ was made by measuring the relative absolute fluorescence over the course of the titration (Hyrc et al., 2000). The ratio of relative fluorescence is proportional to the ratio of metal-bound probe to unbound probe and subsequently the free metal concentration by the use of a conditional constant for the probe-metal complex, K_P':

$$\left(\frac{F - F_{min}}{F_{max} - F}\right)\frac{1}{K_P'} = \frac{[MP]}{\left[P_f\right]K_P'} = [M^+] \quad 8$$

Where F_{min} and F_{max} are the metal-free and metal-saturated fluorescence measurements respectively. F is the fluorescence measured at each point in the titration. With PGSK, the

fluorescence is quenched upon metal binding. In this case the ratio containing the fluorescence measurements must be inverted in Equation 8.

The calibration constants were determined by titrating the probe with metal and measuring the change in fluorescence. For the moderate affinity probe, BTC, NTA was used as a buffering ligand to fix the free metal concentration in the analytical range of the probe. Cd^{2+} and Zn^{2+} ion concentrations were calculated using the formation constants of NTA (Table 4). For the high affinity indicator PGSK, 0.5 M Cl^- was used to buffer the free Cu^+ concentration. Specific values for K_P' were determined for each probe-metal-buffer system by a non-linear fit of fluorescence data to a calculated free metal concentration (Table 1).

4.4. Non-linear determination of stability constants

Equilibrium models were constructed in Microsoft Excel. Equation 4 was used to construct a model of the free metal concentration to fit general stability constants (β_{mlh}) with titrations performed at multiple pH values:

$$[\mathrm{M}^+] = \frac{M_T}{\sum \beta_{mlh}[L^-]^l[H^+]^h + \alpha_{inorg} + K_P'[P_f]} \quad 9$$

Where α_{inorg} represents the inorganic speciation calculated using constants in Table 3. A similar model was constructed to fit the conditional stability constants at each pH:

$$[\mathrm{M}^+] = \frac{M_T}{K_1'[L_f] + K_2'[L_f]^2 + K_P'[P_f]} \quad 10$$

From these calculated free metal concentrations, a model fluorescence value (F_M) could be calculated for each titration point using equation 8. The Solver add-in for Microsoft Excel was used to minimize least squares difference of experimental fluorescence data (F) and modeled

fluorescence (F_M):

$$U = \sum (\log F - \log F_M)^2 \quad 11$$

Conditional stability constants were determined by a non-linear least squares fitting of a direct and an indirect titration at a specific pH. General cumulative stability constants were obtained using a set of six separate titrations, one direct and one indirect in each buffer system. Error analysis was performed using the SolverAid macro (De Levie, 2001). Equilibrium models were verified with VisualMINTEQ (Gustafsson, 2010) and speciation data generated using HySS (Alderighi et al., 1999).

4.5. Kinetic Experiments

Fluorescence readings of Cu(I) titrations in SOW were taken 0, 15, 30, 45, 60, 90, 120 and 150 minutes after the addition of Cu(I). Probe saturation was assumed to indicate the loss of Cu(I) equal to probe concentration (200 nM). Concentration-specific decay rates were determined by the time it took for each titration point to reach saturation. Loss of Cu(I) was modeled using the following equation:

$$\frac{d[Cu(I)]}{dt} = -k[Cu(I)][O_2] \quad 12$$

During these readings the plates remained open to the atmosphere. Oxygen concentration was measured in the stock SOW and used as an estimate of oxygen levels in the titration mixtures. Measurements were made using an Oakton DO 110 oxygen meter, calibrated to 100% saturation in air. The detection limit for the electrode was 1 µM O_2. Values for k (L mol^{-1} min^{-1}) were subsequently calculated for each Cu(I)-ligand system using equation 12.

5. Results

5.1. Measurement of protonation constants for novel dipeptide ligands.

We first determined protonation constants for the ligands used in this study by titrating well-mixed solutions of Arg-Cys, Gln-Cys, cysteine and GSH with 10 mM NaOH. Acid dissociation constants were then obtained from the resulting pH curves (Figure 2, Figure 3) using the Excel-based least squares minimization algorithm CuTiPot (Gutz, 2007). Fits of the thiol titrations resulted in the pK_a values shown in Table 3. The α-amino pK_a values for the four compounds were very close to their recommended values for the molecule (Cys, GSH) or the corresponding amino acid (Arg, Gln) as were the thiol protonation constants for Cys and GSH. However, for Gln-Cys and Arg-Cys, these constants were significantly lower than that of cysteine with pK_a values of 7.5 and 7.2, respectively being fit to the titration. A previous measurement of a thiol group pK_a of 7.25 in the phenylalanine-cysteine dipeptide (Cherifi et al., 1990) indicates such low values are possible. The p*K*a of the guanidine group of Arg-Cys was measured to be 11.7, which falls within the range of values reported for arginine. For the subsequent determination of stability constants, we used the NIST recommended protonation values for cysteine and GSH (Smith et al., 2003) and our newly measured values for Arg-Cys and Gln-Cys.

5.2. Probe calibration

Proper selection and calibration of fluorescent ion indicators is essential for the accurate quantification of the free metal ion concentration and the subsequent modeling of metal speciation. Each probe is responsive to a specific and limited concentration range of the uncomplexed metal ion. This range is defined by the equilibrium relationship between the metal

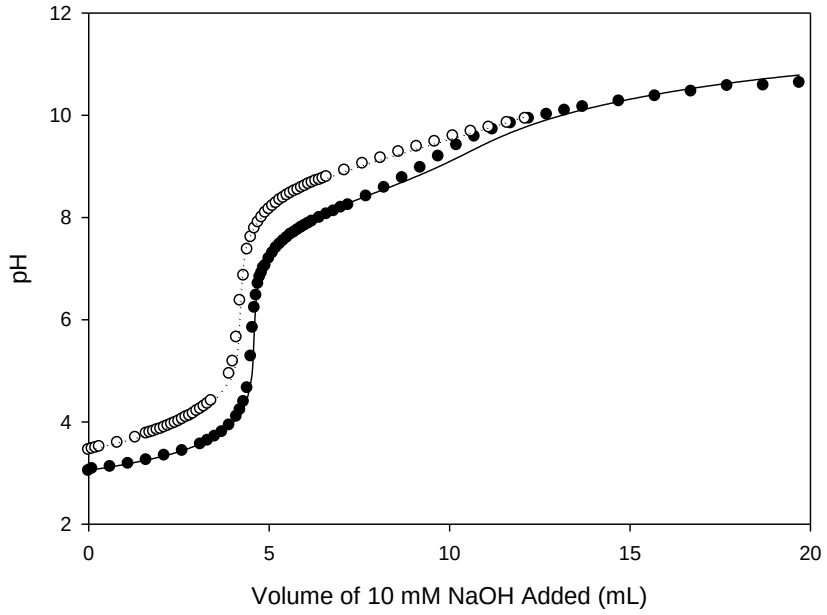

Figure 2. pH titration of 1 mM cysteine (closed circles, solid line) and 1 mM glutathione (open circles, dotted line) with 10 mM NaOH. Circles indicate individual pH measurements and lines are the optimized fits of pKa values.

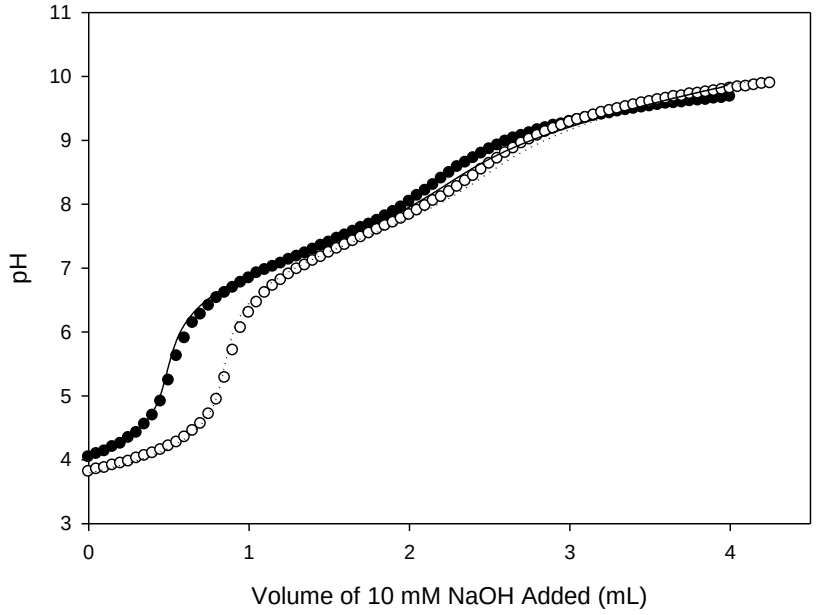

Figure 3. pH titration of 0.4 mM Arg-Cys (closed circles, solid line) and 0.4 mM Gln-Cys (open circles, dotted line) with 10 mM NaOH. Circles indicate individual pH measurements and lines are the optimized fits of pK_a values.

and the probe, K_P'. The optimal concentration range of free metal that can be measured by the probe is typically within one order of magnitude of the inverse of K_P'. The probes used in this study were calibrated directly to a fixed free metal concentration. The resulting constants (Table 1) are conditional with respect to pH, ionic strength and buffer. The fluorescent ion indicators FZ1 and BTC (Molecular Probes) were selected to measure Cd^{2+} and Zn^{2+}. Both indicators exhibit increasing fluorescence upon the addition of metal ion. FZ1 showed low affinity response to micromolar concentrations of Cd^{2+} and Zn^{2+} (Table 1) and therefore did not require the use of a ligand to buffer metal ions for calibration.

Similarities and differences between our values and those of previous calibrations were observed. At pH 7.2, the measured FZ1- Zn(II) constant ($\log K_p$=5.4) was slightly higher than the value reported by Gee at pH 7.0 ($\log K_p$=5.1) (Gee et al., 2002). Measurements of FZ1-Cd(II) complexes yielded calibration constants approximately an order of magnitude higher than the previously reported values (Ogawa and Yoshimura, 2010; Leverrier et al., 2007). This discrepancy is likely a result of buffer selection and our inclusion of inorganic species in calculations. Over the pH range examined here, we would expect a protonation change of the nitrogen in the coordinating iminodiacetic group in FZ1 and therefore an increasing affinity with increasing pH. While this was observed for the FZ1-Zn(II) complex, it was not observed for the FZ1-Cd(II) complex which interestingly showed a slight decreasing affinity with increasing pH. This may have been the result of matrix effects.

BTC contains two sets of iminodiacetic groups which increases its affinity towards divalent cations. For calibration of this probe with Cd(II) and Zn(II), NTA was used as a buffering ligand. Affinity for Zn(II) was consistent with a previously measured value of $\log K_p$ = 7.2 (Hyrc et al., 2000) at pH 7.2 and our values showed an order of magnitude increase over our

pH range. Affinity for Cd(II) was much higher ($\log K_p > 10$) and showed only a modest increase over the pH range.

For measurement of Cu(I), calibrations of the high affinity 1,10-phenanthroline-based indicator PGSK, were performed in the presence of 0.5M NaCl. The Cl^- ions served as a buffer for Cu^+ while stabilizing the cuprous redox state. Under these conditions the calculated free copper concentration ranged from approximately 10^{-13} to 10^{-11}. Fits to the titration data in the presence of PGSK, resulted in log-calibration constants of 11.8, 12.2, and 12.4 for Cu^+ in solutions buffered at pH 7.2, 8.1 and 9.0 respectively. A previous calibration of PGSK at pH 7.2 resulted in a constant of 11.38 in the presence of HEPES (Kim and Ahner, 2006). HEPES has been shown to be reactive with copper (Hegetschweiler and Saltman, 1986) which may explain the slight difference between values.

5.3. Stability constant determination

5.3.1. Glutathione with Cd(II) and Zn(II)

To test the efficacy and limitations of stability constant determination using fluorescent indicators, we first applied this method to a well-studied thiol-metal complex. Cd(II)-GSH complexation has been thoroughly investigated using various techniques (Perrin and Watt, 1971; Fuhr and Rabenstein, 1973; Kadima and Rabenstein, 1990; Leverrier et al., 2007; Chekmeneva et al., 2008; Mah and Jalilehvand, 2010; Ogawa and Yoshimura, 2010). Our results (Table 5, Table 6) agree well with these and other studies (Table 7). Established stability constants for Cd-GSH were used to predict metal speciation at each pH in order select an appropriate indicator and optimize concentrations of metal and ligand. At neutral pH, FZ1 was used for Cd^{2+} quantification and at higher pH BTC was used.

Table 5. Measured conditional stability constants of metal-thiol complexes. N.C. indicates no convergence. SOW Indicates measurement was performed in synthetic ocean water.

		$\log K_1$'			$\log K_2$'		
Metal	**Thiol**	**7.2**	**8.1**	**9.0**	**7.2**	**8.1**	**9.0**
Cd^{2+}	Cys	6.1 ± 0.2	7.7 ± 0.1	9.7 ± 0.1	9.7 ± 1.2	10.2 ± 0.4	12.9 ± 1.6
	GSH	4.9 ± 0	6.9 ± 0.2	8 ± 0.1	7.2 ± 0.2	9.6 ± 0.1	11.6 ± 0.1
	Arg-Cys	4.2 ± 0.3	4.9 ± 0.1		*N.C.*		
Zn^{2+}	Cys	5.0 ± 0.1	6.7 ± 0.1	8.1 ± 1.8	8.4 ± 0.3	10.9 ± 0.2	15 ± 0.2
	GSH	4.2 ± 0.1	6.3 ± 0.1	6.7 ± 0.2	5.7 ± 3.8	9.6 ± 0.3	11.4 ± 0.3
	Gln-Cys	4.6 ± 0.6	6.0 ± 0.1		*N.C.*		
Cu^{+}	Cys	11.1 ± 0.4	11.4 ± 0.5 11.2 ± 0.3 (SOW)	11.3 ± 0.2	15.3 ± 0.4	15.8 ± 0.3	15.6 ± 0.2
	GSH	11.6 ± 0.1	11.9 ± 0.1 11.9 ± 0.1 (SOW)	12.6 ± 0.1	*N.C.*	15.3 ± 0.8	16 ± 0.9
	Arg-Cys	11 ± 0.2	12.1 ± 0.6 12.0 ± 0.1 (SOW)	12.2 ± 0.3	15.8 ± 0.2	16.2 ± 0.6	17.2 ± 0.2
	Gln-Cys	11.4 ± 0.1	12.0 ± 0.2 12.0 ± 0.1 (SOW)	12.7 ± 0.1	15.9 ± 0.1	16.9 ± 0.1	16.8 ± 0.5

Table 6. General stability constants determined by non-linear least squares fitting of metal-thiol titration data. *Indicates that value was solved for by a second iterative fit to the measured conditional constants.

Ligand	**Cys**			**GSH**			**Arg-Cys**	**Gln-Cys**
Metal	*Cd(II)*	*Zn(II)*	*Cu(I)*	*Cd(II)*	*Zn(II)*	*Cu(I)*	*Cu(I)*	*Cu(I)*
ML	10.9 ± 0.2	9.4 ± 0.6		8.3 ± 0.2	7.6 ± 0.1		12.9 ± 0.2	13.0 ± 0.2
MHL			23.0 ± 1.4	15.9 ± 0	15.1 ± 0.1	22.3 ± 0.6	21.2 ± 0.1	22.0 ± 0.1
ML_2	17.0 ± 0.2	18.6 ± 0.1		12.9 ± 0.1	*12.9 ± 0.3		18.2 ± 0.4	
MHL_2				21.8 ± 0.1	20.9 ± 0.4		*26.9 ± 0.4	*26.6 ± 9.7
MH_2L_2			*38.4 ± 7.4	29.5 ± 0.1	28.9 ± 0.3	*35.5 ± 1.1	34.7 ± 0.7	35.9 ± 0.6

Table 7. Previously reported general stability constants used in the calculation of conditional stability constant models for comparison.

Ligand	**Cys**					**GSH**				
Metal	*Cd(II)*		*Zn(II)*		*Cu(I)*	*Cd(II)*		*Zn(II)*		*Cu(I)*
Ref	*a*	*b*	*c*	*b*	*N/A*	*d*	*e*	*d*	*f*	*g*
ML	10.3	10.1	9.08	9.11		8.59	8.5	7.94	7.9	
MHL		15.45	14.64	13.71		15.19	15.7	14.16	14.2	24.5
ML_2	16.92	16.9	18.08	18.21		13.39	12.4	12.41	12.4	
MHL_2	24.97	24.8	24.4	24.51		22.81	22.1	21.56	21.7	
MH_2L_2	30.93	30.76	30.24	30.31		30.45	30.0	28.60	29.0	38.8

a (Berthon, 1995; Cole et al., 1985)
b NIST
c Average of values reported in (Berthon, 1995)
d (Perrin and Watt, 1971)
e (Leverrier et al., 2007)
f (Ferretti et al., 2007)
g (Osterberg et al., 1979)

Direct titrations involving the addition of Cd(II) to solutions of identical GSH concentrations resulted in increase in fluorescence intensity with Cd(II) concentrations (Figure 4A, C & E), whereas the indirect titrations of constant Cd(II) and increasing GSH concentrations resulted in declining fluorescence (Figure 4B, D & F). At pH 7.0, a clear titrand endpoint was observed at equimolar (1:1) concentrations of GSH and Cd in the direct titration (Figure 4a). In this titration a white precipitate was also observed in wells beyond the endpoint. This did not occur in any other titration and is likely the same precipitate of a solid Cd-GSH complex observed by Mah and Jalilehvand et al. (2010). At higher pH, the indicator is saturated well before equimolar ratios are reached.

The use of BTC at pH 8.1 to characterize Cd-GSH equilibrium required very low Cd^{2+} ion concentrations. This was accomplished by using 10 mM GSH in the direct titration and 1 µM cadmium in the indirect titration. At these concentrations, species not included in our model were potentially present. However, we were able to obtain reasonable fits for this pair of titrations. No subsequent combination of indicator, metal and ligand required such high ligand to metal ratios.

Mono and bis conditional stability constants were fit to each set of direct and indirect titrations using equations 8 and 10 and are reported in Table 5. The conditional stability constants indicated that affinity for Cd(II) by GSH increased with increasing pH (Figure 8A). The low error associated with the measured constants for both the mono and the bis complexes indicated that each of these species was sufficiently abundant to drive the concentration of Cd^{2+} and the shape of the titration curve.

Five general stability constants (β_{101}, β_{111}, β_{102}, β_{112}, β_{122}) were also fit simultaneously to the indirect and direct titrations at each pH with low errors (Table 6). The resulting values align closely with those of previous studies. Speciation distribution calculations using these results

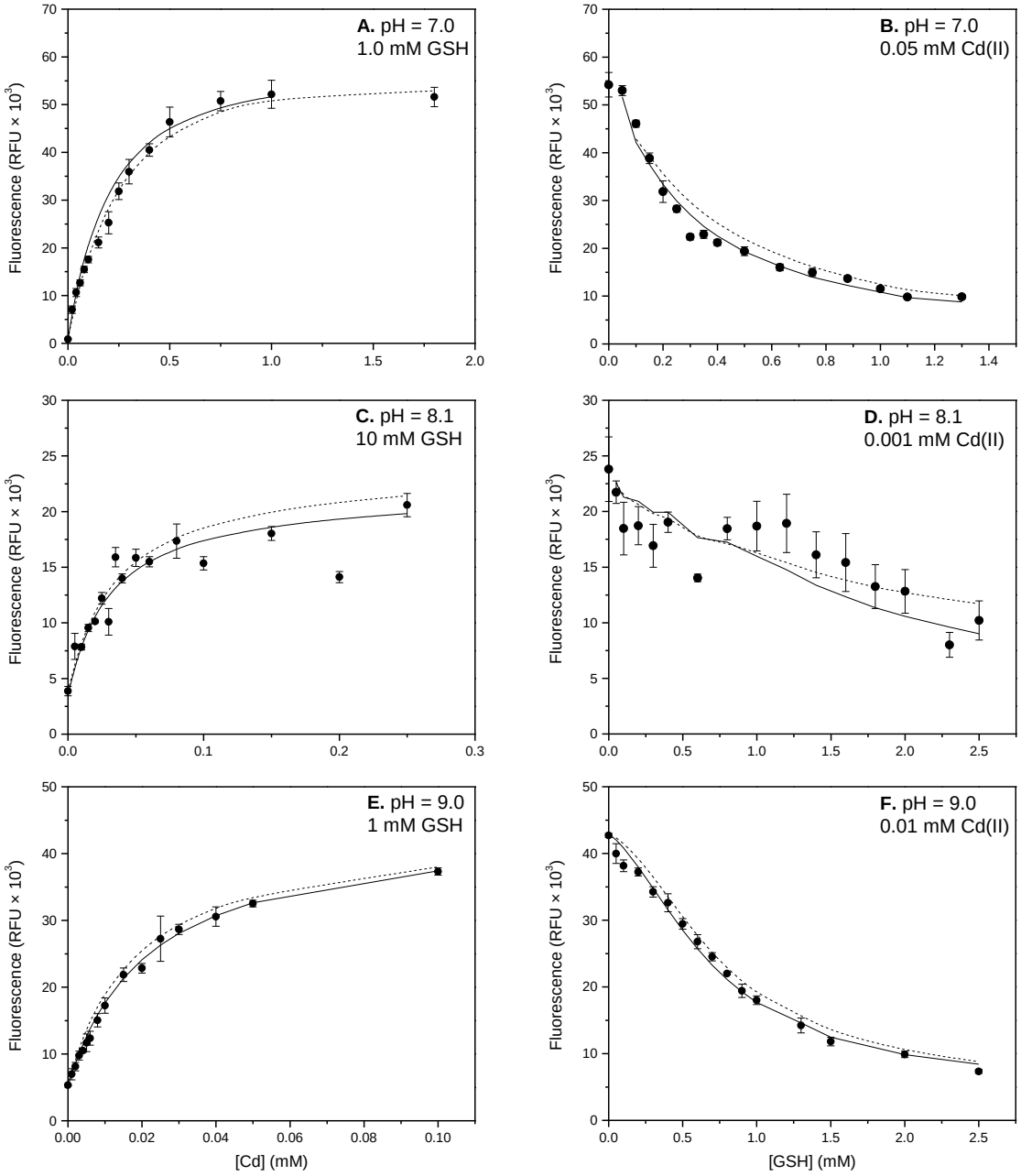

Figure 4. Direct (A,C,E) and indirect (B,D,F) titrations of GSH by Cd(II). Circles represent average of three fluorescence measurements with the standard deviation represented by the error bars. 400nM FluorZin-1 was used as an indicator in titrations A & B. 400nM BTC was employed for titrations C-F. The lines in each titration represent modeled fluorescence using the general (solid) and conditional (dashed) stability constants determined by a nonlinear least squares fit to the measured fluorescence values. These constants can be found in Table 5 (conditional) and Table 6 (general).

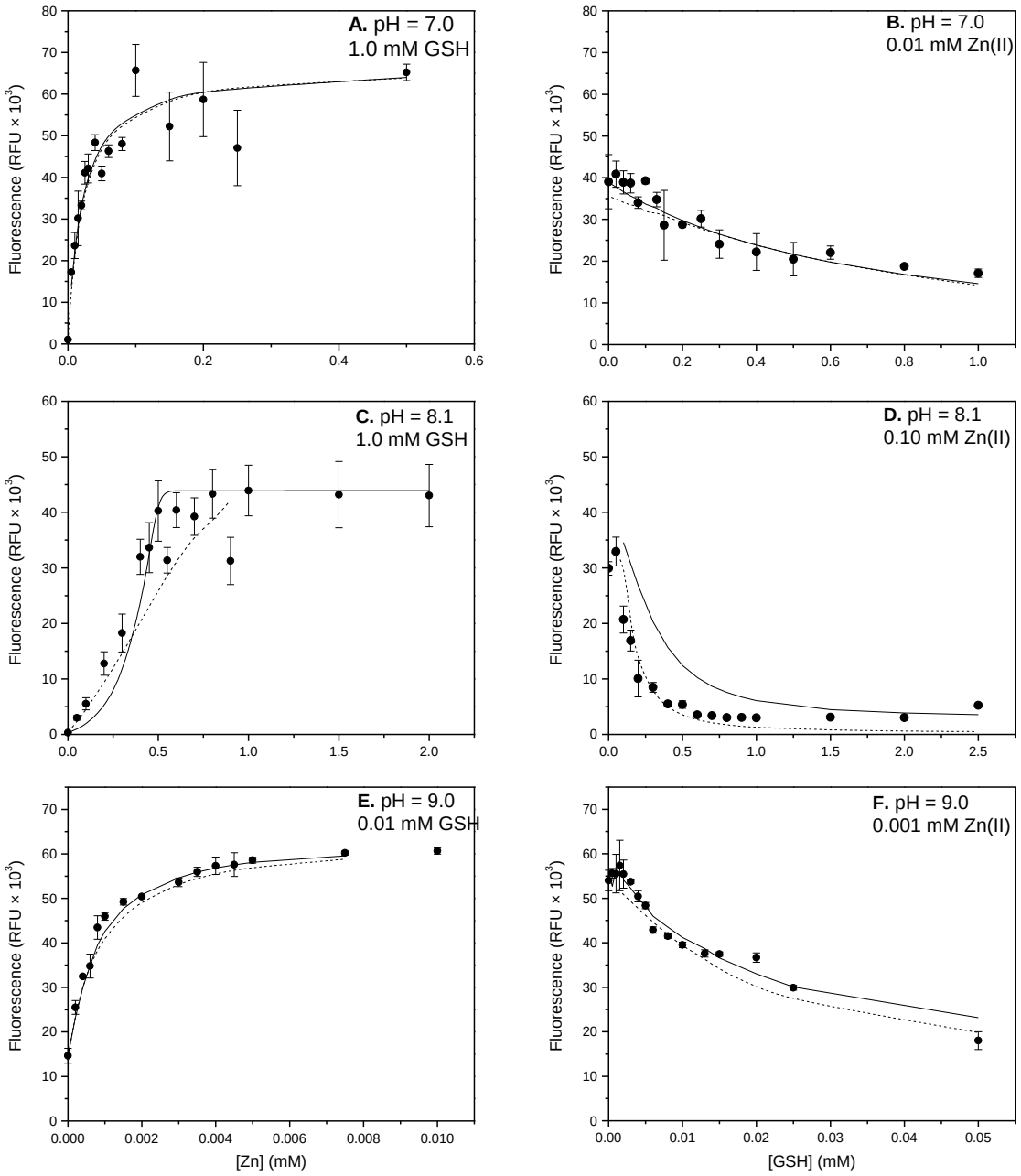

Figure 5. Direct (A,C,E) and indirect (B,D,F) titrations of GSH by Zn(II). Circles represent average of three fluorescence measurements with the standard deviation represented by the error bars. 400nM FluorZin-1 was used as an indicator in titrations A-D. 400nM BTC was employed for titrations E & F. The lines in each titration represent modeled fluorescence using the general (solid) and conditional (dashed) stability constants determined by a nonlinear least squares fit to the measured fluorescence values. These constants can be found in Table 5 (conditional) and Table 6 (general).

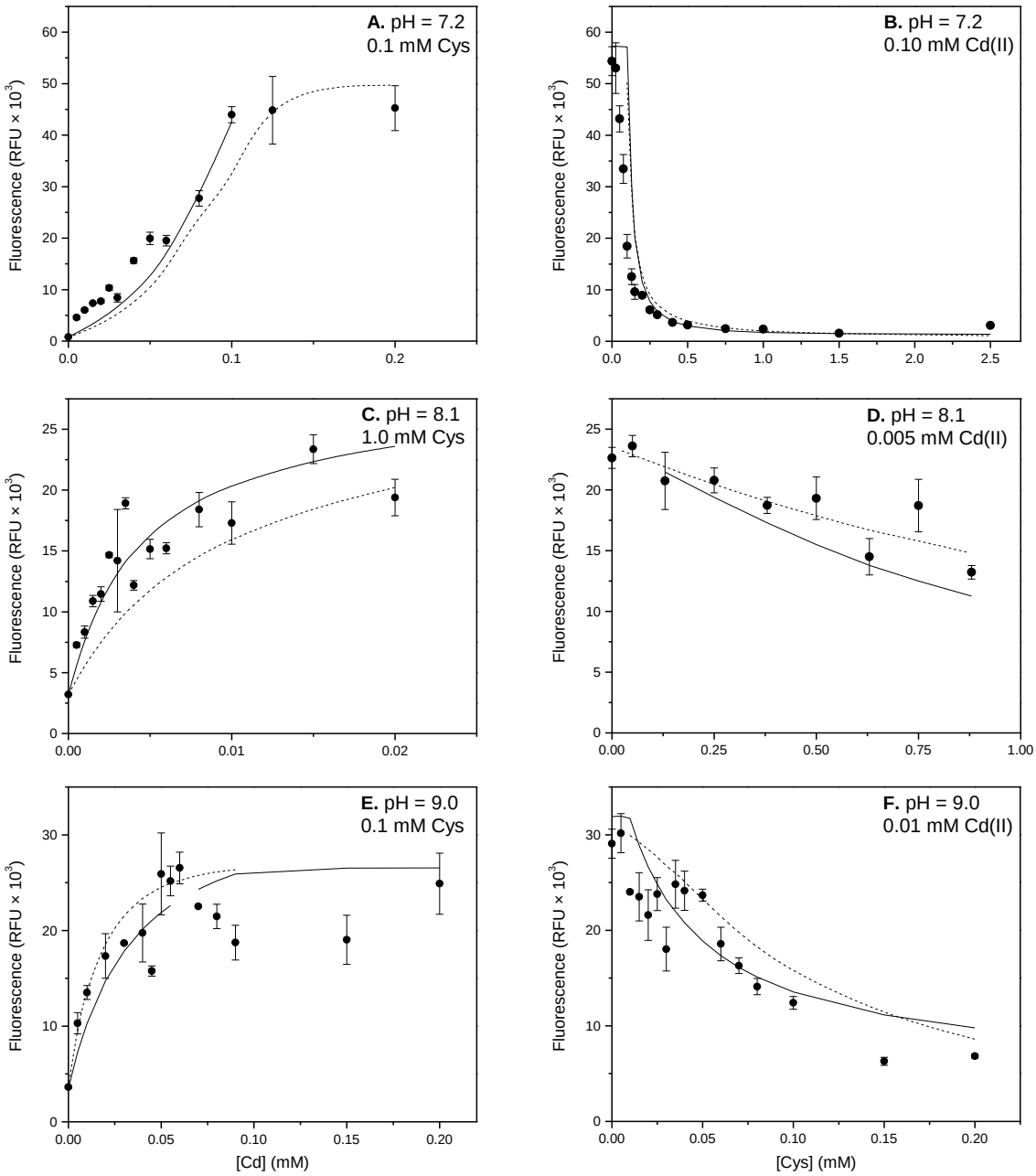

Figure 6. Direct (A,C,E) and indirect (B,D,F) titrations of Cys by Cd(II). Circles represent average of three fluorescence measurements with the standard deviation represented by the error bars. 400nM FluorZin-1 was used as an indicator in titrations A & B. 400nM BTC was employed for titrations C - F. The lines in each titration represent modeled fluorescence using the general (solid) and conditional (dashed) stability constants determined by a nonlinear least squares fit to the measured fluorescence values. These constants can be found in Table 5 (conditional) and Table 6 (general).

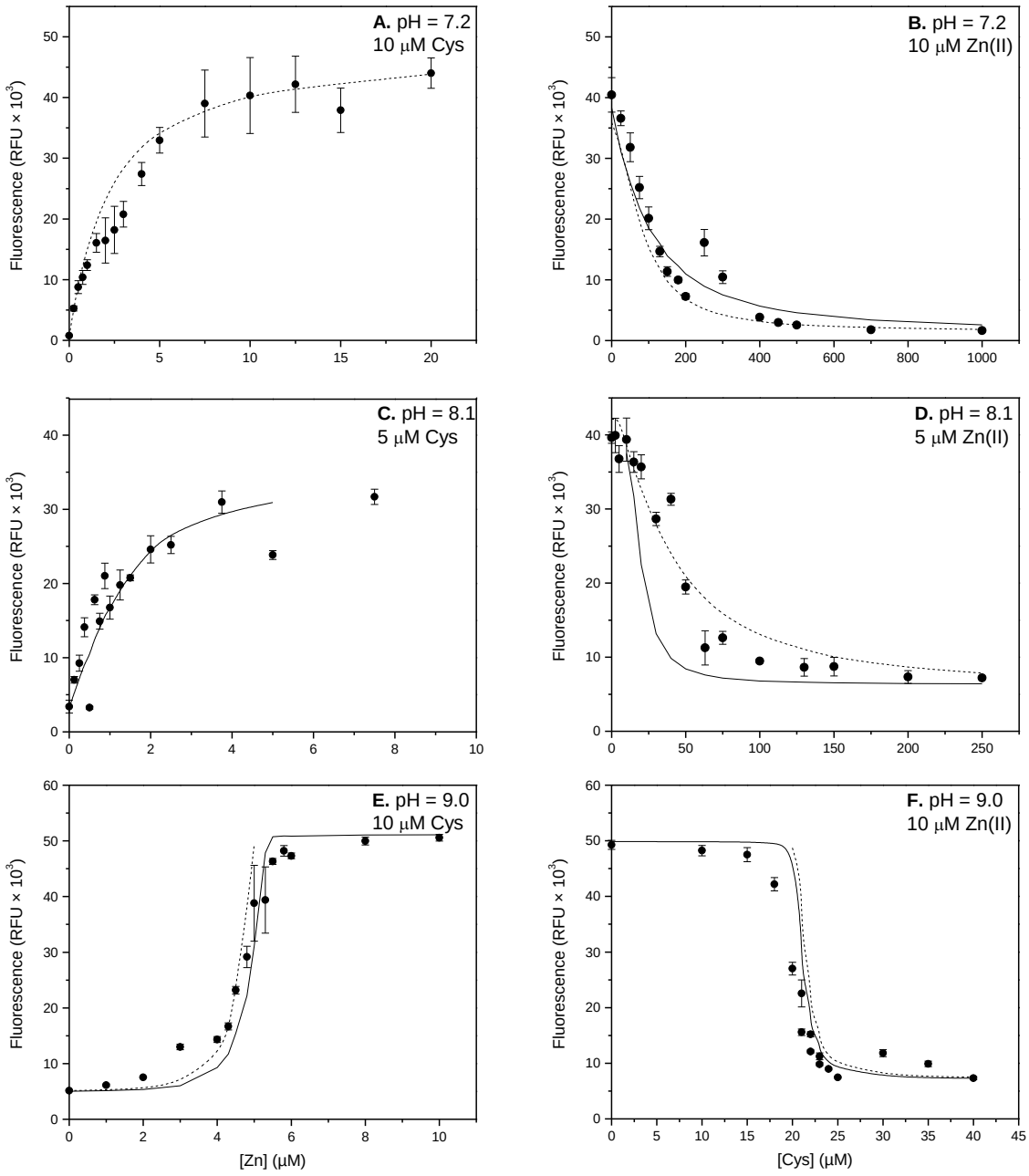

Figure 7. Direct (A,C,E) and indirect (B,D,F) titrations of Cys by Zn(II). Circles represent average of three fluorescence measurements with the standard deviation represented by the error bars. 400nM FluorZin-1 was used as an indicator in titrations A & B. 400nM BTC was employed for titrations C - F. The lines in each titration represent modeled fluorescence using the general (solid) and conditional (dashed) stability constants determined by a nonlinear least squares fit to the measured fluorescence values. These constants can be found in Table 5 (conditional) and Table 6 (general).

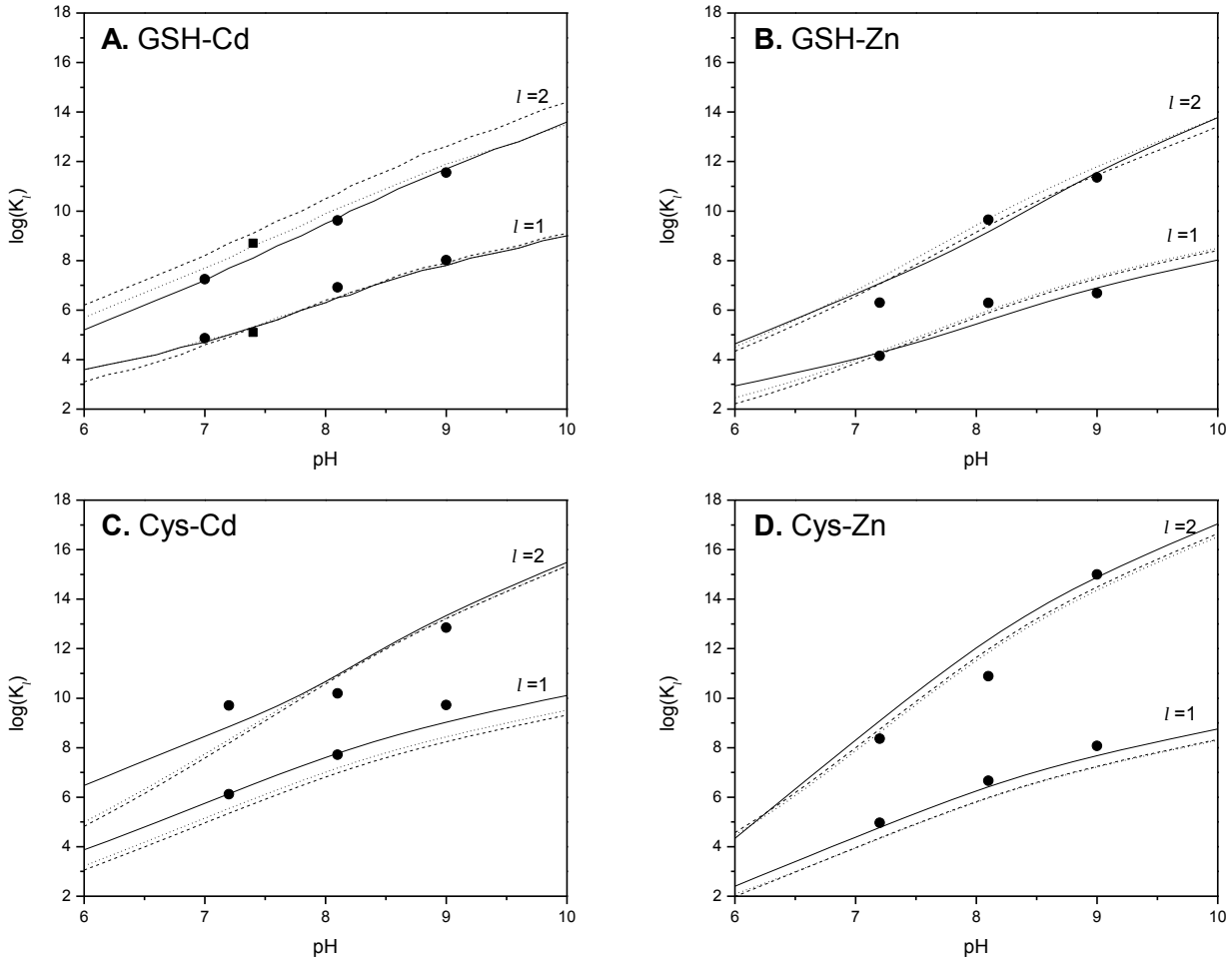

Figure 8. Conditional stability constants plots of Cd^{2+} and Zn^{2+} with GSH and Cysteine. In each panel the bottom series represents mono-complex constants (K_1'), while the top set represents bis-complex constants (K_2'). Circles represent the conditional stability constants for each metal ligand system at the given pH. Squares in panel A are values measured by Ogawa (2010). Lines represent predicted stability constants calculated using Equation 6. In all plots the solid line(-) is of the general stability constants determined in this study. Conditional models represented by dashed (---) and dotted lines (⋯) are respectively calculated using general constants from: A. (Perrin and Watt, 1971) and (Leverrier et al., 2007); B. (Perrin and Watt, 1971) and (Enyedy et al., 2008); C. (Cole et al., 1985) and (Smith et al., 2003); D. Average values of (Berthon, 1995) and (Smith et al., 2003). These values are listed in Table 7.

demonstrate that all five species are present at significant concentrations in at least one of the titrations, with the mono and protonated species favored at lower pH, while unprotonated and bis complexes dominate at higher pH.

Models of predicted conditional stability constants were created using equation 6 using to compare our results with those of previous studies (Figure 8). Our general constants as well as those reported by (Perrin and Watt, 1971) and (Leverrier et al., 2007) were used to predict the conditional constants as a function of pH. The resulting curves aligned well with our pH specific conditional constants. There is also good agreement between our conditional and general stability constants with those reported by Ogawa at pH 7.4.

Direct and indirect titrations were also performed with Zn(II) and GSH (Figure 5). The analytical range of FZ1 and BTC for determination of Zn^{2+} was more suitable for GSH-Zn(II) complexes than for cadmium. The resulting general stability constants for Zn-GSH binding also agree closely with previously published values (Figure 8B). However, in contrast to determining stability constants for all five GSH-Cd(II) species, our initial nonlinear least squares fitting of the GSH-Zn(II) titrations was unable to return a reliable value for the β_{102} constant. The returned value ($\log\beta_{102} = 11.8 \pm 1.6$) was an order of magnitude less than the reported values and did not predict significant concentrations of the unprotonated bis complex. Using the conditional stability constant model (Equation 6), a second nonlinear least squares fit to the individual, pH-specific, conditional stability constants was attempted by adjusting only adjusting β_{102}. This returned a value of 12.9 ± 0.3, close to the value of 12.8 measured by (Ferretti et al., 2007) without substantially changing the overall error, *U* (Equation 11).

5.3.2. Complexes of cysteine with Cd(II) and Zn(II)

Our next series of titrations were used to determine stability constants cysteine complexes of Zn(II) and Cd(II). As there remains some disagreement in studies of these complexes regarding the prevalence of certain protonated species (Berthon, 1995), we initially assumed the presence of all 5 mono and bis species in our speciation model. Titrations of cysteine with Cd and Zn were generally similar to those of GSH exhibiting relatively similar degrees of affinity. However, we observed several more definitive endpoints in these titrations, most notably in the titrations of Zn at pH 9.0 (Figure 7E & f). In these titrations there was a clear rapid change in fluorescence at a 2:1 metal to ligand ratio indicating the dominance of a bis complex. While our fitted value for the mono complex was reasonable, it had a high error associated with it ($logK_1'$ = 8.1 ± 1.9) suggesting a large degree of uncertainty. Conversely, the model remained highly sensitive to the bis constant converging on a value of $logK_2'$ = 15.0 ± 0.2, further demonstrating bis complex dominance at this pH.

When the general stability constants were fit to the respective sets of Zn(II) and Cd(II) cysteine titrations, the model was unable to converge on reasonable values for protonated species ($h > 0$). Subsequent attempts to apply a secondary fit of these constants using the derived conditional constants did not improve these values. This suggested that, at least at neutral to basic pH, the protonated species are not present at a high enough concentration to significantly influence the free metal concentration and therefore the fluorescence curve. However, the values that we did obtain are consistent with those previously reported (Table 6, Table 7). Additionally speciation models using previously reported values also indicate that at neutral-basic pH protonated species of cysteine Cd(II) and Zn(II) complexes are insignificant. While this further supports our methodology, it also demonstrates its limits. These species are dependent on three

variables; limiting one, such as in this case pH, can limit their formation. It may be possible to push the limits of these probes at lower pH, however for the investigation of biological systems, doing so may be irrelevant.

5.3.3. Complexes of Cu(I) with GSH, cysteine, Arg-Cys and Gln-Cys

The central goal of this study was to develop a method for the measurement of stability constants for the redox active metal Cu(I). Titrations were therefore conducted under anaerobic conditions to minimize copper oxidation. Fluorescence was measured immediately after the addition of Cu(I) to the thiol-containing solution. The high affinity copper probe PGSK was a suitable indicator at each pH. Unlike BTC and FZ1, where florescence increases with increasing free metal concentration, the binding of a metal to PGSK quenches its fluorescence resulting in titration curves that exhibit a decrease in fluorescence with increasing free metal ion. In the direct titrations of GSH (Figure 9), Arg-Cys (Figure 11), and Gln-Cys (Figure 12) fluorescence was completely quenched at a 1:1 metal-to-ligand ratio. Titrations of cysteine exhibited full quenching at approximately 1:2, suggesting a weaker complex (Figure 10).

Glutathione formed relatively strong and stable complexes with Cu(I), but consistent with previous work (Osterberg et al., 1979), fewer species were resolved than with Cd(II) and Zn(II) complexes. From the titrations of Cu(I) and GSH (Figure 9) we were able to determine values for mono and bis conditional stability constants complexes at pH 8.1 and 9.0, but only a mono complex was observed at pH 7.2 (Table 5). A fit of the general stability constants resulted in convergence only for one constant ($\log\beta_{111} = 22.3 \pm 0.6$) and the secondary fit using the two bis-conditional constants yielded a reliable value for the fully protonated species ($\log\beta_{122} = 35.5 \pm 1.1$). These results indicate that the bis-complexes and unprotonated species are relatively minor,

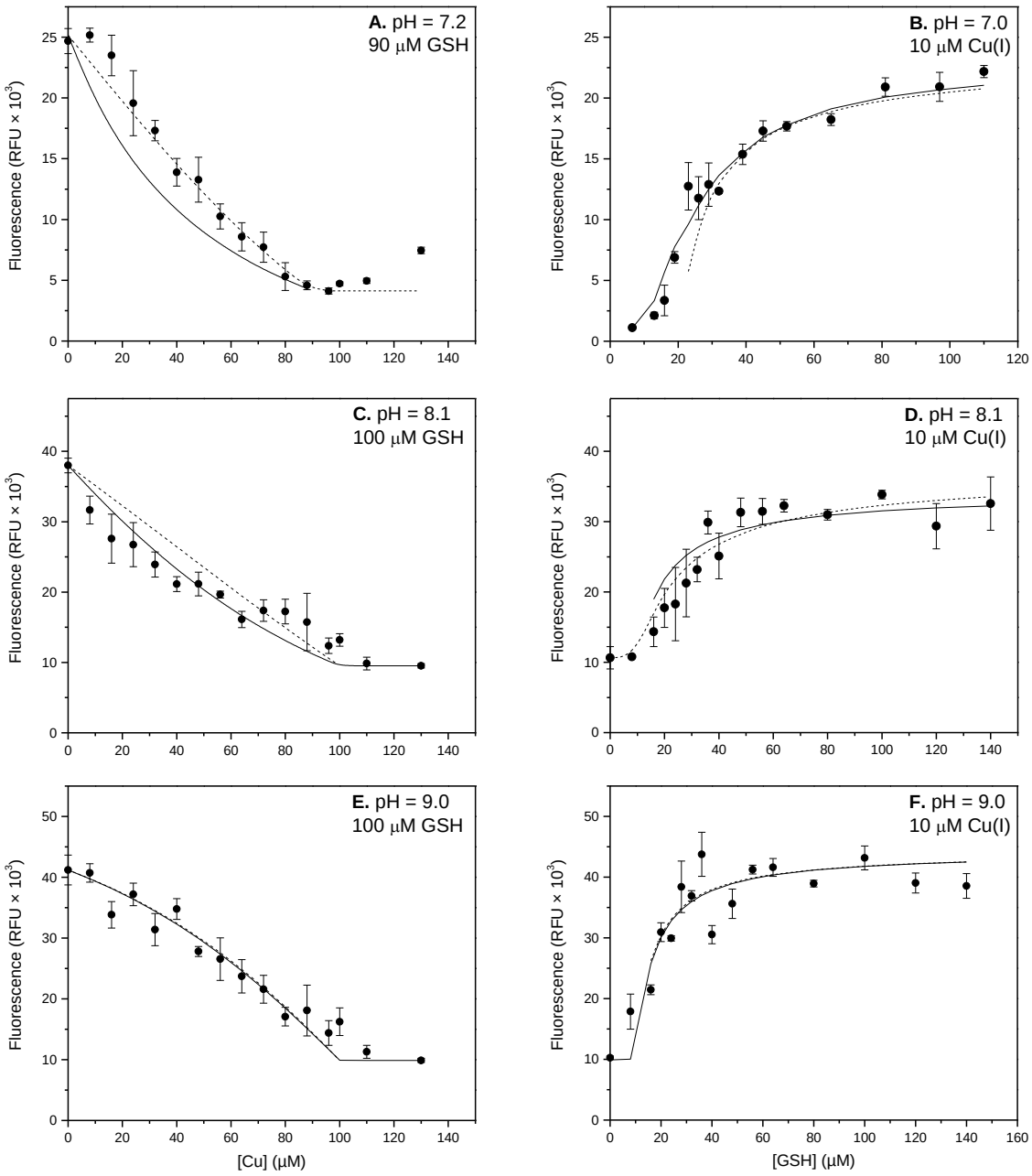

Figure 9. Direct (A,C,E) and indirect (B,D,F) titrations of GSH by Cu(I). Circles represent average of three fluorescence measurements with the standard deviation represented by the error bars. 200nM PGSK was used as an indicator in all titrations. The lines in each titration represent modeled fluorescence using the general (solid) and conditional (dashed) stability constants determined by a nonlinear least squares fit to the measured fluorescence values. These constants can be found in Table 5 (conditional) and Table 6 (general).

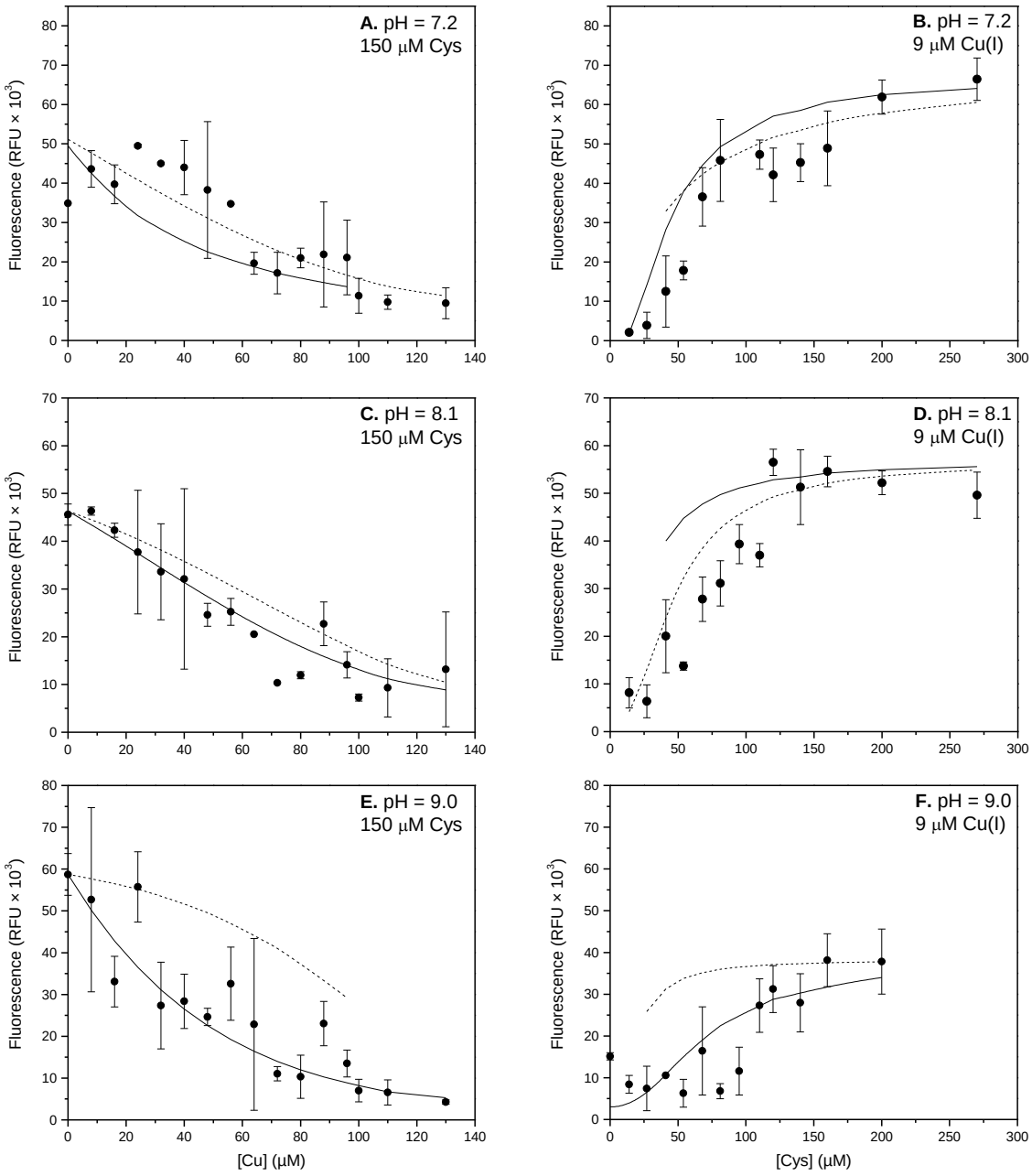

Figure 10. Direct (A,C,E) and indirect (B,D,F) titrations of Cys by Cu(I). Circles represent average of three fluorescence measurements with the standard deviation represented by the error bars. 200nM PGSK was used as an indicator in all titrations. The lines in each titration represent modeled fluorescence using the general (solid) and conditional (dashed) stability constants determined by a nonlinear least squares fit to the measured fluorescence values. These constants can be found in Table 5 (conditional) and Table 6 (general).

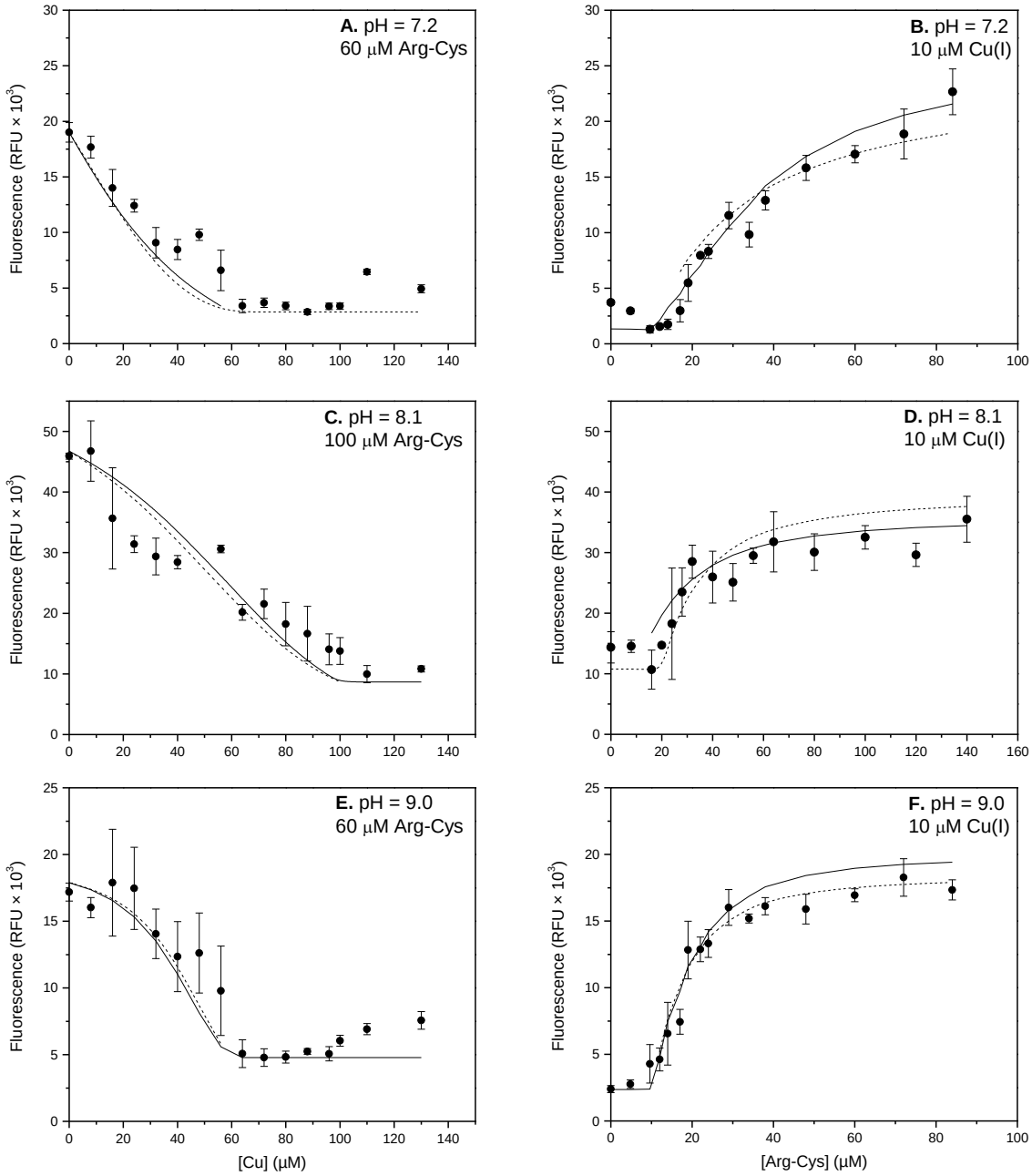

Figure 11. Direct (A,C,E) and indirect (B,D,F) titrations of Arg-Cys by Cu(I). Circles represent average of three fluorescence measurements with the standard deviation represented by the error bars. 200nM PGSK was used as an indicator in all titrations. The lines in each titration represent modeled fluorescence using the general (solid) and conditional (dashed) stability constants determined by a nonlinear least squares fit to the measured fluorescence values. These constants can be found in Table 5 (conditional) and Table 6 (general).

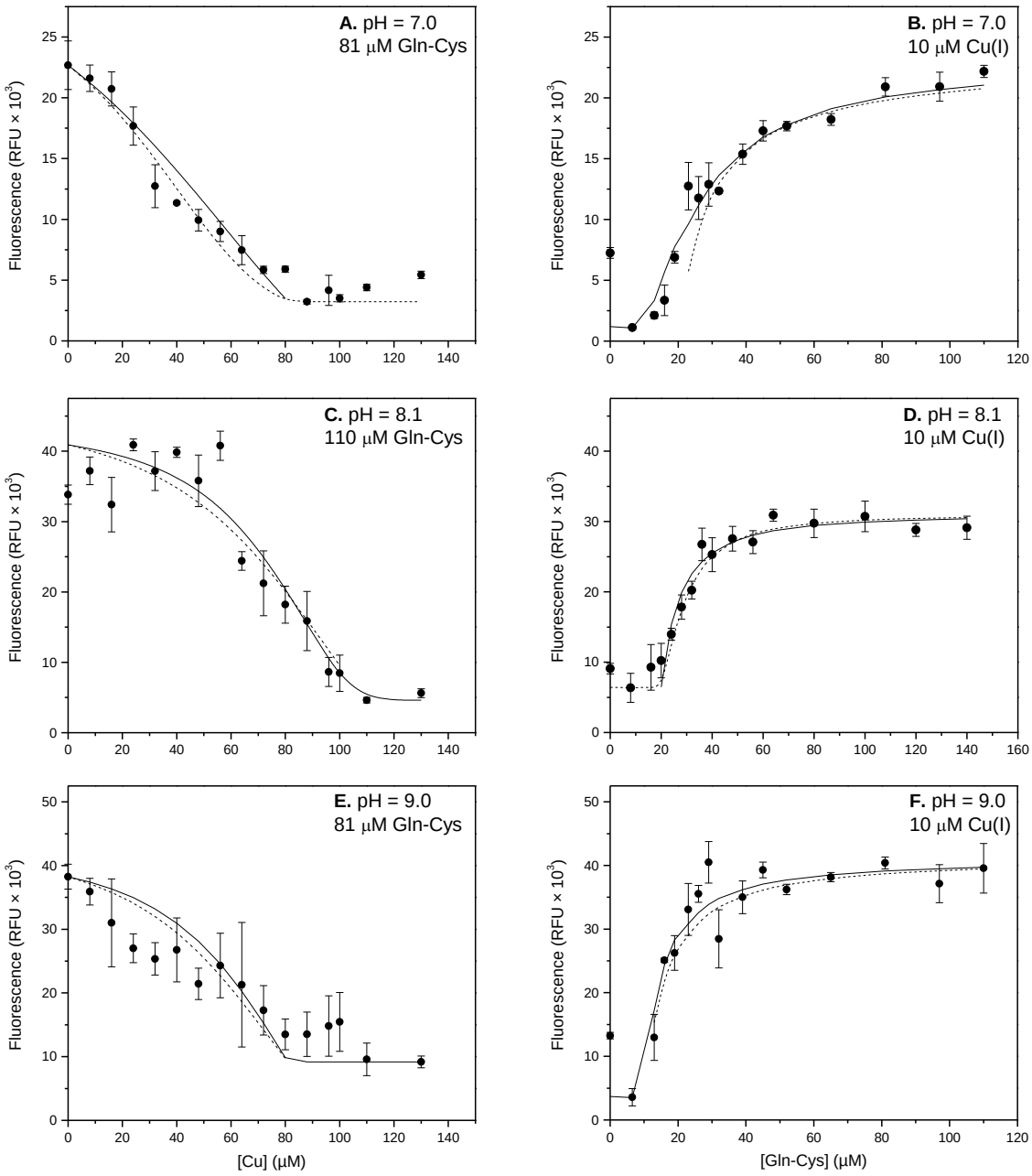

Figure 12. Direct (A,C,E) and indirect (B,D,F) titrations of Gln-Cys by Cu(I). Circles represent average of three fluorescence measurements with the standard deviation represented by the error bars. 200nM PGSK was used as an indicator in all titrations. The lines in each titration represent modeled fluorescence using the general (solid) and conditional (dashed) stability constants determined by a nonlinear least squares fit to the measured fluorescence values. These constants can be found in Table 5 (conditional) and Table 6 (general).

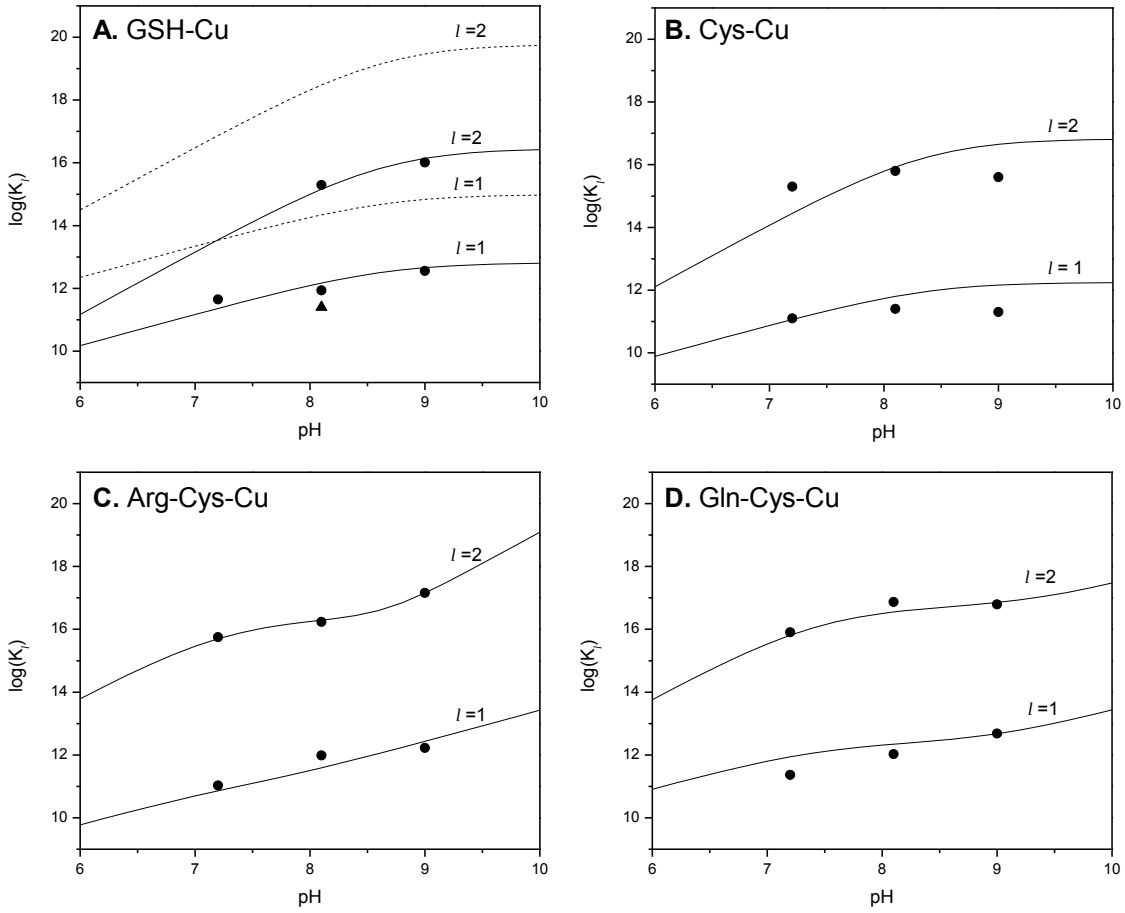

Figure 13. Conditional stability constants plots of Cu(I)-ligand complexes. In each panel the bottom series represents mono-complex constants (K_1'), while the top set represents bis-complex constants (K_2'). Circles represent the conditional stability constants for each metal ligand system at the given pH. Lines represent predicted stability constants calculated using Equation 6. In all plots the solid line(-) is the general stability constants determined in this study. Dotted lines in panel A use the constants provided by Osterberg (1979) and listed in Table 7. The triangle in panel A is the initial measurement of glutathione affinity for copper by Leal and van den Berg (1998)

and that the mono-complex is dominant at the pH range used in this study.

Conditional stability constants derived from titrations involving cysteine (Figure 10, Table 8) confirmed that Cys-Cu(I) complexes were considerably weaker than Cu(I) complexes of GSH. Therefore lower Cu(I) to Cys ratios were used in both direct and indirect titrations. As with GSH complexes of copper only values for protonated complexes were able to be fit to the titration data. A value of 23.0 ± 1.4 was measured for $\log\beta_{111}$. A secondary fit to the conditional constants was required to determine $\log\beta_{122}$ and provided a constant with a high degree of uncertainty ($\log\beta_{122}$ = 38.4 ± 7.5).

Much greater variability is observed in the fluorescence measurements of Cys-Cu(I) titrations than in any other metal ligand system. This noise is likely attributable to the rapid oxidative decay of the Cys-Cu(I) complexes. Any potential effect of this decay on the reliability of our constants would be towards an underestimate on complex stability. It is therefore pertinent to note that our measured conditional stability constant at pH 7.2 ($logK_1'$ = 11.1 ± 0.4 Table 5) is an improvement on a previously reported value ($logK'$ = 9.9) measured using NMR metal ligand titrations at millimolar concentrations of cysteine at the same pH (Rigo et al., 2004). Kinetic considerations are explored in more detail below.

Cu(I) titrations of Arg-Cys (Figure 11) and Gln-Cys (Figure 12) were similar to those of GSH. At pH 8.1 the conditional constants of mono complexes of all three ligands were statistically equivalent (Table 5). However, in contrast to GSH, we were able to measure a conditional constant at pH 7.2 for bis complexes of each dipeptide. Furthermore at higher pH the conditional constants for the dipeptide bis complexes are about an order of magnitude greater than that of GSH (Table 5). The general stability constants of Gln-Cys were similar to those measured for GSH, though in this case ML and MHL_2 constants were able to be determined.

The determination of general stability constants for Arg-Cys complexes of Cu(I) required an adjustment to our speciation model to account for guanidine coordination of copper. This functional group is strongly basic with a pK_a typically estimated to be greater than 12, but values as low as 11.5 have also been reported (Yamauchi and Odani, 1996). For Arg-Cys we determined this pK_a to be 11.7. Therefore in the absence of metals, the guanidine group would be fully protonated at the pH levels used in this study. Several recent studies have demonstrated that guanidine groups can effectively coordinate Cu(I) (Oakley et al., 2004; Wu et al., 2010; Bienemann et al., 2011a; Bienemann et al., 2011b). To allow for guanidine complexation we removed the guanidine protonation constant from our model and treated metal coordination as a simple exchange with the hydrogen. This change in the model resulted in a lower overall error compared to a fit that included the guanidine protonation constant and allowed us to determine stability constants for all five presumed species.

5.3.4. Behavior of Cu(I) complexes in seawater: stability and kinetics.

We are specifically interested in the strength of these complexes in seawater which contains not only Cl^- but also high concentrations of several cations known to interact with organic ligands. Both Mg^{2+} and Ca^{2+} are known to interact to GSH and cysteine, and at marine concentrations have the potential to compete with copper. Unlike BTC and FZ1, PGSK does not significantly interact with these cations which allows for the measurement of stability constants in their presence. We therefore calibrated PGSK affinity (Table 1) for Cu in SOW background (Price et al., 1989) to reexamine the affinity of these ligands for Cu(I).

The affinity of Arg-Cys, Gln-Cys and GSH for Cu(I) did not significantly change when measured in seawater (Table 5, Figure 14). However a small decrease of approximately 0.2 log

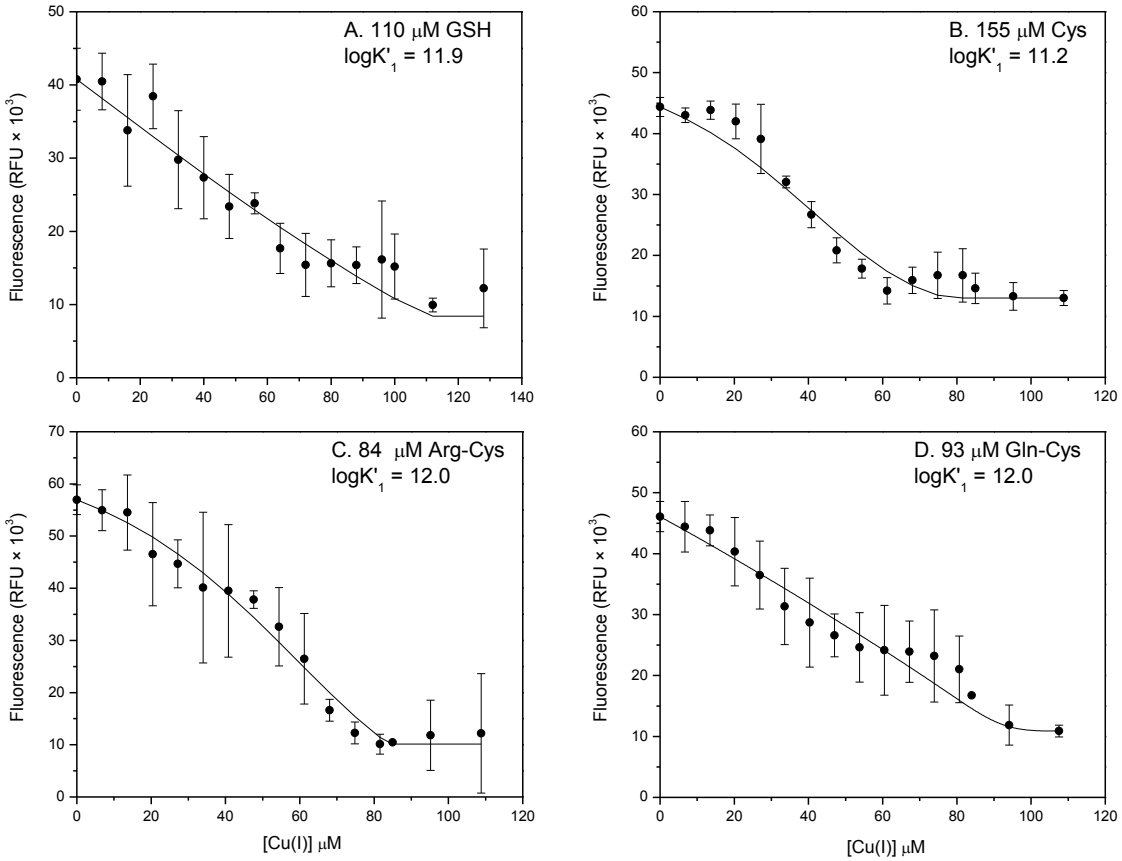

Figure 14. Direct titrations of ligands preformed in the synthetic seawater medium Aquil (pH = 8.1). Circles represent average of three fluorescence measurements with the standard deviation represented by the error bars. 200nM PGSK was used as an indicator in all titrations. The lines in each titration represent modeled fluorescence using the general (solid) and conditional (dashed) stability constants determined by a nonlinear least squares fit to the measured fluorescence values. These constants can be found in Table 5 (conditional) and Table 6 (general).

units was observed in copper titrations of cysteine. We estimated a possible reduction of the conditional constants for these ligands on the order of 0 - 1.5 log units in the presence of Ca^{2+} and Mg^{2+}. Stability constants for these ligands with Ca^{2+} and Mg^{2+} are not well established and there is the potential for a number of side reactions with these ions and other inorganic ligands. Regardless, our results demonstrate that these complexes with Cu(I) are little affected by the presence of competing divalent cations.

Titrations were also performed on mixtures of the ligands. In seawater and batch cultures Arg-Cys, Gln-Cys, cysteine and GSH have all been observed as a mixture and are often assumed to be part of a more diverse pool of ligands. Additionally a mixed-ligand complex, Arg-Cys-Cu(I)-Cys was observed using MALDI/TOF mass spectroscopy in *E. huxleyi* exudates (Dupont et al., 2004). We performed titrations on solutions of cysteine with equimolar amounts of Arg-Cys, Gln-Cys or GSH. These titrations showed little difference from titrations of each polypeptide alone (Figure 15) and the conditional constants were statistically equivalent to those of the mono species (Table 5).

Compared to our titrations of Zn(II) and Cd(II) in which fluorescence was stable overnight, our Cu(I) titrations were not as stable and exhibited changing fluorescence depending on the ligand and its concentration relative to Cu(I). To investigate kinetic stability, we measured the fluorescence of PGSK in the presence of individual Cu(I)-thiol complexes over time (Figure 16). PGSK exhibits decreased fluorescence upon binding Cu(I) or Cu(II) and observed declines may indicate complex instability in the presence of oxygen. Copper cysteine complexes were the least stable followed by Arg-Cys and Gln-Cys which showed intermediate stability, while GSH-Cu(I) complexes were remarkably more stable than the rest (Figure 16).

Fluorescence decay was almost instantaneous for complexes of cysteine indicating that

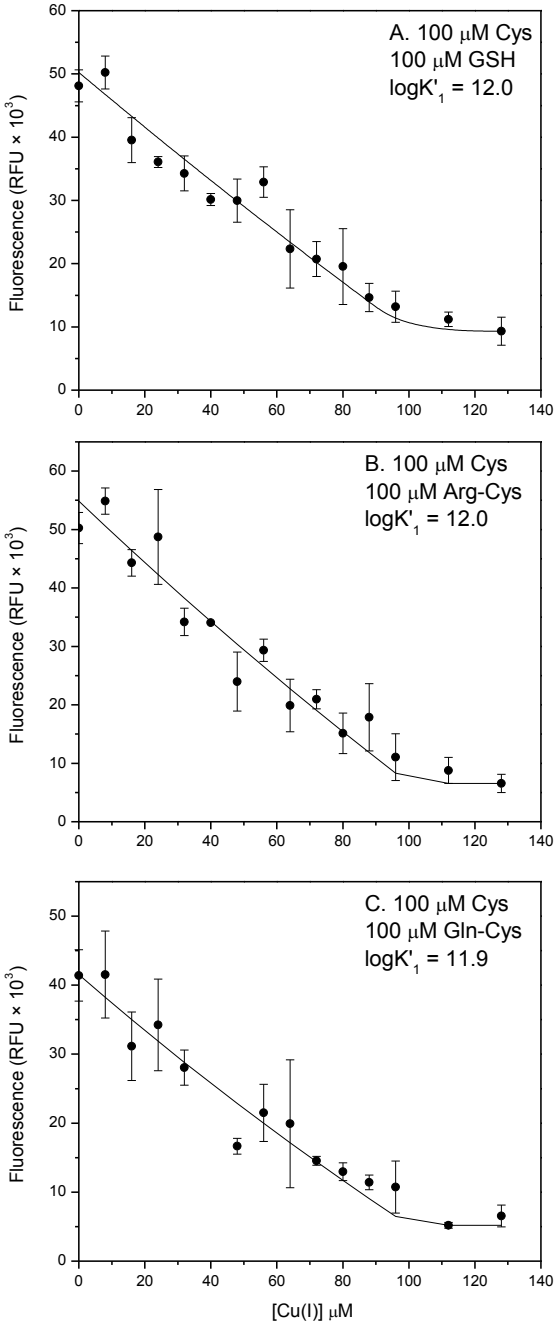

Figure 15. Mixed ligand titrations of GSH (A), Arg-Cys (B) and Gln-Cys (C) with Cysteine in SOW.

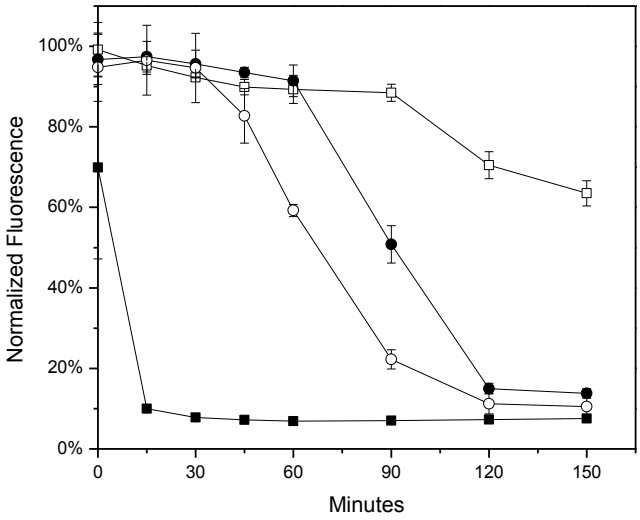

Figure 16. Fluorescence decay measurements of Cu(I)-ligand complexes in SOW with 200 nM PGSK. Total Cu(I) concentrations are approximately 6.8µM. The concentration of Cys (▪) is approximately 20-fold higher than Cu(I), while levels of GSH (□), Arg-Cys (●) or Gln-Cys (◌) are approximately 14-fold.

while the complex may be still relatively strong compared to the Zn and Cd complexes of cysteine it may be kinetically unstable. However it appears that cysteine still provides a moderate amount of stability over uncomplexed copper. Modeling Cu(I) decay in seawater using equation 12 (Sharma and Millero, 1988) with the assumption of oxygen concentration at 10% of saturation we estimated a decay constant of $k_{Cu(I)} = 300\ M^{-1}\ min^{-1}$ for free Cu(I) oxidation. These constant are significantly lower for all thiols ($k_{Cys\text{-}Cu(I)} = 24.3\ M^{-1}\ min^{-1}$; $k_{RC\text{-}Cu(I)} = 4.7\ M^{-1}\ min^{-1}$; $k_{QC\text{-}Cu(I)} = 3.5\ M^{-1}\ min^{-1}$; $k_{GSH\text{-}Cu(I)} = 2.3\ M^{-1}\ min^{-1}$) further demonstrating that these ligands provide stabilization to Cu(I).

6. Discussion

We have shown that a set of fluorescence ion indicators, of varying degrees of affinity, can be effective tools to measure free metal ion concentration and subsequently determine binding constants in the presence of an organic ligand in solutions at neutral to slightly basic pH. This technique is a robust and in some cases, a more effective alternative to traditional acid-base titrations or electrochemical techniques for the determination of stability constants. Measurements were made on microwell plates which reduced the use of reagents, maximized throughput, and enabled rapid analysis of changing solution equilibria. The typical sub-millimolar concentrations of metal and ligand used in this study are representative of biological systems compared to the high millimolar concentrations used in previous studies, allowing for the application of a non-linear least squares fitting of solution equilibria using simplistic speciation models.

Employing a low and high affinity probe, such as FZ1 and BTC respectively, allowed for the measurement of Cd^{2+} and Zn^{2+} at both high and low ion concentrations. By preforming these

titrations at multiple pH's we expanded on the work of Leverrier (Leverrier et al., 2007) and Ogawa (Ogawa and Yoshimura, 2010) to determine a comprehensive set of general stability constants in addition to pH-specific conditional stability constants. Our results (Figure 8) agree well with these studies and are consistent with previous work that measured general stability constants for similar metal-ligand systems (Perrin and Watt, 1971; Leverrier et al., 2007; Chekmeneva et al., 2008).

We have also demonstrated that fluorometric, multiple-pH metal-ligand titrations are a suitable technique for determining stability constants for oxidation prone complexes of Cu(I). This method allowed for the control of several factors that have hindered previous studies of Cu(I) complexation. These fluorometric metal-ligand titrations in pH-buffered, nitrogen-sparged solutions minimized oxidation caused by dissolved oxygen and rapid pH changes typically associated with traditional potentiometric titrations. Further efforts were taken to minimize the effect of oxidation by employing EDTA as masking agent (Kim and Ahner, 2006) to sequester cupric ions generated from residual oxidation of Cu(I).

While these efforts were sufficient to stabilize Cu(I) equilibria for the measurement of stability constants, the fluorescence decay caused by Cu(I) oxidation and the consequential Cu(II) binding by PGSK allowed us to evaluate the kinetic stability of the Cu(I) complexes. While GSH-Cu(I) complexes have been shown to be stable over several hours (Ciriolo et al., 1990) the complex in the presence of oxygen has also been shown to participate in a rapid regenerative cycle involving superoxide (Speisky et al., 2008). This regeneration appears to allow for the apparent kinetic stability of the reduced complex in situations where there is not a good Cu(II) ligand such as in the NMR studies of Ciriolo et al. and Corazza et al. However, in our matrix, PGSK also serves as a strong Cu(II) ligand (logK = 9.8) (Kim and Ahner, 2006), and

would exhibit quenched fluorescence as it removes copper this cycle. The titration curves are snapshots in time of strong metal-thiol complexation undergoing continuous regenerative reactions.

The decay in fluorescence of the respective Cu(I) complexes (Figure 16) is subsequently representative of the forward reaction. In all cases the observed decay constants were significantly lower than that predicted for the decay of inorganic Cu(I) in seawater (Sharma and Millero, 1988). Cu(I) loss was relatively slow in the presence of both dipeptides and GSH while cysteine was far less effective of a Cu(I) stabilizer as complete decay was observed in approximately 30 minutes. This rapid oxidation may explain the poor fit of some of the cysteine titration curves (Figure 10). Despite these limitations our results do present an improvement over previous work and represent the first proposed stability constants for cysteine as well as two novel dipeptides.

Both general stability constants and conditional stability constants were consistent across the four cysteine containing ligands. The reason for this is likely the strong thiol-Cu(I) affinity, as coordination by additional functional groups is likely only to provide marginal improvements in stability. This is demonstrated by the difference between conditional stability constants of cysteine and the peptides. Furthermore the addition of a second thiol coordinating site, through bis-complexation, while still facilitating strong complexation is likely to result in diminishing marginal returns in complex stability. Other factors may also influence affinity as steric effects could limit the benefit of the addition of a second large GSH molecule. This may explain why bis complexes of GSH are slightly weaker than the other bis-complexes that include cysteine. It is also reasonable to assume that the general stability constants should also show similarities, especially in unprotonated species. While the protonated general stability constants do show a

difference between cysteine and the peptides, this is driven by innate differences in proton affinities of the amino group of the ligand, and less by metal affinity.

Previous work on the measurement of Cu(I) affinity constants with several biological, thiol-containing ligands (Table 8) appear to agree with our measurements. BCS has typically been employed in most of these measurements. Xiao et al. (2011) reported a log conditional constant of 15.3 for the dithiothreitol-Cu(I) complex at pH 7.2, but was unable to determine a value for GSH because it is considerably weaker than dithiothreitol. Other BCS titrations have measured log-conditional constants ranging from 15.5 to 16.7 for various dicysteinal peptides (Rousselot-Pailley et al., 2006; Pujol et al., 2010) and 18.8 to 19.2 for tripodal cysteine derivatives (Pujol et al., 2011). Given the approximately three log unit difference between the trithiols and dithols it is reasonable to anticipate from this trend that monothiols, while still strong copper ligands, would have a log-conditional affinity that is less than 13. Our data would fit this trend.

Our results tend to differ from those obtained with electrochemical techniques. The only published general stability constants for Cu(I) with a thiol included in this study were determined for glutathione using electromotive force titrations (Osterberg et al., 1979). Consistent with our results, Osterberg was only able to fit constants for the protonated species, however the measured values ($\log\beta_{111}$ = 24.9, $\log\beta_{122}$ = 38.8) exceed ours by approximately 3 orders of magnitude and would predict a $\log K_1'$ of 13.9 and 14.7 at pH 7.2 and 8.1 respectively. The discrepancy could be attributed to side reactions such as thiol interaction with the mercury electrode surface (Muskal and Mandler, 1999) as well as unaccounted for thiol oxidation or copper disproportionation.

Cathode stripping voltammetry/competitive ligand exchange (CSV-CLE), and some related techniques, have also been employed to determine conditional stability constants. Similar

Table 8. Conditional stability constants of copper-binding ligands compiled from various studies. For known ligands (*) indicates value calculated from available general stability constants using equation 6. For CSV titrations of GSH and Cys: ([ł]) indicates constant is conditional to both metal and ligand; ([ǂ]) is the result of correction for chloride species, conditional to ligand; and ([§]) Assumes bis complexation.

	Ligand	Technique	K'_1 (pH)	K'_2 (pH)	Reference
Monothiols	GSH	EMF Titration	13.9 (7.2)* 14.7 (8.1)*	16.9 (7.2)* 18.5 (8.1)*	(Osterberg et al., 1979)
	GSH	CSV	10.88[ł] (8.35) 16.03[ǂ] (8.35)	32.1[§] (8.35)	(Leal and Van den Berg, 1998)
	GSH	PGSK Titration	11.6 (7.2) 11.9 (8.1) 11.9 (SOW)	13.5 (7.2)* 15.3 (8.1)	This study
	Cys	CSV	11.12[ł] (8.35) 16.28[ǂ] (8.35)	32.6[§] (8.35)	(Leal and Van den Berg, 1998)
	Cys	NMR Metal-Ligand Titration	10.0 (7.2)		(Rigo et al., 2004)
	Cys	PGSK Titration	11.1 (7.2) 11.4 (8.1) 11.2 (SOW)		This study
	RC	PGSK Titration	11.0 (7.2) 12.1 (8.1) 12.0 (SOW)	15.8 (7.2) 16.2 (8.1)	This study
	QC	PGSK Titration	11.4 (7.2) 12.0 (8.1) 12.0 (SOW)	15.9 (7.2) 16.9 (8.1)	This study
Dithiols	DTT	BCS Titration	15.3 (7.0)		(Xiao et al., 2011)
	$GMTCSGCSRP_{cyclic}$	BCS Titration	16.6 (7.4)		(Rousselot-Pailley et al., 2006)
	$GMTCSGCSRP_{linear}$	BCS Titration	16.4 (7.4)		(Rousselot-Pailley et al., 2006)
	$SCWPGRCSPG_{cyclic}$ (P^1)	BCS Titration	16.7 (7.4)		(Pujol et al., 2010)
	$ECNPGWCEPG_{cyclic}$ (P^2)	BCS Titration	15.5 (7.4)		(Pujol et al., 2010)
3xSH	Tripodal-Cysteine (L^1)	BCS Titration	19.2 (7.4)		(Pujol et al., 2011)
	Tripodal-Cysteine (L^2)	BCS Titration	18.8 (7.4)		(Pujol et al., 2011)
	GSH_3	BCS Titration	18.8 (6.0)		(Miras et al., 2008)
Algal Exudates	*Synechococcus*	CSV	13.0		(Croot et al., 2000)
	Skeletonema costatum	CSV	11.6, 12.3		(Croot et al., 2000)
	Thalassiosira weissflogii	CSV	10.6		(Croot et al., 2000)
	Amphidinium carerae	CSV	11.8, 12.2		(Croot et al., 2000)
	Hymenomonas carterae	CSV	10.8		(Croot et al., 2000)
	Emiliania huxleyi	CSV	12.3 11.6		(Leal et al., 1999) (Dupont et al., 2004)

in principle to the fluorometric competing ligand titrations used in this study, free metal concentration is measured by reaction of a copper complex, typically either salicylaldoxime or benzoylacetone, with an electrode. However these techniques suffer from the same drawbacks noted previously with the electromotive force titrations. Despite this, these techniques have been used to measure log-conditional constants between 8 and 14 in a wide variety of systems (Town and Filella, 2000). Conditional log-constants on the order of 10.6-12.3 (Table 8) have been measured for copper-binding ligands observed in the exudates of cultured eukaryotic algae, while a ligand with a log-affinity of 13 is exuded by the cyanobacterium *Synechococcus.*

Using CSV-CLE, Leal (Leal and Van den Berg, 1998) performed Cu(II) titrations on cysteine, GSH and oxidized glutathione (GSSG) in seawater. While the conditional constant for the GSSG-Cu(II) complex was consistent with established general constants (Smith et al., 2003) the authors proposed log-conditional constants of 32.1 and 32.6 for the bis complexes Cu(I)-GSH_2 and Cu(I)-Cys_2 respectively. These values are far larger than our measurements and thus require some assessment. The authors noted that Cu(II) was reduced to Cu(I) via thiol mediated oxidation (Equation 1), however they also assumed that the oxidized thiol would readily revert to its reduced form in seawater. Building on this assumption the authors claimed that a 2:1 thiol-to-metal endpoint was the result of a bis complex and not the result of half the available thiol being oxidized. Others have noted that oxidized thiols are stable in seawater (Crea et al., 2010) and that their trend is towards the oxidized state (Moingt et al., 2010). Additionally no studies have been performed on the behavior of Cu(I) in CSV-CLE experiments or the affinity of the typical CSV-CLE complexing ligands for Cu(I).

Leal and van den Berg's raw measurements of copper affinity (GSH-log$K$ = 10.88; cysteine-log$K$ = 11.12) which did not attempt to correct for the reduced state of copper or a bis

complex, are close to those measured in other studies as well as our own. This may be a coincidental experimental artifact, but could conceivably be a comparable measurement for the copper-complexing capacity of these ligands. Assuming that in CSV-CLE titrations, copper not bound to the thiol is rapidly oxidized to Cu(II) our results would be relatively consistent. More methodological assessment and molecular characterization of copper binding ligands exuded from algae would assist in reconciling these methods.

Our results represent an improvement on the uncertainty associated with the aforementioned electrochemical studies in the characterization of Cu(I) complexation by thiols. By using Cu(I) as a titrant and controlling for its potential oxidation, we were able to avoid several of the complications associated with electrochemical techniques. Arg-Cys and Gln-Cys affinity for Cu(I) are very close to the electrochemically determined values of exudates produced by *E. huxleyi* (Table 8). These dipeptides have been shown accumulate up to extracellular concentrations of 100 nM in copper stressed cultures of *E. huxleyi* (Dupont and Ahner, 2005; Dupont et al., 2004), at concentrations of 10-100 nM in estuarine waters (Chapter 5) and in lower concentrations in the open ocean (Dupont et al., 2006).

Titrations in seawater showed that there was little effect from high concentrations of Mg^{2+} and Ca^{2+} under our experimental conditions. We also measured constants for Arg-Cys with Cd(II) and Gln-Cys with Zn(II) at pH 7.2 and 8.1 in MOPS and Tris buffers respectively, but found the dipeptides to be weaker ligands than GSH or cysteine, almost too weak to be effectively characterized using the low affinity indicator. This is not surprising as, guanidine and amide functional groups are not typically thought of as good divalent ligands. It also demonstrates that the dipeptides have higher degree of metal selectivity compared to cysteine or GSH.

While the Cu(I)-thiol complexes are relatively strong compared to their Zn(II) and Cd(II) counterparts, speciation modeling suggests that this benefit may not extend to surface seawater (Figure 17, Further consideration to speciation is given in the appendix to this chapter). The high concentration of chloride, which forms relatively strong inorganic complexes with Cu(I), already significantly buffers cuprous ion levels. Cu(II) concentrations are more readily controlled by the presence of a ligand with equivalent ion affinity. Since Cu^{+} ion levels are only marginally affected by the presence of a strong thiol ligand, it is unlikely that cells produce these ligands to facilitate direct extracellular buffering of Cu(I). It is also unlikely that thiols are exuded as a mechanism to transform Cu(II) to Cu(I) as a mechanism to lower its bioavailability. Cell surface reductases already facilitate the reduction of Cu(II) to Cu(I) prior to high affinity uptake (Hill et al., 1996; Blaby-Haas and Merchant, 2012) doing so in the bulk media would likely increase copper bioavailability. This would be of more concern if inorganic or other weak ligand complexes are bioavailable to the cell (Aristilde et al., 2012), which may be the case with the resulting chloro-complexes. Regardless of their impact on free cuprous ion concentrations, these thiols can still be found in significant quantities outside the cell. In *E. huxleyi* cultures containing 170 nM extracellular copper, approximately one third of the copper was organically complexed by Arg-Cys (Dupont et al., 2004), roughly the same amount predicted by speciation models using our constants.

These thiol containing ligands may be more important inside cell where chloride levels are lower and these ligands can reach near millimolar concentrations under copper stress (Dupont and Ahner, 2005). These thiols can substantially reduce the free copper concentrations inside the cell at these concentrations. Furthermore their selectivity of the dipeptides for Cu(II) would allow them to strongly modulate copper, while having less of an impact on critical Zn(II)

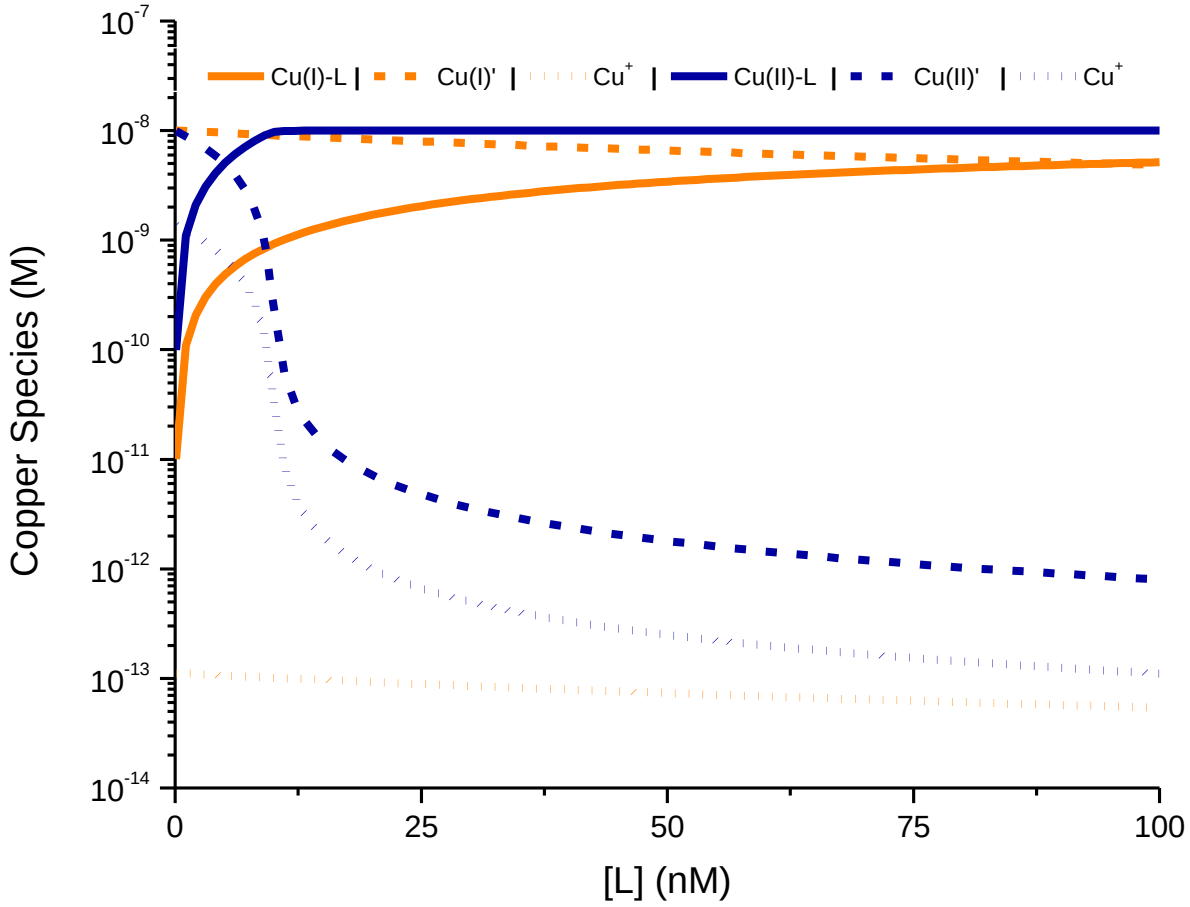

Figure 17. Concentrations of organically complexed (solid), inorganic (dashed), and free ion (dotted) Cu(I) (orange) and Cu(II) (blue) species in the presence of 0 to 100 nM of a ligand (L, log$K^{'}$ = 12.0) in the presence of 10 nM total copper at pH 8.1, 0.55M Cl^{-}. Speciation calculations were performed separately for each oxidation state. Inorganic species formation constants used are listed in Table 2.

levels than GSH. These low-molecular weight complexes may be readily amenable to efflux. There is evidence for such transport in algae as phytochelatin is exported simultaneous with Cd(II) by the diatom *Thalassiosira weissflogii*. Transport of the Cd(II)-phytochelatin complex as well as glutathione conjugates can be facilitated by the *Abc2* ABC-type transporter in yeast (Mendoza-Cózatl et al., 2010).

Regardless of their role inside the cell, thiols do appear to constitute a significant part of the extracellular pool of copper binding ligands and subsequently have impacts on bioavailability. Our results provide improved constants for biologically relevant metal-complexes as well as a new method for determining stability constants for some kinetically unstable metal-ligand complexes. While these results provide new and more reliable information for understanding complexation under physiological conditions, the chemistry of copper in marine systems continues to be an area of uncertainty. The redox behavior of the complexes, monovalent and divalent distribution of copper, and presence of other organic and inorganic ligands, need to be taken into consideration when understanding the importance of biological ligands in extracellular copper homeostasis.

7. Acknowledgements

Potentiometric titrations were performed assistance by Collette Kopon. Funding was provided by NSF Chemical Oceanography (OCE 0451781)

8. References

Ahner BA and Morel FMM. (1995) Phytochelatin Production in Marine-Algae .2. Induction by Various Metals. *Limnology and Oceanography* 40: 658-665.

Al-Farawati R and Van Den Berg CMG. (2001) Thiols in coastal waters of the western North Sea and English Channel. *Environmental Science & Technology* 35: 1902-1911.

Alderighi L, Gans P, Ienco A, et al. (1999) Hyperquad simulation and speciation (HySS): a utility program for the investigation of equilibria involving soluble and partially soluble species. *Coordination Chemistry Reviews* 184: 311-318.

Aristilde L, Xu Y and Morel FMM. (2012) Weak Organic Ligands Enhance Zinc Uptake in Marine Phytoplankton. *Environmental Science & Technology* 46: 5438-5445.

Attari A and Jaselskis B. (1972) Spectrophotometric determination of sulfur dioxide by reduction of iron(III) in the presence of ferrozine. *Analytical Chemistry* 44: 1515-1517.

Berthon G. (1995) Critical Evalution of the Stability-Constants of Metal-Complexes of Amino-Acids with Polar Side-Chains. *Pure and Applied Chemistry* 67: 1117-1240.

Bienemann O, Haase R, Jesser A, et al. (2011a) Synthesis and Application of New Guanidine Copper Complexes in Atom Transfer Radical Polymerisation. *European Journal of Inorganic Chemistry* 2011: 2367-2379.

Bienemann O, Hoffmann A and Herres-Pawlis S. (2011b) (Guanidine)copper complexes: structural variety and application in bioinorganic chemistry and catalysis. *Reviews in Inorganic Chemistry* 31: 83-108.

Blaby-Haas CE and Merchant SS. (2012) The ins and outs of algal metal transport. *Biochimica et Biophysica Acta (BBA) - Molecular Cell Research* 1823: 1531-1552.

Chekmeneva E, Prohens R, Díaz-Cruz JM, et al. (2008) Thermodynamics of Cd2+ and Zn2+ binding by the phytochelatin ([gamma]-Glu-Cys)4-Gly and its precursor glutathione. *Analytical Biochemistry* 375: 82-89.

Cherifi K, Reverend BD-L, Loucheux C, et al. (1990) Transition metal complexes of L-cysteine containing Di- and tripeptides. *Journal of Inorganic Biochemistry* 38: 69-80.

Ciriolo MR, Desideri A, Paci M, et al. (1990) Reconstitution of Cu,Zn-Superoxide Dismutase by the Cu(I).Glutathione Complex. *Journal of Biological Chemistry* 265: 11030-11034.

Cobbett C and Goldsbrough P. (2002) PHYTOCHELATINS AND METALLOTHIONEINS: Roles in Heavy Metal Detoxification and Homeostasis. *Annual Review of Plant Biology* 53: 159-182.

Cole A, Furnival C, Huang ZX, et al. (1985) Computer simulation models for the low-molecular-weight complex distribution of cadmium(II) and nickel(II) in human blood plasma. *Inorganica Chimica Acta* 108: 165-171.

Corazza A, Harvey I and Sadler PJ. (1996) 1H,13C-NMR and X-ray absorption studies of copper(I) glutathione complexes. *European Journal of Biochemistry* 236: 697-705.

Crea P, De Stefano C, Millero F, et al. (2010) Dissociation Constants of Protonated Oxidized Glutathione in Seawater Media at Different Salinities. *Aquatic Geochemistry* 16: 447-466.

Croot PL, Moffett JW and Brand LE. (2000) Production of extracellular Cu complexing ligands by eucaryotic phytoplankton in response to Cu stress. *Limnology and Oceanography* 45: 619-627.

De Levie R. (2001) *How to use Excel in analytical chemistry and in general scientific data analysis*, Cambridge ; New York: Cambridge University Press.
Dryden CL, Gordon AS and Donat JR. (2007) Seasonal survey of copper-complexing ligands and thiol compounds in a heavily utilized, urban estuary: Elizabeth River, Virginia. *Marine Chemistry* 103: 276-288.
Dupont CL and Ahner BA. (2005) Effects of copper, cadmium, and zinc on the production and exudation of thiols by Emiliania huxleyi. *Limnology and Oceanography* 50: 508-515.
Dupont CL, Moffett JW, Bidigare RR, et al. (2006) Distributions of dissolved and particulate biogenic thiols in the subartic Pacific Ocean. *Deep-Sea Research Part I-Oceanographic Research Papers* 53: 1961-1974.
Dupont CL, Nelson RK, Bashir S, et al. (2004) Novel copper-binding and nitrogen-rich thiols produced and exuded by Emiliania huxleyi. *Limnology and Oceanography* 49: 1754-1762.
Enyedy ÉA, Lakatos A, Horváth L, et al. (2008) Interactions of insulin-mimetic zinc(II) complexes with cell constituents: Glutathione and ATP. *Journal of Inorganic Biochemistry* 102: 1473-1485.
Ferretti L, Elviri L, Pellinghelli MA, et al. (2007) Glutathione and N-acetylcysteinylglycine: Protonation and Zn2+ complexation. *Journal of Inorganic Biochemistry* 101: 1442-1456.
Fuhr BJ and Rabenstein DL. (1973) Nuclear magnetic resonance studies of the solution chemistry of metal complexes. IX. Binding of cadmium, zinc, lead, and mercury by glutathione. *J. Am. Chem. Soc.* 95: 6944-6950.
Gee KR, Zhou ZL, Ton-That D, et al. (2002) Measuring zinc in living cells.: A new generation of sensitive and selective fluorescent probes. *Cell Calcium* 31: 245-251.
Gerringa LJA, Herman PMJ and Poortvliet TCW. (1995) Comparison of the linear Van den Berg/Ruzic transformation and a non-linear fit of the Langmuir isotherm applied to Cu speciation data in the estuarine environment. *Marine Chemistry* 48: 131-142.
Gustafsson J. (2010) Visual MINTEQ. 3.0 ed. Stockholm, Sweeden: KTH Royal Institute of Technology
Gutz I. (2007) CurTiPot. 3.2.3 ed. Sao Paulo Brazil.
Hegetschweiler K and Saltman P. (1986) Interaction of copper(II) with N-(2-hydroxyethyl)piperazine-N'-ethanesulfonic acid (HEPES). *Inorganic Chemistry* 25: 107-109.
Hill KL, Hassett R, Kosman D, et al. (1996) Regulated Copper Uptake in Chlamydomonas reinhardtii in Response to Copper Availability. *Plant Physiology* 112: 697-704.
Hyrc KL, Bownik JM and Goldberg MP. (2000) Ionic selectivity of low-affinity ratiometric calcium indicators: mag-Fura-2, Fura-2FF and BTC. *Cell Calcium* 27: 75-86.
Jalilehvand F, Leung BO, Izadifard M, et al. (2006) Mercury(II) cysteine complexes in alkaline aqueous solution. *Inorganic Chemistry* 45: 66-73.
Kadima W and Rabenstein DL. (1990) Nuclear magnetic resonance studies of the solution chemistry of metal complexes. 26. Mixed ligand complexes of cadmium, nitrilotriacetic acid, glutathione, and related ligands. *Journal of Inorganic Biochemistry* 38: 277-288.
Kim H-S, Walsh MJ, Yang H, et al. (2011) Nutrient availability alters levels of non-translationally synthesized nitrogen-rich dipeptides in Emiliania huxleyi. *Aquatic Biology* 12: 215-224.

Kim HS and Ahner BA. (2006) Calibration of Phen Green (TM) for use as a Cu(I)-selective fluorescent indicator. *Analytica Chimica Acta* 575: 223-229.
Leal MFC and Van den Berg CMG. (1998) Evidence for strong copper(I) complexation by organic ligands in seawater. *Aquatic Geochemistry* 4: 49-75.
Leal MFC, Vasconcelos MTSD and van den Berg CMG. (1999) Copper-induced release of complexing ligands similar to thiols by Emiliania huxleyi in seawater cultures. *Limnology and Oceanography* 44: 1750-1762.
Lenz GR and Martell AE. (1964) Metal Chelates of Some Sulfur-Containing Amino Acids. *Biochemistry* 3: 745-&.
Leverrier P, Montigny C, Garrigos M, et al. (2007) Metal binding to ligands: Cadmium complexes with glutathione revisited. *Analytical Biochemistry* 371: 215-228.
Mah V and Jalilehvand F. (2010) Cadmium(II) complex formation with glutathione. *Journal of Biological Inorganic Chemistry* 15: 441-458.
Mendoza-Cózatl DG, Zhai Z, Jobe TO, et al. (2010) Tonoplast-localized Abc2 transporter mediates phytochelatin accumulation in vacuoles and confers cadmium tolerance. *Journal of Biological Chemistry* 285: 40416-40426.
Millis KK, Weaver KH and Rabenstein DL. (1993) Oxidation/reduction potential of glutathione. *The Journal of Organic Chemistry* 58: 4144-4146.
Miras R, Morin I, Jacquin O, et al. (2008) Interplay between glutathione, Atx1 and copper. 1. Copper(I) glutathionate induced dimerization of Atx1. *Journal of Biological Inorganic Chemistry* 13: 195-205.
Moingt M, Bressac M, Bélanger D, et al. (2010) Role of ultra-violet radiation, mercury and copper on the stability of dissolved glutathione in natural and artificial freshwater and saltwater. *Chemosphere* 80: 1314-1320.
Muskal N and Mandler D. (1999) Thiol self-assembled monolayers on mercury surfaces: the adsorption and electrochemistry of ω-mercaptoalkanoic acids. *Electrochimica Acta* 45: 537-548.
Oakley SH, Coles MP and Hitchcock PB. (2004) Structural Consequences of the Prohibition of Hydrogen Bonding in Copper−Guanidine Systems. *Inorganic Chemistry* 43: 5168-5172.
Ogawa S and Yoshimura E. (2010) Determination of thermodynamic parameters of cadmium(II) association to glutathione using the fluorescent reagent FluoZin-1. *Analytical Biochemistry* 402: 200-202.
Osterberg R, Ligaarden R and Persson D. (1979) Copper(I) Complexes of Penicillamine and Glutathione. *Journal of Inorganic Biochemistry* 10: 341-355.
Pearson RG. (1963) Hard and Soft Acids and Bases. *Journal of the American Chemical Society* 85: 3533-&.
Pecci L, Montefoschi G, Musci G, et al. (1997) Novel findings on the copper catalysed oxidation of cysteine. *Amino Acids* 13: 355-367.
Perrin DD and Watt AE. (1971) Complex formation of zinc and cadmium with glutathione. *Biochimica et Biophysica Acta (BBA) - General Subjects* 230: 96-104.
Pompella A, Visvikis A, Paolicchi A, et al. (2003) The changing faces of glutathione, a cellular protagonist. *Biochemical Pharmacology* 66: 1499-1503.
Price NM, Harrison GI, Hering JG, et al. (1989) Preparation and Chemistry of the Artificial Algal Culture Medium Aquil. *Biological Oceanography* 6: 443-461.

Pujol AM, Gateau C, Lebrun C, et al. (2011) A Series of Tripodal Cysteine Derivatives as Water-Soluble Chelators that are Highly Selective for Copper(I). *Chemistry – A European Journal* 17: 4418-4428.

Pujol AsM, Cuillel M, Renaudet O, et al. (2010) Hepatocyte Targeting and Intracellular Copper Chelation by a Thiol-Containing Glycocyclopeptide. *Journal of the American Chemical Society* 133: 286-296.

Rigo A, Corazza A, di Paolo ML, et al. (2004) Interaction of copper with cysteine: stability of cuprous complexes and catalytic role of cupric ions in anaerobic thiol oxidation. *Journal of Inorganic Biochemistry* 98: 1495-1501.

Rousselot-Pailley P, Sénèque O, Lebrun C, et al. (2006) Model Peptides Based on the Binding Loop of the Copper Metallochaperone Atx1: Selectivity of the Consensus Sequence MxCxxC for Metal Ions Hg(II), Cu(I), Cd(II), Pb(II), and Zn(II). *Inorganic Chemistry* 45: 5510-5520.

Sharma VK and Millero FJ. (1988) Oxidation of copper(I) in seawater. *Environmental Science & Technology* 22: 768-771.

Smith R, Martell A and Motekaitis R. (2003) NIST Critical Stability Constants of Metal Complexes Database Version 7.0. 2003 ed.: US Department of Commerce, Gaithersburg, MD

Speisky H, Gómez M, Carrasco-Pozo C, et al. (2008) Cu(I)-Glutathione complex: A potential source of superoxide radicals generation. *Bioorganic & Medicinal Chemistry* 16: 6568-6574.

Town RM and Filella M. (2000) Dispelling the Myths: Is the Existence of L1 and L2 Ligands Necessary to Explain Metal Ion Speciation in Natural Waters? *Limnology and Oceanography* 45: 1341-1357.

Wu Z, Fernandez-Lima FA and Russell DH. (2010) Amino Acid Influence on Copper Binding to Peptides: Cysteine Versus Arginine. *Journal of the American Society for Mass Spectrometry* 21: 522-533.

Xiao Z, Brose J, Schimo S, et al. (2011) Unification of the Copper(I) Binding Affinities of the Metallo-chaperones Atx1, Atox1, and Related Proteins. *Journal of Biological Chemistry* 286: 11047-11055.

Yamauchi O and Odani A. (1996) Stability constants of metal complexes of amino acids with charged side chains .1. Positively charged side chains. *Pure and Applied Chemistry* 68: 469-496.

9. Appendix: Speciation models and predictions of metal thiol complexes

Computational models using stability constants determined in Chapter 1 are presented to demonstrate metal-thiol complex speciation under intracellular and extracellular conditions.

9.1. Calculations

Stability and acid dissociation constants for all species in this study were reported in Chapter 1. Conditional stability constants K_l' were calculated from the general stability constants (β_{mlh}), also reported in Chapter 1, and can be derived from general stability constants using the following equation:

$$K_l' = \frac{\sum_h^1 \beta_{1lh}[H^+]^h}{(1 + \sum_h \beta_{01h}[H^+]^h)^l}$$

Where *m*, *l*, *h*, are the stoichiometric coefficients of the metal, ligand, and proton constituents of the complex. Conditional stability constants modeled from general stability constants were used for prediction of mono or bis complexation because they allow for an efficient determination of complex predominance. A mono bis complex equivalence concentration (L_{50}) of unbound ligand was determined from these conditional constants by defining [L_{50}] as the concentration where [ML] = [ML_2].Substitution of the complex for the components results in:

$$[\mathrm{M}][\mathrm{L}_{50}]\ K_1' = [\mathrm{M}][\mathrm{L}_{50}]^2\ K_2'$$

This simplifies to:

$$\frac{K_1'}{K_2'} = [\mathrm{L}_{50}]$$

or

$$\log K_2' - \log K_1' = pL_{50}$$

This value is conditional with respect to pH. At concentrations higher than [L_{50}], bis-complexes dominate, at concentrations lower than [L_{50}], mono-complexes dominate.

To examine speciation, we calculated pL_{50} values for each complex. Additionally, speciation models as a function of ligand concentration under cytosolic (pH = 7.2, Cl^- = 0.1 M) and marine (pH = 8.1, Cl^- = 0.55 M) conditions. Though our cytosolic model is intended to be applicable to a variety of biological systems, cellular metal concentrations of 17 μM Cd(II), 35 μM Cu(I), and 80 μM Zn(II) used were from the reported average of a survey of marine phytoplankton (Ho et al., 2003). In the marine calculations, 5 nM of each metal was used to represent high metal concentrations to model an elevated pool of metals. Typical surface seawater concentrations for cadmium, copper, and zinc are approximately 1 nM. Chemical speciation calculations were performed using HYSS (Alderighi et al., 1999).

9.2. Speciation predictions

Speciation models and pL_{50} values of Cu(I), Cd(II) and Zn(II) in the presence of biologically observed concentrations of several biogenic thiols indicate that the subsequently formed metal-thiol complexes typically involve a metal to ligand ratio of 1:1 (Table 1, Figure A1, Figure A2, Figure A3, Figure A4). Higher ligand concentrations and pH values will favor the formation of bis complexes. The calculated pL_{50} values indicate that bis complexation will dominate at approximately 0.1-10 mM ligand at pH 7.2 and 0.01 to 1.0 mM at pH 8.1.

The least favorable ligand for bis complexation was GSH. Given that GSH is also the largest ligand, the addition of a second GSH chelator could be hindered by steric effects, though

it appears that cysteine had no advantage over Arg-Cys and Gln-Cys in the formation of bis-Cu(I)-complexes. Glutathione is the most abundant low molecular weight thiol in the cell with concentrations ranging from 0.5-10 mM in a wide variety of animals and algae cells (Pompella, A. et al. 2003). While these levels are below the pL_{50} value bis complexes still start to form at significant concentrations in the cell.

The most favored bis complexes were those of Zn(II) and cysteine (Figure A1). The pL_{50} values for this complex are clear outliers indicating that bis complexes are highly favored at micromolar levels of ligand. This may have biological implications. Cysteine can enhance the bioavailability of Zn(II) to algae in the presence of as strong ligand, presumably through the formation of a ternary complex consisting of Zn(II), a cysteine molecule, and a surface zinc transporter (Aristilde et al., 2012). However the formation of a bis complex results in zinc being inaccessible for uptake. While these concentrations are unlikely in marine systems, cysteine concentrations inside the cell can range from 0.1 to 0.5 mM.

The protonation states of the amine groups of these complexes can vary depending on the complex and pH. In Chapter 1, we were unable to fit $–NH_3^+$ species of cysteine with Zn(II) or Cd(II). Neither were we able to observe $–NH_2$ complexes of Cu(I) with cysteine and glutathione. As such, our models do not include these species. However, models that include reported constants (Berthon, 1995) for protonated Zn(II) or Cd(II) cysteine complexes indicate that $–NH_3^+$ species are insignificant at neutral-to-basic pH. Additionally the only published Cu(I)-GSH stability constants do not include values for $–NH_2$ complexes (Osterberg et al., 1979). Mono complexes of Zn(II) and Cd(II) with glutathione appear to be in transition between $–NH_3^+$ at pH 7.2 (Figure A1) and unprotonated pH 8.1 (Figure A3). Additionally, while Cu(I) complexes of

Arg-Cys and Gln-Cys were mostly protonated at pH 7.2, $-NH_2$ species are significant and do slightly increase at pH 8.1. This behavior is not unexpected as the amine proton affinity typically ranges from 9-10, and is lowered by complexation.

Though thiol metal complexes of Cd(II) and Zn(II) did form at significant levels, the ligands provided little buffering capacity for the divalent cations. Significant reductions of free metal ion concentrations are predicted for the cuprous ion in cytosolic conditions (Figure A2). Chloride forms strong inorganic complexes with Cu(I) resulting in a decline in the free ion concentrations at high concentrations, such as the 0.1 M Cl^- used in cytosolic modeling. Still, the presence of thiols lowered cuprous ion concentrations from approximately 10 nM to below 0.01 nM, with GSH, Arg-Cys, and Gln-Cys being slightly more effective than cysteine. Due to the high chloride concentration in seawater (0.55 M), the presence of thiols is not going to significantly reduce the free metal ion concentrations. Thiol concentrations range from sub-nanomolar in the North Pacific (Dupont et al., 2006) to 50 (Dryden et al., 2007) – 100 (Chapter 5) nM in estuarine environments. While thiols are strong Cu(I) ligands, Cu(I) is already heavily buffered by the presence of chloride ions. Nanomolar concentrations of thiols will only marginally reduce cuprous ion activity in surface sea water. Thiols thus may not be as significant in directly reducing the pool of copper available for uptake in surface seawater. Their presence in surface seawater may be explained by their role in buffering intracellular copper concentrations and subsequent exudation as part of a detoxification mechanism (Dupont et al., 2004; Dupont and Ahner, 2005).

9.3. Figures & Tables

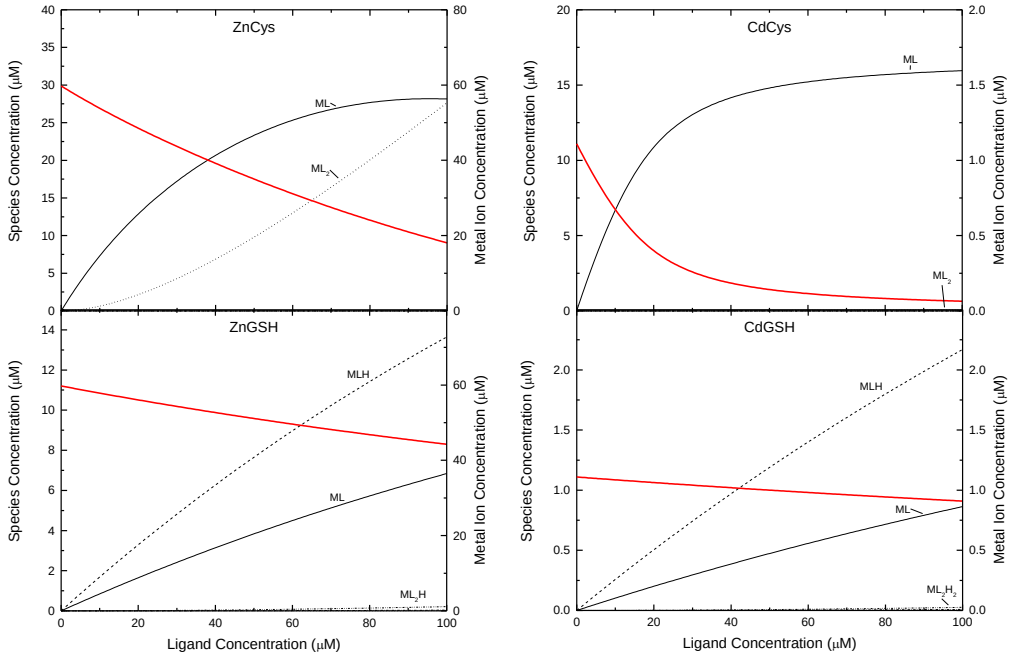

Figure A1. Speciation plots of major complexes (black lines) and free metal ion concentration (red lines) of Zn(II) and Cd(II) complexes of cysteine and GSH. pH = 7.2, Cl^- = 0.1 M, [Zn]= 80 μM, [Cd] = 17 μM.

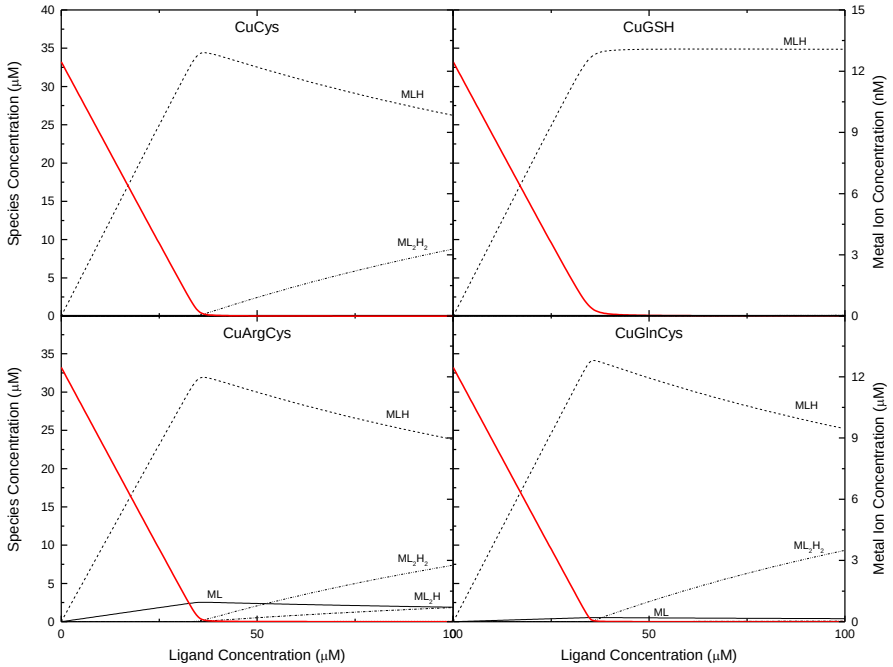

Figure A2. Speciation plots of major complexes (black lines) and free metal ion concentration (red lines) of Cu(I) complexes of cysteine, GSH, Arg-Cys and Gln-Cys. pH = 7.2, Cl^- = 0.1 M, [Cu]= 35 μM.

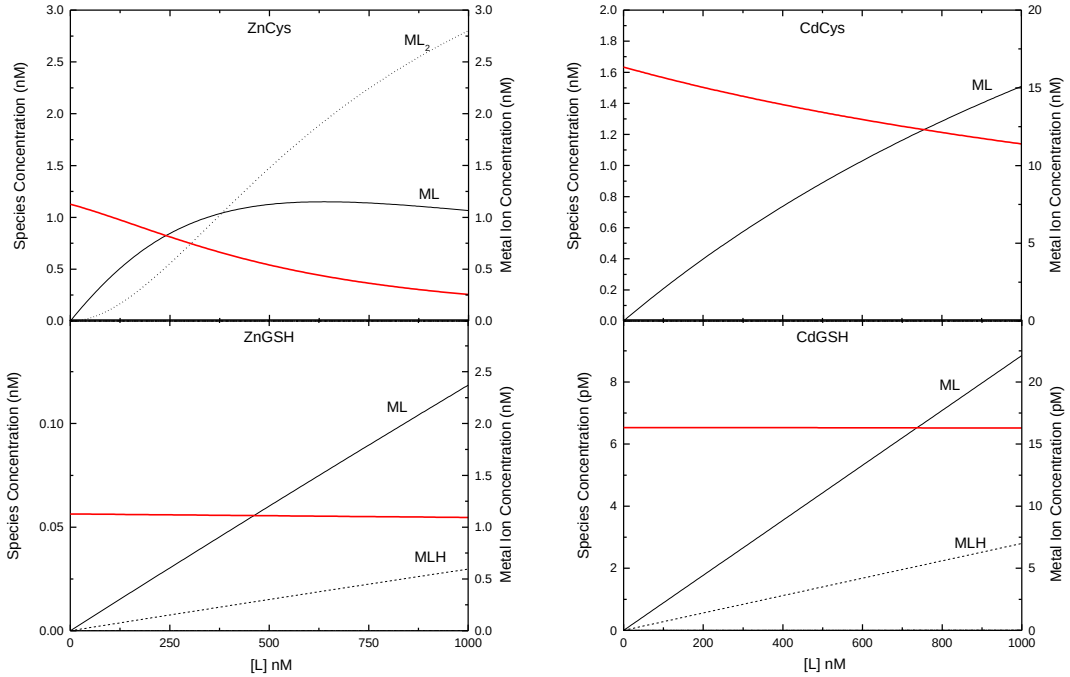

Figure A3. Speciation plots of major complexes (black lines) and free metal ion concentration (red lines) of Zn(II) and Cd(II) complexes of cysteine and GSH. pH = 8.1, Cl^- = 0.55 M, [Zn]= 5 nM, [Cd] = 5 nM.

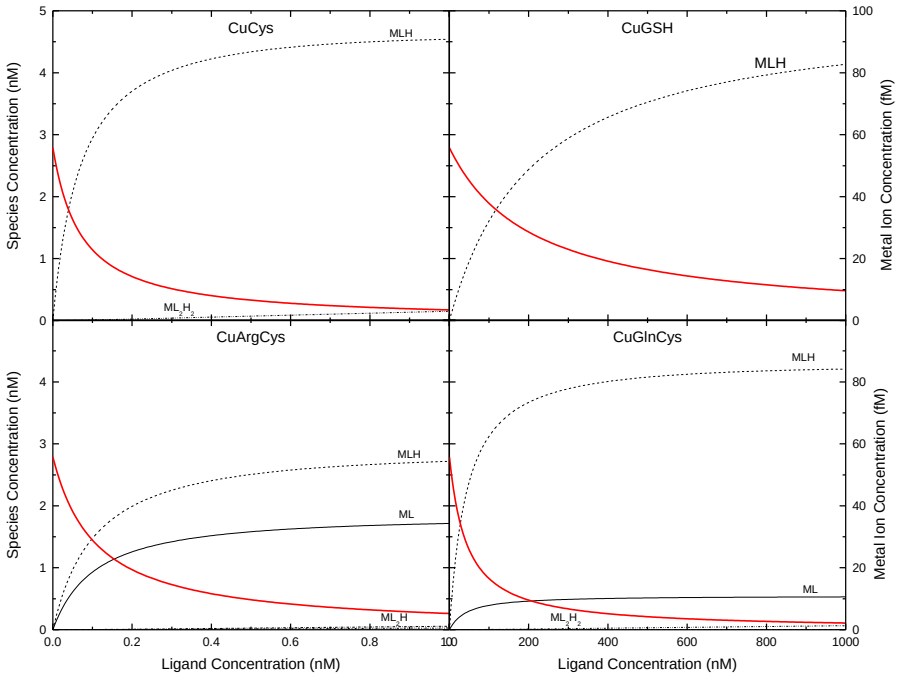

Figure A4. Speciation plots of major complexes (black lines) and free metal ion concentration (red lines) of Cu(I) complexes of cysteine, GSH, Arg-Cys and Gln-Cys. pH = 8.1, Cl^- = 0.55 M, [Cu]= 5nM.

Table 1. pL_{50} values and net charges for selected thiol-metal complexes. pL_{50} represents -log concentration of unbound ligand at which concentration of mono and bis species are predicted to be equal. At free ligand concentrations below this value, mono complexes dominate, at free ligand concentrations higher than this value, bis complexes dominate.

		pL_{50}			
	pH	7.2	8.1	Charge ML	Charge MLH
Zn(II)	GSH	2.6	3.5	-1	0
	Cys	4.4	6.0	0	+1
Cd(II)	GSH	2.4	3.4	-1	0
	Cys	2.7	3.2	0	+1
Cu(I)	GSH	2.2	3.0	-2	-1
	Cys	3.2	4.1	-1	0
	Arg-Cys	3.8	4.4	-1	0
	Gln-Cys	3.7	4.2	-1	0

9.4. References

Alderighi L, Gans P, Ienco A, et al. (1999) Hyperquad simulation and speciation (HySS): a utility program for the investigation of equilibria involving soluble and partially soluble species. *Coordination Chemistry Reviews* 184: 311-318.

Aristilde L, Xu Y and Morel FMM. (2012) Weak Organic Ligands Enhance Zinc Uptake in Marine Phytoplankton. *Environmental Science & Technology* 46: 5438-5445.

Berthon G. (1995) Critical Evalution of the Stability-Constants of Metal-Complexes of Amino-Acids with Polar Side-Chains. *Pure and Applied Chemistry* 67: 1117-1240.

Dryden CL, Gordon AS and Donat JR. (2007) Seasonal survey of copper-complexing ligands and thiol compounds in a heavily utilized, urban estuary: Elizabeth River, Virginia. *Marine Chemistry* 103: 276-288.

Dupont CL and Ahner BA. (2005) Effects of copper, cadmium, and zinc on the production and exudation of thiols by Emiliania huxleyi. *Limnology and Oceanography* 50: 508-515.

Dupont CL, Moffett JW, Bidigare RR, et al. (2006) Distributions of dissolved and particulate biogenic thiols in the subartic Pacific Ocean. *Deep-Sea Research Part I-Oceanographic Research Papers* 53: 1961-1974.

Dupont CL, Nelson RK, Bashir S, et al. (2004) Novel copper-binding and nitrogen-rich thiols produced and exuded by Emiliania huxleyi. *Limnology and Oceanography* 49: 1754-1762.

Ho TY, Quigg A, Finkel ZV, et al. (2003) The elemental composition of some marine phytoplankton. *Journal of Phycology* 39: 1145-1159.

Osterberg R, Ligaarden R and Persson D. (1979) Copper(I) Complexes of Penicillamine and Glutathione. *Journal of Inorganic Biochemistry* 10: 341-355.

Pompella, A., A. Visvikis, et al. (2003). "The changing faces of glutathione, a cellular protagonist." *Biochemical Pharmacology* 66(8): 1499-1503.

CHAPTER 2

Cu(I), Cd(II) & Zn(II) Binding to Cysteine and Cysteine Containing Peptides. 2. Computational Studies of Coordination, Structure and Complex Protonation

1. Abstract

Computational methods were used to evaluate complexation of several low molecular weight thiols (cysteine, glutathione, Arg-Cys and Gln-Cys) with Cu(I), Cd(II) and Zn(II). Speciation models of stability constants in Chapter 1 demonstrate the predominance of certain species under intracellular and marine conditions. Models indicate that Cu(I) complexes are far more likely than Cd(II) and Zn(II) to be protonated. B3LYP density functional theory calculations provide theoretical support for this behavior by demonstrating a significant difference in protonation energies between the divalent and monovalent complexes. Geometries of optimized metal-thiol complexes are also presented and discussed. Coordination by multiple functional groups results in more energetically favorable complexes. Zn(II) and Cd(II) prefer three point coordination while Cu(I) is generally coordinated by two functional groups.

2. Introduction

Complexation of transition metal ions with small organic molecules is a fundamental component of metal homeostasis and transport. Several metals, for which complexation is of particular importance include copper, zinc and cadmium. Copper and zinc are essential enzymatic cofactors. Copper, due to its ability to transition readily between oxidation states of Cu(I) and Cu(II) in biological systems is important in the electron transport chains of respiration and photosynthesis. Zn(II) is critical for protein structure, most notably as part of the zinc finger motif. At higher concentrations, cadmium can substitute for both copper and zinc resulting in toxicity (Das et al., 1997), although some organisms have evolved to allow for cadmium substitution of zinc in certain enzymes (Lane et al., 2005).

Cu(I), Cd(II), Zn(II) exhibit the closed d^{10} shell electron configuration which explains their similar coordination chemistry. Their lack of ligand field stabilization energy allows these metals to exhibit various coordination geometries (Lan et al., 2009), making them relatively flexible metal centers. Soft acid-soft base theory has been used to describe the high degree of affinity of functional groups such as thiols to these metals (Pearson, 1963). As such, copper and zinc are often found highly coordinated by cysteinyl sulfur groups in proteins.

A number of low molecular weight compounds are involved in maintaining cellular homeostasis for these elements via metal complexation. Cysteine-rich metallothioneins regulate copper and zinc in biological systems (Hamer, 1986). Smaller cysteine containing peptides are also involved in managing these metals. Glutathione, present at millimolar levels in the cell, reconstitutes copper into some enzymes (Ciriolo et al., 1990) and is produced by algae under copper and cadmium stress (Ahner et al., 2002). Phytochelatin, an enzymatically produced

oligomer of glutathione, is involved in cadmium detoxification. There is evidence that these and other similar low molecular weight thiols facilitate the exudation or compartmentalization of cadmium or copper as a complex (Dupont et al., 2004; Mendoza-Cózatl et al., 2010). Furthermore, thiols are observed in surface seawater, supposedly as they are exuded from the cell either in a metal complex as described previously or directly to buffer metals extracellularly (Van Den Berg et al., 1988; Al-Farawati and Van Den Berg, 2001; Dupont et al., 2006; Dryden et al., 2007).

Ligands may serve as enhancers or limiters of metal bioavailability. In the case of copper, complexation is thought to reduce bioavailability of this potentially toxic element in surface seawater (Coale and Bruland, 1988). In the case of iron, siderophores facilitate the uptake of this resource that is found at low levels in surface sea water (Vraspir and Butler, 2009). The chemical structure of these complexes is important in influencing bioavailability. Complexes of Zn(II)-cysteine are more bioavailable than EDTA, likely due to their ability to form a ternary complex with zinc transporters (Aristilde et al., 2012). Protonation of the amine group of the natural siderophore desferrioxamine B, is necessary for molecular recognition of the desferrioxamine B-iron complex with a macrocyclic host (Tristani et al., 2009).

Nuclear magnetic resonance, electron paramagnetic resonance, and various spectroscopic techniques have examined the coordination of Cu(I) (Corazza et al., 1996; Rigo et al., 2004), Cd(II) (Perrin and Watt, 1971; Belcastro et al., 2009; Mah and Jalilehvand, 2010) and Zn(II) (Vallee and Auld, 1990; Foley and Enescu, 2007) by cysteine and glutathione. Typically these studies were performed at metal and ligand concentrations much higher than those found under biological conditions. At these concentrations these techniques are likely to observe

polymeric or other highly coordinated metal-ligand complexes that, while chemically fascinating, are likely not biologically or environmentally relevant.

Our study here uses gas-phase computational models and aquatic speciation calculations to investigate the structure, protonation, and distribution of Zn(II), Cd(II) and Cu(I) complexes of the thiols cysteine, GSH, Arg-Cys and Gln-Cys (Figure 1). The latter two, Arg-Cys and Gln-Cys, are novel copper binding ligands which are produced and exuded under copper stress by a marine alga (Dupont et al., 2004). Additionally, we explore coordination by individual functional groups that may improve the complex's stability. While some computational studies have explored the structure of these and similar complexes (Hoyau and Ohanessian, 1997; Foley and Enescu, 2007; Belcastro et al., 2009), we aim to understand the effect of protonation on the stability of certain complexes. This study complements the previous chapter seeking to provide a theoretical explanation for the affinity demonstrated by some metal-thiol complexes, as well as support observed differences in protonation likelihood between divalent and monovalent complexes.

3. Methods

3.1. Density functional theory calculations

Density functional theory (DFT) B3LYP structural models (Lee et al., 1988; Becke, 1993) were used to predict the coordination chemistry, relative stability of complexes, and complexation energies. The effective core potentials of Hay and Wadt (1985) were employed on metals using the LACV3P basis set that includes 6-311G basis set for the nonmetallic atoms. Effective core potentials were used to minimize computational time. The triple-zeta 6-311G was

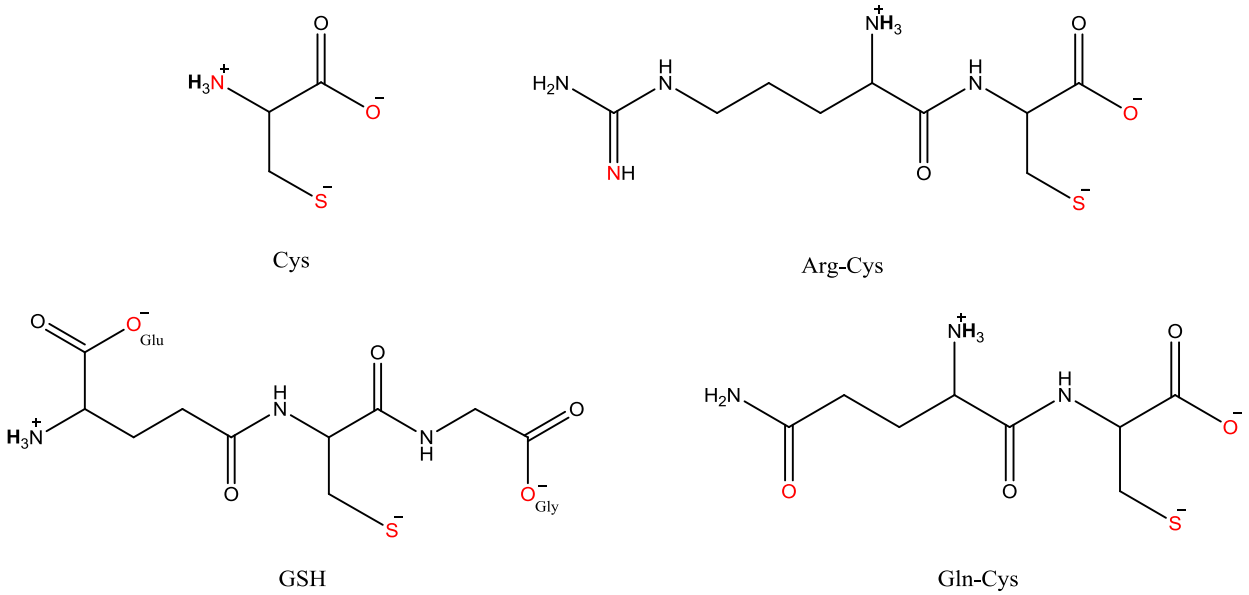

Figure 1. Chemical structures of Cysteine (Cys), Arginine-Cysteine, (Arg-Cys), Glutathione (GSH), and Glutamine-Cysteine (Gln-Cys). Minimizations were performed on structures with and without terminal amine protonation (bolded H). Candidate structures for DFT optimization were developed by coordinating the metal ion with various combinations of atoms highlighted in red.

used to allow for molecular flexibility. We examined cysteine complexes with and without polarization and diffuse functions. For cysteine, application of these functions did not change the relative differences between species (Figure 2) and resulted in an average energy benefit of 88.7± 4.6 kcal/mol. To save computational time no polarization or diffuse functions were applied to the dipeptide or dipeptide models.

Only species with 1:1 stoichiometric ratios were modeled. Schrodinger Jaguar 7.8 (Schrodinger LLC, 2011) was used to optimize structures. All candidate structures were created with a thiol-metal bond. As the peptides contain multiple functional groups, and multiple rotatable bonds, we constructed models that coordinated the metal using the various available functional groups. Coordination sites on each ligand are highlighted in Figure 1. Specific coordination by functional groups is described herein by abbreviations listed in Table 1. Additionally protonated and unprotonated amines are abbreviated as $–NH_3^+$ and $–NH_2$ respectively.

For each optimized complex an overall binding energy (E_B) was calculated using:

$$E_B = E_{ML} - (E_{M^+} + E_L) \qquad 1$$

Where E_{ML}, E_{M^+}, and E_L are the optimized gas phase energies of the metal-ligand complex, the metal, and the ligand respectively. Energies of protonation were determined from the differences in the average energies of binding for protonated complex and its unprotonated counterparts:

$$\overline{E_H} = \overline{E_{BH}} - \overline{E_{B^-}} \qquad 2$$

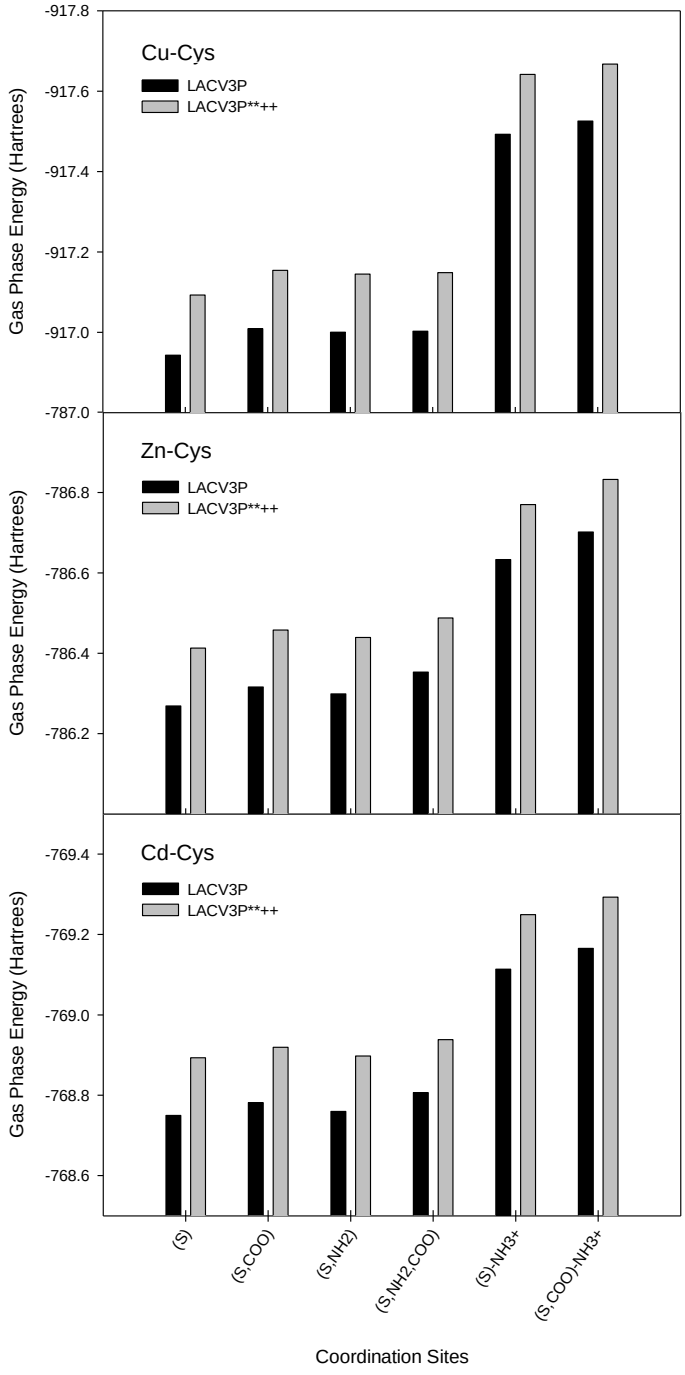

Figure 2. Gas phase optimized energies of Cysteine-metal complexes with different coordination sites. Grey bars indicate calculations that used diffuse (**) and polarization (++) functions on all atoms.

Table 1. Shorthand used to identify metal coordination sites of ligands used in this study.

Functional Group	**Ligands**	**Shorthand**
Thiol	All	S
Terminal Amine	Cys	N
Terminal Carboxyl	Cys, Arg-Cys, Gln-Cys	COO
Glycyl Carboxyl	GSH	COO-Gly
γ-Glutamyl Carboxyl	GSH	COO-Glu
Guanidine	Arg-Cys	GuN
Amide	Gln-Cys	CNO

4. Results and Discussion

4.1. Density functional theory calculations: General considerations

We turned to theoretical methods to provide further evidence for the difference between the proton affinities of divalent and monovalent metal complexes of cysteine and glutathione. To investigate if structure or complex energetics explained this discrepancy, we employed hybrid density functional theory (DFT) optimization calculations at the B3LYP level. All initial candidate structures included thiol metal-coordination. Additional coordination sites were included depending on the ligand, and included available carboxyl groups, a terminal guanidine nitrogen for Arg-Cys, and the amide oxygen for Gln-Cys (Figure 1). We also evaluated amine coordination with cysteine. Candidate structures exhibiting carboxyl coordination were constructed with the metal center being coordinated by a single oxygen atom unless otherwise stated. In almost all optimizations, structures of Zn and Cd complexes were nearly identical in conformation and in relative energy differences. This is especially interesting given that the stability constants of these molecules are relatively similar.

Optimized structures of all candidate structures for cysteine are presented in Figure 3 ($–NH_2$) and Figure 4 ($–NH_3^+$). Lowest energy structures for GSH, Arg-Cys and Gln-Cys are presented in Figure 5, Figure 6, and Figure 7, respectively. Relative binding energies for all structures are presented in Figure 8. Lowest energy optimized structures of Zn(II) and Cd(II) generally exhibited coordination by three functional groups, while those of Cu(I) generally exhibited coordination by two groups. In all cases the coordination by a functional group substantially lowered the binding energy over coordination by just the thiol (S). We also observed that Cd(II) and Zn(II) complexes would coordinate to a peptidyl carbonyl group in

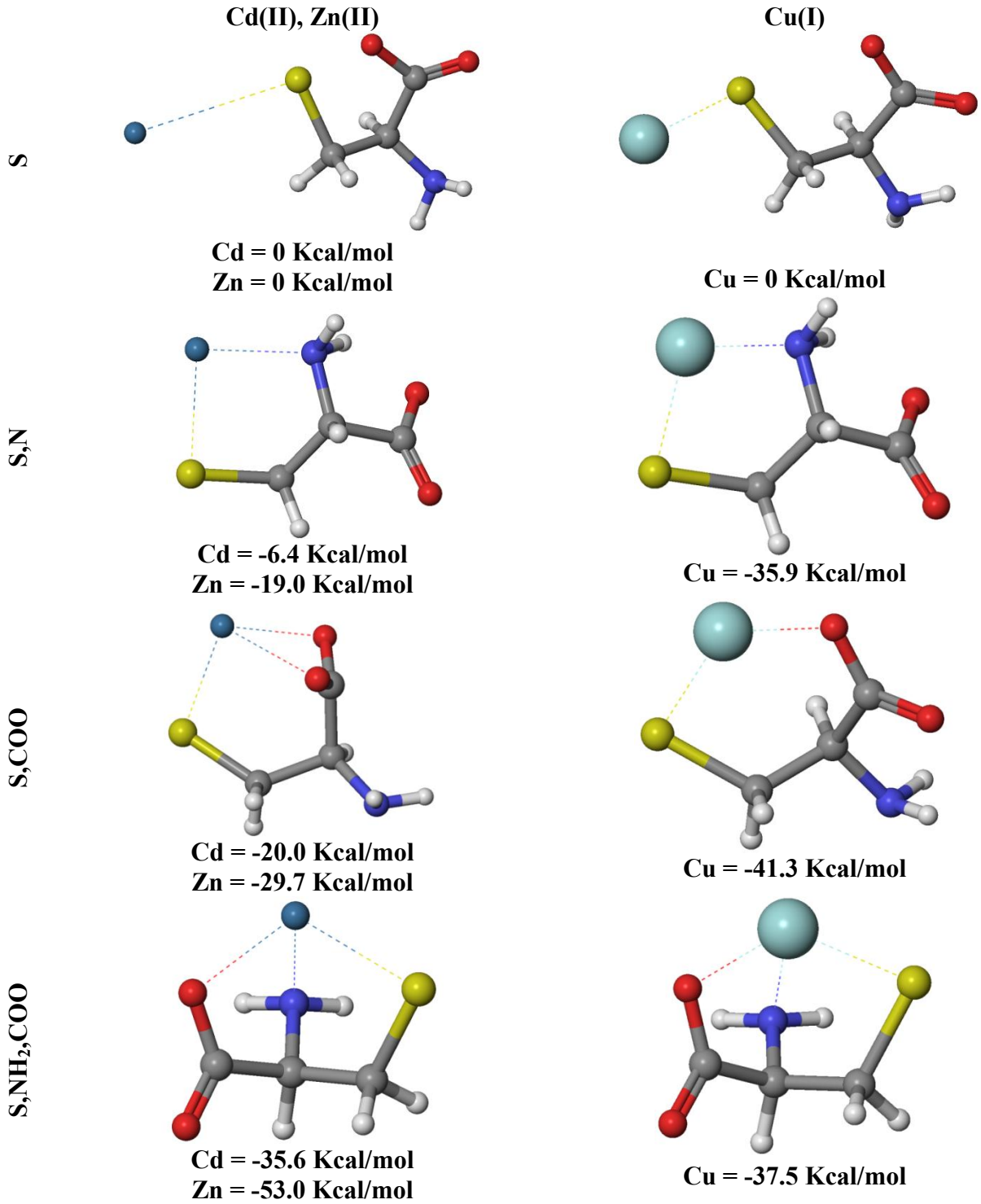

Figure 3. Optimized structures of cysteine metal complexes with energies relative to the highest energy state complex. Figures in left column are of cadmium, but represent the general conformation of zinc cysteine complexes as well.

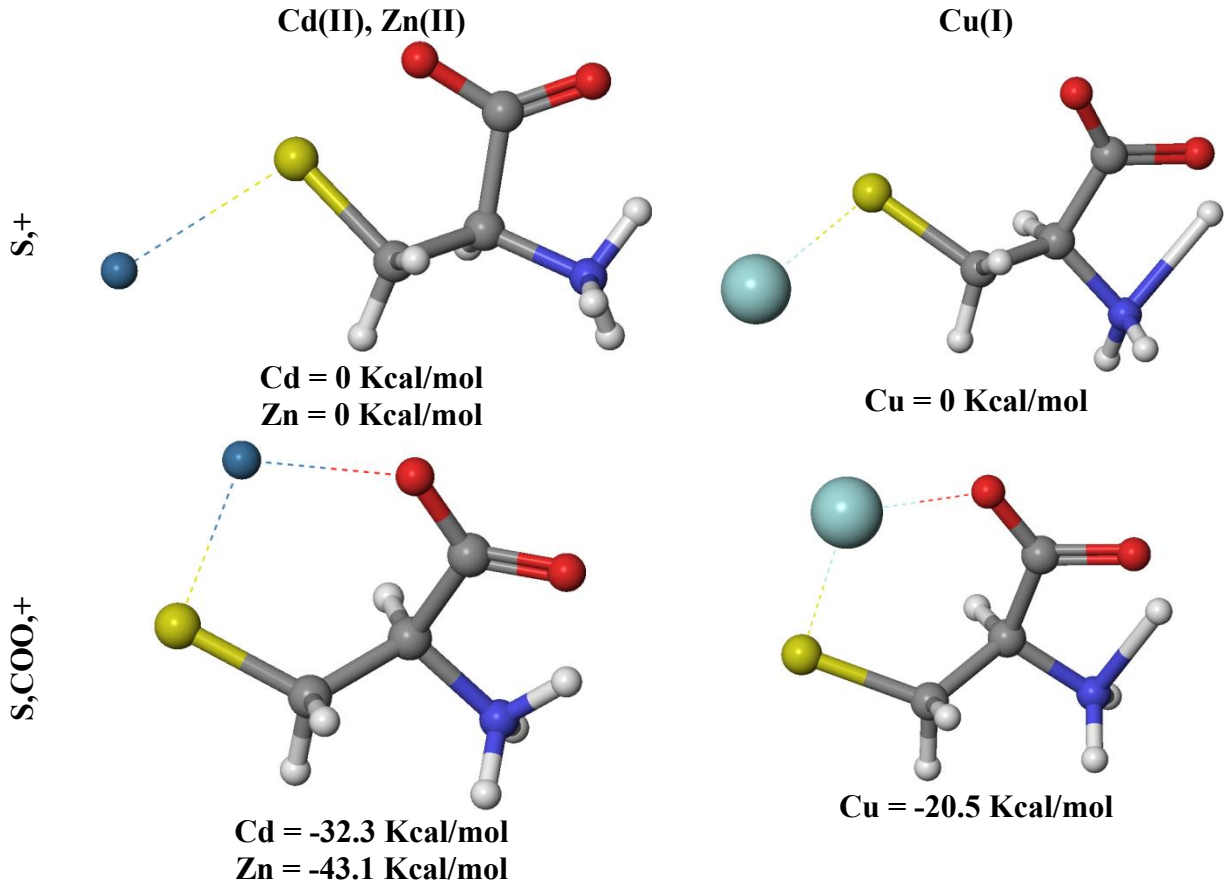

Figure 4. Protonated cysteine metal complexes with energies relative to highest state energy complex. Figures in left column are of cadmium, but represent the general conformation of zinc cysteine complexes as well.

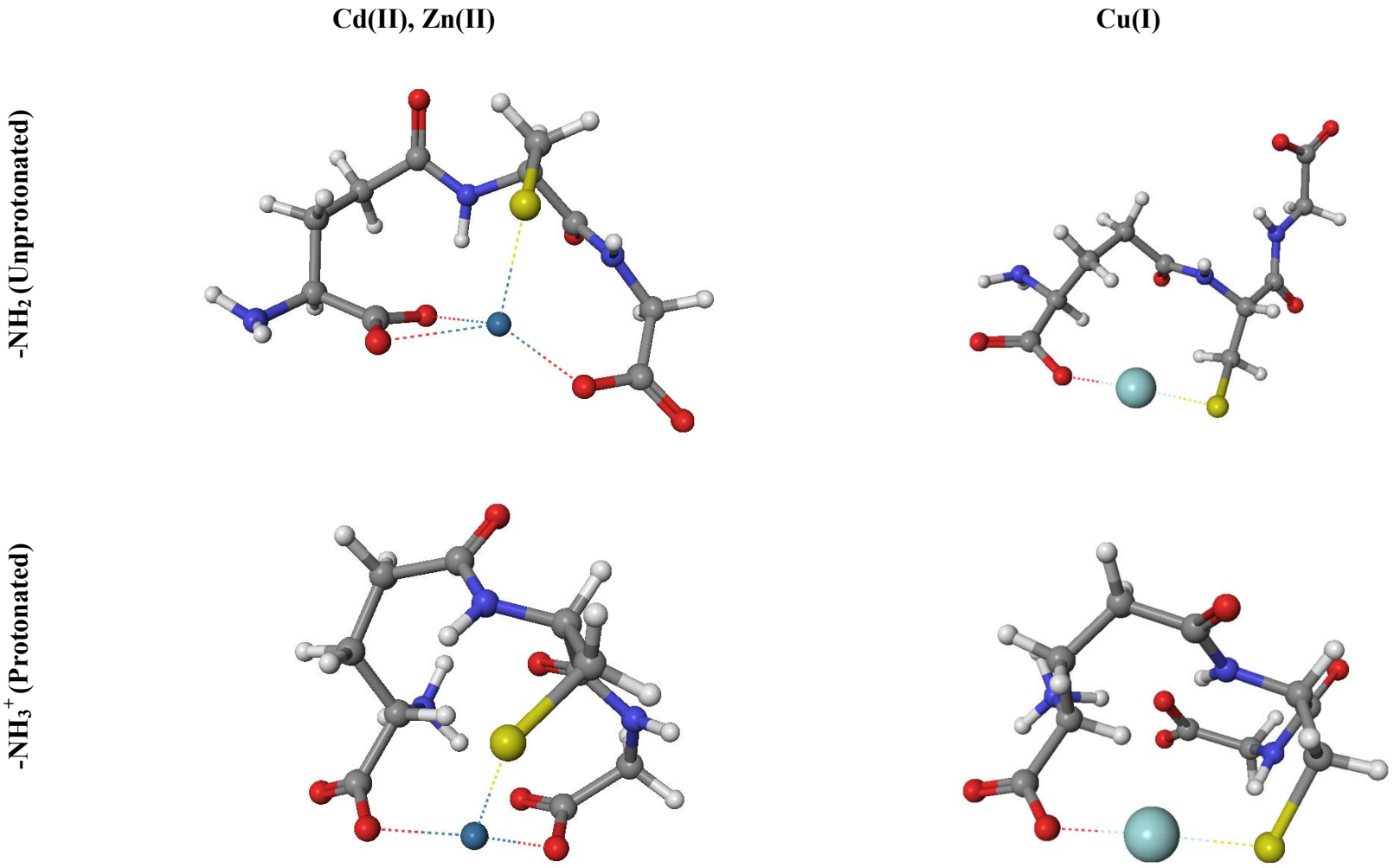

Figure 5. Lowest Energy Structures of GSH

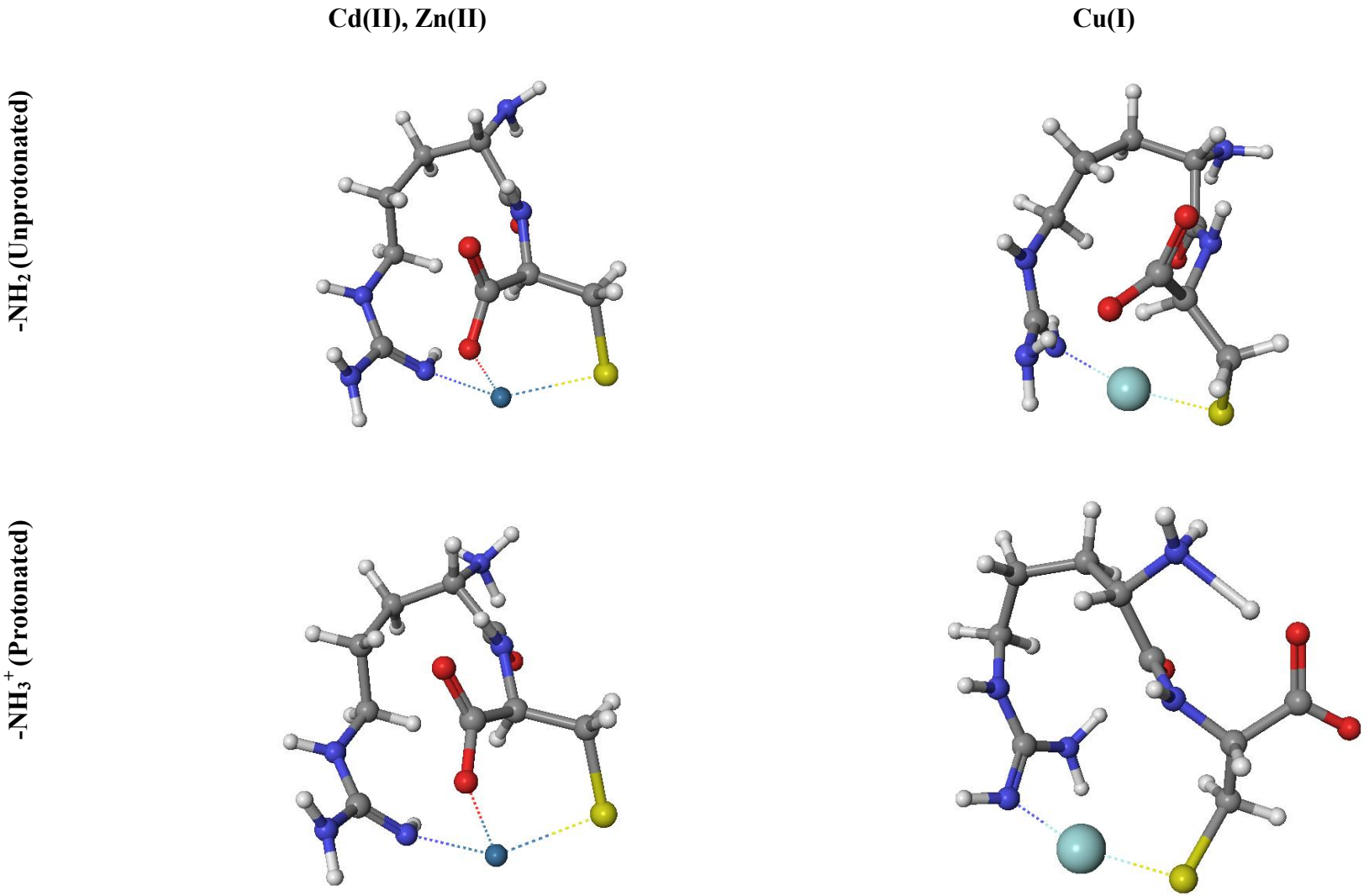

Figure 6. Lowest Energy Structures for Arg-Cys

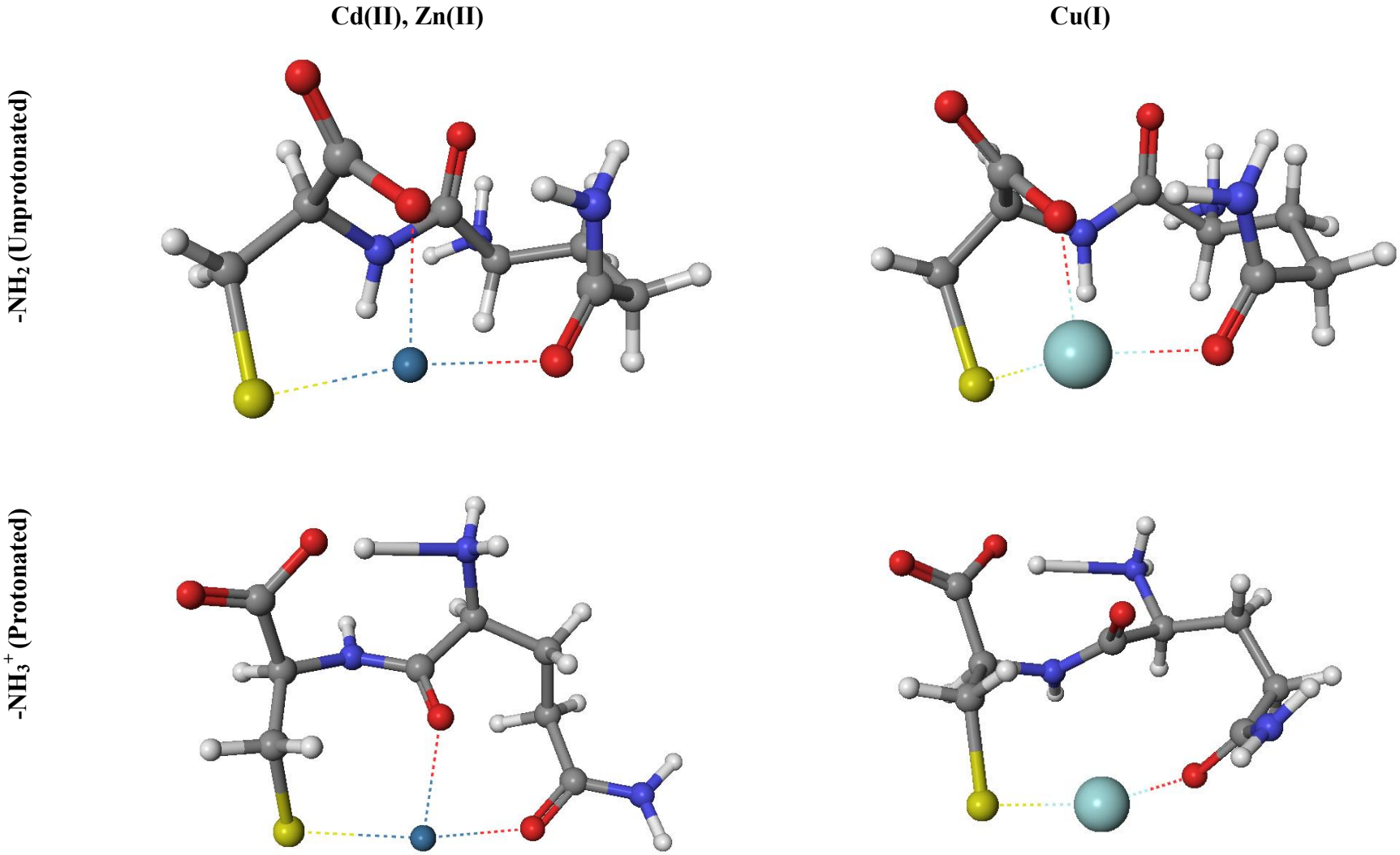

Figure 7. Lowest Energy Structures of Gln-Cys

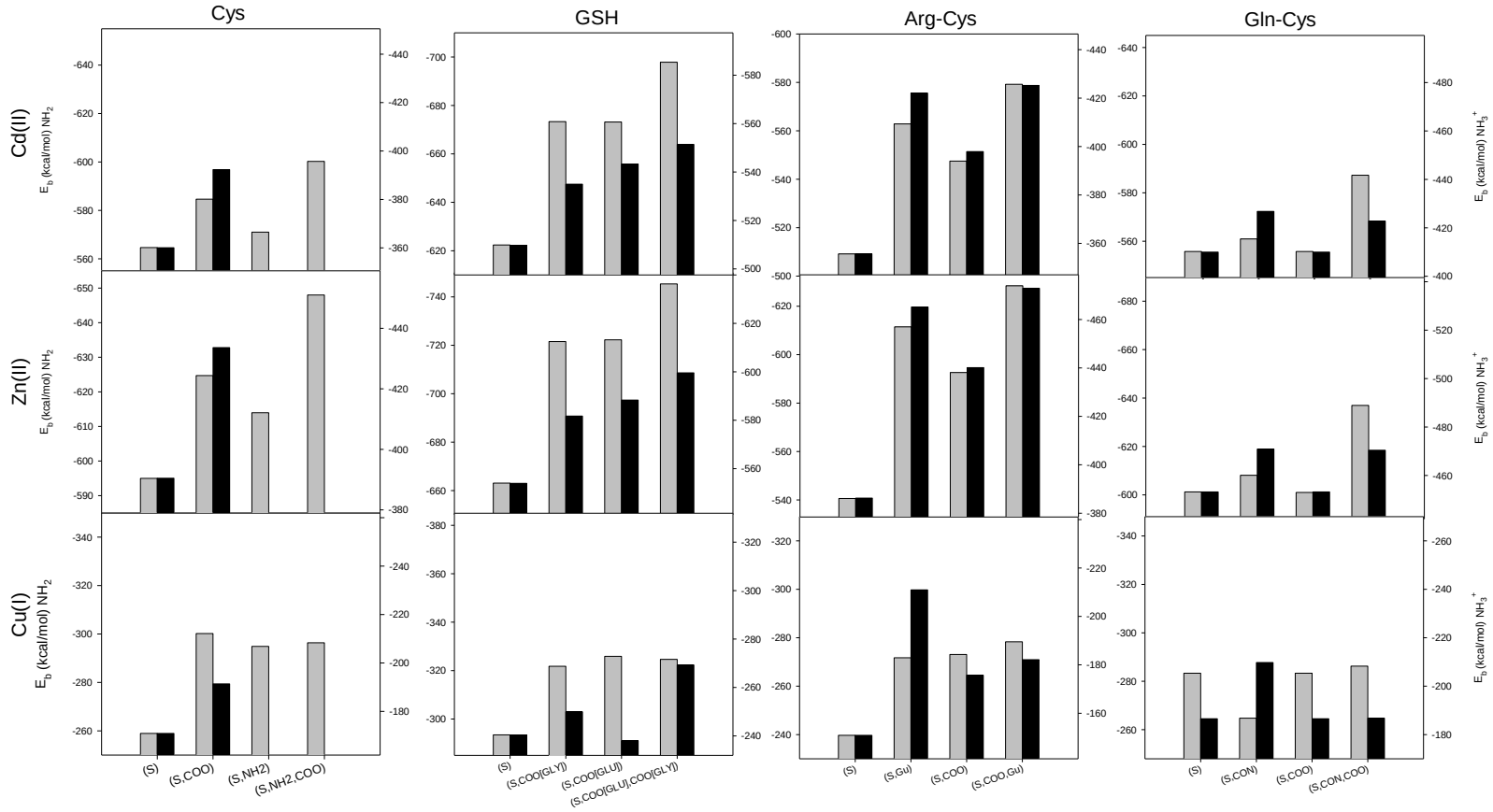

Figure 8. Metal-ligand binding energies E_B for thiol metal complexes included in this study. Grey bars represent unprotonated ($-NH_2$) species, which are scaled to the left axes. Black bars are E_B for species with the terminal amine protonated ($-NH_3^+$) with energies scaled on the right axes. Scales are adjusted to align energy values for (S) conformers of ($-NH_2$) and ($-NH_3^+$). Intervals in each graph are equal to show relative energy differences between conformers. All axes have a range of 100 kcal/mol. *Neither the protonated nor the protonated species converged on a true triply coordinated species.

several instances.

We ran optimizations of Cu(II)-cysteine complexes to discern if the geometry and energy differences were a function of the charge (not shown). In aqueous systems, these complexes are not stable as the thiol donates an electron to Cu(II) reducing it to Cu(I) and oxidizing the thiol. However, gas phase calculations may still be used to explain differences between the divalent metals and the monovalent Cu(II). Like the other divalent metals, Cu(II)-cysteine complexes also favored three coordinate conformers which suggests that the charge of the metal center has an impact on the number of coordination sites.

4.2. Cysteine

For $-NH_2$ cysteine, optimizations were performed on complexes with the metal coordinated solely to the thiol (S), the thiol and the carboxylic acid (S,COO), the thiol and the amine (S,N), and all three functional groups (S,N,COO) (Figure 3, Figure 8). For Cd(II) and Zn(II), the fully coordinated form (S,N,COO) was the most energetically favored, followed by the (S,COO), (S,N), and (S) bound conformers respectively. In contrast, all three multi-coordinated copper species showed very similar energy benefits over the singly coordinated species with the (S,COO) conformer being the most favored. The geometry of the Cu(I)-(S,COO) optimized complex differed from the Zn(II), Cd(II), and Cu(II) (not shown) (S,COO) structures. In this structure Cu(I) is coordinated by one oxygen, coplanar with the carboxylic group while the divalent ions were coordinated by both carboxylic oxygen atoms. Initial alignment of the carboxylic group had no effect on the final optimized structure.

Protonated cysteine complexes favored the (S,COO) coordination scheme over (S) for all

metals (Figure 4). With all metals, the geometry of the (S,COO) complex optimized on the single oxygen conformation, with the metal in coplanar arrangement with the carboxylic acid group. In the case of copper, the extra proton became dislocated, effectively forming a bond with the outward oxygen.

A Raman spectroscopy study of the $Zn(Cys)_2$ complexes demonstrated that both the sulfur and nitrogen groups become unprotonated upon the addition of Zn(II) and that the carboxyl group is involved in coordination (Foley and Enescu, 2007). It is likely that the same groups are involved in complexation in the mono complex. Solid state coordination of Cd(II) has been observed by the cysteinyl sulfur and oxygen (Jalilehvand et al., 2009) or by chloride and the cysteinyl sulfur and oxygen (Faget O et al., 2005). Given these observations as well as the theoretical and experimental similarities with Zn-cysteine complexes, cadmium will likely form a similar coordination scheme.

4.3. Glutathione

Preliminary structures for GSH were constructed with the metal coordinated solely to the thiol (S) as well as the gylcyl carboxylic acid (S,COO[GLY]), the glutamate carboxylic acid (S,COO[GLU]), and both carboxylic acids (S,COO[GLY],COO[GLU]). Complexes with and without glutamyl amine $-NH_3^+$, were considered. Protonation resulted in changes to the relative binding energy (Figure 8) and complex geometry (see Figure 5 for lowest energy example). The optimized (S), (S,COO[GLY]), and (S,COO[GLY]) Cd(II) and Zn(II) conformers of both protonation states demonstrated a geometry where the metal was coordinated by either the cysteinyl-carbonyl or the glutamyl δ-carbonyl group (not shown). This was in addition to the

coordination by the candidate functional groups and indicated a preference by Cd(II) and Zn(II) for coordination by three functional groups. Carbonyl-coordination was not observed with any of the analogous structures of Cu(I). Complexes of Cu(I) furthermore preferred a 2-point coordination causing. As a result the Cu(I)-(S,COO[GLY],COO[GLU]) complex was not stable as the glycyl-carboxylic acid group dislocates from the metal and forms a hydrogen bond with the terminal amine group, subsequently resulting in a geometry that is an alternate form of (S,COO[GLU]) conformation.

The lowest energy states for Zn(II) and Cd(II) were observed with the (S,COO[GLY],COO[GLU]) conformer for both $-NH_3^+$ and $-NH_2$ species (Figure 5). The lowest energy structures for unprotonated complexes of Cu(I) did not significantly vary in binding energies (Figure 8). The addition of a proton disrupted this arrangement and resulted in a lowest energy structure that exhibited (S, COO[GLY]) coordination. This change in conformation occurred despite the fact that the candidate structure for this optimization was of the (S,COO[GLY],COO[GLU]) coordination scheme.

In an evaluation of potentiometric data, Perrin (Perrin and Watt, 1971) suggested that Zn(II) was coordinated by (S, COO[GLU], N) as well as weakly by a peptide nitrogen. NMR work (Fuhr and Rabenstein, 1973; Ferretti et al., 2007) clarified this observation by suggesting that (S) is the primary coordination site for Cd(II), Zn(II), and Hg(II). While Hg(II) doesn't undergo any further coordination, Cd(II) and Zn(II) coordination by other sites is highly variable, and pH dependent, with any amine coordination increasing with pH. At high concentrations and at solid state, Cd(II) is coordinated primarily by sulfur and secondarily by oxygen (Mah and Jalilehvand, 2010). An NMR study of Cu(I)-GSH complexes indicated that Cu(I) coordination is

likely facilitated only by thiol (Corazza et al., 1996).

4.4. Arg-Cys

Arg-Cys structures were constructed for (S), (S,COO), (S,Gu), and (S,COO,Gu) coordination. Metal coordination to the Gu group was through terminal nitrogen that was also bound to single hydrogen and the central guanidine carbon. The same arrangement of Gu coordination of Cu(I) has been used in a previous theoretical study (Corazza et al., 1996). As with GSH, the lowest energy structures of Zn(II) and Cd(II) complexes exhibited a three point (S, COO, Gu) coordination (Figure 6). Furthermore, the (S, COO) and (S, Gu) structures of Zn(II) and Cd(II) optimized to a three point coordination that included peptidyl-carbonyl group, although these were not as energetically favorable as the (S, COO, Gu) coordination. Protonation had no effect on the overall geometries of Cd(II) and Zn(II) complexes, however protonation caused significant changes in those of Cu(I). In general, the relative binding did not change for the optimized structures of Cu(I) candidates. Protonation of the (S, Gu) conformer appeared however, to be highly favored. This was likely due to the formation of a hydrogen bond between the peptide's amino and carboxyl groups (Figure 6). Theoretical optimizations of the Cys-Leu-Arg peptide binding to copper showed similar behavior and was substantiated by parallel mass spectrometry of copper complexed to peptide that contained this sequence (Wu et al., 2010)

4.5. Gln-Cys

Initial geometries for Gln-Cys complexes were constructed for (S), (S,COO), (S,CON), and (S,CON,COO) species. Candidate structures of Gln-Cys that explored amide coordination

utilized an O-Cu binding scheme. Despite soft acid-base theory indicating that Cu(I) preferentially binds to nitrogen, delocalization of nitrogen's loan pair results in increased electronegativity on the oxygen and a positive polarization on the nitrogen. As a result, the glutamyl-oxygen is frequently observed as a copper ligand in Class II Type I copper proteins (Pavelka and Burda, 2008).

Complexes of Zn(II) and Cd(II) again demonstrated a preference for three point coordination. Protonation of the complex however, resulted in a switch in the lowest energy structures from a (S, COO, CON) to a (S, CON)- carbonyl coordination (Figure 7). Optimization of the unprotonated Cu(I)-(S) structure resulted in a geometrically identical structure to that of unprotonated Cu(I)-(S, COO). As such, the E_B of this structure (Figure 8) is not baseline representative of (S) coordination, and also was more stable than the (S, CON) conformation. Additionally, the most optimal conformation was that of (S, SOO, CON), which is the only case of a triply coordinated Cu(I) complex exhibiting the lowest E_B, albeit only slightly more favored than the others Gln-Cys-Cu(I) complexes. In the case of $-NH_3^+$ complexes, the (S, CON) structure exhibited the lowest energy as well as a two point coordination scheme.

4.6. Complex protonation

Linking E_B values to metal-ligand affinity is difficult due to the potential difference between complex behavior in the gas and aqueous phases (Cohen et al., 2008). We are hesitant to equate metal affinity (K) to E_B, due to these limitations associated with DFT and transition metals. However, from our analysis we saw several patterns arise regarding protonation of the complex. In particular, protonation appears to have a large effect on the geometry and E_B of

Cu(I) complexes. To investigate the effect of protonation on overall complex stability, we calculated the energy of complex protonation (Equation 2).

Complexes containing Cu(I) consistently showed a lower energy difference than those of Zn(II) and Cd(II) (Figure 9). For all complexes, cysteine exhibited the highest change in protonation energy. A higher energy requirement for protonation may suggest that the metal is competing with the proton, but also that the proton affinity could be affected by electronic structure changes due to metal complexation. In the peptide complexes, the amide group is less likely to be involved in binding and more likely to be further away from the primary coordinating groups. Average Cu(II)-cysteine protonation energy was 188 kcal/mol (not shown) which is consistent with the values measured for Zn(II) and Cd(II), suggesting that protonation is largely affected by the charge of the metal center.

5. Conclusions

Our theoretical study of the thiol d^{10} metal complexes supports several experimental observations and provides information on the structure of the complexes. The lower energy requirement for Cu(I)-thiol complex protonation is consistent with the favorability of protonated Cu(I)-thiol in aqueous conditions. One reason for this difference may be due to the overall net charge of the copper-thiol which more likely accommodates a proton than that of the divalent metal complexes. Additionally, DFT calculations in the gas phase provide valuable insight into relative degrees of favorability of certain complexes, especially in regard to intramolecular interactions and geometry. These calculations however, neglect potential solvent effects that change how the ligand interacts with the metal in aqueous systems. Given the flexibility of the

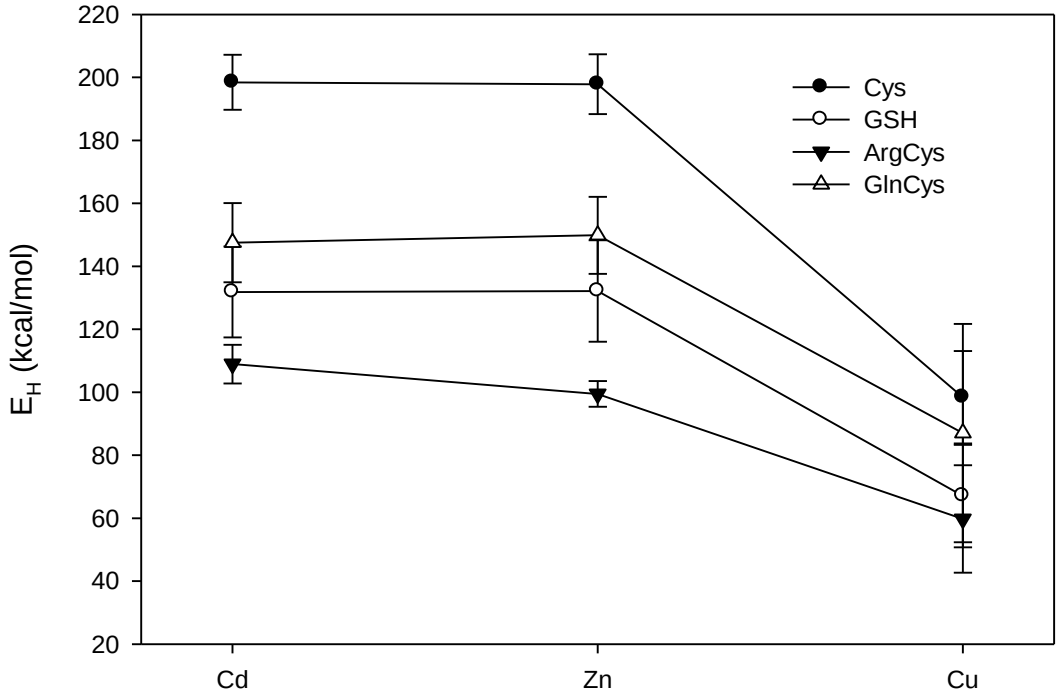

Figure 9. DFT-BP3LY calculated average protonation energy $\overline{E_H}$ of thiol metal complexes. Each point is an average difference of E_B between the $-NH_3^+$ and unprotonated forms of each conformer. Only conformers that were capable of being protonated were considered. Error bars represent the standard deviation of the energy differences.

peptides and the fact that some of the complexes showed only small changes in energy between various coordination schemes, these complexes are not likely to exist in a rigid lowest energy state. Such complex flexibility is more probable in aqueous systems, where water molecules and ternary complexes of many inorganic and organic types are likely to influence coordination and subsequent biochemistry.

6. References

Ahner BA, Wei L, Oleson JR, et al. (2002) Glutathione and other low molecular weight thiols in marine phytoplankton under metal stress. *Marine Ecology-Progress Series* 232: 93-103.

Al-Farawati R and Van Den Berg CMG. (2001) Thiols in coastal waters of the western North Sea and English Channel. *Environmental Science & Technology* 35: 1902-1911.

Aristilde L, Xu Y and Morel FMM. (2012) Weak Organic Ligands Enhance Zinc Uptake in Marine Phytoplankton. *Environmental Science & Technology* 46: 5438-5445.

Becke AD. (1993) *Density?functional thermochemistry. III. The role of exact exchange*: AIP.

Belcastro M, Marino T, Russo N, et al. (2009) The role of glutathione in cadmium ion detoxification: Coordination modes and binding properties – A density functional study. *Journal of Inorganic Biochemistry* 103: 50-57.

Ciriolo MR, Desideri A, Paci M, et al. (1990) Reconstitution of Cu,Zn-Superoxide Dismutase by the Cu(I).Glutathione Complex. *Journal of Biological Chemistry* 265: 11030-11034.

Coale KH and Bruland KW. (1988) Copper Complexation in the Northeast Pacific. *Limnology and Oceanography* 33: 1084-1101.

Cohen AJ, Mori-Sánchez P and Yang W. (2008) Insights into Current Limitations of Density Functional Theory. *Science* 321: 792-794.

Corazza A, Harvey I and Sadler PJ. (1996) 1H,13C-NMR and X-ray absorption studies of copper(I) glutathione complexes. *European Journal of Biochemistry* 236: 697-705.

Das P, Samantaray S and Rout GR. (1997) Studies on cadmium toxicity in plants: A review. *Environmental Pollution* 98: 29-36.

Dryden CL, Gordon AS and Donat JR. (2007) Seasonal survey of copper-complexing ligands and thiol compounds in a heavily utilized, urban estuary: Elizabeth River, Virginia. *Marine Chemistry* 103: 276-288.

Dupont CL, Moffett JW, Bidigare RR, et al. (2006) Distributions of dissolved and particulate biogenic thiols in the subartic Pacific Ocean. *Deep-Sea Research Part I-Oceanographic Research Papers* 53: 1961-1974.

Dupont CL, Nelson RK, Bashir S, et al. (2004) Novel copper-binding and nitrogen-rich thiols produced and exuded by Emiliania huxleyi. *Limnology and Oceanography* 49: 1754-1762.

Faget O G, Felcman J, Giannerini T, et al. (2005) Fourier-transform infrared and Raman spectra of cysteine dichloride cadmium(II) anion: DFT: B3LYP/3-21G(d) structural and vibrational calculations. *Spectrochimica Acta Part A: Molecular and Biomolecular Spectroscopy* 61: 2121-2129.

Ferretti L, Elviri L, Pellinghelli MA, et al. (2007) Glutathione and N-acetylcysteinylglycine: Protonation and Zn2+ complexation. *Journal of Inorganic Biochemistry* 101: 1442-1456.

Foley S and Enescu M. (2007) A Raman spectroscopy and theoretical study of zinc-cysteine complexation. *Vibrational Spectroscopy* 44: 256-265.

Fuhr BJ and Rabenstein DL. (1973) Nuclear magnetic resonance studies of the solution chemistry of metal complexes. IX. Binding of cadmium, zinc, lead, and mercury by glutathione. *J. Am. Chem. Soc.* 95: 6944-6950.

Hamer DH. (1986) Metallothionein1,2. *Annual Review of Biochemistry* 55: 913-951.

Hay PJ and Wadt WR. (1985) Ab initio effective core potentials for molecular calculations.

Potentials for K to Au including the outermost core orbitals. *The Journal of Chemical Physics* 82: 299-310.
Hoyau S and Ohanessian G. (1997) Complexation of small organic molecules by Cu+. *Chemical Physics Letters* 280: 266-272.
Jalilehvand F, Mah V, Leung BO, et al. (2009) Cadmium(II) Cysteine Complexes in the Solid State: A Multispectroscopic Study. *Inorganic Chemistry* 48: 4219-4230.
Lan Y-Q, Li S-L, Fu Y-M, et al. (2009) Syntheses, Structures, and Luminescent Properties of Zinc(II) and Cadmium(II) Coordination Complexes Based on Different (Pyridyl)imidazole Derivatives and 1,4-Benzenedicarboxylate. *Crystal Growth & Design* 9: 1353-1360.
Lane TW, Saito MA, George GN, et al. (2005) A cadmium enzyme from a marine diatom. *Nature* 435: 42-42.
Lee C, Yang W and Parr RG. (1988) Development of the Colle-Salvetti correlation-energy formula into a functional of the electron density. *Physical Review B* 37: 785.
Mah V and Jalilehvand F. (2010) Cadmium(II) complex formation with glutathione. *Journal of Biological Inorganic Chemistry* 15: 441-458.
Mendoza-Cózatl DG, Zhai Z, Jobe TO, et al. (2010) Tonoplast-localized Abc2 transporter mediates phytochelatin accumulation in vacuoles and confers cadmium tolerance. *Journal of Biological Chemistry* 285: 40416-40426.
Pavelka M and Burda JV. (2008) Computational study of redox active centres of blue copper proteins: a computational DFT study. *Molecular Physics* 106: 2733-2748.
Pearson RG. (1963) Hard and Soft Acids and Bases. *Journal of the American Chemical Society* 85: 3533-&.
Perrin DD and Watt AE. (1971) Complex formation of zinc and cadmium with glutathione. *Biochimica et Biophysica Acta (BBA) - General Subjects* 230: 96-104.
Rigo A, Corazza A, di Paolo ML, et al. (2004) Interaction of copper with cysteine: stability of cuprous complexes and catalytic role of cupric ions in anaerobic thiol oxidation. *Journal of Inorganic Biochemistry* 98: 1495-1501.
Schrodinger-LLC. (2011) Jaguar 7.8. New York, NY.
Tristani E, Dubay G and Crumbliss A. (2009) Characterization of second coordination shell ionophore–siderophore host–guest assemblies and binding selectivities in binary and complex mixtures by electrospray ionization mass spectrometry. *Journal of Inclusion Phenomena and Macrocyclic Chemistry* 64: 57-65.
Vallee BL and Auld DS. (1990) Zinc coordination, function, and structure of zinc enzymes and other proteins. *Biochemistry* 29: 5647-5659.
Van Den Berg CMG, Househam BC and Riley JP. (1988) Determination of cystine and cysteine in seawater using cathodic stripping voltammetry in the presence of Cu(II). *Journal of Electroanalytical Chemistry and Interfacial Electrochemistry* 239: 137-148.
Vraspir JM and Butler A. (2009) Chemistry of Marine Ligands and Siderophores. *Annual Review of Marine Science* 1: 43-63.
Wu Z, Fernandez-Lima FA and Russell DH. (2010) Amino Acid Influence on Copper Binding to Peptides: Cysteine Versus Arginine. *Journal of the American Society for Mass Spectrometry* 21: 522-533.

CHAPTER 3

Discerning Copper Uptake and Export in Marine Algae Using Stable Isotopes

1. Abstract

Previous studies have demonstrated that the coccolithophore *Emiliania huxleyi* exhibits lower cellular copper concentrations than many other species of marine algae in absolute, volume-normalized and phosphorus-normalized terms. Furthermore *E. huxleyi* also exhibits high tolerance to levels of copper that are toxic to many other species. We demonstrate that in comparison to the diatom *Thalassiosira pseudonana*, *E. huxleyi* maintains substantially lower quotas, intracellular concentrations and net steady state uptake rates even when grown under very high (10 µM) copper concentrations. *E. huxleyi* also maintains lower net uptake rates over the course of four hours of exposure to copper. The stable isotope ^{65}Cu was used as an uptake tracer. Based on changes in cellular the isotopic ratio, gross isotope uptake was larger than net isotope uptake, suggesting that internalized copper was being rapidly effluxed from *E. huxleyi*. No significant divergence in net and gross uptake was observed in *T. pseudonana*. A two box model was used to confirm this behavior and estimate uptake rates. Copper limited *E. huxleyi* cells were able to attain higher levels of net uptake than replete cultures despite similar net uptake rates, suggesting that efflux is modulated by cellular copper levels. Direct measurement of export from copper loaded cells provided further evidence of a very active efflux mechanism in replete *E. huxleyi*. A novel cellular wash that employed a dithiothreitol-DTPA mixture improved removal of surface bound copper compared to other commonly used rinses.

2. Introduction

Copper is both an essential micronutrient and potentially toxic for marine phytoplankton. As a nutrient it serves a cofactor for a number of ubiquitous enzymes such as the reactive oxygen scavenging superoxide dismutase, the electron transport protein plastocyanin and cytochrome *c* oxidase which facilitates respiration. At high concentrations, copper can itself produce reactive oxygen species or interrupt the assimilation and use other essential cofactors (Sunda and Huntsman, 1998). In the ocean, levels of bioavailable ionic copper can range from those which are limiting (Coale and Bruland, 1988; Moffett and Dupont, 2007) to levels that are toxic (Brand et al., 1986; Mann et al., 2002). This is of particular importance to marine algae as copper is a requirement for iron transport (Peers et al., 2005). Tolerance of high copper concentrations varies significantly across several species of marine algae (Sunda and Huntsman, 1995b) with cyanobacteria being especially sensitive (Mann et al., 2002). Subsequently, copper levels can have an impact on the composition of phytoplankton communities (Moffett et al., 1997).

To maintain homeostasis organisms have developed mechanisms such as uptake regulation, buffering, storage and exclusion to combat high copper concentrations (Nevitt et al., 2012). The implementation (Croot et al., 2000) and effect (Ho et al., 2003) of some of these strategies varies widely across organisms. The globally abundant coccolithophore, *Emiliania huxleyi* maintains a very low copper quotas when compared to other species (Ho et al., 2003; Guo et al., 2012). *E. huxleyi* also exhibits an extraordinarily high tolerance to copper (Brand et al., 1986). While some diatoms such as *T. pseudonana* also exhibit high tolerance, *T. pseudonana* maintains a higher cellular quota of copper. Such differences may be important to understanding the ecological drivers of algae. Given these differences we sought to explore

uptake and export mechanisms in these two species to explain their differences.

Copper uptake in algae follows Michaelis-Menten kinetics (Croot et al., 2003), with both high affinity and low affinity transport systems (Hill et al., 1996; Guo et al., 2010). Other studies have demonstrated rapid assimilation over short periods (Vasconcelos and Leal, 2000; Quigg et al., 2006). High affinity copper uptake is likely facilitated by the ubiquitous Ctr family of transporters which is regulated by copper sensing mechanisms and is ubiquitous in eukaryotes (Nevitt et al., 2012). This process facilitates the transport of Cu(I) across the membrane and thus requires the reduction of available Cu(II). However, in surface seawater, the concentration of bioavailable copper is lowered by the presence of ligands of biological origin (Coale and Bruland, 1988; Moffett, 1995). The mechanism of ligand production and subsequent complexation of copper has yet to be fully discerned but such ligands could be: exuded by the cell lower extracellular copper concentrations from toxic to nutritive levels; or, the product of a mechanism that facilitates exclusion of copper via complex formation and subsequent transport similar to what is observed in the detoxification of Cd(II) by phytochelatin in *Thalassiosira weissflogii* (Lee et al., 1996) or yeast (Mendoza-Cózatl et al., 2010). Neither mechanism is mutually exclusive.

The export of copper, either as a complex or ion, from algae is not as well documented as uptake. Copper exclusion proteins have been identified in the genomes of Synechococcus (Stuart et al., 2009) and Ostreococcus (Palenik et al., 2007). Efflux of copper has been experimentally observed from copper loaded *Nostoc calcicola* (Verma and Singh, 1991) and *Synechococcus* (Croot et al., 2003). Observing export as well as export from cells is made difficult by several factors, notably the potential of simultaneous uptake and export, as well as the difficulty of

sequestering exported copper.

We overcome this difficulty in this paper by using the stable isotope, copper-65 (^{65}Cu) as a tracer (Figure 1) to study uptake and export in *E. huxleyi* and *T. pseudonana*. Stable isotopes have been employed in various environmental and physiological systems to measure nutrient assimilation. Copper efflux has been observed in the bivalve *Corbicula fluminea* using a ^{65}Cu tracer (Croteau et al., 2004; Croteau and Luoma, 2005). However this is the first time we are aware of a work that utilizes a stabile isotope tracer in the study of algal metal uptake and export.

The uptake and export of copper from an algal cell can be expressed as:

$$\frac{dCu_{cell}}{dt} = v_u - v_e \qquad 1$$

Where v_u and v_e are the uptake and export rates (concentration time^{-1}), respectively, and may follow Michaelis-Menten kinetics. The absence, delay, or comparably negligible rate of an export mechanism would result an increase in cellular copper and an equivalent change in the isotopic fractionation and ratio of cellular copper. The presence of an export mechanism, as well as some mixing of the cellular copper pool, would cause a divergence in the absolute net assimilation of copper and the gross isotopic assimilation predicted from the change in the cellular isotopic ratio. Our results show a large difference in copper uptake in *E. huxleyi* as measured by gross isotopic assimilation compared to net uptake. This effect is not observed with *T. pseudonana.* Our analytical measurements of cellular copper were also improved by a novel cell washing solution that is more effective than Cu(II) chelators such as EDTA or DTPA used in previous studies of copper uptake.

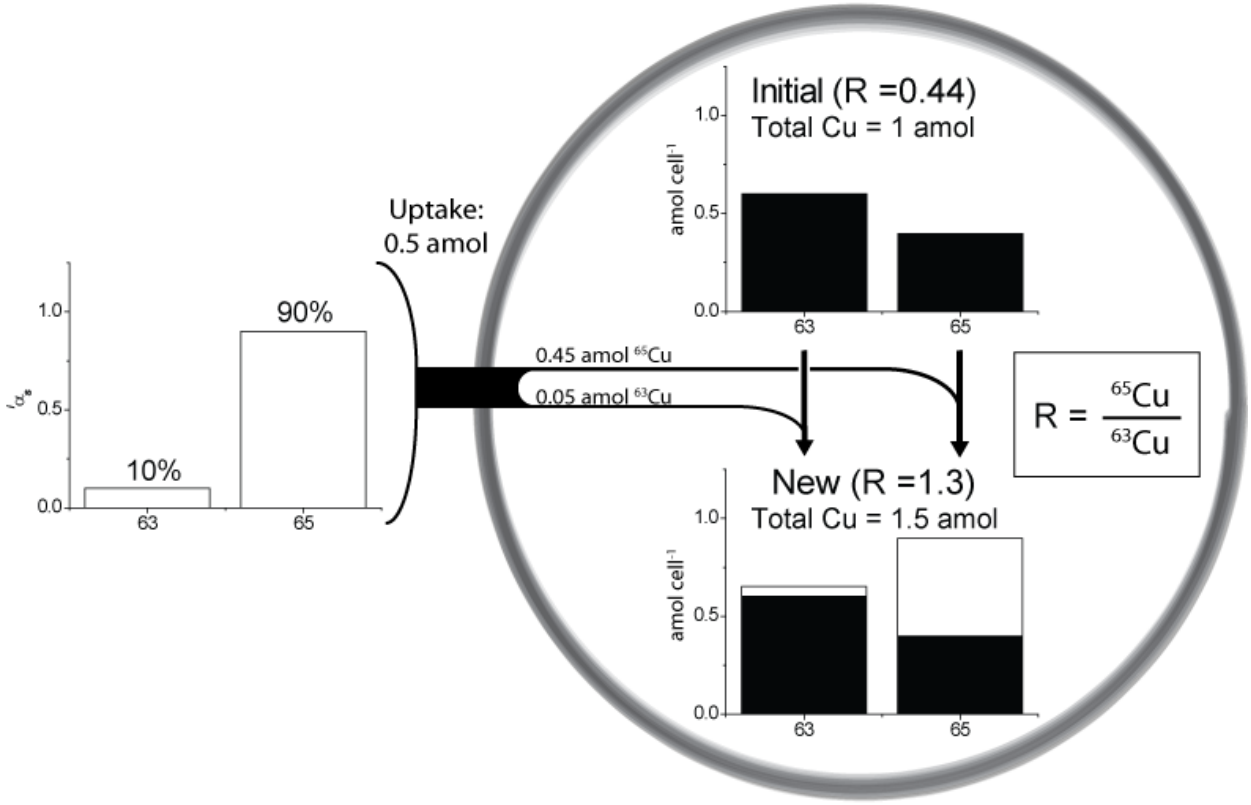

Figure 1. Schematic for uptake of stable isotopes into an algae cell that does not exhibit export. Cells grown under natural copper concentrations (R = 0.44) are exposed to SOW containing isotopically enriched copper spike (90.0% ^{65}Cu). Copper uptake results in the assimilation of spike into the intracellular copper pool increasing the ratio of ^{65}Cu to ^{63}Cu.

3. Methods

3.1. Cultures

The coccolithophore *E. huxleyi* (CCMP 1516) and diatom *T. pseudonana* CCMP 1335 were obtained from the Provasoli-Guillard National Center for Marine Algae and Microbiota (NCMA, Bigelow Laboratory for Ocean Sciences, West Boothbay Harbor, ME, USA). Cell volumes and surface areas were calculated (Table 1) assuming spherical geometry for *E. huxleyi* and cylindrical geometry for *T. pseudonana* using average measurements of cell dimensions provided by the NCMA and used previously by (Quigg et al., 2006; Guo et al., 2010). Axenic cultures of each species were grown in the synthetic ocean water medium Aquil (Price et al., 1989) with some modification of trace metals as described below. All cultures were grown in acid washed polycarbonate bottles under constant lighting conditions of 120 µmol photon m^{-2} s^{-1} at 20°C.

E. huxleyi was grown under reduced iron conditions (Fe_T = 100nM, pFe^{3+} = 20) while *T. pseudonana*, which exhibits reduced growth rates at this concentration (Sunda and Huntsman, 1995a), was grown under high iron conditions (Fe_T = 8.32 µM, pFe^{3+} = 18.1). Both species were grown under replete copper conditions (Cu_T = 20 nM, initial pCu^{2+} = 13.9). Copper limited cultures of both species were grown in reduced iron medium without any added copper for at least three generations. A background copper level of 1 nM (initial pCu^{2+} = 15.2) was estimated from copper measurements of these cells and the assumption that 50% of total copper would be associated with the cells. A similar estimate was made by (Guo et al., 2010). Cultures grown at higher copper concentrations were inoculated with each species in their respective replete Aquil. After three days equimolar Cu(II)-EDTA was added to achieve concentrations from 100 nM to

Table 1. Cellular dimensions and copper quotas measured during exponential growth. Cellular copper quotas measured in cells directly filtered from native Aquil media and rinsed with new rinse procedure.

Species	**Strain ID**	**Cell Volume (μm^3)**	**Surface Area (μm^2)**	**Surface area-to-Volume (μm^{-1})**	**Quota: Cu-limited (amol Cu $cell^{-1}$)**	**Quota: Replete (amol Cu $cell^{-1}$)**
Emiliania Huxleyi	CCMP 1516	144	133	0.92	0.21 ± 0.16	0.78 ± 0.04
Thalassiosira pseudonana	CCMP 1335	80	102	1.29	0.88 ± 0.33	8.86 ± 0.46

Table 2.Isotopic fractions and ratios of natural and isotopically enriched copper. Standard deviations on our measurements are in parentheses.

		R	**$^{63}\alpha$**	**$^{65}\alpha$**
Natural	Observed Range*	0.44221-0.44963	0.68983–0.69338	0.30662–0.31017
	Best Measurement*	0.44563	0.69174	0.30826
	Generally Accepted Value*	0.44613	0.6915	0.3085
	10 ppb measurement	0.4473 ± .016	0.6910 ± .0078	0.3089 ± .0078
Primary Enriched	Predicted (ORNL-Standard)	249	0.004	0.996
	52ppb Measurement	238 ± 52	0.0042 ± 0.0009	0.9958 ± 0.0016
Diluted Spike	Predicted	9	0.1	0.9
	10ppb Measurement	9.25 ± .316	0.0975 ± 0.0033	0.9025 ± 0.0033

*(Berglund and Wieser, 2011)

10 µM. Aquil with no EDTA, trace metal or vitamin amendments (herein referred to as SOW) was used for resuspension and rinses.

Culture growth was monitored in vivo by the fluorescence of *Chl a* (Turner Instruments). Specific growth rates were calculated from a natural log regression of the fluorescence measurements over time. For Cu uptake experiments, cells were collected by centrifugation during mid-exponential phase and resuspended in SOW. *E. huxleyi* and *T. pseudonana* were centrifuged at 7200 RPM and 9000 RPM respectively for 15 minutes at 4°C in 500 mL acid washed polycarbonate centrifuge tubes. *E. huxleyi* cells were rinsed with SOW and resuspended in SOW by light vortexing. *T. pseudonana* cells, which did not pellet as efficiently, were centrifuged a second time at 9000 RPM in 50 mL centrifuge tubes, rinsed with SOW and resuspended in SOW.

3.2. Isotopically enriched copper

Isotopically enriched ^{65}CuO (99.6%) was obtained from Oak Ridge National Laboratory and dissolved in 1mM Ultrapure HCl (Fisher) to a concentration of 124 µM in an acid washed Teflon bottle. A complementary natural isotopic solution was similarly prepared at a concentration of 126 µM. These two solutions were used to make up a 10 µM "spike" solution (90.0% ^{65}Cu) in 0.1M NaCl that had been treated with Chelex (Biorad) to remove trace metals. Concentrations and isotopic fractions were confirmed by ICPMS (Table 2) after making serial dilutions of these stock solutions in 5% ultrapure HNO_3 (Aristar). Two hours prior to each experiment the desired amount of copper spike was diluted into 10mL of trace metal free SOW to allow for equilibration.

3.3. Uptake experiments

Resuspended cells were diluted to biomass concentrations of 0.5 – 1.5 and 1.0 – 3.0 million cells per milliliter for *T. pseudonana* and *E. huxleyi*. These cell densities were consistent with to concentration prior to centrifugation. Resuspensions were made in acid washed polycarbonate bottles filled with SOW from 0.5 – 2.0 L depending on the amount of biomass required for each experiment. Initial (T=0) algal samples for measurement of baseline copper levels and isotope fractionations were immediately taken by collecting cells on an 0.8 µm, 47mm diameter polycarbonate filters (Whatman, Maidstone, UK) that had been acid washed overnight in 1 M ultrapure HCl and rinsed thrice with MilliQ water. Filters were supported on an acid washed polysulfonate funnel filter apparatus (Nalgene, Rochester NY). Between 40 and 125 mL of each sample was filtered in triplicate.

Unless otherwise stated, cells were incubated and washed with 5 mL of a cold SOW solution containing 10 mM diethylenetriaminepentaacetic acid (DTPA, Sigma) and 10 mM dithiothreitol (DTT, Sigma). This solution was made immediately prior to each experiment with freshly dissolved DTT. DTPA was obtained from a 100 mM stock solution prepared in SOW and titrated with Ultrapure NaOH (Fluka) to a pH of 8.1. After 20 minutes of rinse contact, the solution was filtered off and the cells were washed with an additional 10 mL of SOW. Acid washed Teflon forceps were used to fold and place filters into individual, trace metal clean, micro centrifuge tubes which were stored at -20°C until digestion.

Resuspended stock cultures were divided into separate aliquots as required for each experiment. The equilibrated spike solution was added directly to each culture which was immediately and gently shaken to facilitate mixing. Culture bottles were constantly exposed to

light, and during long (>10 mins) intervals between sampling, were stored in the growth chamber. Sampling was performed at various intervals up to four hours using the filtration and washing procedure described above. Duplicate cell counts associated with each stock culture were made using a hemocytometer, cell concentration did not significantly change over the course of each experiment.

3.4. Export experiments

Cultures of *T. pseudonana* and *E. huxleyi* were resuspended in trace-metal-free Aquil exposed to 1000 nM isotopically enriched Cu ($^{65}x = 0.996$, R = 249) for 30 minutes. At this time 100µM DTPA was added to reduce the levels of bioavailable copper in the extracellular media. The culture was then split and one half was cooled to 4°C on an ice bath in a cold room, while the other was kept at 20°C. Filtrations were made of each batch at 60 and 90 minutes after the initial copper addition. Filtered cells were rinsed as described above.

3.5. Copper measurements

Filters were digested in Teflon screw cap vials (Savillex) using 0.8 mL HNO_3 (Aristar Ultra) diluted to 50% with high quality H_2O (Millipore). Vials were heated at 90°C for 8 hours. After the vials had cooled, digests were diluted to 5% HNO_3 using 7.2 mL of ddH_2O and gently mixed. The diluted digests were decanted into acid washed 15 mL centrifuge tubes. To remove undigested silica frustules, diluted digests of *T. pseudonana* were centrifuged at 3000 rpm and the supernatant was pipetted into a fresh centrifuge tube to separate out undigested silica frustules.

Measurements of ^{63}Cu and ^{65}Cu isotopes were made using either an Elan II dynamic reaction cell inductively coupled plasma quadrapole mass spectrometer (DRC-ICP-MS, Perkin Elmer) or an Element II magnetic sector field inductively coupled plasma mass spectrometer (MSF-ICP-MS, Thermo). Copper isotope signals were optimized by adjusting instrumental settings prior to daily analysis or as needed. Elemental standards of natural isotopic abundance (High Purity Standards, Charleston, SC), with concentrations ranging from 1 to 50 ppb were prepared in 5% HNO_3 and compared against other laboratory standards. Separate standard curves were constructed for each isotope. For the DRC-ICP-IMS ammonia gas (Airgas) was used as a collision gas while a solution of 10 ppb gallium was used as an internal standard to monitor for signal stability. When using the MSF-ICP-MS, standard curves were generated every 24 samples and a 5 ppb standard was measured every 6 samples as a quality check, and was used to interpolate a correction factor any signal drift during the course of the run. Using the isotopically enriched copper stock a series of 5 standard isotopic dilutions of copper ranging from natural abundance to 90.0% ^{65}Cu were run on each ICP-MS to measure potential mass bias, which was found to be small (<2%). Analytical errors due to mass bias or instrumental drift were very small in comparison to the biological or replicate variability, which was used for final error propagation.

3.6. Computational details

Equilibrium calculations were performed using VisualMINTEQ (Gustafsson, 2010). Biological uptake and export was modeled using the ode45 function in MATLAB 2011 (Mathworks, Natick, MA).

3.7. Calculation of copper accumulation and assimilation

We evaluated copper uptake using both net copper assimilation and isotopically derived gross assimilation. Net assimilation was calculated from the difference between the initial copper quota and the subsequent cellular quotas at each time point after the cells were exposed to copper. Isotopically derived gross assimilation was calculated from the ratio of ^{65}Cu to ^{63}Cu measured over time. The use of a stable isotopic tracer can help improve interpretation of kinetic models by adding an additional measurable variable (Cobelli et al., 1987). The use of two tracers allows for the deconvolution of export from uptake. Copper is an ideal element for use in isotopic manipulations, since it has only two naturally occurring stable isotopes that occur in relatively close abundance.

The relative abundance ($^{i}\alpha$) of a specific isotope (i) in a sample or standard can be expressed the measured quantity of the isotope over the sum of the number of atoms (N) of each of the copper isotopes:

$$ {}^{i}\alpha = \frac{{}^{i}N}{{}^{63}N + {}^{65}N} \qquad 2 $$

It follows that the sum of the fractions should equal 1 and that the quotient of the relative abundances is equal to the isotopic ratio.

$$ R = \frac{{}^{65}N}{{}^{63}N} = \frac{{}^{65}\alpha}{{}^{63}\alpha} \qquad 3 $$

Relative isotopic abundance for natural samples and experimental spikes are listed in Table 2.

The isotopic ratio of a sample exposed to an isotopically enriched spike is the quotient of

the sums of the initial baseline number of copper atoms (N_0) times a baseline isotopic abundance ($^i\alpha_0$) and the accumulated isotopically spiked copper (N_{sp}) times the spike's isotopic abundance ($^i\alpha_{sp}$):

$$R = \frac{N_0 \cdot {}^{65}\alpha_0 + N_{sp} \cdot {}^{65}\alpha_{sp}}{N_0 \cdot {}^{63}\alpha_0 + N_{sp} \cdot {}^{63}\alpha_{sp}} \quad (4)$$

The gross copper accumulated by the cell at a specific time point, $N_{sp,t}$, can thus be solved for given quality measurements of N_0 prior to the addition of a copper spike, and subsequent measurements of the ratio at each time point (R_t):

$$N_{sp,t} = N_0 \frac{R_t {}^{63}\alpha_0 - {}^{65}\alpha_0}{{}^{65}\alpha_{sp} - R_t {}^{63}\alpha_{sp}} \quad (5)$$

Given no loss of copper from the cell, $N_{sp,t}$ calculated from R_t, should equal the net absolute assimilation of copper. Alternatively, the presence of an export mechanism would result in a loss of copper from the cell that has a lower relative abundance of ^{65}Cu than the copper being assimilated. This would cause an additional increase in cellular *R* and subsequently overpredict the isotopically calculated value N_{sp}. Furthermore, the copper exported from the cell, relatively lower in ^{65}Cu, will cause the overall relative abundance of the spike in the media ($^{65}\alpha_{sp}$) to decline over the course of the experiment.

To address export we developed a two box model based on Equation 1:

$$\frac{d^i N_m}{dt} = v_e {}^i\alpha_c - v_u {}^i\alpha_m \quad (6)$$

$$\frac{d^i N_c}{dt} = -v_e {}^i\alpha_c + v_u {}^i\alpha_m \quad (7)$$

Where ^iN_m is amount of a specific copper isotope in the media; ^iN_c is the amount of a specific

copper isotope in the cell; ($^{i}\alpha_{m}$) is the isotope fraction of *i* in the media, ($^{i}\alpha_{c}$) is the isotope fraction of *i* in the cell. Preliminary calculations revealed that any change in the relative isotopic abundances of the spike in the media due to efflux would be extremely small allowing us to assume that $^{63}\alpha_{sp}$ and $^{65}\alpha_{sp}$ were constant over the course of the experiment. Complete modeling of our data required us to use an additional uptake term in Equation 6 and Equation 7 to account for a rapid initial sorption (v_s) of copper with a time-decay constant (τ):

$$^{i}\alpha_{m} v_s e^{-t/\tau} \qquad 8$$

Uptake rates were calculated for both initial (v_s) and mid-term uptake (v_u) from both net and isotopically derived measurements. Initial rates were determined by difference of the baseline cellular measurement and the first measurement after copper addition. Mid-term rates were calculated by linear regression from the first measurement through four hours after copper addition. Relative isotopic abundances of the uptake rates (Table 4, $^{i}\alpha_{\Delta Cu/\Delta t}$) were calculated by dividing the calculated uptake rate for an isotope (*i*) by the total uptake rate of copper. Rates are reported on a per cell basis. Dimensions of both organisms in this study were roughly similar. As such normalization based on volume would not significantly alter the calculated and observed relative differences.

4. Results

4.1. Removal of surface bound Cu

Most previous studies that have worked on the quantification of cellular copper in algal cells have utilized either DTPA or EDTA at concentrations up to 10 mM to remove surface bound copper (Cullen and Sherrell, 1999; Vasconcelos and Leal, 2000; Croot et al., 2000; Quigg

et al., 2006). In our experiments, both of these ligands reduced total cellular copper measurement by approximately 10% (DTPA wash shown in Figure 2A), which is consistent with these earlier studies. However in our initial uptake experiments using the DTPA wash, we were unable to observe any linear biological uptake over any time period and instead observed a rapid saturation of cellular copper and isotopic ratios. Similar behavior has been observed in *E. huxleyi* when exposed to Cu(II) for 10 minutes (Vasconcelos and Leal, 2000). We hypothesized that the rapid saturation was due to incomplete removal of surface bound Cu and that Cu(II)-chelator based rinses were incapable of removing it. Copper may be bound by surface sites that outcompete these chelators, or be bound as Cu(I) which does not form strong complexes with EDTA or DTPA.

In testing this hypothesis, we used thiol-based chelators because thiols are effective Cu(I) ligands and may also reduce strongly bound Cu(II) thereby releasing it. We tested several thiols, including cysteine, glutathione (GSH), and dithiothreitol (DTT), and found that while the biogenic ligands did offer some improvement over DTPA (data not shown), DTT was the most effective at removing surface copper especially at concentrations of 10 mM (Figure 2A). The concomitant decline in the isotopic ratio facilitated by the 10 mM rinse solution indicates that it was primarily the isotopic spike that was being removed. Increasing the contact time of the wash increased Cu removal in experiments ranging from 2.5 to 20 minutes, but beyond 20 minutes no further reduction was observed (Figure 2B). The copper that was removed was predominantly ^{65}Cu and the isotopic ratio of the cellular Cu at 20 min and 30 min were statistically indistinguishable (Figure 2B).

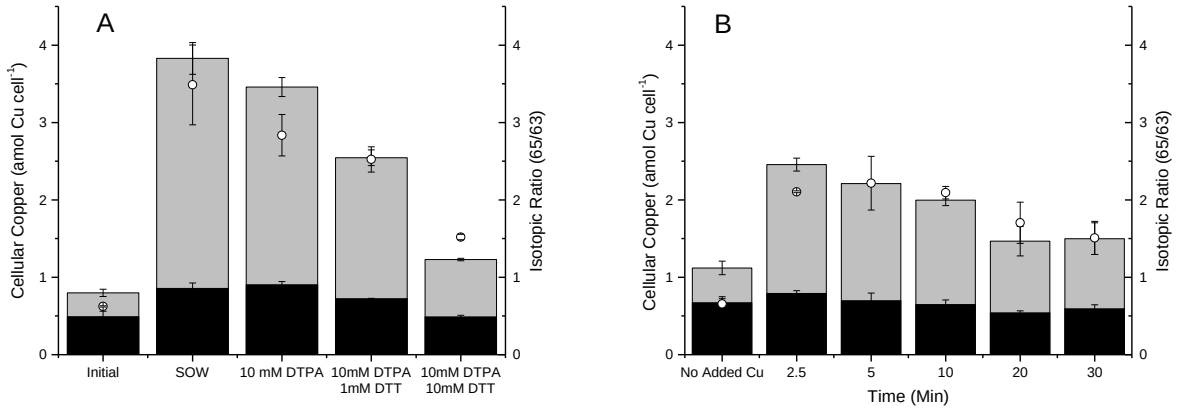

Figure 2. Removal of surface bound copper. Bars represent absolute measurement of cellular copper (^{63}Cu-Black, ^{65}Cu-Grey). Open circles are measurements of the ^{65}Cu-^{63}Cu ratio. Replete *E. huxleyi* cells were resuspended in SOW and an initial copper quota was measured. Cells were then exposed to 100 nM Cu(II) for 10 minutes and then filtered. Panel A shows the effect of different rinse solutions on copper levels. Cells were soaked in rinse solution for 10 minutes, after which the rinse solution was filtered off and rinsed again with SOW. Panel B demonstrates the effectiveness of a 10 mM DTPA, 10 mM DTT solution from t = 0 to 30 minutes.

4.2. Regulation of cellular copper levels

Several studies of copper quotas in marine algae have reported that *E. huxleyi* maintains a significantly lower Cu quota than other organisms (Ho et al., 2003; Quigg et al., 2006); this is especially true of oceanic strains (Guo et al., 2012). Our measurements of copper quotas in batch cultures grown over a range of 0 - 10 µM of EDTA-buffered copper (initial pCu = 15.2 – 11.2) show that in absolute and volume normalized terms, copper levels are substantially lower in *E. huxleyi* cultures than in cultures of *T. pseudonana* (Table 3). At the highest copper concentration, *T. pseudonana's* growth rate declined by a third from the maximum measured growth rate, indicating an induction of copper stress. Conversely *E. huxleyi* was able to maintain its maximum growth rate at all Cu concentrations. A comparison of the steady state uptake rates, the product of the specific growth rate and cellular quota (Morel, 1987), confirms that at all copper concentrations *E. huxleyi* exhibits lower net assimilation rates. Even when exposed to the highest copper concentration, *E. huxleyi* maintains a lower net copper assimilation rate than when *T. pseudonana* is cultured in the presence of 500 times less copper (0.32 vs. 0.38 amol $cell^{-1}$ hr^{-1}). It is also worth noting that we measured Cu(I) concentrations in spent medium from the highest copper treatments, using the colorimetric indicator BCS, and found that up to 50% of the total copper was in the form of Cu(I). While this had little impact on this study it highlights the need to better understand the redox behavior of copper in marine systems.

Distinct differences in copper uptake were also observed in replete cultures of *E. huxleyi* and *T. pseudonana* resuspended in SOW and exposed for shorter periods of time to unbuffered copper at concentrations ranging from 10 nM to 10 µM. Initial uptake rates calculated from cellular accumulation after 10 minutes of copper exposure are very rapid for both organisms

Table 3. Growth rates, cellular copper concentrations, and calculated steady state uptake rates for *E. huxleyi* and *T. pseudonana*. Cells were grown in EDTA-buffered Aquil medium. *E. huxleyi* cultures were grown at 100nM Fe_T, while *T. pseudonana* cultures were grown at 100nM Fe_T.

	$[Cu]_T$ (nM)	**Initial pCu (-log[Cu^{2+}])**	**Growth Rate (d^{-1})**	**Cellular Cu (amol $cell^{-1}$)**	**$[Cu]_{cell}$ (µM)**	**Steady State accumulation rate ρ^{ss} (amol $cell^{-1}$ hr^{-1})**
T. pseudonana	0	15.2	0.20	0.9 ± 0.3	11.1 ± 4.1	0.007
	20	13.9	1.02	8.9 ± 0.5	111.4 ± 5.8	0.38
	100	13.2	1.23	19.6 ± 1.2	246.3 ± 14.5	1.00
	1000	12.2	1.11	31.6 ± 0.9	397.2 ± 11.0	1.46
	10000	11.2	0.82	125.0 ± 4.4	1571.9 ± 55.0	4.26
E. huxleyi	0	15.2	0.34	0.2 ± 0.1	1.4 ± 1.1	0.003
	20	13.9	0.54	0.8 ± 0.0	5.5 ± 0.3	0.018
	100	13.2	0.52	1.5 ± 0.4	10.2 ± 2.6	0.032
	1000	12.2	0.51	13.9 ± 1.1	96.3 ± 7.4	0.29
	10000	11.2	0.52	15.0 ± 2.1	104.1 ± 14.4	0.32

(Figure 3A) and always greater than midterm uptake rates measured during the interval of 10 minutes to four hours (Figure 3B). Short-term uptake was negligible at low concentrations (10 - 50 nM). At intermediate concentrations (100 – 2000 nM), uptake in *T. pseudonana* increased far more than in *E. huxleyi*, but at higher concentrations (5000 - 10000 nM) uptake was comparable between the two species. In contrast mid-term uptake rates for *E. huxleyi* remained significantly below the rates measured in *T. pseudonana* at 1000 nM and above (Figure 3B). Mid-term uptake rate declined in in the range of 250-500 nM after steadily increasing (Figure 3B inset). This may be a result of the high variability observed in cellular copper measurements for this organism.

Whether the rapid short-term uptake rates are largely due to burst phase kinetics or a small amount of irremovable surface bound copper cannot be completely resolved. The fraction of total copper that was removable declined as concentrations increased (not shown). This may indicate a drop in efficiency in the wash or that the surface binding sites are becoming saturated with copper. In the case of the latter, cells resuspended in copper free medium and subsequently challenged with copper may exhibit a rapid assimilation facilitated by transporters that become inactive in the absence of copper. Upon the addition of copper the transporters may not be in steady state resulting in an initial rapid phase of uptake. Such burst phase kinetics has been observed with enzymes that reduce copper prior to uptake (Miura et al., 2005).

4.3. Isotope tracer time course measurements

Isotopically enriched copper was employed to determine whether copper export was responsible for low uptake rates observed in *E. huxleyi.* Copper uptake was measured over the course of 4 hours with algae cultures resuspended in trace-metal-free SOW and exposed to 100

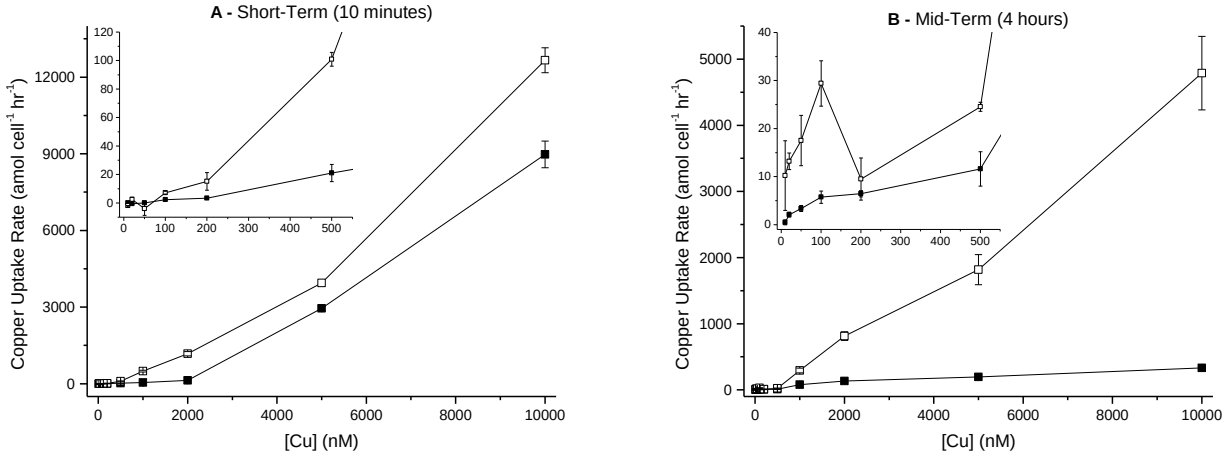

Figure 3. Short-term and mid-term copper uptake rates in replete *E. huxleyi* (▪) and *T. pseudonana* (□) cells resuspended in varying levels of total copper. Short-term rates were calculated from the change in cellular copper concentrations after 10 minutes of exposure. Mid-term rates were calculated from the difference between the 10-minute measurement and a measurement made after 240 minutes.

nM isotopically enriched copper (90% ^{65}Cu). Both total copper and the isotopic ratio were measured, allowing for the calculation of net assimilation and what we have termed isotopically-derived assimilation or gross uptake (Equation 3). Baseline copper quotas (N_0) and isotope fractionation ($^i\alpha_b$) measurements were determined for resuspended Cu-limited and replete *T. pseudonana* and *E. huxleyi* cells prior to the addition of any extracellular copper. Quotas were consistent ($P < 0.05$ by Student's-t) with cells filtered directly from native growth medium (Table 1) as well as quotas measured in other studies (Ho et al., 2003; Quigg et al., 2006).
As in previous experiments, both organisms, under replete and Cu-limited conditions exhibited fast short-term uptake rates (0 - 10 minutes) compared to the rates measured thereafter during the interval from 10 to 240 minutes (Figure 4). Short-term uptake rates were not significantly different for replete cultures of *E. huxleyi* and *T. pseudonana* (Table 4, $P < 0.05$ by Student's-t). Cu-limitation caused short-term uptake to increase in *T. pseudonana* cells, while surprisingly lower short-term uptake in Cu-limited *E. huxleyi*.

Over four hours replete cultures of *T. pseudonana* exhibited somewhat linear uptake of copper, nearly doubling the cellular copper concentration (Figure 4A). A concomitant increase in the cellular isotopic ratio was also observed in that time period. The isotopic fractionation of the uptake rate was (Table 4) was consistent with concentration driven uptake of the isotopic spike. Remarkably different kinetics were observed over same time period by replete *E. huxleyi* (Figure 4C). Cellular copper levels nearly tripled in the first 15 minutes, driven by uptake of ^{65}Cu which rapidly overtook levels of ^{63}Cu. Total cellular copper then only increased by about 0.5 amol over the next 110 minutes and then leveled off at approximately 2 amol cell^{-1}. However, during this time period the isotopic ratio also increased significantly, indicating a changing pool of

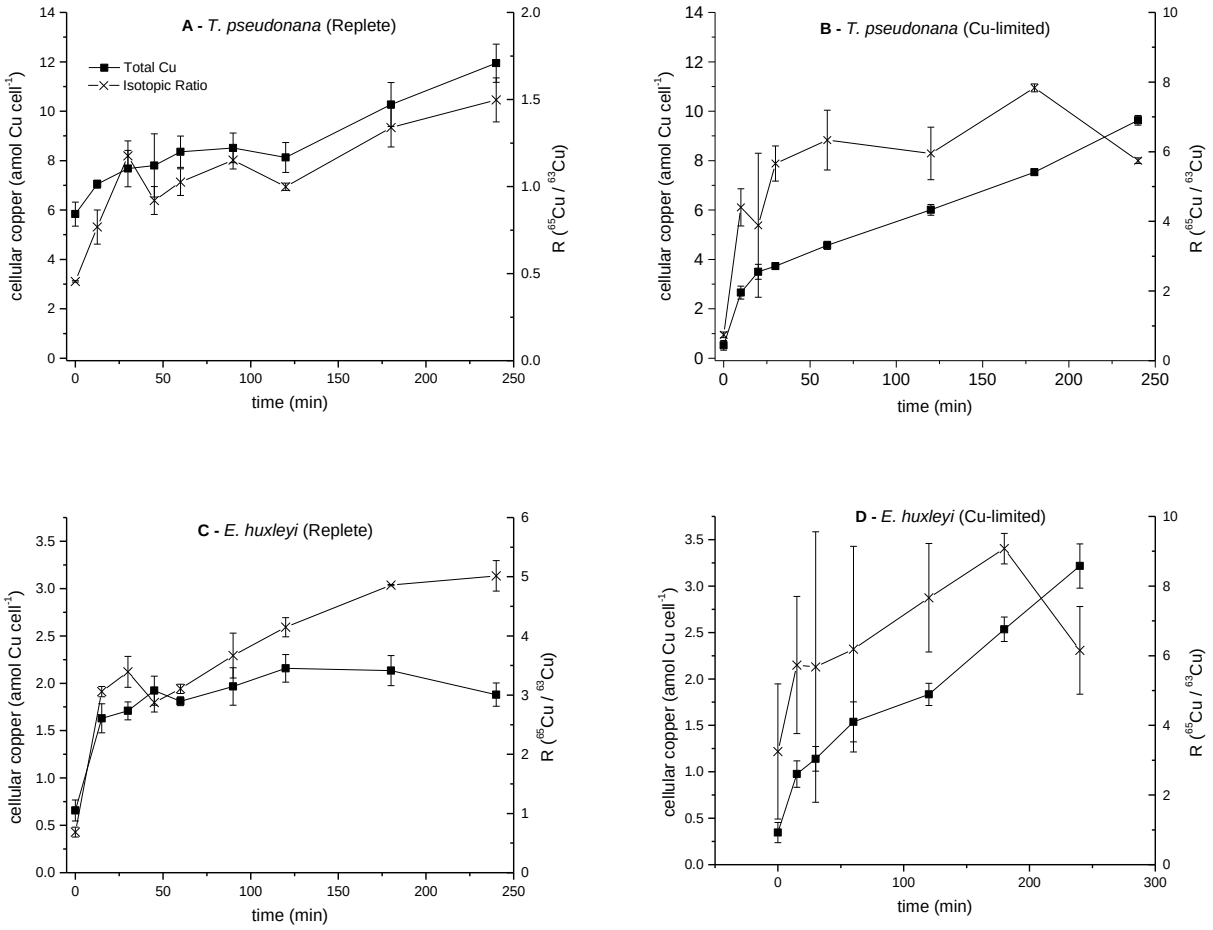

Figure 4. Cellular measurements of total copper (▪) and the isotopic ratio (×) in replete and Cu-limited *T. pseudonana* and *E. huxleyi* cultures. Cells were resuspended in SOW and amended with 100 nM isotopically enriched ^{65}Cu (90%).

Table 4. Measured net and isotopically calculated gross (Equation 5) uptake rates for in Cu-replete and Cu-limited cultures exposed to 100 nM copper spike (90% ^{65}Cu). Initial rates are measured uptake in the first data point, (10 or 15 minutes). Mid-term rates are the slope of the linear regression curve from the first spiked time point through 4 hours. Estimated pCu = 8.3.

		Initial Rate (amol cell^{-1} h^{-1})		**Mid-term rate (amol cell^{-1} h^{-1})**		**Mid-term rate relative abundance**	
Species	*Cu*	*Net*	*Gross*	*Net*	*Gross*	$^{63}\alpha_{\Delta Cu/\Delta t}$	$^{65}\alpha_{\Delta Cu/\Delta t}$
T. pseudonana	+	4.9 ± 0.7	6.2 ± 2.2	1.1 ± 0.1	0.9 ± 0.1	0.18 ± 0.05	0.82 ± 0.11
	-	12.8 ± 1.6	14.1 ± 3.5	1.7 ± 0.1	Saturated	0.10 ± 0.02	0.90 ± 0.03
E. huxleyi	+	3.9 ± 0.6	6.3 ± 0.5	0.05 ± 0.03	[ł] 0.8 ± 0.1	[ǂ]	[ǂ]
	-	2.5 ± 0.4	2.4 ± 0.2	0.5 ± 0.1	Saturated	0.07 ± 0.04	0.93 ± 0.11

[ł] A uptake rate of 0.4 amol cell^{-1} h^{-1} was estimated for this condition by fitting the assimilation data to an uptake-export model (Equations 6, 7, & 8). [ǂ] Could not be determined due to a negative ^{63}Cu assimilation rate.

intracellular copper. Furthermore mid-term uptake of ^{65}Cu was 0.090 ± 0.030 amol cell^{-1} hr^{-1}, while ^{63}Cu levels declined at a rate of 0.036 ± 0.006 amol cell^{-1} hr^{-1} resulting in a net uptake rate of 0.054 ± 0.030 amol cell^{-1} hr^{-1} (data not shown).

In Cu-limited cells, both species exhibited similar biphasic kinetics, marked by a rapid initial accumulation followed by slower uptake over four hours (Figure 4B & D, Table 4). As expected, initial copper quotas of both species were significantly lower than replete cells, and were consistent with measurements made on cells harvested directly from native SOW (Table 1). The higher than natural isotopic ratio (R= 3.2) measured in Cu-limited *E. huxleyi* at the initial time point was likely caused by contamination of the growth medium by the frequent handling of the ^{65}Cu stock solution in the laboratory. This was routinely observed in other Cu-limited cultures. Isotopic ratios in both Cu-limited cultures quickly saturated and were prone to high error due to the very low initial cellular levels of copper.

Cu-limitation resulted in a fivefold and 50% increase in mid-term net uptake for both *E. huxleyi* and *T. pseudonana* respectively (Table 4). Both *T. pseudonana* treatments and Cu-limited *E. huxleyi* exhibited mid-term absolute uptake rates of copper that were representative of concentration dependent uptake of the spike solution. In these cultures, the isotopic fractionation of the assimilated copper was statistically equivalent to the fractionation of the isotopic enriched copper spike (Table 4).

Of the four cultures exposed to copper, only the replete *E. huxleyi* culture failed to exhibit concentration dependent uptake consistent with the isotopic spike. In fact ^{63}Cu measurements declined slightly while ^{65}Cu levels increased, indicating that there must be some mechanism removing copper from the cell. Despite the leveling off of net assimilated copper, the isotopic

ratio steadily increased over the course of the experiment (Figure 4C). Using the isotopic ratios and initial cellular copper quotas, both shown in Figure 4, we used Equation 5 to calculate gross assimilated copper and compared these values with those measured for net assimilation (Figure 5). This comparison reveals that over the course of 4 hours isotopically calculated gross assimilation diverges considerably from net assimilation in cultures of *E. huxleyi* (Figure 5A) but not *T. pseudonana* (Figure 5B). In *E. huxleyi*, the mid-term isotopically-derived gross uptake rate (0.8 ± 0.1 amol cell^{-1} hr^{-1}) suggests that there was continued uptake of the isotopic spike. This resulted in a significant discoordination (Pearson's $r = 0.53$) between the isotopically derived calculated copper uptake and measured net copper uptake (Figure 5A & C). In contrast net and gross assimilation in *T. pseudonana* (Figure 5B & C) were more correlated ($r = 0.91$).

It appears that after an initial rapid period the absolute copper levels in replete *E. huxleyi* quickly achieve steady state while the isotopic ratios in the cell and the media do not. To further demonstrate we applied a two box isotopic uptake and export model that incorporates equations 6, 7 and 8. In the case of *E.* huxleyi ($N_0 = 0.66$ amol cell^{-1}), steady state was assumed by setting the mid-term export (v_e) and uptake (v_u) rates equal. A value of 0.42 cell^{-1} hr^{-1} was fit for these parameters (Figure 5A). For cultures of *T. pseudonana* ($N_0 = 5.8$ amol cell^{-1}), no export was assumed (v_e=0) and v_u was fit at 1.2 amol cell^{-1} hr^{-1} (Figure 5B). In both cases the initial rapid sorption was modeled with an initial rate (v_i) of 1.8 amol cell^{-1} hr^{-1} with a time decay constant (τ) of 15 min.

We were unable to perform a similar analysis in Cu-limited cells. Due to their low initial copper levels, the isotopic ratio of spiked cultures saturated rapidly, making it difficult to calculate gross uptake over the medium term. As such we can neither confirm nor exclude the

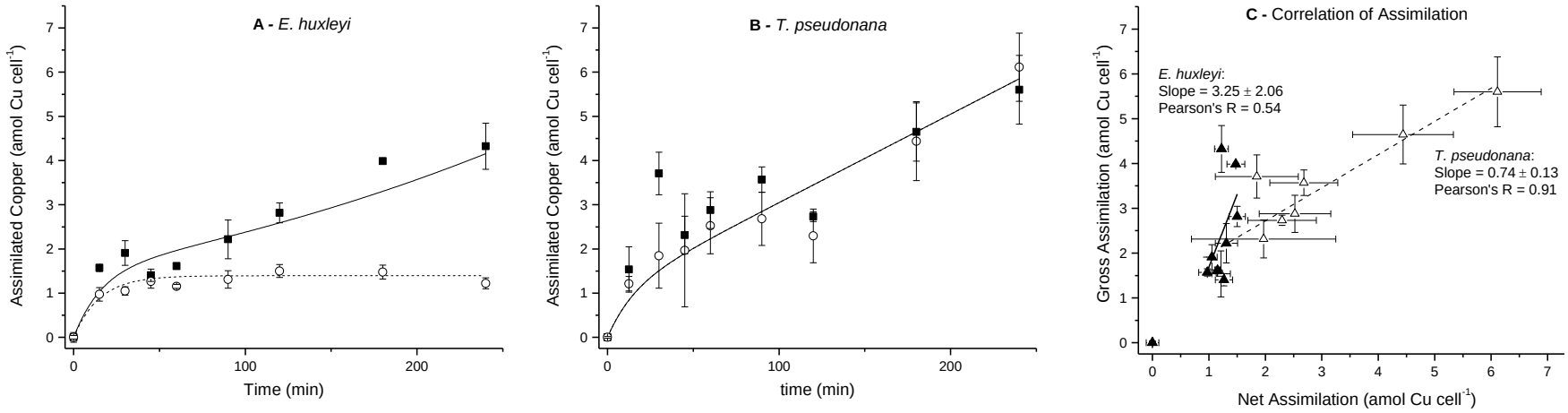

Figure 5. Calculated copper uptake in cultures of *E. huxleyi* (A) and *T. pseudonana* (B). Net assimilation (○) was calculated from the difference between the initial copper concentration and the measured total concentration at each time point. Isotopically derived assimilation was(▪) were calculated from the isotopic ratio at each time point and the initial copper concentration using Equation 5. Solid lines represent modeled absolute assimilation and dotted lines follow the model of isotopically derived uptake. Modeled parameters are listed in the ext. Since export was not included in the model for *T. pseudonana* net and isotopically derived assimilation models are identical. Panel (C) demonstrates the correlation of isotopically measured uptake and absolute uptake for *T. pseudonana* (Δ) and *E. huxleyi* (▲). A linear regression was fitted to each of the assimilation datasets to demonstrate correlation of measurements: *T. pseudonana* (dotted line); *E. huxleyi* (solid line)

presence of active export in Cu-limited cultures, however we do notice that in *E. huxleyi* under limitation (Figure 4D) net uptake and total copper exceed the net uptake and steady state level observed in replete cells (Figure 4C), indicating that any present export is far less active than in replete cells.

4.4. Direct Measurement of Export

Independent experiments were performed to directly measure export from cells. Resuspended cells were exposed to 1000 nM copper for 30 minutes at which point DTPA was added to limit the bioavailability of Cu(II). During the exposure period, *T. pseudonana* cells accumulated approximately 83 amoles of copper (7.5% of total added copper) and while *E. huxleyi* gained 48 attomoles (4% of total added copper). After 30 minutes in the presence of DTPA, the cellular copper decreased to 10% and 60% of loaded levels in *E. huxleyi* and *T. pseudonana* respectively (Figure 6). In both species, export slowed substantially over the next half hour (t = 60 min) suggesting desaturation of the export mechanism.

Export for both species was temperature dependent. Export was reduced by approximately 13% and 20% in *E. huxleyi* and *T. pseudonana* in DTPA amended loaded cell cultures that were reduced from 20 to 4^{o} C. The temperature decline was not immediate and thus it remains likely that export was still substantial under cold conditions. However, cold-induced reduction of rates indicate that that export is the result of a biological process rather than leakage or ligand-induced diffusion. Furthermore, cell division is too slow to cause the observed reductions in cellular Cu levels.

Copper loaded *T. pseudonana* exposed to the cold demonstrated increased copper in the

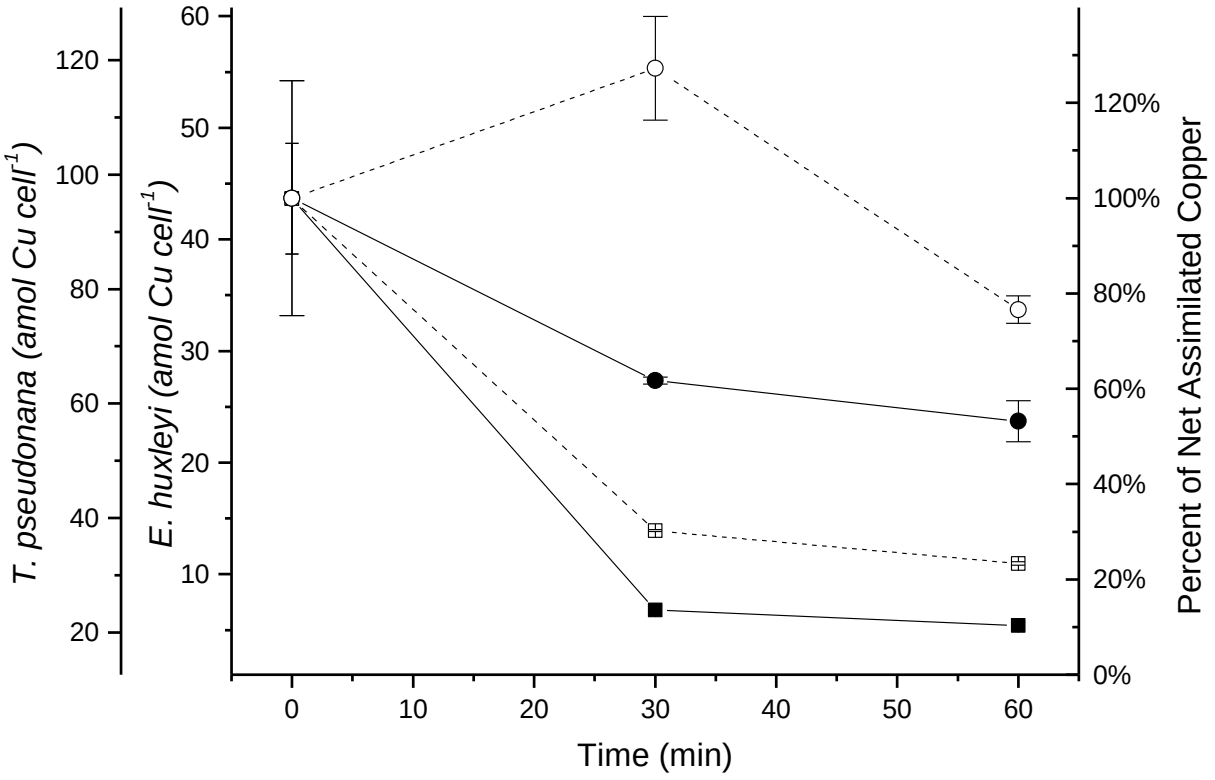

Figure 6. Export of copper from *E. huxleyi* (squares) and *T. pseudonana* (circles). Resuspended algae cells were exposed to 1 µM Cu(II) for 30 minutes and total cellular concentration was measured (T=0, dotted line). 100 µM DTPA was then added. The culture was split and half put on ice in a cold room (4°C) (open symbols), the other half were kept at room temperature (20°C). Dotted line represents the cellular copper concentration prior to copper exposure. Where not shown error bars are within the symbol.

first 30 minutes after DTPA exposure. This may be due to latent uptake of an elevated Cu(I) pool in cultures of *T. pseudonana*. In this species the surface reduction of extracellular copper is roughly 10 fold more efficient than in *E. huxleyi* (Chapter 4). As Cu(I) is not readily complexed by DTPA it is likely that this larger pool is still available for uptake . The subsequent decline over the next half hour as well as the initial decline observed in the first half hour of *T. pseudonana* at room temperature indicates active export. However, this is not sufficient to maintain steady state concentrations, as observed in the time course experiments for *E. huxleyi*, while the export observed here with *E. huxleyi* is.

5. Discussion

E. huxleyi, a widespread and ecologically important coccolithophore, is able to maintain higher relative growth rates under severe copper stress than a wide sampling of phylogenetically diverse marine phytoplankton demonstrating a strong tolerance for copper (Brand et al., 1986). Furthermore *E. huxleyi* has a relatively small copper requirement (Table 1) in absolute terms and when normalized to phosphorus (Ho et al., 2003; Guo et al., 2012). In this study we compared *E. huxleyi* with the diatom *T. pseudonana* to demonstrate that these differences in cellular copper quotas are to a large extent driven by a rapid copper export mechanism in *E. huxleyi* that is active in replete cultures, but not in those that are copper limited. Conversely export was only observed from Cu-stressed *T. pseudonana* cells.

Accurate assessment of cellular copper concentrations, especially in cells exposed to uncomplexed copper proved to be somewhat challenging. Cu(I) can be generated by surface reducatases (Hill et al., 1996; Andreazza et al., 2011) and then strongly bound by ligands such as

thiols (cysteine, methionine) or imines (histidine) potentially present in surface proteins. Even in trace metal buffered medium, Cu(I) can accumulate to significant levels (Chapter 4). Previous cell washing treatments only utilized EDTA or DTPA and thus may not remove this strongly bound copper. We found that using a 10 mM DTT containing cellwash was critical for the removal of the majority of surface bound copper. While the use of a thiol in a cellular wash has been demonstrated before showing improved removal of mercury in comparison to EDTA (Le Faucheur et al., 2011), thiols should be particularly effective reagents to remove copper, as they binds strongly to Cu(I) (Chapter 1) and can reduce and remove strongly bound Cu(II). While we found that cysteine and DTT had similar washing efficiencies, we opted to use DTT primarily because it is stronger than cysteine and cysteine has been shown to increase the bioavailability of some metals (Aristilde et al., 2012; Schaefer and Morel, 2009).

Given these considerations previous copper uptake studies should thus be treated with care, especially those, such as in ours, that include experiments where copper is added free and unbuffered. Vasconcelos and Leal (2000) reported rapid assimilation of copper into *E. huxleyi* upon the addition of uncomplexed copper that was similar to our measurements prior to development of the DTT wash. While these authors dismissed the possibility of incomplete removal from the cell surface, our results indicate that after exposure to uncomplexed copper at concentrations between 100 and 2000 nM for 10 minutes the majority of copper associated with the cells is strongly bound to the surface (data not shown). While this artifact is likely less pronounced at lower concentrations, Quigg et al. (2006) measured net uptake rates that resulted the doubling of cellular copper quotas in *E. huxleyi* and *T. pseudonana* within minutes upon the addition of 7 nM copper. This exceeded our measured uptake rates, and may still represent

significant surface binding, despite the relatively low addition of copper.

Previous studies of copper uptake in algae have employed measurements of either radio isotopes or absolute copper. Absolute measurements of algal copper using electrochemical techniques (Vasconcelos and Leal, 2000) or atomic absorption spectroscopy (Chang and Reinfelder, 2000) are less sensitive than radioisotopes measurements, thus requiring copper additions that may exceed those observed in environmental systems. In contrast the radioisotopes ^{64}Cu and ^{67}Cu can provide superb sensitivity (Croot et al., 1999; Croot et al., 2003; Quigg et al., 2006; Guo et al., 2010), however these isotopes are short lived and require special handling. While high resolution inductively coupled plasma mass spectroscopy does provide some benefit in sensitivity over other absolute measurements, it does not match the sensitivity of radioisotopes, hence required the use of higher levels of unbuffered copper. However its primary benefit is derived from ability to measure multiple isotope of copper allowing for absolute measurement of the total element and fractionation of individual isotopes. This property allows export to be mathematically discerned from uptake (Croteau et al., 2004; Cobelli et al., 1987). As R diverges from unity small numerical changes in the denominator, arising from error in ^{63}Cu measurement, can propagate to increase uncertainty in R through to the calculation of gross uptake. As such, the design of experiments necessitated proper selection of the isotopic spike ratio to ensure that the isotopic ratio over the course of the experiment did significantly diverge from unity. Additionally we could not calculate isotopically derived assimilation from cultures where the amount in internalized copper rapidly exceeded the initial cellular quota, such as cultures under copper limitation or replete cultures that were spiked with high levels (>1000nM) of copper.

When these conditions were fulfilled we were not only able to measure copper uptake in two species of marine algae but also observe the divergence of gross-isotopic assimilation and absolute net assimilation in copper replete cultures of *E. huxleyi*. The fit of a biological uptake-export model to the isotopic measurements of uptake in replete *E. huxleyi* cells resulted in an estimate of 0.4 amol cell^{-1} hr^{-1} for uptake and export rates. With uptake and export equal, the cell attains a steady state level of copper while still exhibiting a gradual increase in the ratio of ^{65}Cu to ^{63}Cu. Direct uptake in *T. pseudonana* is only 2 to 3 times greater than this value (Table 4). This is substantially lower than what the differences in cellular quotas as well as steady state and net uptake rates would suggest and further highlights the need for export to be invoked.

Efflux of copper is not well described in eukaryotes. In prokaryotes, P_{1B}-ATPase mediated ion channel efflux from the cytoplasm to the periplasm has been shown to be a route for copper detoxification (Rensing et al., 2000; Osman and Cavet, 2008; Nies, 2003). Direct export of copper from copper-over-loaded cells has been observed in the cyanobacterium *Nostoc* (Verma and Singh, 1991) and *Synechococcus* (Croot et al., 2003). Direct export from *Synechococcus* cells ($[Cu]_{cell}$ = 10 µM) was approximately 0.024 amol cell^{-1} hr^{-1} and maximum efflux was estimated at 0.22 amol cell^{-1} hr^{-1}. Copper- exposed replete *E. huxleyi* cells ($[Cu]_{cell}$ = 14 µM) in our time course experiments exhibited rates approximately twice this, while our measurement of direct export suggested that efflux in copper-loaded cells ($[Cu]_{cell}$ = 300 µM) was at least 74 nM amol cell^{-1} hr^{-1}. This large rate in comparison to the maximum rate for *Synechococcus* is likely a result of *E. huxleyi's* larger surface area and the higher copper concentration of these cells. Croot indicated that such mechanisms are likely going to be concentration dependent and follow Michaelis-Menten kinetics, and larger cell sizes would likely

contain more transport sites. Concentration defendant kinetics may also explain why we are able to see some export even in Cu-loaded *T. pseudonana* while none was observed in time course experiments at 10-fold less copper exposure.

In eukaryotic algae metal export has been significantly understudied compared to uptake, but as with uptake is likely going to be influenced by the presence of metal coordinating ligands inside the cell. Both *Synechococcus* and the toxic dinoflagellate, *Amphidinium carterae*¸ a eukaryote with a relatively low copper quota(Ho et al., 2003), produce and exude a strong copper binding ligand (Croot et al., 2000; Croot et al., 2003). *E huxleyi* is known to exude high concentrations of two cysteine containing dipeptides under copper stress (Dupont and Ahner, 2005), Arg-Cys and Gln-Cys. These compounds can be rapidly synthetized (Kim et al., 2011), strongly bind copper with somewhat more metal-specificity than other low molecular weight thiols such as GSH (Chapter 1) and have been observed to be exuded with copper (Dupont et al., 2004). Currently, only *E. huxleyi* has been observed to produce these compounds at significant concentrations, which can be upwards of 100 µM each in copper stressed cells. At these concentrations these ligands are strong enough to buffer intracellular copper concentrations and the cell then has no need to synthesize larger and expensive copper storage proteins such as metallothioneins. Also unlike storage proteins which would result in a large increase in intracellular copper as seen in cultures of *T. pseudonana,* these low molecular weight complexes would also be easier to transport. It is possible that these compounds play a significant role in *E. huxleyi's* copper export mechanism. Low molecular weight thiol-containing polypeptides have been shown to facilitate export in a cadmium detoxification mechanism in the diatom *Thalassiosira weissflogii* (Lee et al., 1996). In higher plants and yeast, Cd detoxification involves

phytochelatins ($(\gamma\text{-Glu-Cys})_n\text{Gly}$, $n \geq 2$) binding to cadmium inside the cell followed by removal of the complex from the cytosol via an *Abc2* an ABC-type transporter(Mendoza-Cózatl et al., 2010). Homologues of this mechanism are found in other kingdoms. The mechanism encoded by this gene can also facilitate the exclusion of glutathione conjugates.

While phytochelatins are ubiquitous in eukaryotic algae, the ability of *E. huxleyi* to produce alternate detoxification mechanism may give it a significant advantage. Copper levels naturally fluctuate in surface sea water between limiting and toxic. While copper binding ligands found outside the cell may reduce copper bioavailability from toxic to tolerable, some extracellular ligands may enhance uptake, such as cysteine with zinc in *T. pseudonana* and *E. huxleyi* (Aristilde et al., 2012) or desferrioxamine B in yeast (Yun et al., 2000). The last line of defense is intracellular regulation of copper. Our results expand on previous work by demonstrating that copper export is utilized to maintain copper homeostasis in *E. huxleyi*. The use of stable isotope traces found that export is active even while the organism is actively taking up copper. The ability to readily modulate copper levels could explain why *E. huxleyi* can tolerate higher copper concentrations than many other species. Such a mechanism may give it a substantial biological advantage in waters that are prone to higher copper concentrations such as coastal zones or during upwelling events.

6. Acknowledgements

We thank Professors Lou Derry and John Helmann for use of their inductively coupled plasma mass spectrometers. Zhen Ma and Gregg McElwee provided support on these instruments. Funding was provided by NSF Chemical Oceanography (OCE 0451781).

7. References

Andreazza R, Okeke B, Pieniz S, et al. (2011) Bioreduction of Cu(II) by Cell-Free Copper Reductase from a Copper Resistant <i>Pseudomonas sp. NA. *Biological Trace Element Research* 143: 1182-1192.

Aristilde L, Xu Y and Morel FMM. (2012) Weak Organic Ligands Enhance Zinc Uptake in Marine Phytoplankton. *Environmental Science & Technology* 46: 5438-5445.

Berglund M and Wieser ME. (2011) Isotopic compositions of the elements 2009 (IUPAC Technical Report). *Pure and Applied Chemistry* 83: 397-410.

Brand LE, Sunda WG and Guillard RRL. (1986) Reduction of marine phytoplankton reproduction rates by copper and cadmium. *Journal of Experimental Marine Biology and Ecology* 96: 225-250.

Chang SI and Reinfelder JR. (2000) Bioaccumulation, Subcellular Distribution, and Trophic Transfer of Copper in a Coastal Marine Diatom. *Environmental Science & Technology* 34: 4931-4935.

Coale KH and Bruland KW. (1988) Copper Complexation in the Northeast Pacific. *Limnology and Oceanography* 33: 1084-1101.

Cobelli C, Toffolo G, Bier DM, et al. (1987) Models to interpret kinetic data in stable isotope tracer studies. *American Journal of Physiology - Endocrinology And Metabolism* 253: E551-E564.

Croot PL, Karlson B, van Elteren JT, et al. (1999) Uptake of 64Cu−Oxine by Marine Phytoplankton. *Environmental Science & Technology* 33: 3615-3621.

Croot PL, Karlson B, van Elteren JT, et al. (2003) Uptake and efflux of Cu-64 by the marine cyanobacterium Synechococcus (WH7803). *Limnology and Oceanography* 48: 179-188.

Croot PL, Moffett JW and Brand LE. (2000) Production of extracellular Cu complexing ligands by eucaryotic phytoplankton in response to Cu stress. *Limnology and Oceanography* 45: 619-627.

Croteau M-N and Luoma SN. (2005) Delineating copper accumulation pathways for the freshwater bivalve Corbicula using stable copper isotopes. *Environmental Toxicology and Chemistry* 24: 2871-2878.

Croteau M-N, Luoma SN, Topping BR, et al. (2004) Stable Metal Isotopes Reveal Copper Accumulation and Loss Dynamics in the Freshwater Bivalve Corbicula. *Environmental Science & Technology* 38: 5002-5009.

Cullen JT and Sherrell RM. (1999) Techniques for determination of trace metals in small samples of size-fractionated particulate matter: phytoplankton metals off central California. *Marine Chemistry* 67: 233-247.

Dupont CL and Ahner BA. (2005) Effects of copper, cadmium, and zinc on the production and exudation of thiols by Emiliania huxleyi. *Limnology and Oceanography* 50: 508-515.

Dupont CL, Nelson RK, Bashir S, et al. (2004) Novel copper-binding and nitrogen-rich thiols produced and exuded by Emiliania huxleyi. *Limnology and Oceanography* 49: 1754-1762.

Guo J, Annett AL, Taylor RL, et al. (2010) Copper-Uptake Kinetics of Coastal and Oceanic Diatoms. *Journal of Phycology* 46: 1218-1228.

Guo J, Lapi S, Ruth TJ, et al. (2012) The Effects of Iron and Copper Availability on the Copper Stoichiometry of Marine Phytoplankton. *Journal of Phycology* 48: 312-325.
Gustafsson J. (2010) Visual MINTEQ. 3.0 ed. Stockholm, Sweeden: KTH Royal Institute of Technology
Heumann KG. (2004) Isotope-dilution ICP–MS for trace element determination and speciation: from a reference method to a routine method? *Analytical and Bioanalytical Chemistry* 378: 318-329.
Hill KL, Hassett R, Kosman D, et al. (1996) Regulated Copper Uptake in Chlamydomonas reinhardtii in Response to Copper Availability. *Plant Physiology* 112: 697-704.
Ho TY, Quigg A, Finkel ZV, et al. (2003) The elemental composition of some marine phytoplankton. *Journal of Phycology* 39: 1145-1159.
Kim H-S, Walsh MJ, Yang H, et al. (2011) Nutrient availability alters levels of non-translationally synthesized nitrogen-rich dipeptides in Emiliania huxleyi. *Aquatic Biology* 12: 215-224.
Le Faucheur S, Tremblay Y, Fortin C, et al. (2011) Acidification increases mercury uptake by a freshwater alga, Chlamydomonas reinhardtii. *Environmental Chemistry* 8: 612-622.
Lee JG, Ahner BA and Morel FMM. (1996) Export of cadmium and phytochelatin by the marine diatom Thalassiosira weissflogii. *Environmental Science & Technology* 30: 1814-1821.
Mann EL, Ahlgren N, Moffett JW, et al. (2002) Copper Toxicity and Cyanobacteria Ecology in the Sargasso Sea. *Limnology and Oceanography* 47: 976-988.
Mendoza-Cózatl DG, Zhai Z, Jobe TO, et al. (2010) Tonoplast-localized Abc2 transporter mediates phytochelatin accumulation in vacuoles and confers cadmium tolerance. *Journal of Biological Chemistry* 285: 40416-40426.
Miura T, Sasaki S, Toyama A, et al. (2005) Copper Reduction by the Octapeptide Repeat Region of Prion Protein: pH Dependence and Implications in Cellular Copper Uptake†. *Biochemistry* 44: 8712-8720.
Moffett JW. (1995) Temporal and Spatial Variability of Copper Complexation by Strong Chelators in the Sargasso-Sea. *Deep-Sea Research Part I-Oceanographic Research Papers* 42: 1273-1295.
Moffett JW, Brand LE, Croot PL, et al. (1997) Cu Speciation and Cyanobacterial Distribution in Harbors Subject to Anthropogenic Cu Inputs. *Limnology and Oceanography* 42: 789-799.
Moffett JW and Dupont C. (2007) Cu complexation by organic ligands in the sub-arctic NW Pacific and Bering Sea. *Deep-Sea Research Part I-Oceanographic Research Papers* 54: 586-595.
Morel FMM. (1987) Kinetics of Nutrient Uptake and Growth in Phytoplankton. *Journal of Phycology* 23: 137-150.
Nevitt T, Öhrvik H and Thiele DJ. (2012) Charting the travels of copper in eukaryotes from yeast to mammals. *Biochimica et Biophysica Acta (BBA) - Molecular Cell Research* 1823: 1580-1593.
Nies DH. (2003) Efflux-mediated heavy metal resistance in prokaryotes. *FEMS Microbiology Reviews* 27: 313-339.
Osman D and Cavet JS. (2008) Chapter 8 Copper Homeostasis in Bacteria. In: Allen I. Laskin SS and Geoffrey MG (eds) *Advances in Applied Microbiology*. Academic Press, 217-247.

Palenik B, Grimwood J, Aerts A, et al. (2007) The tiny eukaryote Ostreococcus provides genomic insights into the paradox of plankton speciation. *Proceedings of the National Academy of Sciences* 104: 7705-7710.
Peers G, Quesnel SA and Price NM. (2005) Copper requirements for iron acquisition and growth of coastal and oceanic diatoms. *Limnology and Oceanography* 50: 1149-1158.
Price NM, Harrison GI, Hering JG, et al. (1989) Preparation and Chemistry of the Artificial Algal Culture Medium Aquil. *Biological Oceanography* 6: 443-461.
Quigg A, Reinfelder JR and Fisher NS. (2006) Copper uptake kinetics in diverse marine phytoplankton. *Limnology and Oceanography* 51: 893-899.
Rensing C, Fan B, Sharma R, et al. (2000) CopA: An Escherichia coli Cu(I)-translocating P-type ATPase. *Proceedings of the National Academy of Sciences* 97: 652-656.
Schaefer JK and Morel FMM. (2009) High methylation rates of mercury bound to cysteine by Geobacter sulfurreducens. *Nature Geoscience* 2: 123-126.
Stuart RK, Dupont CL, Johnson DA, et al. (2009) Coastal Strains of Marine Synechococcus Species Exhibit Increased Tolerance to Copper Shock and a Distinctive Transcriptional Response Relative to Those of Open-Ocean Strains. *Applied and Environmental Microbiology* 75: 5047-5057.
Sunda WG and Huntsman SA. (1995a) Iron uptake and growth limitation in oceanic and coastal phytoplankton. *Marine Chemistry* 50: 189-206.
Sunda WG and Huntsman SA. (1995b) Regulation of Copper Concentration in the Oceanic Nutricline by Phytoplankton Uptake and Regeneration Cycles. *Limnology and Oceanography* 40: 132-137.
Sunda WG and Huntsman SA. (1998) Interactions Among Cu2+, Zn2+, and Mn2+ in Controlling Cellular Mn, Zn, and Growth Rate in the Coastal Alga Chlamydomonas. *Limnology and Oceanography* 43: 1055-1064.
Vasconcelos MTSD and Leal MFC. (2000) Adsorption and Uptake of Cu by Emiliania huxleyi in Natural Seawater. *Environmental Science & Technology* 35: 508-515.
Verma SK and Singh HN. (1991) Evidence for energy-dependent copper efflux as a mechanism of Cu2+ resistance in the cyanobacterium Nostoc calcicola. *FEMS Microbiology Letters* 84: 291-294.
Yun C-W, Ferea T, Rashford J, et al. (2000) Desferrioxamine-mediated Iron Uptake in Saccharomyces cerevisiae: Evidence for Two Pathways of Iron Uptake. *Journal of Biological Chemistry* 275: 10709-10715.

CHAPTER 4

Bioavailability of Copper in the Presence of Thiols

1. Abstract

Thiols have been previously measured at varying concentrations in surface seawater and estuaries. As strong copper ligands they are likely to complex a portion of Cu(I) in surface seawater, however their impact on the bioavailability of copper to marine algae is uncertain. Despite affinity of thiols for Cu(I), speciation models predict that free cuprous ion concentrations are already heavily buffered by the presence of chloride, a strong inorganic Cu(I) ligand. The presence of thiols will thus have only a marginal effect on reducing bioavailable copper. In this study test this prediction by examining the bioavailability of thiol complexes to two species of marine algae. Uptake experiments were designed to control the copper ion oxidation states. At high thiol concentrations, Cu(I) uptake is reduced by approximately half in replete cultures of *Emiliania huxleyi*, a coccolithophore, and *Thalassiosira pseudonana,* a diatom. However, uptake of Cu(I) in the presence of a thiol is still substantially higher than in cultures exposed to Cu(II) and a strong Cu(II) ligand, suggesting that thiols may not be as effective in limiting bioavailability. Cysteine was able to enhance Cu(I) uptake in copper limited cells and in cultures pre-exposed to Cu(II)-EDTA. Copper limitation increases surface reduction and cysteine uptake in *E. huxleyi*. Cysteine uptake rates, similar to that of copper, may indicate that a copper cystine complex is being assimilated.

2. Introduction

In surface seawater copper is bound to organic ligands of likely biological origin. The concentration of total copper in surface sea water typically ranges from 1-2 nM, while ligand concentrations are typically one order of magnitude higher. Elevated concentrations of copper and organic ligands have been observed in coastal and estuarine waters (Vachet and Callaway, 2003). These ligands can strongly bind copper and subsequently reduce the free ion concentrations from toxic to tolerable levels (Coale and Bruland, 1988; Moffett and Dupont, 2007).The composition of the pool of copper binding ligands is diverse (Croot et al., 1999) and largely unidentified. However, it has been shown to be partly composed of thiols (Al-Farawati and Van Den Berg, 2001; Dupont et al., 2006; Dryden et al., 2007). Several species of marine algae can produce and exude thiols, such as glutathione, under copper stress (Tang et al., 2005). The coccolithophore *Emiliania huxleyi* produces two unique dipeptides Arg-Cys and Gln-Cys when exposed to elevated copper levels (Dupont and Ahner, 2005). These compounds may be part of a copper detoxification mechanism as copper-Arg-Cys complexes are observed extracellularly (Dupont et al., 2004). Thiols can strongly complex copper in its reduced, cuprous, state. Complexes of Cu(I) with several cysteine containing peptides are relatively strong (logK' = 11-12). However, at the observed concentrations in seawater, thiols are in competition with chloride ions that would likely dominate Cu(I) speciation (Chapter 1). Subsequently, thiols only marginally reduce the cuprous free ion concentrations in surface seawater. Furthermore, thiols can also facilitate the reduction of Cu(II) to Cu(I) (Pecci et al., 1997; Aliaga et al., 2010) prior to complexation:

$$2\,RSH + Cu(II) \longrightarrow RS\cdot + RS - Cu(I) \qquad \text{Equation 1.}$$

The reduction of copper is typically facilitated by cell surface reductases as a required precursor to, cuprous ion dependent, high affinity copper uptake. The bioavailability of copper could thus be increased by the presence of thiols. In that case, Cu(II) ligands are likely to be more effective than thiols at limiting cellular assimilation of copper. However, high cellular concentrations of these thiols would suggest that their role in detoxification may be of highest importance inside the cell. At these levels, thiols would likely be far more effective in complexing Cu(I) and buffering free ion concentrations than in surface seawater. The presence outside the cell could be explained by efflux of the Cu(I) thiol complexes in a similar fashion to the detoxification of cadmium facilitated by phytochelatins (Lee et al., 1996; Mendoza-Cózatl et al., 2010).

Few studies have examined the bioavailability of copper-ligand bioavailability to marine algae. Exudates of several species can have both adverse and productive effects on algal growth presumably due to their ability to alter the bioavailability of various metals (Vasconcelos et al., 2002). Uptake of copper has been shown to be enhanced by some ligands but reduced by others (Semeniuk et al., 2009). Cysteine can enhance zinc uptake in the presence of a stronger ligand such as EDTA (Aristilde et al., 2012). Additionally, there are a several examples of molecular mimicry in which metal uptake is enhanced by complexation with a transport-prone molecule (Bridges and Zalups, 2005), most notably in the case in which methyl mercury hitchhikes on cysteine uptake though a large amino acid transporter (Simmons-Willis et al., 2002).

In this paper we demonstrate that thiol ligands can reduce the bioavailability of copper only at high concentrations, that are not typically found in surface seawater. We also demonstrate several mechanisms in which copper uptake is enhanced by the presence of cysteine. Our

experiments were designed with the aim of discerning the complexation and assimilation of the cuprous and cupric ions and the ability of thiols to facilitate copper reduction. We also explore the effect of biologically mediated copper reduction. Our results further clarify the role of copper binding ligands in surface seawater.

3. Methods

3.1. Culturing

The coccolithophore *E. huxleyi* (CCMP1516) and the centric diatom *Thalassiosira pseudonana* (CCMP1335) were obtained from the Provasoli-Guillard National Center for Marine Algae and Microbiota (Bigelow Laboratory for Ocean Sciences, West Boothbay Harbor, ME, USA). Axenic cultures were grown in acid washed polycarbonate bottles under constant lighting conditions of 120 µmol photon m^{-2} s^{-1} at 20°C. Growth was monitored via fluorescence measurements of *Chl a* (Turner Instruments). Specific growth rates were calculated from a natural log regression of the fluorescence measurements over time.

Cells were cultured in the synthetic ocean water medium Aquil (Price et al., 1989). Aquil with no trace metals or vitamins added (hereafter designated SOW) was used in cellular resuspensions and washes. In growth media trace metal ion concentrations were buffered with 100 µM EDTA. *E. huxleyi* and *T. pseudonana* were grown under total iron concentrations of 100 nM (initial pFe^{3+} = 20) and 8.32 µM (initial pFe^{3+} = 18.1) respectively. These iron concentrations were sufficient to maintain maximal growth rates for both species (Sunda and Huntsman, 1995). The total copper concentrations for replete cultures was 20 nM (initial pCu^{2+}= 13.8). Cu-limited cultures were prepared by growing cells for at least three generations in 100

nM iron containing Aquil with no added copper. Background copper for these cultures was estimated to be 1 nM (initial pCu^{2+}= 15.2) based upon the assumption that 50% of the total copper was associated with the cells. A similar estimate was made by (Guo et al., 2010).

When cultures reached mid-exponential growth cells were harvested by centrifugation in 500 mL acid washed polycarbonate centrifuge tubes at 4°C. *E. huxleyi* cells were pelleted at 7200 RPM for 10 minutes. *T. pseudonana* cells were concentrated by 15 minutes of centrifugation at 9000 RPM for 10 minutes, after which the supernatant was decanted and the concentrated cells were centrifuged again in 50 mL acid washed polystyrene centrifuge tubes for 15 minutes at 9000 RPM. Pellets of both species were gently rinsed with SOW and resuspended by slowly vortexing in fresh SOW to a desired biomass concentration.

3.2. Reductants and thiol ligands

Stock solutions of reductants and Cu(I)-ligands were made daily prior to each experiment. Primary 10 mM stock solutions of cysteine (Baker), reduced GSH (Sigma), and ascorbate (Sigma) were prepared in SOW and used within four hours. The cysteine containing dipeptides Arg-Cys and Gln-Cys were synthetized at 99% purity by Anaspec (Freemont, CA) and dissolved in high quality Milli-Q water and split into several stock aliquots which were then frozen and stored at -80°C until use. Daily stock solutions of 1 mM Arg-Cys and Gln-Cys were prepared by diluting the stock in SOW and adding equimolar $NaBH_4$ (Sigma) to reverse the effects of oxidation. This solution was allowed to react for an hour to allow for decay of the borohydride ion. Concentrations of thiol stocks were confirmed using Elman's Reagent or fluorescent derivatization, the method for which is described elsewhere (Dupont et al., 2004).

3.3. Production of Cu(I) and Cu(I) complexes for use in uptake experiments

Cu(I) used in uptake experiments, was generated by gaseous reduction (Attari and Jaselskis, 1972) by bubbling $SO_{2(g)}$ through a 1 mM solution of Cu(II)O dissolved in 1 mM HCl and 100 mM NaCl. $SO_{2(g)}$ was generated by adding 50% sulfuric acid to dry sodium sulfate while stirring in generation flask. Gas was delivered through acid washed PVC (Tygon) tubing into the copper stock, bubbling for 15 minutes. Dissolved $SO_{2(g)}$ was subsequently sparged out of the copper stock by bubbling through ultrahigh purity $N_{2(g)}$ (Airgas) for 45 minutes. At this point the pH was slowly titrated to a pH of 6.5-7.0 using 0.1 M Ultrapure NaOH (Fluka). An aliquot of the solution was removed and treated with 10 mM bathocuproine disulfonate (BCS, Sigma) to confirm Cu(I) concentration. The procedure of measuring the absorbance of this complex is described below. The reduced copper stock was continuously bubbled with $N_{2(g)}$ until use which was always within four hours. BCS measurements indicated that the concentration of Cu(I) did not change during this time. In experiments where Cu(I) was added with either cysteine, GSH, Arg-Cys or Gln-Cys, the ligand and Cu(I) was combined in 5 mL of SOW and allowed to equilibrate for 15 minutes before addition to an algae culture.

3.4. Biological uptake experiments

Two types of copper uptake experiments were performed. The first measured direct assimilation of either Cu(I) or Cu(II) by cells in the absence or in the presence of various complexing ligands. The second tested the ability of several reductants to reduce Cu(II) in equilibrium with EDTA thereby increasing the bioavailability of Cu to the cell. In each type of experiment, cells were resuspended in SOW at concentrations of approximately 0.5-1.5 million

cells per milliliter for *T. pseudonana* and 1.5-3 million cells per milliliter for *E. huxleyi*. These biomass concentrations were roughly equivalent to the biomass concentration prior to centrifugation from the growth medium. A portion of this cell suspension was sampled for initial cellular copper concentrations. The remainder was then aliquoted into separate batches to test uptake.

In the direct assimilation experiments, uncomplexed Cu(I) and Cu(II) as well as Cu(I) in the presence of several thiols or Cu(II) preequlibriated with either EDTA or GSSG were added to resuspended algae cultures. Each treatment was gently shaken and kept under constant light for 60 minutes at which point samples were taken from each treatment. Cu(II)-reductant release experiments were performed by adding preequilibrated Cu(II)-EDTA at concentrations of 100 nM Cu and 1000 nM EDTA to the resuspended cultures. After 30 minutes of exposure a sample was taken and the culture aliquoted into four separate batches. One batch was kept as a control, while 500 nM of either cysteine, GSH or ascorbate was added to each of the other three. Each batch was stored in the growth chamber and were sampled after 30 minutes. At each time point, triplicate samples were taken for copper measurement (described below) and duplicate samples were taken for cell counts. Cell counts were made using a Neubauer Improved hemocytometer.

3.5. Cellular copper measurements

Algae cell samples were gently filtered (5 kpsi vacuum) onto acid washed 0.8 µm polycarbonate membrane filters (Whatman) using acid washed polysulfonate funnels and supports (Nalgene). Surface bound copper was removed by washing cells with SOW containing 10 mM DTPA and 10 mM DTT (Sigma) for 20 minutes followed by a rinse with 10 mL SOW.

Filters were stored in acid washed microcentrifuge tubes at -20°C until digested.

Filters were digested in Teflon screw cap vials (Savillex) using 0.8 mL 50% HNO_3 (Aristar Ultra), diluted with high quality H_2O (Millipore). Vials were heated at 90°C for 8 hours and then allowed to cool. Digests were diluted to a final volume of 8 mL and HNO_3 concentration of 5%. Diluted digests were gently mixed and decanted into acid washed 15 mL centrifuge tubes, leaving the filter. To remove undigested silica frustules, diluted digests of *T. pseudonana* were centrifuged at 3000 rpm and the supernatant was pipetted into a fresh acid washed centrifuge tube.

Measurements of both ^{63}Cu and ^{65}Cu isotopes were made using either an Elan II dynamic reaction cell inductively coupled plasma quadrapole mass spectrometer (DRC-ICP-MS, Perkin Elmer) or an Element II magnetic sector field inductively coupled plasma mass spectrometer (MSF-ICP-MS, Thermo). Copper isotope signals were optimized by adjusting instrumental settings prior to daily analysis or as needed. Elemental standards from 1 to 50 ppb (High Purity Standards) were prepared in 5% HNO_3 and compared against other laboratory standards. For the DRC-ICP-MS ammonia (Airgas) was used as a collision gas while a solution of 10 ppb Gallium was employed as an internal standard. When using the MSF-ICP-MS, standard curves were generated every 24 samples and a 5 ppb copper standard was measured every 6 samples as a quality check. The 5 ppb standard was used to interpolate a correction factor any signal drift during the course of the run. Instrumental errors were very small in comparison to the biological or replicate variability, which was used for final error propagation.

3.6. Production of Cu(I) from complexed Cu(II) by reducing agents

We designed a series of experiments to test the ability of thiols to generate Cu(I) from Cu(II) ligand complexes. Previously the colorimetric Cu(I) ion indicator neocuproine has been used employed to quantify thiols in by measuring the rapid thiol-facilitated 1:1 reduction of Cu(II) to Cu(I) (Besada et al., 1989). In these experiments we utilized bathocuproine disulfonate(BCS), an analogous Cu(I) indicator with a larger molar absorptivity, to measure Cu(I) production from several strong complexes of Cu(II). Assays were performed in acid washed 96 well plates (Corning). The Cu(II) ligands 1,4,8,11-tetraazacyclotetradecane (Cyclam), 1,4,8,11-tetraazacyclotetradecane-1,4,8,11-tetraacetate (TETA), DTPA, oxidized glutathione (GSSG) and NTA were obtained from Sigma, while EDTA was obtained from Fisher. Stock solutions containing 1.0 mM ligand and 0.5 mM Cu(II)O were prepared in MilliQ water and allowed to equilibrate overnight prior to each assay. Dilutions of Cu(II)-ligand stocks were made to achieve a final concentration of 50 µM Cu(II) and 100 µM ligand. Copper affinities, kinetic parameters and estimiated free cupuric ion concentration under these conditions are listed in (Table 1) BCS was added to each well to achieve a final concentration of 1 mM. SOW was added as needed to ensure a final uniform volume of 200 µL after the addition of all reagents. Solutions of the reductants cysteine, GSH, ascorbate and dithiothreitol (DDT, Sigma) were prepared in SOW immediately prior to addition. Plates were loaded into a Synergy4 Microplate Reader Spectrophotometer (BioTek) and the desired reductant was added via auto dispenser to achieve reductant-to-metal ratios of 0, 0.5, 0.6, 0.8, 1 and 2, 4 and 10. Absorbance of the BCS-Cu(I) complex at a wavelength of 483 nm was measured immediately after the addition of each reductant and periodically thereafter for 90 minutes. Cu(I) concentrations were calculated using

Table 1. Conditional stability constants of Cu(II) ligands and concentrations of the cupric ion and inorganic cupric complexes in SOW. Total Cu(II): 50 µM; Total L: 100 µM.

L	**logK'**	**[Cu^{2+}]**	**Cu'**	**K s^{-1}**
Cyclam	22.1	8.11E-23	1.54E-21	
TETA	15.4	3.59E-16	6.14E-15	
DTPA	12.5	3.03E-13	5.73E-12	5.50E-01[ǂ]
EDTA	10.2	6.19E-11	1.17E-09	7.80E-02[ǂ]
GSSG	10.1	8.08E-11	1.45E-09	
NTA	8.6	2.67E-09	5.64E-08	5.60E-02[ǂ]

[ǂ] pH 6.0 (van Doornmalen et al., 2002)

an emissivity constant of 12,700 M^{-1} cm^{-1}.

3.7. Extracellular production of Cu(I)

A similar experiment was performed to test the ability of both species of phytoplankton to produce Cu(I) from Cu(II). BCS has been previously employed to observe cell surface reduction in *T. weissflogii* (Jones et al., 1987). We devised a similar experiment to test *E. huxleyi* and *T. pseudonana* under copper limiting and replete conditions. In our experiments, 9 mL of concentrated resuspended algae culture was aliquoted as needed into polysulfonate centrifuge tubes. Concentrations of *T. pseudonana* and *E. huxleyi* cells were approximately 10 million and 30 million cells per milliliter, or 10-fold the biomass concentration prior to centrifugation. BCS was added to achieve a final concentration of 1.0 mM. Cu(II) or preequlibrated Cu(II)-EDTA was added to attain a final concentration of 100 µM Cu(II) and 1.0 mM EDTA. The volume was immediately brought up to 10 mL with SOW. Starting at 5 minutes after the addition of Cu(II), samples were taken periodically over a period of 150 minutes. At each time point an 800 µL aliquot was pipetted into a 1.7 mL microcentrifuge tube and immediately centrifuged at 3000 rpm for 5 minutes. Duplicate 200 µL aliquots of the cell-free supernatant were pipetted into an acid washed 96-well plate. Absorbance of the Cu(I)-BCS complex was measured following the collection of all samples as a measure of the Cu(I) generated. Background measurements of Cu(I)-BCS formation were made in spent media.

3.8. Measurement of cysteine uptake

Radiolabeled [^{35}S]cysteine was obtained from GE Life Sciences, diluted to a specific

activity of 100 Ci mol^{-1}, and aliquoted into separate stocks which were subsequently stored frozen at -20°C until use. *E. huxleyi* cells were resuspended at a concentration of 1.5-3 million cells per milliliter and aliquoted into separate bottles. Cultures used in temperature studies were chilled to 4°C. The [^{35}S]cysteine stock was then added as needed to each bottle. When added with a metal, cystine was allowed to equilibrate for 15 minutes in the presence of either Cu^{+}, Cu^{2+}, Zn^{2+} (sulfate salt, Sigma) or Cd^{2+} (chloride salt, Sigma). At 5 minute intervals from 0-30 minutes, 20 mL aliquots were removed from each treatment and filtered onto GF/A filters. To halt cysteine uptake, filters were washed with, 5 mL of 1 mM unlabeled cysteine in ice cold SOW followed by 10 mL ice cold SOW. Cellular [^{35}S]cysteine was measured by liquid scintillation counting.

3.9. Computational

Equilibrium calculations were performed using VisualMINTEQ (Gustafsson, 2010) and log-conditional stability constants of 11.2 and 12 for cysteine and glutathione Cu(I) complexes respectively (Chapter 1). Background concentrations of ions in SOW were used all in speciation calculations.

4. Results

4.1. Copper assimilation in the presence of thiols

In *E. huxleyi* experiments the addition of copper to the culture medium either as unbound Cu(I) or Cu(II) had no statistical influence on the amount of Cu assimilated by the cells (Figure 1A & C). In contrast assimilation of the cuprous ion was double that of the cupric ion in *T.*

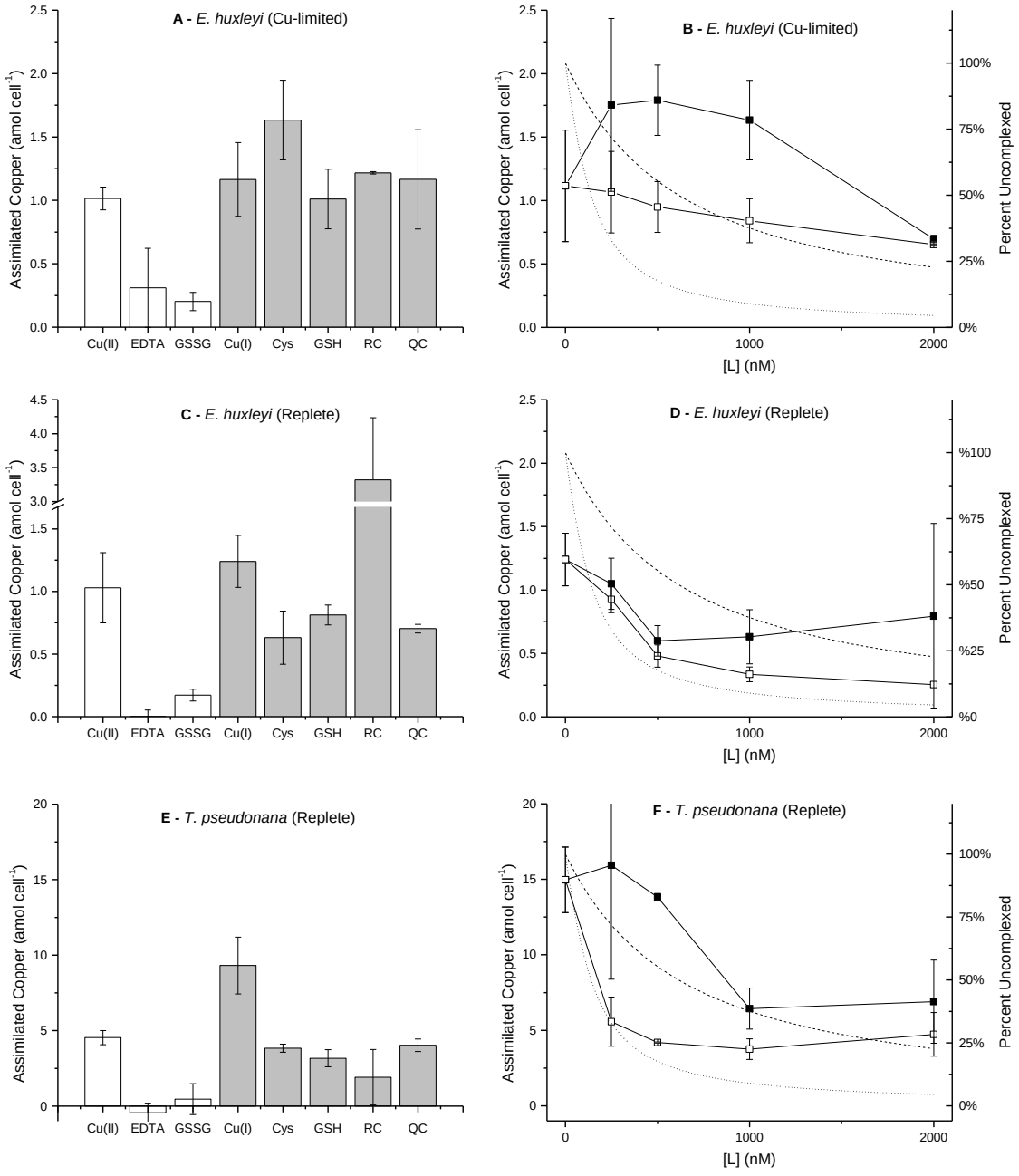

Figure 1. Copper uptake after 60 minutes in the presence of copper ligands. *T. pseudonana* cells were resuspended in SOW. Left panels show uptake after the addition of preequlibrated spikes of 100nM Cu(I) (grey bars) or Cu(II) (white bars) with or without 1000nM of Cu(I) and Cu(II) ligands. Right panels show uptake of 100nM Cu(I) in the presence of increasing concentrations of Cysteine (filled squares), or GSH (empty squares).

pseudonana (Figure 1E). Both EDTA and GSSG were highly effective at blocking Cu(II) assimilation in all cultures (Figure 1A, C & E). The presence of various thiols had a mixed effect on the assimilation of Cu(I). In replete cultures of *E. huxleyi*, assimilation was reduced by approximately 50% when Cu(I) was added in the presence of cysteine, GSH or Gln-Cys but doubled in the presence of Arg-Cys (Figure 1C). In Cu-limited cultures of *E. huxleyi* the thiols did not appear to depress assimilation (Figure 1A), with cysteine inciting a slight, yet statistically significant ($P < 0.05$ by Student's *t* test) increase over assimilation of unbound Cu(I). Assimilation in *T. pseudonana* did appear to favor Cu(I) over Cu(II), however the presence of all four thiols reduced Cu uptake.

Copper assimilation is further dependent on the concentration of thiol ligand (Figure 1B, D, &F). Generally higher concentrations of both thiols reduced copper assimilation, but culture-specific and thiol-specific differences were observed. The assimilation of copper by *T. pseudonana* in the presence of cysteine or glutathione appears to be correlated to the fraction of copper not bound to a thiol (Figure 1F). This was also somewhat true for the replete culture of *E. huxleyi* (Figure 1D), but assimilation in the presence of cysteine closely followed that of glutathione at low thiol concentrations, before slightly increasing at higher concentrations (Figure 1B). Copper limitation of *E. huxleyi* results in increased copper assimilation in the presence of cysteine. Under limitation the presence of glutathione appeared to have little effect on net assimilated copper. Furthermore, the presence of cysteine from 250 – 1000 nM actually increases the amount of assimilated copper. Cu-limitation appears to induce some functional change that allows for increased bioavailability of Cu-thiol, particularly Cu-cysteine complexes to the cell.

Our previous work investigated the uptake of copper added as Cu(II) in the absence of any coordinating ligands by the organisms *T. pseudonana* and *E. huxleyi.* Export of Cu from replete *E. huxleyi* cells resulted in lower net assimilation compared to gross Cu uptake during experiments longer than 1 hour; experiments described in this chapter are shorter in duration therefore the data is only reported as measured total assimilated Cu. To confirm that export was not significantly affecting our results isotopically enriched copper was employed to calculate assimilation (Chapter 3) from changes in the cellular isotopic ratios. Differences between this value and the total assimilated value were negligible in this study.

We are also able to show that cysteine can increase the bioavailability of copper that is strongly complexed by EDTA (Figure 2). The addition of 500 nM cysteine after a half hour of exposure to 50 nM Cu(II) pre-equilibrated with 1000 nM EDTA was able to increase cellular copper levels over the next 30 minutes in all cultures. Uptake was most pronounced in relation to the initial cellular copper concentrations in Cu-limited *E. huxleyi* with copper quotas nearly tripling following the addition of cysteine. Replete *E. huxleyi* cells showed only a modest increase of 0.15-0.25 amol cell^{-1} which was comparable to the relative amount of copper assimilated by replete *T. pseudonana* cells.

Conversely, the addition of glutathione and did not increase uptake compared to Cu(II)-EDTA exposed control cells that were not treated with a reductant. Neither did the non-copper binding reductant ascorbate which has been demonstrated to reduce extracellular copper and increase copper uptake in yeast cultures (Hassett and Kosman, 1995).In some cases, inexplicable decreases were observed with ascorbate and glutathione addition.

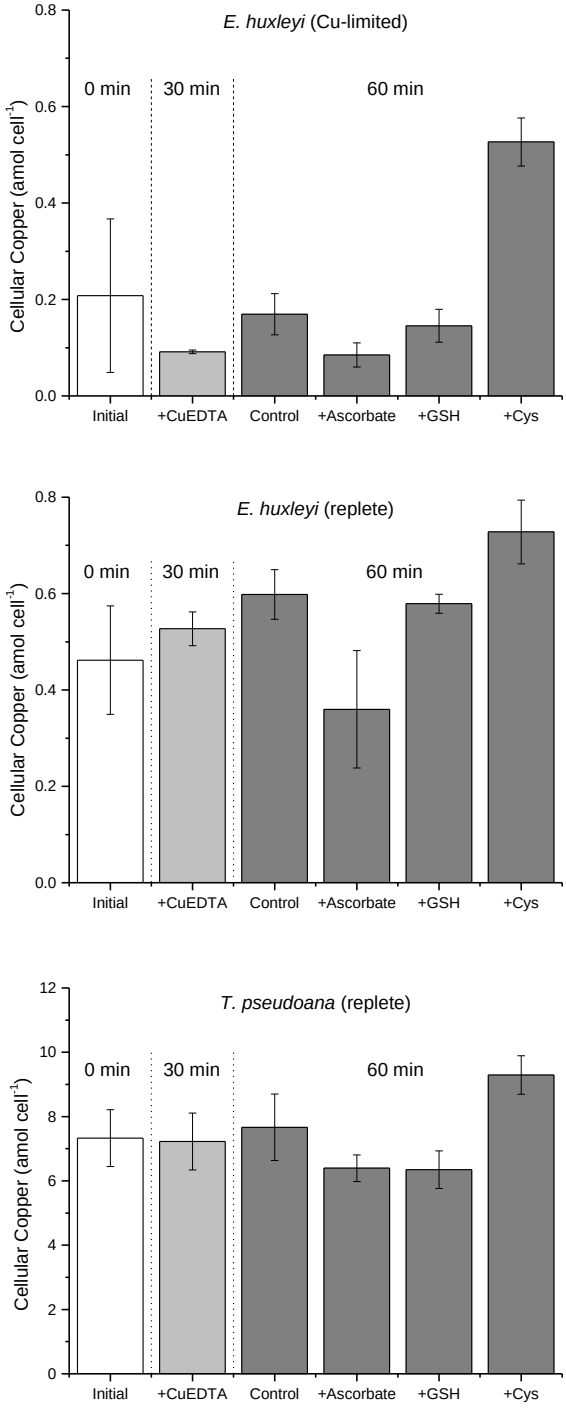

Figure 2. Copper uptake from cells exposed to 1000 nM EDTA, 50 nM Cu(II) for 30 minutes and then 500 nM of either ascorbate, cysteine or GSH for an additional 30 minutes. In E. huxleyi panel grey bars represent Cu-limited cells and black bars replete cells. Only replete T. pseudonana cultures were used in these experiments.

4.2. Thiol mediated release of Cu(I) from strong Cu(II)-ligand complexes

To demonstrate a chemical mechanism for the reductive release of Cu(I) from strong Cu(II ligands, we employed the strong Cu(I) colorimetric indicator bathocuproine disulfonate to measure the production of Cu(I) upon the addition of thiols to pre-equilibrated mixtures of Cu(II) and various Cu(II) ligands. Upon the addition of cysteine, GSH, and ascorbate Cu(I) was generated from complexes of EDTA, DTPA, and NTA. Generation of Cu(I) from the very strong ligands, TETA and cyclam, was negligible (Figure 3). Only cysteine was able to generate a small amount of Cu(I) (<1μM) in the presence of TETA. The rate of Cu(I) production varied with both the chelator and the reductant. Cysteine was the most effective reductant, 50 μM of which was able to facilitate very rapid reduction of Cu(II) that went to completion in under 15 minutes. Cu(I)-BCS production by GSH was substantially slower, and the addition of 50 μM GSH to solutions of EDTA and NTA did not result in complete reduction in under an hour. Differences caused by individual Cu(II) ligands were most pronounced when using GSH. Generation of the Cu(I)-BCS complex by GSH was fastest in the presence of DTPA, followed by NTA and EDTA. Higher concentrations of either cysteine or GSH promoted more rapid reduction (not shown). Additions of either GSH that were less than 50 μM resulted in slower production of Cu(I) that either reached or approached a concentration that was equimolar to the amount of reductant.

While the addition of 25 μM ascorbate resulted in rapid equimolar production of Cu(II) (Figure 3C), higher concentrations of ascorbate resulted in lower overall, albeit still rapid, production of Cu(I)-BCS (data not shown). Ascorbate has been long and widely used to reduce Cu(II) to Cu(I) for a variety of analytical uses (Yebra-Biurrun, 2000). However, high

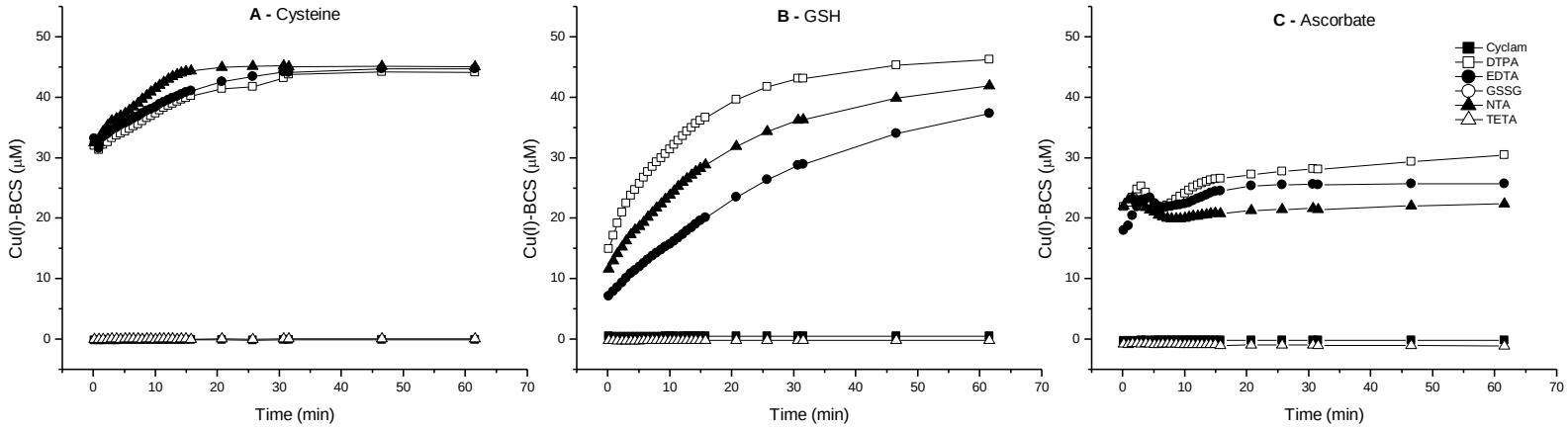

Figure 3. Production of Cu(I) from 50 μM Cu(II) in the presence of several strong Cu(II) chelator by 50 μM of Cysteine (A), 50 μM GSH (B) or 25 μM of ascorbate (C). While Cu(I) production at this addition of ascorbate was rapid and equimolar higher concentrations of ascorbate had a negative effect on absorbance.

concentrations of ascorbate in the presence metal-ligand complexes can catalyze the generation of reactive oxygen species which results in the autoxidation of ascorbate (Burkitt and Gilbert, 1990; Buettner and Czapski, 1986; Xu et al., 2000). It is unclear if these effects are present at the concentrations used in the reduction-uptake experiments (Figre 2?). Conceivably it could explain why no uptake is observed with the addition of ascorbate. Regardless such secondary reactions highlight the specificity of the reductant, such as cysteine, needed for efficient reduction and stabilization prior to uptake.

The relative differences in Cu(I)-production facilitated by these reductants may give hints to the mechanism of reduction, which could be either on the complex or on the free metal ion. The slow production of Cu(I) by GSH was a surprise. Our initial tests as well as a previous study indicate that in the absence of a chelator this reaction should achieve completion in under 15 minutes (Besada et al., 1989). The contrasting behavior of cysteine and GSH, as well as the effect of concentration on rate of reduction, may indicate that cysteine and ascorbate may be highly effective at reducing complexed copper. In contrast the complex may not be accessible to reduction by GSH and that the observed rate of reduction is limited by the dissociation of Cu(II) from the chelator. The relative rates of Cu(I) production by GSH from Cu(II) ligand complexes is consistent with measured rates of Cu(II) dissociation from DTPA, NTA and EDTA at pH 6.0 (Table 1) (van Doornmalen et al., 2002). It may also be possible that reduction could occur via both pathways at different rates. Regardless of the exact mechanism of Cu(I) production from Cu(II) complexes, it does appear that cysteine does offer a considerable advantage over GSH with respect to increasing the bioavailability of Cu to cells.

4.3. Surface reduction of copper

The primary mechanism of copper reduction prior to uptake is facilitated by cell surface reductases (Blaby-Haas and Merchant, 2012). Previous work has shown that their activity can be measured by using BCS as a Cu(I) indicator (Jones and Morel, 1988). This study further demonstrated that reductases could act on some Cu(II) complexes, but no reduction was observed with Cu(II)-EDTA. We performed similar experiments with and without EDTA in the presence of replete and Cu-limited cells to test the reductive ability of *T. pseudonana* and *E. huxleyi* cells in fresh media.

Uncomplexed copper was rapidly reduced in all cultures (Figure 4). Reduction by *T. pseudonana* was near complete after two hours, while *E. huxleyi* reduced approximately half of the Cu(II) in the same time fame. The presence of a complexing ligand slowed Cu(I) production significantly, but low levels of Cu(I) production was observed even after background correction. Given the slow production rate in the presence of EDTA, as well as the high copper and biomass concentrations, reduction was likely occurring on the buffered free cupric ion, that once removed is replenished by dissociation of Cu(II)-EDTA complex.

Copper limitation of *E. huxleyi* resulted in an increase in reduction of both uncomplexed and complexed Cu(II). Surprisingly no change in reduction rates was observed in cultures of Cu-limited *T. pseudonana*. However, reduction in *T. pseudonana* was approximately 10 fold faster than those of either *E. huxleyi* culture indicating that its mechanism was already highly efficient. To demonstrate that the enhanced uptake rate was part of a biological response in *E. huxleyi* we performed assays over a range of uncomplexed Cu(II) concentrations (Figure 5). Michaelis-Menten kinetics were observed in measurement of reduction and confirmed using a

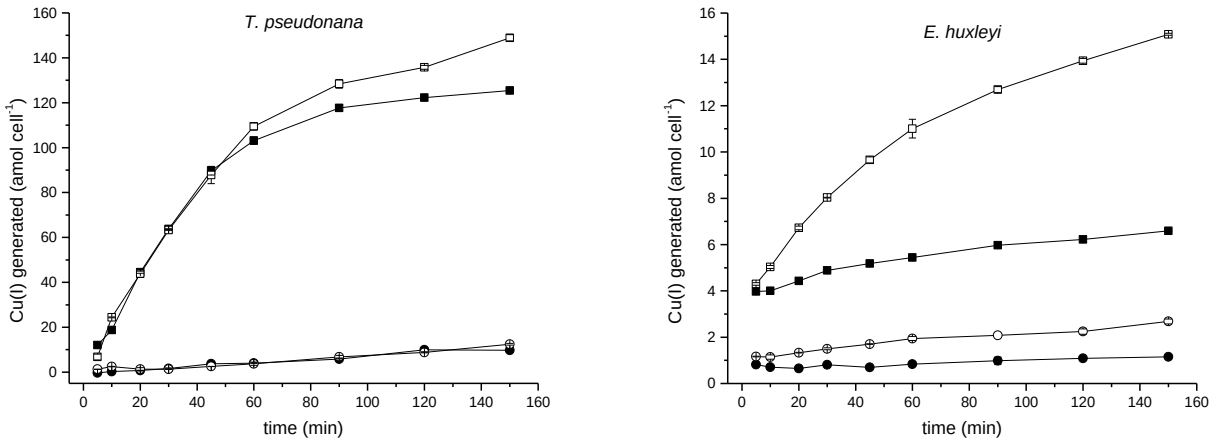

Figure 4. Generation of Cu(I) by *T. pseudonana* and *E. huxleyi*. Copper-limited (open symbols) and replete cultures (filled) of each species were exposed to 100 µM Cu(II) either as a Cu-EDTA complex (circles) or as free ion (squares). All cultures had a background of 1 mM BCS.

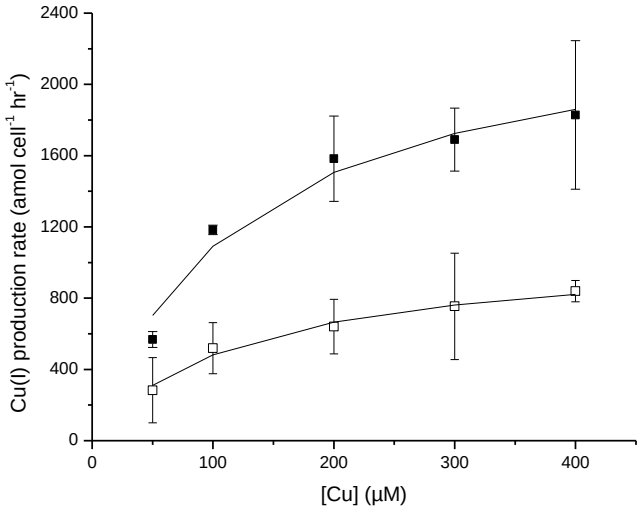

Figure 5. Copper(I) production rates in cultures of replete (○) and Cu-limited (▪) *E. huxleyi*. Lines represent nonlinear least squares fit of $V = V_{max}[Cu]/(K_m+[Cu])$. Fitted constants were Km = 123 ± 32 µM and V_{max} = 40.5 ± 3.9 amol cell^{-1} min^{-1} for Cu-limited cells and Km = 249 ± 71 µM and V_{max} = 18 ± 1 amol cell^{-1} min^{-1} for replete cells.

kinetic model. Nonlinear least-squares fitting of the data returned half saturation constants were 123 ± 22 µM and 249 ± 71 µM for Cu-limited and replete cells respectively V_{max} increased from 18 ± 1 amol cell^{-1} min^{-1} in replete cultures to 91 ± 13 amol cell^{-1} min^{-1} in Cu-limited cultures. These changes suggest not only an increase in the number of reductases (V_{max}) but also a higher affinity of those on the cell surface for Cu(II) (Km) in response to low copper levels.

4.4. Uptake of cysteine as a probable pathway

Finally, we measured uptake of cysteine by both replete and Cu-limited *E. huxleyi* using radiolabeled (^{35}S)cysteine. Uptake of cysteine by *E. huxleyi* follows Michaelis-Menten enzyme kinetics and was surprisingly enhanced under Cu-limitation (Figure 6A). Using a nonlinear-least squares fit of the Michaelis-Menten parameters we calculated a K_m of 368 ± 217 nM and V_{max} of 8.9 ± 4.6 amol cell^{-1} hr^{-1} for the replete cells and a K_m of 408 ± 90 nM and V_{max} of 50.5 ± 6.2 amol cell^{-1} hr^{-1} in Cu-limited cells. This would suggest upregulation of cysteine transporters under Cu-limitation.

Attempts to inhibit uptake of 100 nM cysteine using 100 µM glycine or glutamine did not result in any significant changes (Figure 6B, $P < 0.05$ by Student's *t* test) indicating that the transporter is likely cysteine-specific. Uptake of 100 nM cysteine was not slowed by the presence of equimolar levels of Cu(I), Cu(II), Zn(II), Cd(II). Roughly a sixth of the cysteine is complexed with Cu(I) under the experimental concentrations. Given that cysteine uptake does not decline with the addition of Cu(I) (in fact is slightly higher) it is possible that copper may be assimilated with the cysteine. Inhibition was achieved at lower temperatures (Figure 6B) with a Q_{10} temperature coefficient of 2.1 for Cu-limited cells.

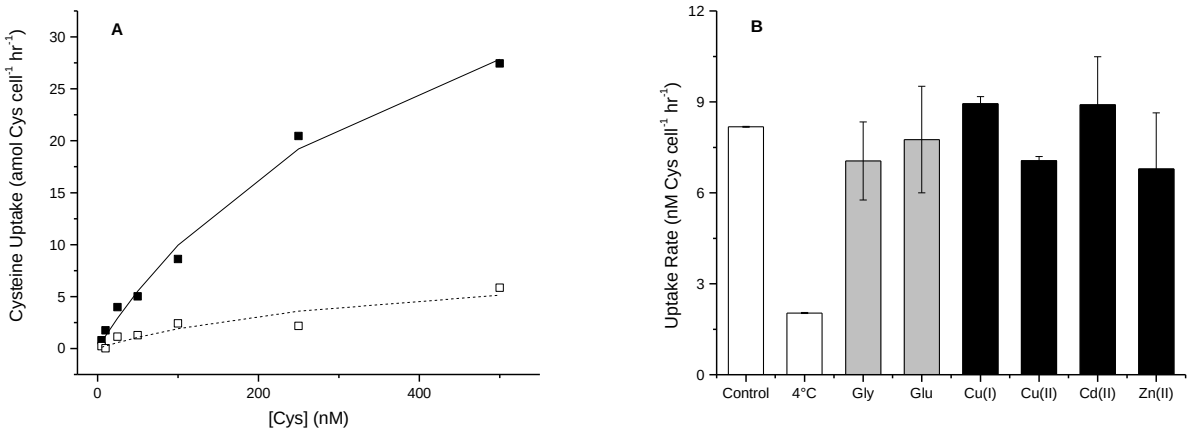

Figure 6. Uptake of cysteine by *E. huxleyi*. Panel A shows uptake in replete (□) and Cu-limited (▪) cells. Lines represent the least-squares Michaelis-Menten fit of the kinetic parameters reported in the text. Panel B shows uptake rates by Cu-limited *E. huxleyi* of under varying conditions: 100 nM cysteine only at 20°C and 4°C (white bars); 100 nM cysteine in the presence of 100 µM glycine or glutamine (grey bars); and 100 nM cysteine in the presence of equimolar concentrations of several dissolved metals. Uptake rates were calculated over 30 minutes after the addition of [^{35}S]cysteine.

5. Discussion

The role of organic, copper-complexing ligands in reducing the toxicity of copper in surface seawater cannot be understated. Some, if not most, reduce extracellular bioavailable copper ion concentrations from toxic to more tolerable levels. In algal cultures EDTA is used in this capacity to buffer Cu(II) concentrations. We demonstrated that oxidized glutathione (GSSG), a Cu(II) ligand present in seawater (Crea et al., 2010) and with a Cu(II)-affinity equivalent to that of EDTA, is nearly effective as EDTA at reducing uptake over the course of an hour (Figure 1A, C & E). While GSSG is one of many, mostly unidentified copper ligands, a proportion of which are likely to coordinate Cu(II) through carboxylic or amine functional groups as in the case of EDTA or GSSG complexes. The strength and concentration of these complexes can vary depending on species and regime. However their presence can substantially reduce the concentration of free and inorganic cupric species (Figure 7) and limit the copper available to low-affinity copper transporters (Figure 8-1) and to surface reductases (Figure 4, Figure 8-A) that would produce Cu(I) available for high-affinity transport (Figure 8-3).

A recent field study of copper uptake by the surface microbiota also demonstrated EDTA reduced copper uptake compared to the absence of a strong ligand, however in contrast to our results the study demonstrated that copper in the presence of GSSG was bioavailable (Semeniuk et al., 2009). This difference is likely best explained by exposure time as these experiments were performed over the course of 8 hours and the authors hypothesize that the GSSG is reduced to GSH. This could be facilitated by several reductive mechanisms, however associated copper would immediately cause the re-oxidation of GSH back to GSSG and produce Cu(I). Our results demonstrate that this form of copper is more bioavailable than bound Cu(II) whether or

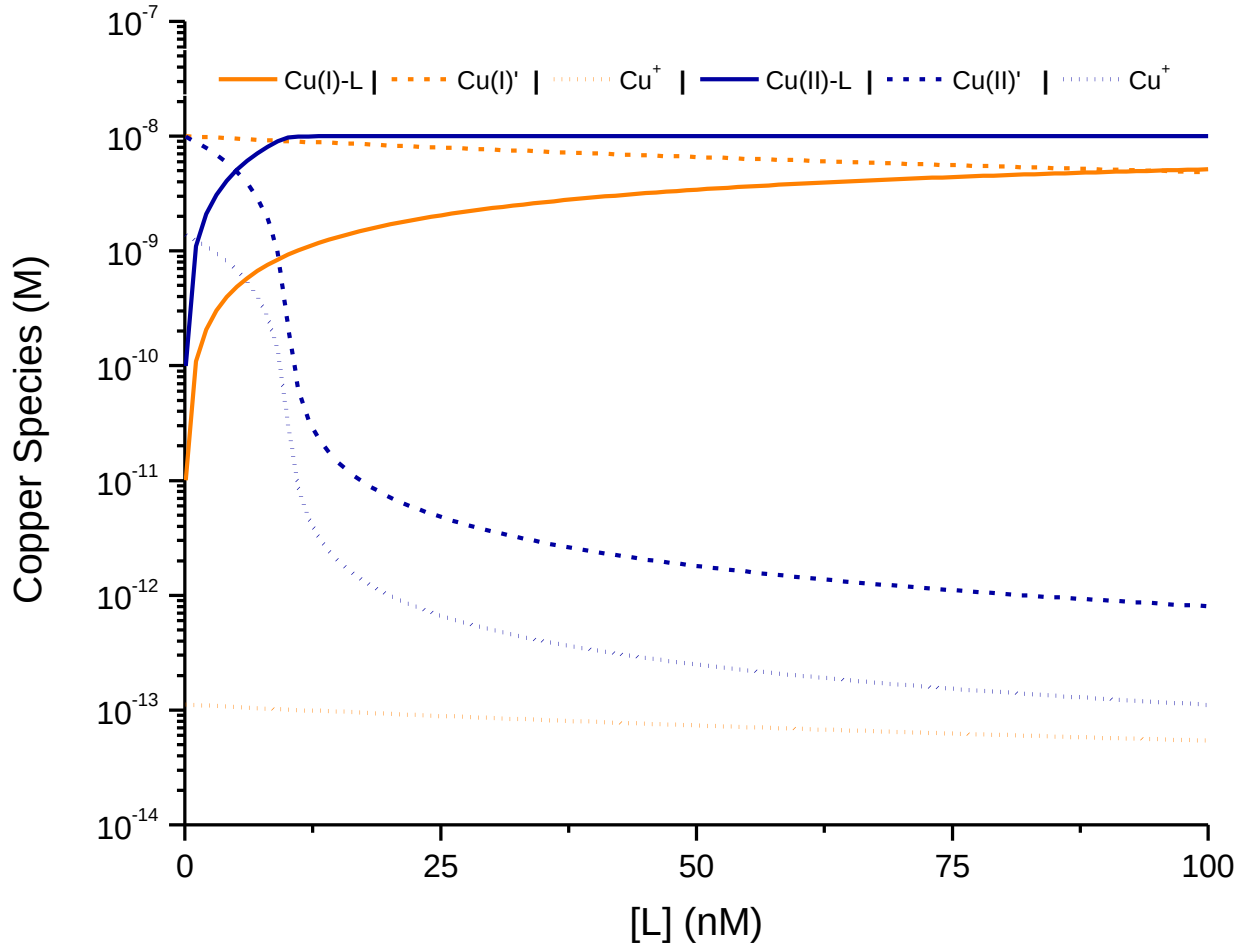

Figure 7. Concentrations of organically complexed (solid), inorganic (dashed), and free ion (dotted) Cu(I) (orange) and Cu(II) (blue) species in the presence of 0 to 100 nM of a ligand (L, log$K^{'}$ = 12.0) in the presence of 10 nM total copper at pH 8.1, 0.55M Cl^{-}. Speciation calculations were performed separately for each oxidation state. Inorganic species formation constants used are listed in Chapter 1, Table 2

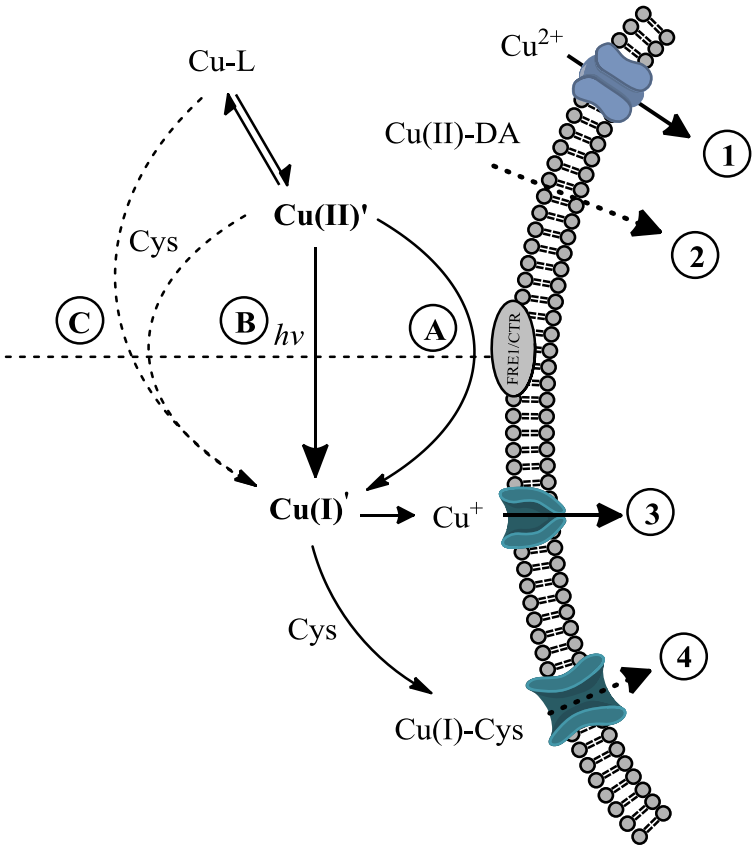

Figure 8. Mechanisms for copper reduction and assimilation: (A) Reduction of Cu(II) by cell surface reductases. (B) Photochemically mediated production of Cu(I) (Moffett and Zika, 1983). (C) Thiol facilitated reduction, demonstrated in this paper. (1) Low affinity uptake of the Cu^{2+} ion. (2) Domoic Acid modulation of copper uptake observed by (Wells et al., 2005). (3) High affinity uptake of the Cu^{+} ion. (4) Uptake of a Cu(I)-Cys complex proposed in this paper.

not a ligand is present. The oxidation state of copper and thiol is thus subsequently critical to understanding bioavailability. Culture and multiple field studies demonstrate that similar thiolate ligands are also highly prevalent. Thiols can range from subnanomolar levels in surface seawater (Dupont et al., 2006) to approximately 100 nM in estuarine environments (Chapter 5). In cultures of copper stressed *E. huxleyi* the dipeptide Arg-Cys can complex as much as one-third of the extracellular copper (Dupont and Ahner, 2005).

Unfortunately, despite a large number of natural and culture studies of copper behavior with marine algae and their exudates, there is very little consideration for oxidation state of copper or in studies that include it, that of the thiol. Additionally little attention is paid to the behavior of Cu(I). Despite its instability in sea water (Sharma and Millero, 1988), Cu(I) fractions of up to 10% have been measured in surface seawater (Moffett and Zika, 1988) and up to 80% in estuaries (Buerge-Weirich and Sulzberger, 2004). Both reactive photochemistry (Figure 8-B) (Moffett and Zika, 1983) and cell surface reduction (Jones et al., 1987; Hill et al., 1996; Blaby-Haas and Merchant, 2012) (Figure 8-A) have been implicated in production of the cuprous ion.

The chemistry of Cu(I) in seawater is fundamentally different than that of Cu(II). While Cu(I) does form a strong bond with thiols, the high chloride concentration in seawater drives the formation of Cu(I)-chloride complexes to effectively out compete thiol at concentrations typically observed in surface seawater (Chapter 1). Subsequently the presence of thiols can only marginally reduce the concentration of the cuprous ion and its inorganic complexes (Figure 7). Our results clearly demonstrate this disconnect between thiol-cuprous complexes and cupric complexes as Cu(I) in the presence of thiols is more bioavailable than complexed Cu(II) (Figure 1A, C & E). While increasing concentrations of thiols can further lower bioavailability (Figure

1E, F), these high concentrations are not observed in surface seawater (Dupont et al., 2006), or coastal and estuarine systems (Al-Farawati and Van Den Berg, 2001; Laglera and van den Berg, 2006; Dryden et al., 2007) (Chapter 5).

What then is to be made of the role of thiols in surface seawater given their high concentrations? It is possible that they are involved in the metabolism of other metals, yet the ability of organisms such as *E. huxleyi* to exude them under Cu-stress (Dupont and Ahner, 2005) underscores that they still likely are involved in somewhat of alleviating the toxic effects of copper. At the high micromolar levels observed in cellular extracts (Dupont and Ahner, 2005) (Chapter 5), these thiols would act as an effective buffering mechanism of Cu(I) in the cell where it is more thermodynamically favored and present at higher concentrations than in surface seawater. Detoxification of copper could be further facilitated by efflux of these complexes. Similar behavior is observed in the detoxification of cadmium by phytochelatins. Simultaneous phytochelatin and cadmium efflux has been observed in the diatom *Thalassiosira weissflogii* (Lee et al., 1996) and Cd-phytochelatin complexes as well as GSH conjugates can be transported across the membrane by *Abc2* an ABC-type transporter in yeast that has homologues across kingdoms (Ortiz et al., 1995) (Mendoza-Cózatl et al., 2010).

While the intracellular behavior of these thiols as an intracellular detoxification mechanism offers a robust explanation for their importance, the transient effects of thiols on copper in the extracellular medium still appears to be significant. We have shown that both cysteine can rapidly reduce strongly bound Cu(II) in a SOW matrix (Figure 8-C) while reduction by GSH proceeds to completion at a slower pace (Figure 3). Due to the rapid dissociation of these complexes reduction likely occurs on unbound Cu(II) causing a disequilibrium and

cascading dissociation of the Cu(II)-EDTA complex. The superoxide induced reduction of Fe(III) in equilibrium with EDTA proceeded by complex dissociation rather than by direct reduction of the complex (Kustka et al., 2005).

The exudation of thiols to reduce copper bioavailability outside the cell is unlikely. While reduction would lower the free ion concentration this would not necessarily reduce copper's bioavailability. First, the cuprous ion is a substrate for the high affinity copper uptake system and algae utilize surface reductases for its production at the cell surface (Blaby-Haas and Merchant, 2012). Second reduction from a strong Cu(II) ligand could substantially increase the concentration of weak inorganic copper species (Figure 7). Uptake of the chemically analogous Ag(I) is not slowed by the formation of chloride complexes (Campbell et al., 2002), and in some cases uptake is enhanced by their formation (Fortin and Campbell, 2000). Satellite reduction would make more copper available to the cell not less.

Our experiments show that this is in fact what is happening. Cysteine is facilitating the satellite reduction of Cu(II) in the presence of EDTA allowing for increased copper uptake (Figure 2). This mechanism appears to be specific for cysteine as no uptake was observed when either GSH or ascorbate was used a reductant, likely as a result of their inefficiency in reducing copper (Figure 3). This mechanism provides an alternative to surface reduction of copper prior to high affinity uptake. Additionally while copper limitation does induce an increase in cell surface reduction of copper, the presence of EDTA hinders its effectiveness. Subsequently satellite reduction by cysteine becomes a more effective mechanism for copper uptake in Cu-limited cells.

In addition to observing cysteine enhanced uptake in the presence of Cu-EDTA

complexes we also observed elevated levels of uptake in Cu-limited *E. huxleyi* cells exposed solely to Cu(I)-cysteine (Figure 1A). While we did observe some variability across our assimilation measurements, such as a large assimilation of copper in the presence of Arg-Cys (replete *E. huxleyi*, Figure 1C) our measurements in the presence of 250-1000 nM cysteine (Figure 1A) consistently showed elevated assimilation. Additionally preliminary experiments, at 1000 nM cysteine measured assimilation that was double that of unbound Cu(I), however we were unable to reproduce these results.

We hypothesized that copper could "hitchhike" on cysteine transport via molecular mimicry. Though we were unable to demonstrate specific transport of a copper-cysteine complex, enhanced uptake of cysteine under Cu-limitation (Figure 6A) suggests a mechanistic link between cysteine uptake and copper acquisition. Furthermore the addition of copper did not appear to have any impact on cysteine uptake, which one would expect if the cysteine-Cu complex was unavailable for transport. Assuming that cysteine uptake does not vary when bound to copper, the uptake rate of the complex (v_{CuCys}) via such a mechanism can be determined from the kinetic parameters of the enzyme (v_{max}, K_m), the total concentration of cysteine ($\mathrm{Cys_T}$) and the concentration of the complex (CuCys):

$$v_{CuCys} = \frac{v_{max}[CuCys]}{[Cys_T] + K_m} \qquad \text{Equation 2}$$

Given the kinetic parameters determined from the data presented in (Figure 6A), at 1000 nM cysteine and 100 nM Cu(I), the maximum copper assimilated via cysteine transport would be approximately 2.2 amol cell^{-1} in Cu-limited cultures and 0.4 amol cell^{-1} in replete cultures of *E. huxleyi* after an hour of exposure. In Cu-limited cultures Cu(I) uptake was approximately 0.5

amol cell^{-1} higher with cysteine (0.5 amol cell^{-1}) than without (1.0 amol cell^{-1}). Furthermore since approximately 62% of the copper is organically complexed, the portion of the rate attributable to cuprous ion transport would be proportionally less or 38%of Cu(I) uptake rate measured in the absence of a ligands. This would result in approximately 1.2 amol cell^{-1} copper being transported by cysteine, slightly less than half of the maximum complex uptake rate of 2.2 amol cell^{-1} predicted for these conditions.

Significant uptake of Cu-thiol complexes is unlikely in marine systems, especially if as presumed such complexes are used to facilitate copper detoxification. However cysteine uptake in *E. huxleyi* is upregulated under copper-limitations. Cysteine enhanced uptake of metals has been described to varying degrees in a number of biological systems(Bridges and Zalups, 2005), with several demonstrations of transport of a cysteine-metal complex. Notably the human large neutral amino acid transporter can transport the methylmercury-cysteine complex (Simmons-Willis et al., 2002). Cysteine and other weak ligands including GSH enhance uptake of Zn(II) in the presence of EDTA in cultures of *T. pseudonana* and *E. huxleyi* (Aristilde et al., 2012). In the absence of EDTA cysteine reduced Zn(II) uptake, suggesting that while cysteine and other weak ligands can lower the bioavailability of Zn(II), when in competition with EDTA, they are comparatively bioavailable. While our experiments demonstrate an analogous, albeit mechanistically different, competitive role for cysteine, we also see evidence for cysteine enhancing uptake independent of the initial complexation state of copper.

The upregulation of cysteine transport under Cu-limitation to enhance copper uptake necessitates the presence of cysteine in the extracellular environment. Though cysteine has been measured in surface seawater (Van Den Berg et al., 1988; Dupont et al., 2006), its source is

unclear and could include the direct exudation of cysteine, release from cell rupture or from the degradation of cysteine-containing compounds present via exudation or rupture. The strategic exudation of compounds designed to increase the bioavailability of metals have been observed before. Siderophores are employed for iron acquisition by cyanobacteria (Ferreira and Straus, 1994) and are readily observed in iron-limiting surface seawater (Vraspir and Butler, 2009). While copper concentrations in surface sea water are unlikely to be limiting, copper does play a role in high affinity iron uptake (Price, 2005; Peers et al., 2005; Maldonado et al., 2006). Furthermore strategic copper acquisition may be necessary for cells under iron limitation. The Cu(II)-binding neurotoxin domoic acid has been proposed to be part of an extracellular copper acquisition system in *Pseudo-nitzschia* under iron limitation (Figure 8-2) (Wells et al., 2005).

The study of copper-organic complexes in marine systems has typically focused on the ability of ligands of biological origin to lower free copper ion concentrations substantially and thus bioavailability. We have demonstrated that bioavailability of copper to two common marine algae can be both increased and decreased by the addition of certain thiols cystine in the presence of a strong ligand via a reductive release mechanism. Furthermore copper-limited *E. huxleyi* cells can enhance the assimilation of copper bound to thiols, and in particular cysteine, possibility via the upregulation of cysteine transporters. These results highlight the need to further understand the composition of extracellular copper binding ligands in surface seawater as well as their sources and sinks in managing copper bioavailability.

6. Acknowledgements

We think Lou Derry and John Helmann for use of their inductively coupled plasma mass spectrometers. Zhen Ma and Gregg McElwee provided support on these instruments. Funding was provided by NSF Chemical Oceanography (OCE 0451781)

7. References

Al-Farawati R and Van Den Berg CMG. (2001) Thiols in coastal waters of the western North Sea and English Channel. *Environmental Science & Technology* 35: 1902-1911.

Aliaga M, Carrasco-Pozo C, López-Alarcón C, et al. (2010) The Cu(I)–glutathione complex: factors affecting its formation and capacity to generate reactive oxygen species. *Transition Metal Chemistry* 35: 321-329.

Aristilde L, Xu Y and Morel FMM. (2012) Weak Organic Ligands Enhance Zinc Uptake in Marine Phytoplankton. *Environmental Science & Technology* 46: 5438-5445.

Attari A and Jaselskis B. (1972) Spectrophotometric determination of sulfur dioxide by reduction of iron(III) in the presence of ferrozine. *Analytical Chemistry* 44: 1515-1517.

Besada A, Tadros N and Gawargious Y. (1989) Copper(II)-neocuproine as colour reagent for some biologically active thiols: Spectrophotometric determination of cysteine, penicillamine, glutathione, and 6-mercaptopurine. *Microchimica Acta* 99: 143-146.

Blaby-Haas CE and Merchant SS. (2012) The ins and outs of algal metal transport. *Biochimica et Biophysica Acta (BBA) - Molecular Cell Research* 1823: 1531-1552.

Bridges CC and Zalups RK. (2005) Molecular and ionic mimicry and the transport of toxic metals. *Toxicology and Applied Pharmacology* 204: 274-308.

Buerge-Weirich D and Sulzberger B. (2004) Formation of Cu(I) in Estuarine and Marine Waters: Application of a New Solid-Phase Extraction Method To Measure Cu(I). *Environmental Science & Technology* 38: 1843-1848.

Buettner GR and Czapski PG. (1986) Ascorbate Autoxidation in the Presence of Iron and Copper Chelates. *Free Radical Research* 1: 349-353.

Burkitt MJ and Gilbert BC. (1990) Model Studies of the Iron-Catalysed Haber-Weiss Cycle and the Ascorbate-Driven Fenton Reaction. *Free Radical Research* 10: 265-280.

Campbell PGC, Errécalde O, Fortin C, et al. (2002) Metal bioavailability to phytoplankton—applicability of the biotic ligand model. *Comparative Biochemistry and Physiology Part C: Toxicology & Pharmacology* 133: 189-206.

Chen LH and Chung CS. (1988) Steric and macrocyclic effects in the dissociation kinetics of cyclic and open-chain tetraamine complexes of copper(II) in strongly acidic, aqueous media. *Inorganic Chemistry* 27: 1880-1883.

Coale KH and Bruland KW. (1988) Copper Complexation in the Northeast Pacific. *Limnology and Oceanography* 33: 1084-1101.

Crea P, De Stefano C, Millero F, et al. (2010) Dissociation Constants of Protonated Oxidized

Glutathione in Seawater Media at Different Salinities. *Aquatic Geochemistry* 16: 447-466.
Croot PL, Moffett JW and Luther GW. (1999) Polarographic determination of half-wave potentials for copper-organic complexes in seawater. *Marine Chemistry* 67: 219-232.
Dryden CL, Gordon AS and Donat JR. (2007) Seasonal survey of copper-complexing ligands and thiol compounds in a heavily utilized, urban estuary: Elizabeth River, Virginia. *Marine Chemistry* 103: 276-288.
Dupont CL and Ahner BA. (2005) Effects of copper, cadmium, and zinc on the production and exudation of thiols by Emiliania huxleyi. *Limnology and Oceanography* 50: 508-515.
Dupont CL, Moffett JW, Bidigare RR, et al. (2006) Distributions of dissolved and particulate biogenic thiols in the subartic Pacific Ocean. *Deep-Sea Research Part I-Oceanographic Research Papers* 53: 1961-1974.
Dupont CL, Nelson RK, Bashir S, et al. (2004) Novel copper-binding and nitrogen-rich thiols produced and exuded by Emiliania huxleyi. *Limnology and Oceanography* 49: 1754-1762.
Ferreira F and Straus N. (1994) Iron deprivation in cyanobacteria. *Journal of Applied Phycology* 6: 199-210.
Fortin C and Campbell PGC. (2000) Silver uptake by the green alga Chlamydomonas reinhardtii in relation to chemical speciation: Influence of chloride. *Environmental Toxicology and Chemistry* 19: 2769-2778.
Guo J, Annett AL, Taylor RL, et al. (2010) COPPER-UPTAKE KINETICS OF COASTAL AND OCEANIC DIATOMS1. *Journal of Phycology* 46: 1218-1228.
Gustafsson J. (2010) Visual MINTEQ. 3.0 ed. Stockholm, Sweeden: KTH Royal Institute of Technology
Hassett R and Kosman DJ. (1995) Evidence for Cu(II) Reduction as a Component of Copper Uptake by Saccharomyces cerevisiae. *Journal of Biological Chemistry* 270: 128-134.
Hill KL, Hassett R, Kosman D, et al. (1996) Regulated Copper Uptake in Chlamydomonas reinhardtii in Response to Copper Availability. *Plant Physiology* 112: 697-704.
Jones GJ and Morel FMM. (1988) Plasmalemma Redox Activity in the Diatom Thalassiosira. *Plant Physiology* 87: 143-147.
Jones GJ, Palenik BP and Morel FMM. (1987) TRACE METAL REDUCTION BY PHYTOPLANKTON: THE ROLE OF PLASMALEMMA REDOX ENZYMES1, 2. *Journal of Phycology* 23: 237-244.
Kustka AB, Shaked Y, Milligan AJ, et al. (2005) Extracellular Production of Superoxide by Marine Diatoms: Contrasting Effects on Iron Redox Chemistry and Bioavailability. *Limnology and Oceanography* 50: 1172-1180.
Laglera LM and van den Berg CMG. (2006) Photochemical oxidation of thiols and copper complexing ligands in estuarine waters. *Marine Chemistry* 101: 130-140.
Lee JG, Ahner BA and Morel FMM. (1996) Export of cadmium and phytochelatin by the marine diatom Thalassiosira weissflogii. *Environmental Science & Technology* 30: 1814-1821.
Maldonado MT, Allen AE, Chong JS, et al. (2006) Copper-dependent iron transport in coastal and oceanic diatoms. *Limnology and Oceanography* 51: 1729-1743.
Mendoza-Cózatl DG, Zhai Z, Jobe TO, et al. (2010) Tonoplast-localized Abc2 transporter mediates phytochelatin accumulation in vacuoles and confers cadmium tolerance.

Journal of Biological Chemistry 285: 40416-40426.
Moffett JW and Dupont C. (2007) Cu complexation by organic ligands in the sub-arctic NW Pacific and Bering Sea. *Deep-Sea Research Part I-Oceanographic Research Papers* 54: 586-595.
Moffett JW and Zika RG. (1983) Oxidation-Kinetics of Cu(I) in Seawater - Implications for Its Existence in the Marine-Environment. *Marine Chemistry* 13: 239-251.
Moffett JW and Zika RG. (1988) Measurement of Copper(I) in Surface Waters of the Sub-Tropical Atlantic and Gulf of Mexico. *Geochimica et Cosmochimica Acta* 52: 1849-1857.
Ortiz DF, Ruscitti T, McCue KF, et al. (1995) Transport of Metal-binding Peptides by HMT1, A Fission Yeast ABC-type Vacuolar Membrane Protein. *Journal of Biological Chemistry* 270: 4721-4728.
Pecci L, Montefoschi G, Musci G, et al. (1997) Novel findings on the copper catalysed oxidation of cysteine. *Amino Acids* 13: 355-367.
Peers G, Quesnel SA and Price NM. (2005) Copper requirements for iron acquisition and growth of coastal and oceanic diatoms. *Limnology and Oceanography* 50: 1149-1158.
Price NM. (2005) The Elemental Stoichiometry and Composition of an Iron-Limited Diatom. *Limnology and Oceanography* 50: 1159-1171.
Price NM, Harrison GI, Hering JG, et al. (1989) Preparation and Chemistry of the Artificial Algal Culture Medium Aquil. *Biological Oceanography* 6: 443-461.
Semeniuk DM, Cullen JT, Johnson WK, et al. (2009) Plankton copper requirements and uptake in the subarctic Northeast Pacific Ocean. *Deep Sea Research Part I: Oceanographic Research Papers* 56: 1130-1142.
Sharma VK and Millero FJ. (1988) Oxidation of copper(I) in seawater. *Environmental Science & Technology* 22: 768-771.
Simmons-Willis TA, Koh AS, Clarkson TW, et al. (2002) Transport of a neurotoxicant by molecular mimicry: the methylmercury-L-cysteine complex is a substrate for human L-type large neutral amino acid transporter (LAT) 1 and LAT2. *Biochemical Journal* 367: 239.
Sunda WG and Huntsman SA. (1995) Iron uptake and growth limitation in oceanic and coastal phytoplankton. *Marine Chemistry* 50: 189-206.
Tang D, Shafer MM, Karner DA, et al. (2005) Response of Nonprotein Thiols to Copper Stress and Extracellular Release of Glutathione in the Diatom Thalassiosira weissflogii. *Limnology and Oceanography* 50: 516-525.
Vachet RW and Callaway MB. (2003) Characterization of Cu(II)-binding ligands from the Chesapeake Bay using high-performance size-exclusion chromatography and mass spectrometry. *Marine Chemistry* 82: 31-45.
Van Den Berg CMG, Househam BC and Riley JP. (1988) Determination of cystine and cysteine in seawater using cathodic stripping voltammetry in the presence of Cu(II). *Journal of Electroanalytical Chemistry and Interfacial Electrochemistry* 239: 137-148.
van Doornmalen J, Wolterbeek HT and de Goeij JJM. (2002) Analysis of copper complex lability using 64Cu-equilibration techniques and free-ion selective radiotracer extraction. *Analytica Chimica Acta* 464: 141-152.
Vasconcelos MTSD, Leal MFC and van den Berg CMG. (2002) Influence of the nature of the exudates released by different marine algae on the growth, trace metal uptake, and

exudation of Emiliania huxleyi in natural seawater. *Marine Chemistry* 77: 187-210.
Vraspir JM and Butler A. (2009) Chemistry of Marine Ligands and Siderophores. *Annual Review of Marine Science* 1: 43-63.
Wells ML, Trick CG, Cochlan WP, et al. (2005) Domoic Acid: The Synergy of Iron, Copper, and the Toxicity of Diatoms. *Limnology and Oceanography* 50: 1908-1917.
Xu A, Vita JA and Keaney JF. (2000) Ascorbic acid and glutathione modulate the biological activity of S-nitrosoglutathione. *Hypertension* 36: 291-295.
Yebra-Biurrun MC. (2000) Flow injection determination methods of ascorbic acid. *Talanta* 52: 367-383.

CHAPTER 5

Measurements of Thiol Containing, Copper Binding Dipeptides in Several Phylogenetically Diverse Species of Marine Algae and an Estuary

1. Abstract

Several phylogenetically diverse species of eukaryotic marine algae are surveyed for production of the copper binding peptides Arg-Cys and Gln-Cys. Production appears to be widespread although not universal. Both thiols were observed at high particulate and dissolved concentrations in the Chesapeake Bay. No response to the addition of nitrogen or copper was observed in field samples. These results show that the thiols Arg-Cys and Gln-Cys are more widespread geographically and biologically than previously thought.

2. Introduction

The complexation of copper by a pool of organic ligands is well documented in aquatic ecosystems (Town and Filella, 2000). These ligands of presumed biological origin are of particular importance in marine systems where they facilitate the reduction of free copper ion concentrations from toxic to tolerable levels (Coale and Bruland, 1988; Moffett, 1995; Moffett and Dupont, 2007). This pool of ligands is diverse with copper binding affinity of exudates varying among species (Croot et al., 1999; Croot et al., 2000). Some of these ligands include thiols that are "cysteine-like and glutathione like" (Al-Farawati and Van Den Berg, 2001).

The dipeptides Arg-Cys and Gln-Cys are found in cell extracts and exudates of the marine coccolithophore *Emiliania huxleyi* (Dupont et al., 2004). Furthermore *E. huxleyi* produced elevated particulate and dissolved levels upon exposure to high concentrations of copper, cadmium, and zinc (Dupont and Ahner, 2005). Particulate concentrations also increase under luxury nitrogen and were consumed under subsequent depletion indicating that these nitrogen-rich peptides may additionally be involved in nitrogen storage (Kim et al., 2011). Along with nanomolar levels of cysteine, glutathione (GSH), and the glutathione precursor γGlu-Cys, both Arg-Cys and Gln-Cys were measured at sub-nanomolar levels in the North Pacific (Dupont et al., 2006). A copper binding ligand with a copper affinity comparable to exudates of *E. huxleyi* and an *m/z* equal to that that of Arg-Cys (*m/z* =277) was found in the Chesapeake Bay (Vachet and Callaway, 2003) further providing evidence of the pervasiveness of these ligands.

It is likely that these ligands bind to copper inside the cell and are then exported in a similar manner to the elimination of cadmium by phytochelatin (Mendoza-Cózatl et al., 2010; Lee et al., 1996). Though they exhibit a similar affinity for Cu(I) to that of GSH, both Arg-Cys

and Gln-Cys are weaker Cd(II) or Zn(II) ligands than GSH, indicating a Cu(I) selectivity (Chapter 1). This specificity as well as their size may give these compounds an advantage over GSH or expensive metallothioneins in buffering intracellular concentrations of copper.

Synthesis of Arg-Cys has been observed before in *Escherichia coli*. The dipeptide appears to be a product of the deacylation of Arg-tRNA^{Arg} in the presence of cysteine facilitated by the Arginyl-tRNA synthetase (Jakubowski, 1995). The thiol group of cysteine appears to be essential for this reaction to take place. It also appears possible for Gln-Cys to be produced via a similar mechanism as cysteine conjugates of isoleucine and valine were facilitated by their respective aminoacyl tRNA synthetases. Both of which, as well as Arginyl-tRNA and Glutamyl-tRNA syntheses, are Class I aminoacyl tRNA synthetases. While it is not known if this is the same pathway that enables *E. huxleyi* to generate these dipeptides, it provides a non-ribosomal mechanism for their production.

A preliminary survey of marine algae measured low levels of Gln-Cys produced by the coccolithophore *Gephyrocapsa oceanica* (Dupont et al., 2004). Here we expand the list of species known to produce these copper binding ligands. To determine if there is a response to copper and nitrogen levels, cultures were grown under copper stress or luxury nitrogen prior to analysis. We also report the measurements of these thiols in the field.

3. Methods

3.1. Culturing

Cultures of several species of marine phytoplankton (Table 1) were obtained from the Provasoli -Guillard National Center for Culture of Marine Phytoplankton (CCMP, currently the

Table 1. Species of marine phytoplankton used in this study.

Classification	Species	Clone ID (CCMP)	Arg Cys Observed	Gln-Cys Observed	Log K of copper binding ligand
***Prymnesiophyceae* – coccolithophore**	*E. huxleyi*	373	Yes	Yes	11.6[1], 11.8-12.2[2]
***Prymnesiophyceae* – coccolithophore**	*E. huxleyi*	1516	Yes	Yes	11.6[1], 11.8-12.2[2]
***Prymnesiophyceae* – flagellate**	*Isochrysis sp.*	1323	Yes	Yes	
***Prymnesiophyceae* – flagellate**	*Isochrysis galbana*	1324	No	Yes	
Diatom – centric	*Thalassiosira weissflogii*	1336	No	No	10.6[3]
Diatom – centric	*Thalassiosira pseudonana*	1335	Very low	Very Low	
Diatom – penate	*Phaeodactylum tricornutum*	632	Yes	Very Low	
Diatom – chain	*Skeletonema costatum*	2092	No	No	11.6 - 12.3[3]
Dinoflagellate	*Amphidinium carterae*	1314	Yes	No	11.8 – 12.2[3]
Mamiellaceae	*Ostreococcus sp.*	2972	Very Low	Yes	
Mamiellaceae	*Micromonas pusilla*	1545	No	No	

[1] (Dupont et al., 2004)
[2] (Leal et al., 1999)
[3](Croot et al., 2000)

National Center for Marine Algae, NCMA), Boothbay Maine. Species were selected based upon several factors which included model species for several classifications of algae as well as those that are known to produce copper binding ligands.

Cultures were grown axenically in the synthetic ocean water medium Aquil (Price et al., 1989) with trace metals buffered by 100 µM EDTA. Since several of the selected species had high iron requirements, the final total iron concentration was set to 8.32 µM (initial pFe^{3+} = 18.1). Prior to culturing in Aquil, the dinoflagellates *A. carterae* and the picoplankton *Ostreococcus* and *M. pusilla* were cultured for several generations in 50% Aquil, 50% f/2 medium (Guillard, 1975).

Initial copper levels were set at 20 nM (initial pCu^{2+} = 13.9). To test if species exhibited increased production of Arg-Cys and Gln-Cys under copper stress, 10 µM copper (initial pCu^{2+} = 11.2) was added as a preequilibrated equimolar EDTA complex three days after inoculation. To induce luxury nitrogen conditions, phosphorus was reduced to 10 µM sodium phosphate, instead of the standard 100 µM.

Cultures were grown in acid-washed polycarbonate bottles at 20°C under constant lighting of 120 µmol photon m^{-2} s^{-1}. Growth was monitored via fluorescence (Turner Instruments). Chlorophyll *a* (Chl *a*) measurements were made by filtering 5 mL of culture onto a 25 mm glass fiber filter (GF/F, Whatman). Chl *a* was then extracted in the dark by immersing the filter in a 5 mL solution of 45% dimethyl sulfoxide, 45% acetone and 10% water for 6 hours (Shoaf and Lium, 1976). The fluorescence of the extract was subsequently measured and Chl *a* calculated using a standard curve that was constructed from serial dilutions of a standard Chl *a* extract of spinach that was measured spectrophotometrically (Beckman Instruments).

3.2. Thiol quantification

Cultures were harvested during mid-exponential growth by gently filtering between 25 and 200 mL of individual cultures through 25 mm GF/F filters. Filters were stored in liquid nitrogen until extraction. Extraction and derivation of thiols with the fluorescent probe monobromobimane is described elsewhere (Dupont et al., 2004). Derivatized thiols were quantified following separation using a reverse-phase C-16 amide column (Supelco Discovery, 2.1 x 250 mm) using a method described in (Kim et al., 2011).

Except for *Ostreococcus* and *M. pusilla,* thiols were normalized to cell count and reported on a per cell basis. With each sampling, cell densities were determined by counting cells on a Neubauer Improved hemocytometer. Cell sizes, particularly for *E. huxleyi*, were sensitive to the various nutrient treatments. Thiol measurements for *Ostreococcus* and *M. pusilla* were normalized to Chl *a* as their small size made counting difficult.

3.3. Field measurements

Field sampling was performed on Monday July 27, 2009 at three sites (Figure 1, Table 2) in the Southern Chesapeake Bay (Virginia, USA). This estuary is heavily impacted by shipping and industrial use. Sampling was performed by collecting estuary water from location on piers, set out at least 50 yards from the shore. Chl *a* extractions were performed on 30 mL of filtered biomass.

Dissolved thiols were measured by immediately derivatizing filtered estuary water. 10 mL of estuary water was passed through a sterile 0.2 µm Acrodisc filter (Whatman). Duplicate aliquots of 800 µL were derivitized with monobromobimane using the method described by

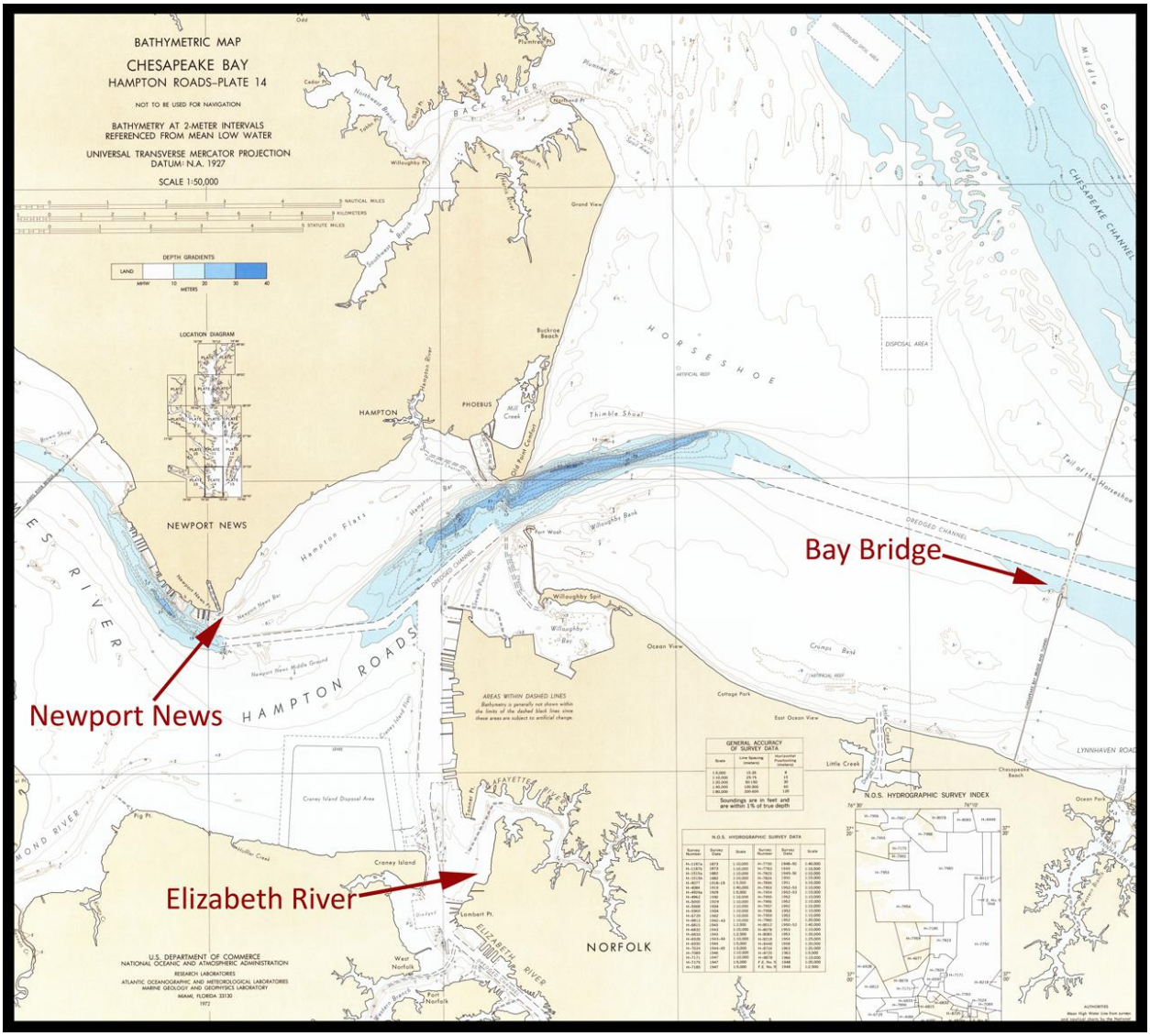

Figure 1. Sampling locations in the Chesapeake Bay near Newport News and Norfolk VA

Table 2. Location data, Chlorophyll *a* measurements, dissolved thiol, particulate thiols and relative changes in particulate thiol concentrations after the addition of 100 mM $NaNO_3$ or 100 µM $CuSO_4$. Relative increases were calculated as the change in ChlA normalized particulate thiols after 24 hours. Increases are bolded, italicizes are used to indicate declines.

Site Name	*Newport News (James River)*	*Elizabeth River*	*Bay Bridge*
Latitude	36.967215	36.886202	36.967217
Longitude	-76.408834	-76.317887	-76.114085
ChlA (µg/L)	13.6 ± 0.3	87.6 ± 26.3	10.8 ± 0.1
Dissolved Thiols			
Arg-Cys (nM)	26.7	101.9	105.3
Cys (nM)	902.5	1887.2	1572.5
Gln-Cys (nM)	None detected	20.6	16.6
Arg-Cys (mM $gChlA^{-1}$)	1.96	1.16	9.76
Cys (mM $gChlA^{-1}$)	66.21	21.52	145.79
Gln-Cys (mM $gChlA^{-1}$)	None detected	0.23	1.54
Particulate Thiols			
Arg-Cys (nmol L^{-1})	**0.043 ± 0.001**	**0.540 ± 0.008**	**0.032 ± 0.0103**
Cys (nmol L^{-1})	**0.598 ± 0.096**	**11.947 ± 5.055**	**0.459 ± 0.039**
Gln-Cys (nmol L^{-1})	**0.133 ± 0.007**	**2.117 ± 0.547**	**0.141 ± 0.019**
Arg-Cys (µM $gChlA^{-1}$)	14.8 ± 0.25	73.4 ± 13.3	15.6 ± 5.0
Cys (µM $gChlA^{-1}$)	203.8 ± 22.9	1557.3 ± 369.3	224.1 ± 18.9
Gln-Cys (µM $gChlA^{-1}$)	45.6 ± 0.3	208.6 ± 18.1	69.2 ± 9.1

Dupont et al. (2004). Derivitized samples were stored at 4°C until measurement, which was within three days of derivitization.

Particulate thiol production in response to nitrogen and copper levels was also tested for. Aliquots of estuary water at each site were inoculated with either 100 nM $CuSO_4$ (Sigma) or 100 μM $NaNO_3$ and kept under constant light. After 24 hours of exposure each treatment was filtered in duplicate for thiol derivitization and measurement.

4. Results and Discussion

4.1. Thiol production assay

We assayed a diverse array of marine phytoplankton for thiol production by growing algae under replete, luxury nitrogen and copper stressed conditions. The latter two conditions have been shown to increase production of the dipeptides in *E. huxleyi* (Kim et al., 2011; Dupont and Ahner, 2005). The strains of algae surveyed are listed in Table 1. Of these species no production was observed in cultures of the picoplankton *Micromonas pusilla* (1546) or the diatoms *Thalassiosira weissflogii* (1336) and *Skeletonema coastatum* (2092).

Production varied widely across the remaining species (Figure 2). Both strains of *E. huxleyi* had the greatest levels of production each showing copper and nitrogen responses that have been previously observed (Dupont and Ahner, 2005; Kim et al., 2011). The most closely related species to *E. huxleyi* are the two *Isochrysis* isolates. While *Isochrysis sp.* (1324) exhibited significant levels of Gln-Cys and measurable levels of Arg-Cys, no Arg-Cys and very little cysteine and Gln-Cys were measured in cultures of *Isochrysis galbana* (1323).

Production by the diatoms also varied significantly. Levels of Arg-Cys and Gln-Cys were

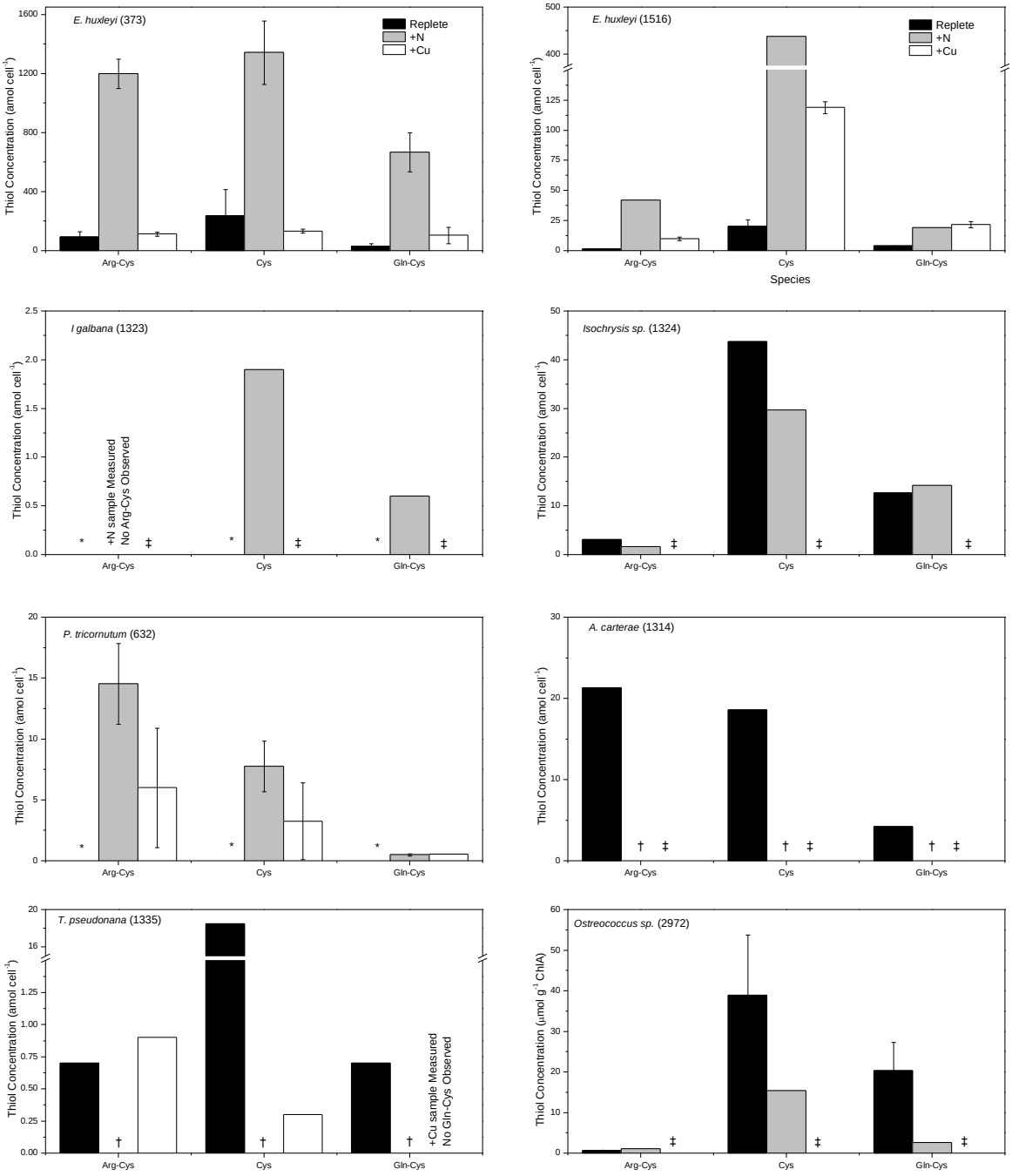

Figure 2. Measured levels of particulate Arg-Cys, Cys and Gln-Cys from cells grown under standard growth (black bars), luxury nitrogen (grey bars), and copper stressed (white bars) conditions. All concentrations are expressed in attomol cell-1 except for those of Ostreococcus sp. which is normalized to Chl a. Cultures for which thiol concentrations were not tested are indicated by * for replete, † for luxury nitrogen and ‡ for copper stressed.

close to the detection limit in cultures of *T. pseudonana* (1335) while significant levels of cysteine were measured. Production of Arg-Cys by *Phaeodactylum tricornutum* (632) was relatively high under luxury nitrogen, while only low levels of Gln-Cys were measured. Similar production levels were measured in the dinoflagellate *Amphidinium carterae* (1314). The picoplankton *Ostreococcus sp.* (2972) appears to be a good producer of Gln-Cys, but not Arg-Cys.

Previous work has demonstrated that Arg-Cys can be produced via an amino-deacylation reaction catalyzed by arginyl-tRNA synthetase, a reaction that appeared to be facilitated by other tRNA synthetases (Jakubowski, 1995). In this mechanism arginine is an inhibitor, while charged Arg-tRNA^{Arg} and cysteine are substrates. Given this, it is likely that there could be a connection between high cysteine levels which are observed in *E. huxleyi* and production of these dipeptides. In the case of the two *Isochrysis* isolates, 1323 and 1324, it appears that 1324 is far more cysteine rich, and also produces significant levels of Arg-Cys and Gln-Cys than 1323. This was not the case with *T. pseudonana* which had substantial cysteine but very little dipeptide production. We attempted to utilize the quantitative real time polymerase chain reaction to measure expression of arginyl-tRNA synthetase and glutamyl-tRNA synthetase to see if these enzymes were upregulated under our treatments in *E. huxleyi* (1516) and *T. pseudonana* (1335). Initial experiments did not produce clear results.

Concentrations and copper affinities of exudates from several organisms included in this study have been measured using electroanalytical techniques (Table 1) (Leal et al., 1999; Croot et al., 1999; Croot et al., 2000). Of these, *A. carterae and S. costatum* produce ligands of comparable copper affinity to that of *E. huxleyi*. Exudates of *A. carterae* appear to consist of at

least three copper binding ligands with log-conditional stability constants of approximately 12 (Croot et al., 1999). Further evaluation indicated that one of these ligands appears to be a Cu(I) binding ligand while another was chemically similar to the ligand produced by *S. costatum*. This supports of our measurement of Arg-Cys and Gln-Cys in *A. carterae* but not *S. costatum.*

4.2. Field measurements

Arg-Cys and Gln-Cys have been observed in surface seawater at sub-nanomolar levels in the subarctic Pacific (Dupont et al., 2006). Despite their low levels, concentrations of dissolved thiols were relatively high compared to particulate thiols which suggest that they were exudated. In coastal and estuarine waters, higher concentrations of glutathione, cysteine, and unidentified thiols have been observed (Le Gall and van den Berg, 1993; Al-Farawati and Van Den Berg, 2001; Vachet and Callaway, 2003). One of the unidentified sulfur containing copper-binding ligands from the Chesapeake Bay had a *m/z* of 277 which is identical to the expected *m/z* of Arg-Cys.

Copper concentrations in the Chesapeake are elevated, in part, due to the presence of various industrial and shipping-associated anthropogenic sources (Gupta and Karuppiah, 1996). Total copper concentrations in the Elizabeth River range between 10-25 nM (Dryden et al., 2007). Between 25 and 56 nM of copper binding ligands, with a log*K*' of approximately 12, buffer the free ion concentration to a pCu^{2+} between 12.2 and 11.5. This measurement is higher than observed in surface sea water. The Chesapeake Bay is also highly eutrophic due to high levels of nitrogen and phosphorus loading (Paerl, 2009). Given these factors, the region provided the ideal waters to observe high concentrations of Arg-Cys and Gln-Cys.

Levels of Arg-Cys were highest at the Bay Bridge and Elizabeth River Sampling sites (Table 2); the same two sites where Gln-Cys was measured. Cysteine levels were also highest at these two sites. Dissolved thiols exceeded particulate thiols in all measurements, indicating that thiols are continuously being exported. The abundance of Arg-Cys in comparison to Gln-Cys is consistent with the observations of Vachet and Callaway (2003) that identified mass peaks representative of Arg-Cys but not Gln-Cys. We observed that certain species produce one of these dipeptides, but not the other, which makes it reasonable to assume that similar distributions are possible in the environment.

While the measurements in the Elizabeth River may indicate a biological response to high copper levels, especially given the vicinity to a major naval ship yard, we did not expect to find equivalent concentrations at the Bay Bridge sampling site. Additionally, the ratio of dissolved thiols to particulate was higher at the Bay Bridge site than at any other site. Bay Bridge is the furthest from land and closest to the open ocean that led us to expect dilution. Tidal effects may explain this discrepancy as the Newport News and Elizabeth River sites were sampled prior to high tide, and the Bay Bridge sample was taken as the tide was receding. However, the Bay Bridge also had the lowest chlorophyll measurements indicating that tidal flows may not be sufficient to explain the difference from the other sites.

Attempts to stimulate thiol production by amending estuarine waters with nitrogen and copper were not successful. While nitrogen increased Chl *a* substantially over the control (Figure 3A), total particulate thiol concentrations did not significantly change with the addition of either nitrate or copper (Figure 3B-D). Rapid dipeptide production has only been previously observed upon nitrogen addition to nitrogen-limited cells (Kim et al., 2011). Attempts to stimulate

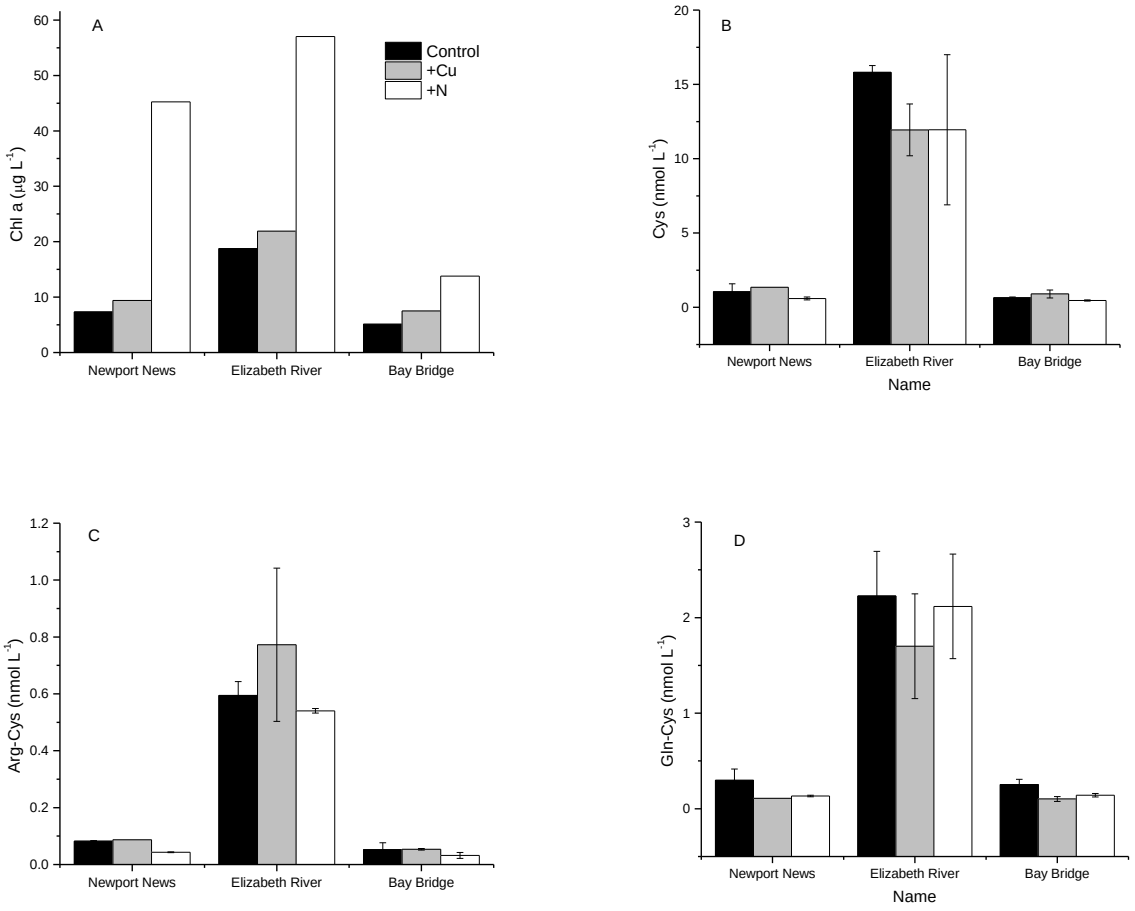

Figure 3. Particulate measurements of Chl *a* (A), cysteine (B), Arg-Cys (C), and Gln-Cys(D) after 24 hour incubation of estuarine water upon. Grey and white bars represent cultures to which 100 nM $CuSO_4$ and 100 µM $NaNO_3$ were added respectively. Black bars represent no addition controls.

dipeptide production in cells that are already awash with nitrogen may not result in increased production. Copper levels in the estuary are also high and the addition of 100 nM Cu(II) may have been insufficient to overcome background ligand concentrations that are likely present.

5. Conclusions

We demonstrated that several species of phylogenetically diverse eukaryotic algae can produce significant cellular levels of Arg-Cys and Gln-Cys. Production is not universal and several species will only produce one thiol but not the other. Production in surveyed species is less than that observed in *E. huxleyi*. Increased production under luxury nitrogen and copper stress were also not observed, though experimentation is necessary. The latter response suggests that these thiols are involved in a copper buffering and export mechanism that may allow *E. huxleyi* to tolerate higher copper concentrations than other organisms. Measurement of these thiols in a heavily impacted estuary demonstrates that these thiols are ecologically prevalent.

6. Acknowledgements

Collette Kopon, Sarah Fields, and Mark Loria assisted in sample processing and Brianna Walsh for assisted in field sampling. Funding for culture work was provided for by NSF Chemical Oceanography (OCE 0451781). Funding for field sampling was made possible by a small grant provided by the sponsored Biogeochemistry and Environmental Biocomplexity NSF IGRET at Cornell University (DGE 0221658))

7. References

Al-Farawati R and Van Den Berg CMG. (2001) Thiols in coastal waters of the western North Sea and English Channel. *Environmental Science & Technology* 35: 1902-1911.

Coale KH and Bruland KW. (1988) Copper Complexation in the Northeast Pacific. *Limnology and Oceanography* 33: 1084-1101.

Croot PL, Moffett JW and Brand LE. (2000) Production of extracellular Cu complexing ligands by eucaryotic phytoplankton in response to Cu stress. *Limnology and Oceanography* 45: 619-627.

Croot PL, Moffett JW and Luther GW. (1999) Polarographic determination of half-wave potentials for copper-organic complexes in seawater. *Marine Chemistry* 67: 219-232.

Dryden CL, Gordon AS and Donat JR. (2007) Seasonal survey of copper-complexing ligands and thiol compounds in a heavily utilized, urban estuary: Elizabeth River, Virginia. *Marine Chemistry* 103: 276-288.

Dupont CL and Ahner BA. (2005) Effects of copper, cadmium, and zinc on the production and exudation of thiols by Emiliania huxleyi. *Limnology and Oceanography* 50: 508-515.

Dupont CL, Moffett JW, Bidigare RR, et al. (2006) Distributions of dissolved and particulate biogenic thiols in the subartic Pacific Ocean. *Deep-Sea Research Part I-Oceanographic Research Papers* 53: 1961-1974.

Dupont CL, Nelson RK, Bashir S, et al. (2004) Novel copper-binding and nitrogen-rich thiols produced and exuded by Emiliania huxleyi. *Limnology and Oceanography* 49: 1754-1762.

Guillard RRL. (1975) *Culture of phytoplankton for feeding marine invertebrates,* New York, USA.: Plenum Press.

Gupta G and Karuppiah M. (1996) Heavy metals in sediments of two Chesapeake Bay tributaries — Wicomico and Pocomoke Rivers. *Journal of Hazardous Materials* 50: 15-29.

Jakubowski H. (1995) Synthesis of cysteine-containing dipeptides by aminpacyl-tRNA synthetases. *Nucl. Acids Res.* 23: 4608-4615.

Kim H-S, Walsh MJ, Yang H, et al. (2011) Nutrient availability alters levels of non-translationally synthesized nitrogen-rich dipeptides in Emiliania huxleyi. *Aquatic Biology* 12: 215-224.

Le Gall A-C and van den Berg CMG. (1993) Cathodic stripping voltammetry of glutathione in natural waters. *Analyst* 118: 1411-1415.

Leal MFC, Vasconcelos MTSD and van den Berg CMG. (1999) Copper-induced release of complexing ligands similar to thiols by Emiliania huxleyi in seawater cultures. *Limnology and Oceanography* 44: 1750-1762.

Lee JG, Ahner BA and Morel FMM. (1996) Export of cadmium and phytochelatin by the marine diatom Thalassiosira weissflogii. *Environmental Science & Technology* 30: 1814-1821.

Mendoza-Cózatl DG, Zhai Z, Jobe TO, et al. (2010) Tonoplast-localized Abc2 transporter mediates phytochelatin accumulation in vacuoles and confers cadmium tolerance. *Journal of Biological Chemistry* 285: 40416-40426.

Moffett JW. (1995) Temporal and Spatial Variability of Copper Complexation by Strong Chelators in the Sargasso-Sea. *Deep-Sea Research Part I-Oceanographic Research Papers* 42: 1273-1295.

Moffett JW and Dupont C. (2007) Cu complexation by organic ligands in the sub-arctic NW Pacific and Bering Sea. *Deep-Sea Research Part I-Oceanographic Research Papers* 54: 586-595.
Paerl H. (2009) Controlling Eutrophication along the Freshwater–Marine Continuum: Dual Nutrient (N and P) Reductions are Essential. *Estuaries and Coasts* 32: 593-601.
Price NM, Harrison GI, Hering JG, et al. (1989) Preparation and Chemistry of the Artificial Algal Culture Medium Aquil. *Biological Oceanography* 6: 443-461.
Shoaf WT and Lium BW. (1976) Improved extraction of chlorophyll a and b from algae using dimethyl sulfoxide. *Limnology and Oceanography* 21.
Town RM and Filella M. (2000) Dispelling the Myths: Is the Existence of L1 and L2 Ligands Necessary to Explain Metal Ion Speciation in Natural Waters? *Limnology and Oceanography* 45: 1341-1357.
Vachet RW and Callaway MB. (2003) Characterization of Cu(II)-binding ligands from the Chesapeake Bay using high-performance size-exclusion chromatography and mass spectrometry. *Marine Chemistry* 82: 31-45.

CONCLUSIONS AND FUTURE WORK

1. General conclusions

Stability constants of thiol-Cu(I) complexes of several biogenic thiols were measured using a fluorescent ion indicator. Various precautions were taken to minimize oxidation of Cu(I) and interference from Cu(II). The reported constants are the first for cysteine, Arg-Cys and Gln-Cys, while those of glutathione provide an alternative to previously reported values. Log-conditional stability constants for these complexes in surface seawater ranged from approximately 11 for cysteine to 12 for the low molecular weight peptides. Speciation models predict that nanomolar concentrations of these thiols in surface seawater would have little effect on lowering free cuprous ion concentrations due to heavy competition from chloride. The presence of these thiols would also have little impact on reducing the bioavailability of Cu(I) to marine algae. Cu(II) ligands with analogous affinity would likely be more effective than thiols in reducing extracellular copper bioavailability. However, inside the cell where these thiols are present at high micromolar concentrations, speciation models indicate that thiols would be very effective at buffering copper. Arg-Cys and Gln-Cys also have high specificity for Cu(I) over other metals.

Bioavailability experiments confirmed the predictions of speciation models. While thiols, at concentrations in excess of what is observed in surface seawater, were able to reduce copper uptake, they were not as effective as Cu(II) ligands in limiting bioavailability. Surprisingly, in some cases bioavailability was increased. Uptake in the presence of thiols was enhanced in copper-limited cells of the coccolithophore *Emiliania huxleyi*, particularly in the presence of

cysteine, where uptake of Cu(I) exceeded that of uncomplexed Cu(I). Furthermore, cysteine is able to increase the bioavailability of copper that is strongly complexed by EDTA, presumably through the reduction of the Cu(II)-EDTA complex and subsequent facilitation of uptake. Similar behavior is not observed with glutathione or the biological reductant ascorbate. The mechanism was observed in replete cultures of *E. huxleyi* and the diatom *Thalassiosira pseudonana* and is enhanced in copper-limited *E. huxleyi*. Copper limitation also enhances the activity of surface reductases and the uptake of cysteine. Cysteine uptake rates are comparable to those observed with cysteine enhanced copper uptake and may suggest that copper is being assimilated with cysteine in addition to uptake via cuprous ion transporters.

Previous research has demonstrated that *E. huxleyi* maintains lower copper quotas than many other eukaryotic algae. This remains true over a range of copper concentrations as *E. huxleyi* cells are able to maintain lower cellular quotas in comparison to the diatom *T. pseudonana*. Stable isotopes of copper were used as biological tracers to demonstrate a divergence between net and gross assimilated copper in *E. huxleyi,* indicating the loss of copper from the cell. This export mechanism is constitutive and facilitates export even during active uptake of copper. Under the same conditions, *T. pseudonana* demonstrates continuous accumulation. Furthermore, while both copper loaded *E. huxleyi* and *T. pseudonana* demonstrate export, elimination of copper from *E. huxleyi* is far more rapid than from *T. pseudonana*.

Both dipeptides were measured in a diverse array of marine phytoplankton, though at levels below those observed in *E. huxleyi.* High concentrations of Arg-Cys and Gln-Cys were also measured in the highly polluted and nutrient loaded Chesapeake Bay, further demonstrating their ecological prevalence.

High affinity copper uptake is facilitated by the surface reduction of Cu(II) to Cu(I) followed by the transport across the membrane of Cu(I). Cu(II) is already heavily complexed in surface seawater. The exudation of thiols could potentially cause the reduction of Cu(II), potentially complexed, in the bulk media. Furthermore thiols provide little additional buffering capacity of Cu(I). It is therefore unlikely that thiols are exuded with the purpose of directly lowering the bioavailability of copper outside the cell.

E. huxleyi produces high concentrations of the copper-specific Arg-Cys and Gln-Cys while under copper stress. Inside the cell these dipeptides are likely to provide substantial buffering capacity that could alleviate the toxic effects of high copper, potentially without affecting the speciation of other metals. Meanwhile, Cu(I) complexes would represent a substantial portion of the cellular copper pool. Since export is highly efficient in keeping cellular concentrations low, it is conceivable that the complexed cellular copper is being subsequently exported. Such a mechanism has an analogue in the detoxification of cadmium by phytochelatin, and would explain why these thiols are also observed outside the cell. This ability to rapidly exclude copper would give *E. huxleyi* a distinct ecological advantage in waters that are prone to high copper concentrations.

2. Future work

2.1. Evaluation of the behavior of Cu(I) and Cu(I) complexes

The behavior of Cu(I) in surface seawater is poorly understood. Beyond its oxidation kinetics (Sharma and Millero, 1988; Moffett and Zika, 1983) and photochemical generation

(Moffett and Zika, 1987) few studies have examined its biochemical behavior or generation. Additionally, the tools used to measure it remain limited (Moffett et al., 1985; Buerge-Weirich and Sulzberger, 2004). If Cu(I) is addressed in studies of copper-ligand binding in surface seawater it is often given only a passing mention. Unfortunately many of the analytical techniques used to measure copper assume a Cu(II) oxidation state when measuring the affinity of copper binding ligands. While this may be descriptive in a number of environments in which Cu(II) and Cu(II) ligands dominate, the presence of thiols either knowingly or unknowingly could have an impact on results. This may be of particular concern in culture studies, where higher cell densities are likely going to increase the surface mediated reduction of Cu(II) to Cu(I). Evaluation of the behavior of Cu(I) with the competitive ligands, as well as the behavior of thiols exposed to the electrodes used in voltammetry, would aid in the interpretation of electroanalytical studies of copper binding ligands.

There are conflicting studies regarding the redox behavior of thiols in surface seawater. Several suggest that oxidized glutathione dissociates into its reduced form (Leal and Van den Berg, 1998; Semeniuk et al., 2009). Other studies provide evidence that the trend is towards net oxidation (Moingt et al., 2010; Crea et al., 2010). Our work suggests that at least in the short term they are stable in their initial form. This has impacts on some of the electroanalytical methods mentioned above. More importantly, however, is the effect on copper chemistry. Oxidized glutathione is a reasonably strong Cu(II) ligand and, as we have shown, it is more effective than its reduced form in limiting the bioavailability of copper. If thiols are exuded as a complex with Cu(I), it is pertinent to know how long these complexes are stable before they dissociate and to know for how long the thiols are stable in their reduced form. Copper

concentrations, photochemistry and biological factors are all likely to impact the behavior of thiols outside the cell.

Recent studies have shown that Cu(I)-thiol complexes can also generate superoxide (Aliaga et al., 2010; Speisky et al., 2009; Speisky et al., 2008). Superoxide plays a role in the redox cycling of several elements, including iron and manganese, both of which have biological implications (Learman et al., 2011; Kustka et al., 2005). Cells could potentially exude Cu(I)-thiol complexes to promote the production of extracellular superoxide for defense or nutrient acquisition purposes.

2.2. Synthesis of a Cu(I) specific fluorescent ion indicator for seawater

A highly sensitive and highly specific Cu(I) ion indicator would help to elucidate the role of Cu(I) in marine systems. While the fluorescent ion indicator Phen Green SK was suitable for measurement of Cu(I) in controlled systems, it is limited by its lack of copper ion selectivity. As a 5-substituted derivative of 1,10 phenanthroline PhenGreenSK can readily bind Hg(II), Pb(II), Zn(II), Fe(II), Ni(II), Cd(II), Cu(I), Cu(II). Methylation of the 2 and 9 positions, would make this indicator a binding analogue of the Cu(I) specific neocuproine. Due to the presence of 4 and 7-substituted phenyl groups, bathocuproine would not be a suitable precursor. If this new compound is strongly fluorescent, it would be a suitable indicator for Cu(I) measurement in environmental and biological systems. Utilization of this compound in tandem with a reductant could also facilitate the measurement of total copper.

2.3. Structural evaluation of copper-thiol complexes

Further structural investigation of thiol metal complexes is also warranted. We attempted to characterize Cu(I)-GSH complexes via electrospray mass spectrometry (ESI-MS). Analysis of solutions of Cu(I)-GSH resulted in mass spectra of a Cu(II)-GSSG complex indicating that both the glutathione molecule and copper were being oxidized. Attempts to mitigate oxidation by running the electrospray source in both positive and negative ion mode and utilizing a platinum electrode as an ionization source (Kertesz and Van Berkel, 2001; Tsikas et al., 2000) did not succeed. Recent advancements suggest that this artifact can be overcome. Cu(I) complexes of a cysteine containing octapeptide were characterized using MALDI/TOF-MS (Wu et al., 2010). Fragmentation of this molecule suggested that Cu(I) was being coordinated by the cysteinyl thiol. The use of a novel cooper salt matrix consisting of α -cyano-4-hydroxycinnamic acid (Wu et al., 2009) aided in the formation of these Cu(I) complexes. Additionally, Cu(I)-peptide analyses were performed using a sacrificial copper electrode (Prudent and Girault, 2008), however this method also generated Cu(II) which subsequently oxidizes any cysteine present (Prudent and Girault, 2009). While not yet ideal for the evaluation of Cu(I)-thiol complexes, paired with a copper detection instrument, ESI-MS could still provide a first analytical step in identifying novel copper binding ligands.

2.4. Uptake and ocean acidification

Increasing ocean acidity will have various impacts on trace metal speciation and uptake. Acidification has been shown to affect iron uptake in coccolithophores and diatoms (Shi et al., 2010). Similar reduction in iron uptake has been shown to slow nitrogen fixation in

Trichodesmium (Shi et al., 2012). The effect of lower pH levels decreased Cd(II) and Zn(II) bioavailability, however this change was also driven by the presence of a change in speciation in weak ligands of Cd(II) and Zn(II) (Xu et al., 2012). The effect of acidification on copper speciation and bioavailability is unclear, but it is likely to be substantially affected by the change in complexing capacity of copper ligands. Given the potential diversity of responses to copper, experiments to test the effect of pH levels on copper uptake should be performed on a diversity of species.

2.5. Expression studies

Proteomic or genomic methods would further help unravel the copper detoxification mechanism of *E. huxleyi*. Given that arginyl tRNA synthethase has been shown to facilitate Arg-Cys production in *E. coli* (Jakubowski, 1995), we could use qRT-PCR to see if arginyl and glutatmyl tRNA synthethases, are upregulated under copper stress in *E. huxleyi*. These synthetases should be further examined as a potential source for these dipeptides. Additionally, expression of specific ABC-type transporters should also be explored. Proteomic measurement of copper stressed cells would provide insight into which enzymes are involved in copper detoxification. The availability of genomes of a wide variety of marine phytoplankton, including *E. huxleyi*, allows for further bioinformatic evaluation.

3. References

Aliaga M, Carrasco-Pozo C, López-Alarcón C, et al. (2010) The Cu(I)–glutathione complex: factors affecting its formation and capacity to generate reactive oxygen species. *Transition Metal Chemistry* 35: 321-329.

Buerge-Weirich D and Sulzberger B. (2004) Formation of Cu(I) in Estuarine and Marine Waters: Application of a New Solid-Phase Extraction Method To Measure Cu(I). *Environmental Science & Technology* 38: 1843-1848.

Crea P, De Stefano C, Millero F, et al. (2010) Dissociation Constants of Protonated Oxidized Glutathione in Seawater Media at Different Salinities. *Aquatic Geochemistry* 16: 447-466.

Jakubowski H. (1995) Synthesis of cysteine-containing dipeptides by aminpacyl-tRNA synthetases. *Nucl. Acids Res.* 23: 4608-4615.

Kertesz V and Van Berkel GJ. (2001) Minimizing analyte electrolysis in an electrospray emitter. *Journal of Mass Spectrometry* 36: 204-210.

Kustka AB, Shaked Y, Milligan AJ, et al. (2005) Extracellular Production of Superoxide by Marine Diatoms: Contrasting Effects on Iron Redox Chemistry and Bioavailability. *Limnology and Oceanography* 50: 1172-1180.

Leal MFC and Van den Berg CMG. (1998) Evidence for strong copper(I) complexation by organic ligands in seawater. *Aquatic Geochemistry* 4: 49-75.

Learman DR, Voelker BM, Vazquez-Rodriguez AI, et al. (2011) Formation of manganese oxides by bacterially generated superoxide. *Nature Geosci* 4: 95-98.

Moffett JW and Zika RG. (1983) Oxidation-Kinetics of Cu(I) in Seawater - Implications for Its Existence in the Marine-Environment. *Marine Chemistry* 13: 239-251.

Moffett JW and Zika RG. (1987) Photochemistry of copper complexes in sea water. *Photochemistry of environmental aquatic systems. American Chemical Society*: 116-130.

Moffett JW, Zika RG and Petasne RG. (1985) Evaluation of bathocuproine for the spectrophotometric determination of copper(I) in copper redox studies with applications in studies of natural waters. *Analytica Chimica Acta* 175: 171-179.

Moingt M, Bressac M, Bélanger D, et al. (2010) Role of ultra-violet radiation, mercury and copper on the stability of dissolved glutathione in natural and artificial freshwater and saltwater. *Chemosphere* 80: 1314-1320.

Prudent M and Girault HH. (2008) On-line Electrogeneration of Copper–Peptide Complexes in Microspray Mass Spectrometry. *Journal of the American Society for Mass Spectrometry* 19: 560-568.

Prudent M and Girault HH. (2009) The role of copper in cysteine oxidation: study of intra- and inter-molecular reactions in mass spectrometry. *Metallomics* 1: 157-165.

Semeniuk DM, Cullen JT, Johnson WK, et al. (2009) Plankton copper requirements and uptake in the subarctic Northeast Pacific Ocean. *Deep Sea Research Part I: Oceanographic Research Papers* 56: 1130-1142.

Sharma VK and Millero FJ. (1988) Oxidation of copper(I) in seawater. *Environmental Science & Technology* 22: 768-771.

Shi D, Kranz SA, Kim J-M, et al. (2012) Ocean acidification slows nitrogen fixation and growth in the dominant diazotroph Trichodesmium under low-iron conditions. *Proceedings of*

the National Academy of Sciences 109: E3094–E3100.
Shi D, Xu Y, Hopkinson BM, et al. (2010) Effect of Ocean Acidification on Iron Availability to Marine Phytoplankton. *Science* 327: 676-679.
Speisky H, Gómez M, Burgos-Bravo F, et al. (2009) Generation of superoxide radicals by copper-glutathione complexes: Redox-consequences associated with their interaction with reduced glutathione. *Bioorganic & Medicinal Chemistry* 17: 1803-1810.
Speisky H, Gómez M, Carrasco-Pozo C, et al. (2008) Cu(I)-Glutathione complex: A potential source of superoxide radicals generation. *Bioorganic & Medicinal Chemistry* 16: 6568-6574.
Tsikas D, Raida M, Sandmann J, et al. (2000) Electrospray ionization mass spectrometry of low-molecular-mass S-nitroso compounds and their thiols. *Journal of Chromatography B: Biomedical Sciences and Applications* 742: 99-108.
Wu Z, Fernandez-Lima FA, Perez LM, et al. (2009) A New Copper Containing MALDI Matrix That Yields High Abundances of [Peptide + Cu]+ Ions. *Journal of the American Society for Mass Spectrometry* 20: 1263-1271.
Wu Z, Fernandez-Lima FA and Russell DH. (2010) Amino Acid Influence on Copper Binding to Peptides: Cysteine Versus Arginine. *Journal of the American Society for Mass Spectrometry* 21: 522-533.
Xu Y, Shi D, Aristilde L, et al. (2012) The effect of pH on the uptake of zinc and cadmium in marine phytoplankton: Possible role of weak complexes. *Limnology and Oceanography* 57: 293.